An investigation into the impact of microvascular leakage on neutrophil transendothelial migration as analysed using murine models of inflammation

A thesis submitted in partial fulfilment of the requirements of the Degree of Doctor of Philosophy

By

Charlotte Owen-Woods

Centre for Microvascular Research

William Harvey Research Institute

Barts & The London School of Medicine and Dentistry

Queen Mary University of London

Charterhouse Square

London

EC1M 6BQ

Statement of Originality

I, Charlotte Owen-Woods, confirm that the research included within this thesis is my own work or that where it has been carried out in collaboration with, or supported by others, that this is duly acknowledged below and my contribution indicated. Previously published material is also acknowledged below.

I attest that I have exercised reasonable care to ensure that the work is original, and does not to the best of my knowledge break any UK law, infringe any third party's copyright or other Intellectual Property Right, or contain any confidential material.

I accept that the College has the right to use plagiarism detection software to check the electronic version of the thesis.

I confirm that this thesis has not been previously submitted for the award of a degree by this or any other university.

Signature: Charlotte Owen-Woods

……..

Date: 05-Jan-2021

Acknowledgments

I would like to thank all those who have supported me throughout my PhD in both a professional and personal manner. I have met incredible people at Queen Mary University of London and I am grateful to everyone in the team for making my experience so positive. Their humour, support and guidance have been instrumental in the completion of my PhD.

First and foremost, I would like to thank Prof. Sussan Nourshargh for her continuous support and supervision throughout the PhD and for providing me with the opportunity to study such a fascinating area of research. I would also particularly like to thank Dr. Régis Joulia for his partnership throughout our research project and co-authored publication. Furthermore, I would like to give special thanks to Dr. Mathieu Benoit-Voisin and Dr. Matthew Golding for their support and guidance throughout the PhD and thesis writing process. My thanks also go to Prof. Ken Suzuki for his words of encouragement and acting as my secondary supervisor. I am also grateful to Dr. David Budd and Dr. Augustin Amour for their project input, support and reassurance throughout the PhD and in particular during my time working at GlaxoSmithKine.

I would also like to thank everyone, past and present in microvascular research. To my friends and colleagues, I cannot thank you all enough for your support over the past four years. In particular, I would like to thank Ross for his training from the start of my PhD and his continued support. Special thanks also go to Lorena, Natalia, Loïc, Monja and Anna for their help throughout my PhD and more importantly, on a personal level for all the laughs and being great friends. You all made my experience, so thank you!

Importantly, I would like to like to thank my family for all the support I have been given. In particular, my parents for their continuous support and words of encouragement. To Max, I cannot put into words the support and patience you have shown me over the past 4-years.

Lastly, I would like to thank the funding bodies for supporting the investigations conducted throughout my PhD, namely, the BBSRC and GlaxoSmithKline.

Abstract

Controlled opening of endothelial-cell (EC) junctions is vital in regulating vascular permeability and neutrophil transendothelial migration (TEM) during acute inflammation. Although both phenomena can occur independently, as supported by distinct molecular pathways, the potential inter-play of these two responses requires further exploration. In this thesis, we investigated the impact of microvascular leakage on neutrophil TEM and the potential downstream pathophysiological consequences.

To this aim, as part of this project, a confocal intravital microscopy platform was developed for simultaneous analysis of neutrophil TEM and vascular permeability within the murine cremaster muscle microcirculation. The inflammatory reactions employed were driven by locally administered LTB_4, or IL-1β ± vasoactive agents (e.g. histamine/VEGF), or by a model of IR-injury. The findings provide direct evidence for the ability of inflammatory reactions characterised by enhanced microvascular leakage to promote an aberrant mode of neutrophil TEM, known as reverse (r)TEM. This response is characterised by neutrophils that have partially breached the endothelium and move in a retrograde mode, thus returning into the lumen. Interestingly, genetic functional deficiency or pharmacological blockade of VE-cadherin-dependent hyper-permeability reduced the frequency of neutrophil rTEM. Mechanistically, this migration behaviour was driven by excessive diffusion of tissue-derived CXCL1 through EC junctions into the plasma, resulting in a disrupted chemotactic gradient across the endothelium. Development of a novel tracking method allowed us to demonstrate that rTEM neutrophils exhibited a pro-inflammatory phenotype and disseminated into the blood and lung circulation. Presence of these cells in lungs was associated with vascular damage. Finally, we identified distinct roles for TNF-receptors in controlling vascular permeability and neutrophil migration during IR-injury.

Collectively, the findings of this thesis provide a causal link between increased local microvascular leakage induction and disrupted localisation of chemotactic directional cues across the endothelial barrier, resulting in aberrant mode of neutrophil migration and subsequent distant organ damage.

Contents

List of Figures

List of Tables

List of Movies

All videos are available in OneDrive shared file (See Appendix 1.)

Video 1: A representative example of the neutrophil TEM & vascular leakage response during IR-injury induced cremasteric inflammation

Video 2: An example of normal neutrophil TEM (nTEM) during IR-injury induced cremasteric inflammation

Video 3: An example of neutrophil reverse TEM (rTEM) during IR-injury induced cremasteric inflammation

Video 4: Neutrophil TEM, vascular leakage and neutrophil rTEM as induced by IL-1β + histamine cremasteric inflammation

Video 5: Labelling of rTEM neutrophils in the cremaster muscle with anti-Ly6G-biotin Ab and strept-AF647

Abbre*via*tions

Ab	Antibody
ACK	Ammonium-chloride-potassium
ACKR	Atypical chemokine receptor
ADCC	Antibody-dependent cellular cytotoxicity
AF	Alexa Fluor
ALI	Acute lung injury
AP	Activating protein
APC-Cy	Allophycocyanin-cyanine
ARDS	Acute respiratory distress syndrome
α-SMA	Alpha-smooth muscle actin
BBB	Blood brain barrier
BM	Bone marrow
bp	base pair
BV	Brilliant violet
BSA	Bovine serum albumin
C5a	Complement component 5a
CARD	Caspase recruitment domain-containing protein
CCL	C-C motif chemokine ligand
CD	Cluster of differentiation
CDC	Complement-dependent cytotoxicity
CNS	Central nervous system
COPD	Chronic obstructive pulmonary disease
Cre	Cre recombinase
CRP	C reactive protein
CVD	Cardiovascular disease

CXCL	Chemokine (C-X-C) ligand
CXCR	Chemokine (C-X-C) receptor
DAMP	Danger associated molecular pattern
DHR	Dihydrorhodamine
DNA	Deoxyribonucleic acid
EAP	Endothelial adhesive platforms
EC	Endothelial cell
EM	Extracellular matrix
EDTA	Ethylenediaminetetraacetic acid
EGFP	Enhanced green fluorescent protein
ELISA	Enzyme linked immunosorbent assay
ELR	glutamine-leucine-arginine
ERM	Ezrin, radixin and moesin
ESAM	Endothelial cell adhesion molecule
ESL	E-selectin ligand
EYFP	Enhanced yellow fluorescent protein
FACS	Fluorescence-activated cell sorting
FCS	Foetal calf serum
f/f	Flox/flox
FITC	Fluorescein isothiocyanate
fMLP	N-formylmethionine-leucyl-phenylalanine
g	Gram
GM	Genetically modified
G/(M)-CSF	Granulocyte/(macrophage)-colony stimulating factor
g/RCF	Relative Centrifugal Force
GAGs	Glycosaminoglycans
G-CSF	Granulocyte-colony stimulating factor

GPCR	G protein coupled receptor
Gy	Gray
HBP	Heparin binding protein
HCAM	Homing cell adhesion molecule
HDCs	Haematopoietic derived cells
Hist	Histamine
HRP	Horseradish peroxidase
hr	Hour/s
HSCs	Haematopoietic stem cells
Hz	Hertz
ICAM	Intercellular cell adhesion molecule
IF	Immunofluorescence
IL	Interleukin
IFN	Interferon
iRhom2	Inactive rhomboid protein 2
IR	Ischaemia reperfusion
IVM	Intravital microscopy
i.p.	Intraperitoneal
i.s.	Intrascrotal
i.v.	Intravenous
JAM	Junctional adhesion molecule
kDa	Kilodalton
KLH	keyhole limpet hemocyanin
KO	Knock out
LBRC	Lateral border recycling compartment
LBD	Lectin binding domain
LER	Low expression region

LFA	Lymphocyte function associated antigen
LPS	Lipopolysaccharide
LT-A_4 or -B_4 or -C_4	Leukotriene A_4 or B_4 or C_4
LVWO	Lung vascular washout
LysM	Lysosome M
mAb	Monoclonal antibody
MAC	Macrophage antigen
MAPK	mitogen-activated protein kinase
MBL	Mannose binding lectin
min	Minute/s
ml	Milliliter/s
MLC(K)	Myosin-light chain (kinase)
mm	Millimetre
MMPs	Matrix Metalloproteinase
MPO	Myeloperoxidase
MRP8	Myeloid-related protein 8
NADPH	Nicotinamide adenine dinucleotide phosphate
NE	Neutrophil elastase
NETs	Neutrophil extracellular traps
NHP	Non-human primates
NO/S	Nitric oxide/synthase
ns	Not significant
PA	Photoactivation
PAMP	Pathogen associate molecular pattern
PBS	Phosphate buffered saline
PB	Pacific blue
PC	Photoconversion

PCR	Polymerase chain reaction
PE	Phycoerythrin
Pe	Péclet number
PE-Cy	Phycoerythrin-cyanine
PECAM	Platelet endothelial cell adhesion molecule
PE-Dazzle	Phycoerythrin-Dazzle
PFA	Paraformaldehyde
pg	Picogram
PGE_2	Prostaglandin E2
PI3K	phosphoinositide 3-kinase
PSGL	P-selectin glycoprotein
qPCR	Quantitative polymerase chain reaction
RA	Rheumatoid arthritis
ROSA-EYFP	R26-stop-enhanced yellow fluorescent protein
rIM	Reverse interstitial migration
(r) - MFI	(relative) – mean fluorescence intensity
ROI	Region of interest
ROS	Reactive oxygen species
RNA	Ribonucleic acid
rTEM	Reverse transendothelial migration
SB	Sorting buffer
SEM	Standard error of the mean
SHP	Src homology region 2 domain-containing phosphatase
SNP	Single nucleotide polymorphism
SOD	Superoxide dismutase
SP	Surfactant protein
Strept	Streptavidin

TACE	Tumor necrosis factor-α-converting enzyme
TEER	Transendothelial electrical resistance
TEM	Transendothelial migration
TGF-β	Transforming growth factor beta
TLR	Toll-like receptor
(s or m) - TNF	(Soluble or membrane) - tumour necrosis factor
TNFR	Tumour necrosis factor receptor
TRADD	TNFR-associated death domain
TRAF	TNFR-associated factor
TPM	Transpericyte migration
TRITC-dextran	Tetramethylrhodamine isothiocyanate-dextran
Tyr	Tyrosine
VCAM	Vascular cell adhesion molecule
VE-C or -cadherin	Vascular endothelial cadherin
VEGF	Vascular endothelial growth factor
VEGFR	Vascular endothelial growth factor receptor
VE-PTP	Vascular endothelial protein tyrosine phosphatase
VLA	Very late antigen
v/v	Volume/volume
VVO	Vesiculo-vascular organelle
w/v	Weight/volume
WPB	Weibel-Palade bodies
WT	Wildtype

Publications arising from this work

C. Owen-Woods, R. Joulia, A. Barkaway, L. Rolas, B. Ma, A. Fee Nottebaum, K. P. Arkill, M. Stein, T. Girbl, M. Golding, D. O. Bates, D. Vestweber, M.B. Voisin & S. Nourshargh. (2020). *Local microvascular leakage promotes trafficking of activated neutrophils to remote organs.* Journal of Clinical Investigations. 130, 5, 2301-2318. DOI: 10.1172/JCI133661 (See Appendix 2).

List of presentations

Charlotte Owen-Woods, Régis Joulia, Bin Ma, Anna Barkaway, Ross King, Dietmar Vestweber, Mathieu-Benoit Voisin, Sussan Nourshargh (2018). **Microvascular leakage promotes aberrant neutrophil transendothelial migration.** UK Adhesion Meeting (London, September 2018). *Poster presentation.*

Charlotte Owen-Woods, Régis Joulia, Bin Ma, Anna Barkaway, Ross King, Dietmar Vestweber, Mathieu-Benoit Voisin, Sussan Nourshargh (2019). **Microvascular leakage promotes aberrant neutrophil transendothelial migration.** William Harvey Day (London, January 2019). *Oral presentation.*

Charlotte Owen-Woods, Régis Joulia, Bin Ma, Anna Barkaway, Dietmar Vestweber, Mathieu-Benoit Voisin, and Sussan Nourshargh (2019). **Microvascular leakage promotes neutrophil reverse transendothelial migration *in vivo*.** Cell Adhesion and Migration in Inflammation and Cancer – Zoo Meeting (Rotterdam, May 2019). *Poster presentation.*

Chapter 1

Introduction

1.1. Acute inflammation and the innate immune response

Inflammation is a natural host defence reaction that is fundamentally mediated by the innate and/or the adaptive immune systems in response to infections or tissue damage. Inflammation aims to rapidly eliminate the initial cause of insult, i.e. removal of pathogens, dead cells and debris, in addition to, initiating tissue repair and remodelling. Inflammation is defined by five classical signs: *dolor* (pain), *calor* (heat), *rubor* (redness), *tumor* (swelling) and *functio laesa* (loss of function) (Majno and Joris, 2004). Redness and heat develop as a consequence of increased blood flow, and swelling results from increased leakage of plasma proteins and fluid into the damaged tissue. Pain results from an active release of neuropeptides that enable stimulation of the sensory nerves, and finally, loss of function can occur if the inflammatory response remains unresolved or becomes dysregulated.

Inflammatory responses are triggered within minutes (Chen et al., 2018) by the recognition of "pathogenic/danger signals", comprising distinct chemical motifs known as 'pathogen-associated molecular patterns' (PAMPs) or 'damaged-associated molecular patterns' (DAMPs) (Zindel and Kubes, 2020). These factors can be released by foreign microorganisms or damaged tissue and cells, respectively, into the interstitial tissue. Such molecules are recognised by pattern recognition receptors (PRRs), for instance toll-like receptors (TLRs), that are expressed on the surface of resident/sentinel immune cells (e.g. macrophages, dendritic cells and mast cells) and non-immune cells (e.g. fibroblasts and endothelial cells [ECs]) in the tissue (Andonegui et al., 2009; Zindel and Kubes, 2020). One such example is the endotoxin, lipopolysaccharide (LPS), a PAMP that can be detected by the cell surface PRR, TLR_4, expressed primarily on monomyelocytic cells. Once activated, these cells release a plethora of preformed and *de novo* synthesised inflammatory and pro-permeability mediators *via* the NF-κB pathway (Newton and Dixit, 2012). These mediators contribute to the activation of other resident cells (e.g. ECs and pericytes), thus further amplifying the inflammatory response. The principal mediators involved here include numerous cytokines such as tumour necrosis factor (TNF) and interleukin-1β (IL-1β), various C-X-C and C-C motif chemokines (e.g. CXCL1, CXCL2, CXCL8, CCL2, CCL5), lipids and eicosanoids such as leukotriene (LT)B_4 and vasoactive factors such as vascular endothelial growth factor

(VEGF) and histamine in addition to numerous reactive oxygen species (ROS) (Thomas and Schroder, 2013; Park-Windhol and D'Amore, 2016). Collectively, this leads to both the recruitment and directed migration of immune cells derived from the bone marrow (BM) such as monocytes and of particular interest to this thesis, neutrophils (refer to section 1.5) and the initiation of an enhanced vascular leakage response at the site of insult (Newton and Dixit, 2012). Resident (e.g. dendritic cells and macrophages) and migrated (e.g. neutrophils) immune cells are then able to eliminate the invading pathogen or remove dead cells in the interstitial tissue *via* the release a variety of bactericidal factors or by targeted phagocytosis (Julier et al., 2017). The return of homeostasis is supported by the synthesis of several mediators that hinder further recruitment of leukocytes, counteract pathways that lead to leukocyte survival, and transitioning of cells, especially macrophages, from a pro-inflammatory to pro-clearance phenotype for the removal of apoptotic cells. These factors include, prostaglandin (PGE) -E_2 and D_2 which induce lipid mediator class switching for the formation of lipoxins, E- & D- series resolvins and protectins. In addition, expression of the anti-inflammatory cytokines IL-10 and transforming growth factor (TGF)-β is upregulated, while negative feedback loops are initiated to inhibit further synthesis of inflammatory cytokines (e.g. TNF) to support the resolution of the inflammatory response (Serhan et al., 2008; Sugimoto et al., 2016). After successful clearance of the pathogen or damaged cells, immune cells are able to secrete a range of growth factors to promote tissue repair (e.g. VEGF and platelet-derived growth factor (PDGF)) (Julier et al., 2017) (detailed in **Fig. 1.1**). However, if acute inflammation remains unresolved or becomes dysregulated, this cascade of events can result in excessive tissue damage, which is a common feature of many inflammatory diseases such as cardiovascular and pulmonary conditions including stroke, sepsis, pneumonia and trauma (Fan et al., 2018).

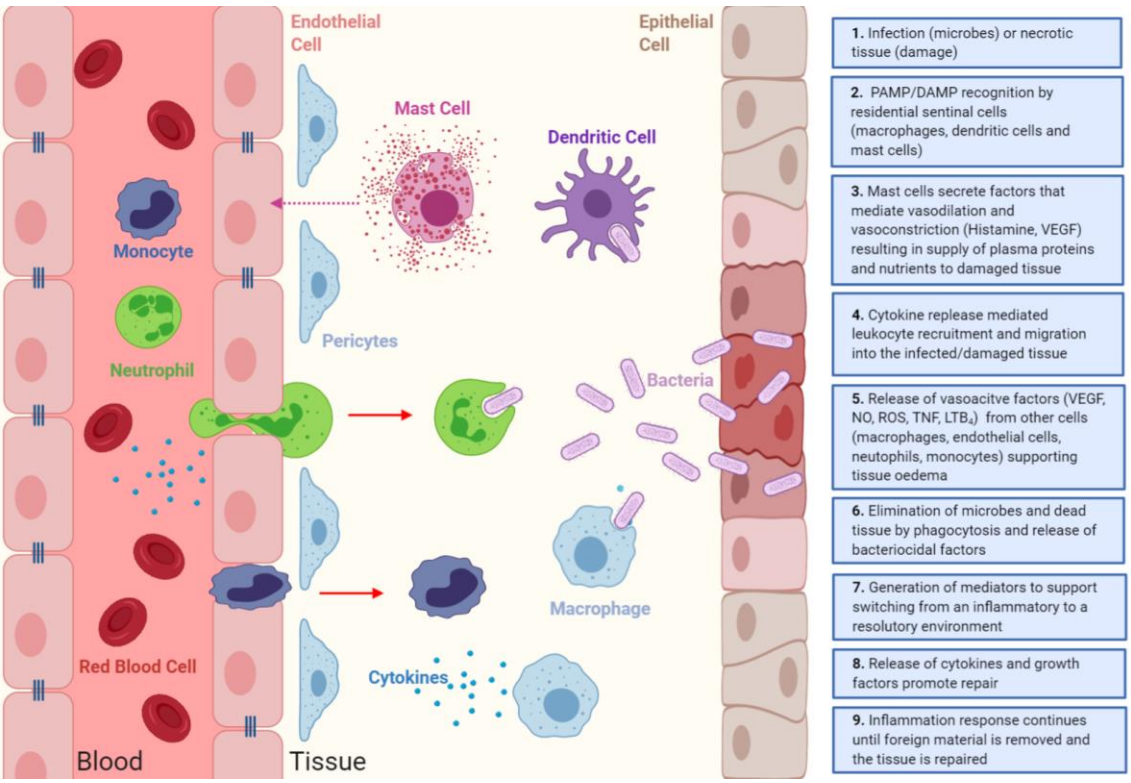

Figure 1.1. Pathogen or injury-induced activation of the innate immune response. Schematic illustrating PAMP/DAMP-mediated activation of resident innate immune cells (macrophages, dendritic cells and mast cells) *via* their PRR's. This results in the release of pro-inflammatory mediators and chemoattractants in order to mobilise and recruit, amongst other cells, neutrophils and monocytes. In addition, the inflammatory response initiates the release of pro-permeability inducing agents, thus supplying the tissue with essential plasma proteins. Once recruited, neutrophils play a key role in pathogen killing and tissue repair processes. Furthermore, specific resolutory mediators are generated to support the transition back from an inflammatory to homeostatic environment. If the acute inflammatory response remains unresolved or hyperactivated this can result in an acute response evolving into a chronic response in addition to triggering the adaptive immune response.

1.2. Pathological acute inflammation and distant organ injury

Whilst acute inflammation is usually a beneficial response functioning to resolve harmful effects of injury or infection, under excessive or prolonged stimulation, this reaction can become dysregulated with pathogenic consequences. Examples of diseases caused by dysregulated acute inflammation are tissue fibrosis, acute lung injury (ALI) and acute respiratory distress syndrome (ARDS) (Chen et al., 2018). Although commonly triggered by local inflammatory insults, a life-threatening feature of these conditions is damage to distant organs as illustrated following ischaemia reperfusion (IR)-injury (Grace, 1994).

IR-injury is an insult associated with tissue damage that results from a period of reduced blood supply, usually to an organ (e.g. during transplantation) or limb (e.g. post trauma), resulting in hypoxia. During hypoxia, anaerobic respiration becomes the predominant source of energy leading to increased local concentrations of lactic acid with a consequent reduced pH. Under these acidic conditions, normal enzymes and protein functions become dysregulated, leading to a failure of local homeostasis (Grace, 1994; Rodrigues and Granger, 2010). As a consequence, prolonged ischaemia leads to loss of essential cell functions, resulting in the release of DAMPs and stress signals into the extracellular space and cell death. The only means to protect cell damage is the rapid restoration of blood flow, known as reperfusion. Paradoxically, reperfusion is a double-edged sword as it can result in further injury. The sudden return of oxygen leads to a cascade of reactions mediated by ROS that cause further tissue damage (Grace, 1994). In addition, reperfusion is followed by enhanced local vascular permeability and increased levels of neutrophil recruitment and transendothelial migration (TEM) which act to enhance the inflammatory response further. Our understanding that exacerbated localised inflammation can lead to adverse systemic pathologies has a been a keen area of interest over the decades (Kalia et al., 2005). For example, IR-injury of the intestines, lung, heart, kidney, liver and skeletal muscle have been associated with distal (or secondary) organ damage (Kalogeris et al., 2012; Faubel and Edelstein, 2016). In particular, as the lungs are one of the first organs to be exposed to ischaemia induced hypoxic blood, they are particularly susceptible to secondary injury, which can manifest as ALI.

ALI is a serious pathological condition often encountered following major surgery, with >200,000 cases/year in the US alone and has a high associated mortality rate (~40%). Even patients that survive ALI usually experience lingering adverse effects on quality of life resulting from the onset of pulmonary fibrosis, and consequent permanent reduction in lung capacity (Johnson and Matthay, 2010). This disease is classically characterised by tissue oedema and enhanced neutrophil infiltration, whereby the latter can exacerbate the former *via* the release of various pro-inflammatory mediators (discussed in section 1.4.3) and proteases, such as neutrophil elastase (NE) and cathepsin G (Soehnlein et al., 2008; Grommes and Soehnlein, 2011). Fundamentally, these proteases result in damage and degradation of the endothelial basement

membrane and EC junction proteins, a series of responses that ultimately leads to a severe reduction in endothelial integrity and enhanced lung permeability. Increased passage of plasma proteins and fluid into the alveoli then prohibits effective gaseous exchange, at which point ARDS and failure of the respiratory system ensue (Raghavendran et al., 2008; Johnson and Matthay, 2010; Dushianthan et al., 2011). Currently, our understanding as to precisely how locally induced inflammation can lead to the development of distant organ injury, is underdeveloped. Therefore, gaining greater insight into the mechanisms driving dysregulated local inflammation and the subsequent development of secondary organ injury could be informative for the design of therapeutic interventions.

1.3. Neutrophils in homeostasis and physiological inflammation

Neutrophils are terminally differentiated leukocytes, measuring approximately 12-15 µm (7 µm in mice) in diameter and are the most abundant cell type in human blood (50-70% of total white blood cells) (Rosales, 2018; Wright et al., 2010). Neutrophils originate from haematopoietic stems cells (HSCs) in the BM, which during haematopoiesis become committed to the myeloblastic lineage in the presence of granulocyte colony stimulating factor (G-CSF). HSCs initially differentiate into granulocyte-monocyte progenitors (GMPs), which then require two major phases to develop into mature neutrophils: a proliferative stage during which GMPs differentiate into myeloblasts, promyelocytes and myelocytes followed by a non-proliferative stage into metamyelocytes, immature neutrophils before ultimately terminally differentiating into mature neutrophils (~10^{11} cells per day) (Rosales, 2018; Ng et al., 2019). The release of mature neutrophils from the BM into the blood circulation is tightly regulated under homeostatic (i.e. healthy) conditions, with only 1-2% of the total neutrophil population circulating at any one time, the vast majority being retained in the BM. Immature neutrophils are retained in the BM by stromal cells expressing vascular cell adhesion molecule (VCAM)-1 and CXCL12 (cognate ligands for neutrophil-derived α4β1 integrin (very late antigen (VLA)-4) and CXCR4, respectively). Upon maturation in response to G-CSF, neutrophil precursors begin to downregulate VLA-4 and CXCR4 (Martin et al., 2003) and increase their expression of CXC receptor 2 (CXCR2) and TLR_4, allowing neutrophils

to respond to chemokines such as CXCL1 and PAMPs/DAMPs, respectively (De Filippo et al., 2013; Sawant et al., 2016), culminating in reduced retention and egression of mature neutrophils from the BM. Once released, mature neutrophils have a relatively short lifespan, surviving between 8-12 hours in the circulation and 1-2 days in the interstitial tissue, though this issue remains contentious (Hellebrekers et al., 2018).

Following an inflammatory insult or infection, circulating inflammatory cytokines, (e.g. CXCL1) stimulate the BM for a rapid release *en masse* of neutrophils (and other leukocytes) into the peripheral blood. Circulating neutrophils are then recruited to the site of insult. Neutrophils are one of the earliest responders to sites of inflammation where they adhere and crawl along the endothelium adjacent to the site of injury and/or infection, before ultimately migrating through the vascular barrier into the interstitial tissue. The latter series of events is known as the leukocyte adhesion cascade (Ley et al., 2007) (detailed in section 1.5).

Neutrophils are considered to exist in three states: resting, primed or fully activated states. Under basal resting conditions neutrophils ensure their toxic intracellular components are retained. Neutrophils have various cytokines, receptors and bactericidal molecules contained in four main preformed granular stores: azurophilic (primary), specific (secondary) and gelatinase (tertiary) granules in addition to secretory (quaternary) vesicles listed from least to most readily released and the order in which they are formed in the BM during neutrophil maturation (**Fig. 1.2**) (Borregaard et al., 1996; Cowland and Borregaard, 2016). Transition between the resting and primed state is mediated by priming agents such as bacterial products, G-CSF, IL-8 (CXCL8) and various cytokines (e.g. TNF, interferon (IFN)-γ) (Hallett and Lloyds, 1995). Priming can occur within minutes and involves mobilisation of preformed receptors stored in granules such as cluster of differentiation molecule (CD)11b (i.e. α_M-subunit of the integrin macrophage-1 antigen (MAC-1)) and the integrin, lymphocyte function-associated antigen (LFA)-1, to the cell membrane. In addition, priming leads to activation of transcription factors such as NF-κB, that initiates *de novo* synthesis of receptor molecules and cytokines (Wright et al., 2010). Neutrophil priming can also occur following interaction with activated ECs and during TEM (Condliffe et al., 1998; Summers et al., 2010). Activation of neutrophils typically occurs at the site of their TEM, where they exert innate immune functions including the synthesis and release of chemokines

including CXCL1 and CXCL2 (human homologue known as CXCL8) and cytokines including IL-1β and TNF (Finsterbusch et al., 2014). Furthermore, neutrophils are able to secrete a variety of pro-permeability factors that reduce the integrity of the endothelial barrier (described in detail in section 1.4.3).

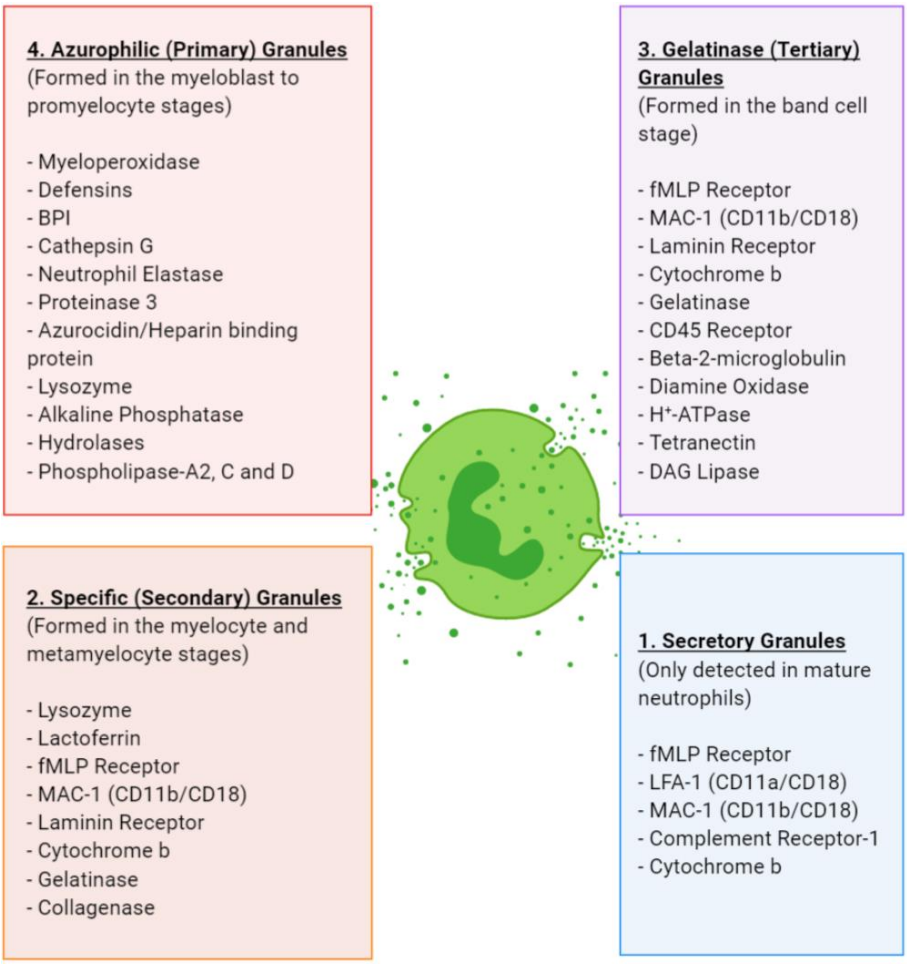

Figure 1.2. Neutrophil intracellular granules and their contents. Schematic detailing the principal four granular storage compartments of neutrophils, namely, azurophilic, specific, gelatinase, secretory and their key known contents. Secretory granules are the most readily released and the last to be stored during neutrophil maturation. Figure based on data summarised by Cowland & Borregaard 2016.

Neutrophils exhibit a diverse range of effector functions including phagocytosis of opsonised microbes, degranulation, intracellular killing, formation of neutrophil extracellular traps (NETs) and modulation of the adaptive immune response (Lacy, 2006; Wright et al., 2010). Most of these responses induce the production and/or release of toxic products such as oxygen-dependent ROS and degrading proteases into the environment, which have the potential to be harmful to the host tissue. It is therefore

critical that neutrophil migration and specialized cytotoxic neutrophil functions are tightly regulated (Thomas and Schroder, 2013). During oxygen dependent killing, bacteria opsonised with c-reactive protein (CRP), mannose-binding lectin (MBL) or surfactant proteins (SP)-A or D or *via* direct PAMP recognition, become engulfed by neutrophil formed pseudopodia and ingested into a phagosome. This phagosome then fuses with a lysosome to form a phagolysosome. The lysosome is a low pH environment, containing preformed products from primary and secondary granules such as anti-microbials (cathelicidins and defensins), hydrolytic enzymes (lysozyme and proteases) and oxidative species (ROS and NOS) (**Fig. 1.2**). ROS generation requires the enzyme nicotinamide adenine dinucleotide phosphate (NADPH) oxidase which converts oxygen to superoxide ion (O_2^-). Other ROS species such as hydrogen peroxide (H_2O_2) and hypochlorous acid (HClO) are further generated in the presence of the enzyme superoxide dismutase (SOD) and myeloperoxidase (MPO), respectively. In addition, ROS and other non-oxidative mediators, including NE and lysozyme, can be released from the cell *via* degranulation to kill extracellular pathogens (Borregaard et al., 1996). However, inappropriate or uncontrolled release of ROS can accumulate in the vascular bed where they can compromise the integrity of the endothelial barrier which subsequently results in enhanced tissue oedema. Neutrophils also have the capacity to release NETs *via* a process known as NETosis, which comprises an additional method of microbial entrapment and neutralisation (Papayannopoulos, 2018). This process firstly requires delobulation of the nucleus and disassembly of the nuclear envelope. Chromatin then decondenses and is released into the cytoplasm, where it forms a net-like structure. This 'net' is then released from the cell where it is then able to capture, immobilise and kill pathogens with antimicrobial peptides such as NE and MPO, calprotectin and defensins (Urban et al., 2009; Papayannopoulos, 2018).

Due to the plethora of neutrophil effector functions, a hypothesis has emerged suggesting the existence of neutrophil sub-populations, some with tissue specific functions beyond their generic elimination of inflammatory insults (**Fig. 1.3**) (Silvestre-Roig et al., 2016; Rosales, 2018; Ng et al., 2019). For example, in the mouse spleen, a neutrophil sub-population exhibiting a $CD62L^{low}$ (L-selectin), $CD11b^{high}$ and intercellular adhesion molecule (ICAM)-1^{high} phenotype has been shown to be important in the initiation of the adaptive immune response by releasing cytokines that mediate somatic

hypermutation and antibody (Ab) production by B-lymphocytes (Puga et al., 2012). Another sub-population of neutrophils identified in mice, exhibiting upregulated expression of the CC chemokine receptor (CCR)-7, LFA-1 and CXCR4, selectively migrates into lymph nodes during bacterial infection and to a lesser extent following sterile scratch injury of the skin, where they mediate activation of T-lymphocytes (Beauvillain et al., 2011; Hampton et al., 2015; Hampton and Chtanova, 2016). Interestingly, in LPS-challenged healthy human volunteers, a distinct subset of neutrophils defined by their $CD11c^{high}$, $CD11b^{high}$, $CD16^{high}$ and $CD62L^{low}$ surface expression profile, were found to suppress T-cell proliferation in a ROS- and CD11b-dependent manner (Pillay et al., 2010, 2012). Further, in mice and humans, it is thought that a $CD49d^{high}$, $CXCR4^{high}$ and VEGF-receptor 1^{high} (VEGFR1) neutrophil sub-population plays a role in mediating angiogenesis under hypoxia conditions (Massena et al., 2015) and in promoting tumour vascularisation (Jablonska et al., 2010). Indeed, the role of neutrophils in cancer is a complex and developing area of research. During cancer, neutrophils are capable of exhibiting different phenotypes, including their stage of maturation, tumour cytotoxicity and immune suppression, which are influenced by the type of cancer and the stage of tumour advancement. For example, Sagiv et al., identified in humans and mice, two distinct neutrophil subsets that were classified as high density- (HDN) and low density-neutrophils (LDN) (Sagiv et al., 2015). Whilst HDNs comprised solely of mature neutrophils, LDNs encompassed both mature and immature neutrophils with impaired neutrophil functions. Of these, LDNs were preferentially upregulated in cancer and were derived from HDN populations in the blood *via* stimulation with TGF-β, or directly from immature granulocyte pools in the BM (Sagiv et al., 2015). Following migration into tumour sites, thereby becoming known as "tumour-associated neutrophils" (TANs), HDN and LDN subpopulations have been associated with cytotoxic (i.e. anti-tumour, known as N1) and immunosuppressive (i.e. pro-tumour, known as N2) functions, respectively (Rosales, 2018). However, our understanding of neutrophil sub-populations still remains in its infancy and there is no consensus on precisely what defines a distinct and true neutrophil subset, whereby subsets have been defined by their tissue localisation, maturation state, phenotype and effector functions. On this basis, these sub-populations may even include neutrophils that exhibit varying modes of migrational motility during inflammation, a concept further explored in section 1.7 (Németh et al., 2020). Others have suggested that true subsets should be defined by transcriptional

and/or epigenetic profiles to avoid cases of mistaken identity (Ng et al., 2019). For example, it has also been noted that many of the aforementioned sub-populations share many of the phenotypic differences identified between young and “aged” neutrophils in the circulation, whereby the latter exhibit greater expression of CXCR4, ICAM-1, CD11b, VLA-4 and decreased expression of CD62L and CXCR2 (**Fig. 1.3**) (Rosales, 2018).

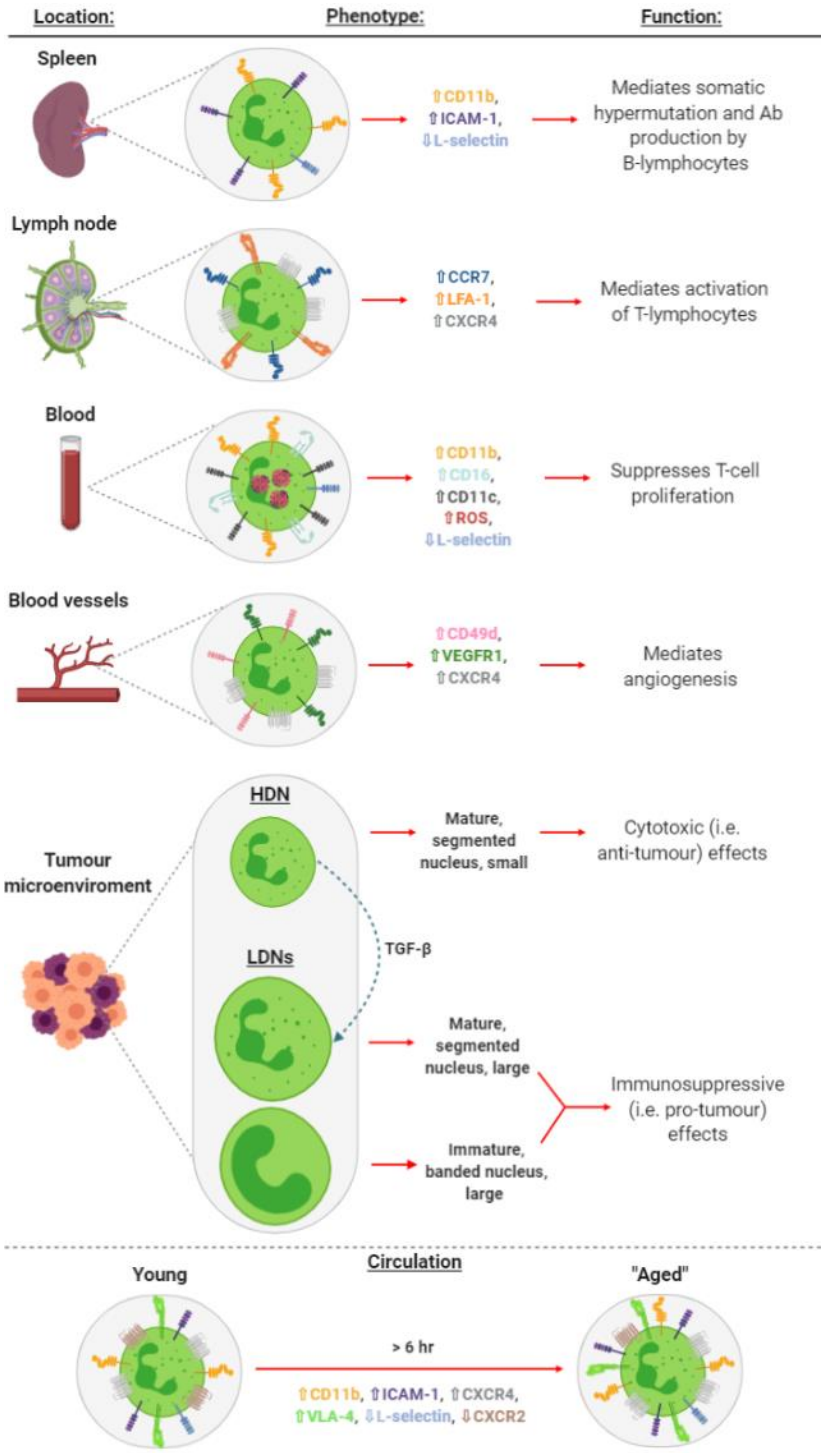

Figure 1.3. Schematic summarising neutrophil sub-populations. During infection or stimulation by LPS, the first three neutrophil subsets have been found to modulate the innate immune system *via* B- (spleen) and T-lymphocyte (lymph nodes) activation, or suppression of T-cell proliferation (cells isolated from the blood, *in vitro*). In addition, a phenotypically unique neutrophil subset has been identified in hypoxic tissue where it mediates angiogenesis. At least three additional subsets, collectively categorised as either HDNs or LDNs, are known to mediate immune responses during tumourigenesis. Although to what extent these neutrophils represent true sub-populations (i.e. are destined for their stated roles) as opposed to a product of their surroundings or their natural aging whereby distinct phenotypic changes have been observed between “young” and “aged” circulating neutrophils remains unclear.

At the end of their life, neutrophils in the tissue undergo apoptosis followed by monocyte-, macrophage- and dendritic cell-mediated phagocytosis (Summers et al., 2010; Lim et al., 2020). Furthermore, phagocytosis of dead neutrophils also results in reduction of macrophage derived IL-23, which in turn reduces IL-17 and G-CSF production resulting in reduced granulopoiesis (Stark et al., 2005; Rosales, 2018). In contrast, "aged" neutrophils (i.e. those present in the blood for >6 hrs) in the blood upregulate expression of CXCR4 allowing them to return to the BM for clearance by stromal macrophages (Rosales, 2018).

1.4. The Endothelial barrier and vascular permeability

The vasculature is an essential structure that maintains hydrostatic pressure, ensures a continuous and efficient supply of oxygen, nutrients, and fluids to tissues, and controls immune cell migration during inflammation (Claesson-Welsh, 2015). There are 5 main types of blood vessels: arteries, arterioles, capillaries, venules and veins. This thesis is mainly concerned with post-capillary venules that connect capillaries and veins and are the chief site of leukocyte migration and vascular leakage during inflammation. The vascular barrier of post-capillary venules is composed of a single, semi-permeable layer of cobblestone-like ECs surrounded by a thin basement membrane and pericyte layer. ECs, in particular, are the first and primary barrier to transmigrating leukocytes. Individual ECs are anchored to each other through transmembrane junctional molecules that are classically divided into three key groups: gap junctions, tight junctions and adherens junctions (Matter and Balda, 2003; Lampugnani, 2012).

Gap junctions are comprised of the transmembrane proteins, connexins, that aggregate to form hexameric structures known as connexons. These semi-permeable structures form channels between adjacent ECs allowing for intercellular communication by permitting the passage of small molecules, such as Ca^{2+} ions, amino acids and nucleotides (Okamoto and Suzuki, 2017). Tight junctions predominantly consist of protein complexes including claudin and occludin transmembrane proteins, members of the junctional adhesion molecule (JAM) family, endothelial cell-selective adhesion molecule (ESAM) and intracellular adapters such as ZO-1 and ZO-2 (Matter and Balda,

2003). Adherens junctions are predominantly populated by molecules of the cadherin family, in particular, VE-cadherin; a cornerstone molecule in both vascular permeability and neutrophil TEM (**Fig. 1.4**). Although tight junctional molecules are often depicted to be located in closer proximity to the apical side, and adherens molecules closer to the basolateral side, both are in fact distributed throughout the EC junction (Dejana, 2004; Duong and Vestweber, 2020). Collectively, these proteins play a fundamental role in junctional stabilization, through their anchorage to the EC actin cytoskeleton, and in the regulation of endothelial permeability. Of note, other adhesion molecules expressed at EC junctions include platelet endothelial cell adhesion molecule-1 (PECAM-1, also known as CD31) and CD99 which are detailed in section 1.5.3.1.

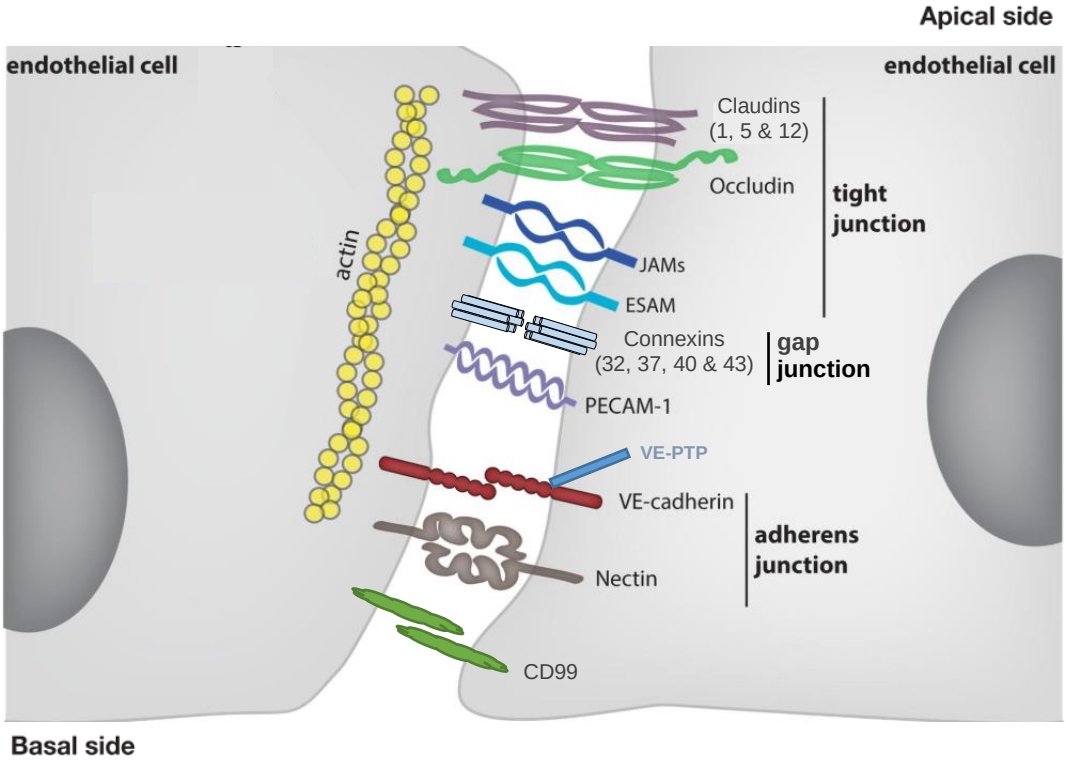

Figure 1.4. Schematic illustrating the fundamental EC junctional structures required to maintain the integrity of the endothelium. ECs are anchored together by gap (connexins)-, tight (claudins, occludin, JAMs & ESAM)- and adherens (VE-cadherin & nectin)-junctional proteins that form intercellular homophilic interactions between adjacent ECs. Stability of the endothelial barrier is maintained *via* anchorage of these paracellular junctional molecules to the EC actin cytoskeleton. Key molecules, including JAMs, ESAM, PECAM-1, VE-cadherin and CD99, play essential roles in controlling vascular permeability and neutrophil migration responses. Figure adapted from Duong & Vestweber 2020.

Under basal conditions, only molecules under 40 kDa can freely diffuse across the EC barrier (known as plasma *filtrate*) (Nagy et al., 2008). Passage of larger molecules

however requires active disruption of the EC barrier e.g. by the pro-permeability agent histamine, whereby molecules as large as 2,000 kDa are able to move through EC junctions (known as plasma *exudate*) (Egawa et al., 2013). Vascular hyper-permeability is a hallmark response during acute inflammation and functions to supply damaged and infected tissues with essential blood-borne immunoregulatory and pro-inflammatory proteins (e.g. immunoglobulins and components of the complement cascade). Overtime, these plasma proteins and fluids are drained by the tissue lymphatics. The lymphatics have a slow filtration rate of the interstitial tissue to ensure sufficient availability of nutrients and signalling molecules, including various hormones and cytokines, to the cells present within the tissue (Randolph et al., 2017). However, when the endothelial integrity is severely disrupted, plasma leakage through the endothelium occurs at a rate exceeding the capacity of the tissue lymphatics to drain the excess fluid, resulting in tissue oedema (Bates and Harper, 2002; Randolph et al., 2017).

In addition to histamine, vascular permeability can be modulated by various factors including bradykinin, substance P, ROS, TNF and VEGF. Although many of these factors result in the destabilisation of EC junctions and/or induction of EC vesicular transcytosis, leakage can also be indirectly modulated through induction of vasodilation, resulting in changes in blood pressure and thus flow rate. There are two pathways by which hyper-vascular permeability can occur: transcellular or paracellular (**Fig. 1.5**).

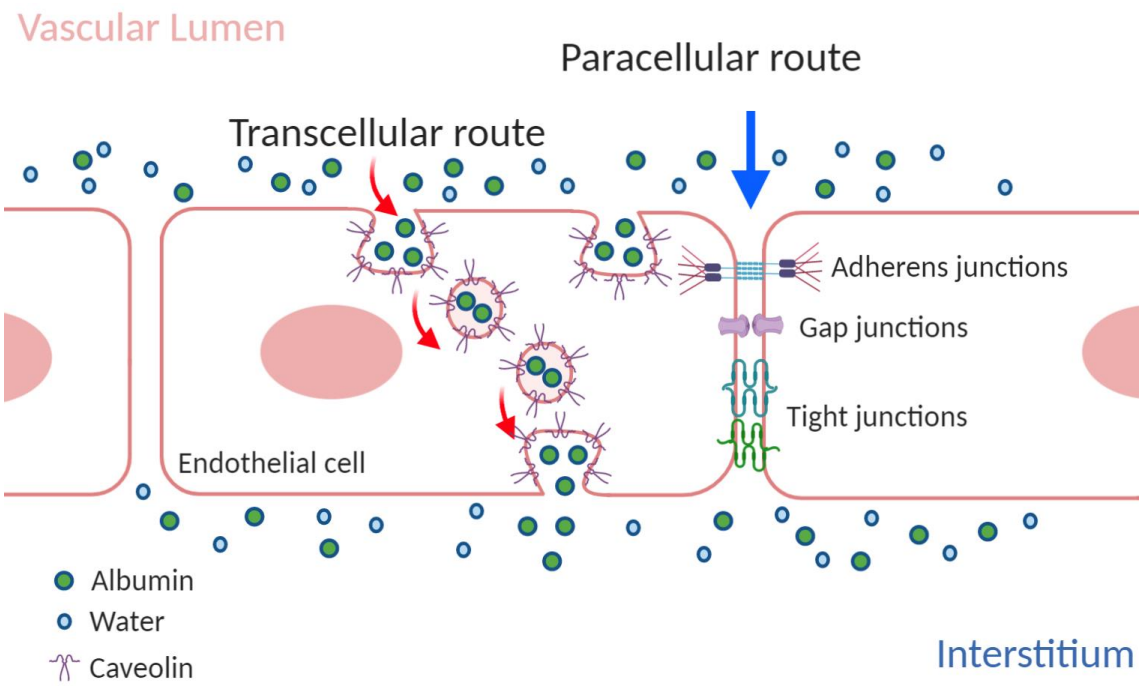

Figure 1.5. Schematic depicting endothelial para- and trans-cellular permeability routes. Under basal conditions, the endothelial layer tightly regulates the exchange of plasma- and tissue-bound solutes and fluids. Under certain inflammatory conditions (e.g. IR-injury), the endothelial barrier becomes compromised and more permeable allowing for greater passage of fluid from the blood into the tissue. EC permeability can occur by two key routes, either paracellularly or transcellularly. Paracellular leakage is associated with reduced/loosened EC-EC contact following internalisation of junctional adhesion proteins such as VE-cadherin and exertion of intracellular pulling forces on the EC membrane, which can in some tissues form fenestrate structures. Transcellular leakage is mediated by the formation of an EC 'pinch', that is then released as a vesicle into the cytoplasm and trafficked across the EC.

1.4.1. Transcellular endothelial permeability

Transcellular vascular permeability involves the formation of vesiculo-vascular organelles (VVO), whereby vesicles or vacuoles are formed at the endothelial membrane. These structures transport solutes and proteins from the apical (luminal) to basolateral (abluminal) side, through the EC body. The current understanding of VVO transcytosis is in its infancy, but it is thought to primarily support the movement of larger macromolecules unable to move through the paracellular junctions. This transport route has been shown to occur in normal, inflamed and tumour supplying vasculature (Caruso et al., 2001; Dvorak and Feng, 2001). During this process, caveolae form within regions of the plasma membrane by establishing a 'pinch', which is then released as a vesicle

into the cytoplasm. The vesicle is then trafficked across the body of the cell to the basolateral side where it fuses with the plasma membrane and its contents are released into the perivascular space (**Fig. 1.5**). However, whether VVOs originate from caveolae remains contentious. For example, caveolin-1 (a major caveolae protein) null mice exhibit a reduction in vascular leakage but have a similar frequency of VVO formation. This suggests VVOs may not be derived from caveolae and thus highlights a need for further investigation (Schubert et al., 2001; Chang et al., 2009). The difficulty in studying the origin of VVOs is primarily due to a lack of suitable loss-of-function mouse models, in addition to the technical limitation that VVOs cannot be studied by conventional light microscopy (Claesson-Welsh, 2015).

1.4.2. Paracellular endothelial permeability

The most comprehensively studied and primary route of enhanced vascular leakage occurs paracellularly, through EC junctions. Here, endothelial integrity is maintained by a dynamic combination of adherens and tight junctional molecules, the distribution of which can vary between different vascular beds. For example, in the BBB where vascular leakage is more tightly controlled, EC junctions are primarily populated by tight junction molecules to minimise leakage into the parenchymal space. However, in the majority of vascular beds, adherens junctions provide a semi-permeable barrier and comprise the 'gatekeepers' that govern controlled vascular leakage (Claesson-Welsh, 2015). One of the most fundamental junctional molecules in regulating vascular permeability is VE-cadherin (**Fig. 1.6**). The extracellular domain of this adherens molecule forms homophilic cis dimers that then form trans dimers with the adjacent EC (Sidibé and Imhof, 2014; Dejana and Orsenigo, 2013). Stability of VE-cadherin is determined by recruitment of γ-, β- & p120- catenin to the cytosolic tail. These, in turn, connect to the EC actin cytoskeleton through the actin binding proteins α-catenin, vinculin and eplin (Gavard, 2014). In addition, γ-catenin is involved in maintaining the association between VE-cadherin and the transmembrane protein, vascular endothelial protein tyrosine phosphatase (VE-PTP), which supports the stability of VE-cadherin at the junction by sequestering tyrosine-induced phosphorylation (Nottebaum et al., 2008; Gavard, 2014). p120-catenin is also particularly important in maintaining VE-cadherin junctional

stability through associations with α-catenin, however rescue of VE-cadherin stability in p120 KO mice still leads to reduced endothelial integrity (Herron et al., 2011). This suggests a wider role for p120-catenin which remains largely unexplored. However, following ligation of pro-permeability factors such as VEGF, histamine and/or TNF to their cognate receptors, this interactome becomes destabilised, culminating in internalisation of VE-cadherin and induction of vascular leakage. This follows the dissociation of VE-PTP from VE-cadherin, which occurs within 5 min of ligand binding (Nottebaum et al., 2008), and subsequent hyperphosphorylation of tyrosine residues Y658 and Y685, the latter being further discussed in Chapter 4 (Sukriti et al., 2014). Of note, dephosphorylation of another VE-Cadherin residue, Y731, has been shown to lead to enhanced leukocyte migration as discussed in section 1.5.3.1 (Potter et al., 2005; Wessel et al., 2014). Phosphorylation of these specific tyrosine residues can lead to augmented interactions with associated catenins. For example, phosphorylation of the residue Y658 leads to dissociation from p120-catenin, leading to endocytosis of VE-cadherin *via* the formation of clathrin-coated vesicles, which results in destabilisation of the EC junction (Potter et al., 2005). However, receptor dissolution at the junction is transient, whereby VE-cadherin re-establishes at the membrane within 15 min post cessation of stimulus application (Gaudry et al., 1997), known in part to be due to rapid recycling of the receptor (Fukuhra et al., 2006; Orsenigo et al., 2012). In addition, EC integrity can be compromised following influx of Ca^{2+} ions and by activation of small GTPases, namely RhoA, Rac and CDC42, that lead to the phosphorylation of myosin light chains (MLC) (Wojciak-Stothard and Ridley, 2002). Consequently, catenin mediated contraction of actomyosin stress fibres occurs, which in turn leads to pulling forces exerted on the EC membrane. Ultimately, this directly disrupts the intercellular adhesion contacts and induces vascular permeability (Qiang et al., 2009; Azzi et al., 2013). Under basal conditions, activation of RhoA is inhibited by the key junctional-stabilising transmembrane tyrosine kinase receptor, Tie-2 (Frye et al., 2015). Tie-2 activates the GTPases, Rac-1 and Rap-1, which prevent phosphorylation of MLCs and subsequent dissolution of actomyosin stress fibres, thus preventing their contractility; a function which is compromised following VE-PTP-dependent de-phosphorylation as induced by pro-permeability agents (Winderlich et al., 2009; Frye et al., 2015).

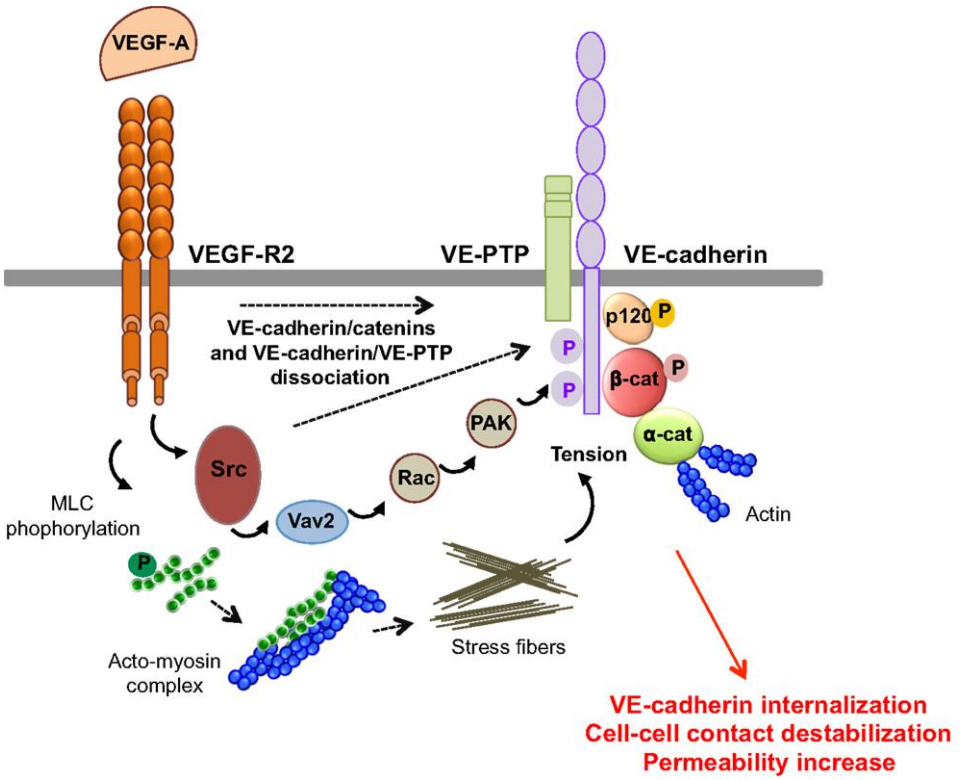

Figure 1.6. Regulation of VE-cadherin internalisation at EC junctions to induce vascular permeability. VE-cadherin is expressed at the EC junction and plays a vital role in maintaining EC-EC contact and the integrity of the vascular barrier. However, following ligation of a pro-permeability mediator such VEGF (as depicted) or other factors including TNF and histamine to their EC-expressed cognate receptors, VE-PTP dissociates from VE-cadherin, allowing for Src-dependent phosphorylation of specific VE-cadherin intracellular residues, Y658 and Y685, and its binding partners β- and p120-catenin, and MLCs. Downstream, this leads to VE-cadherin internalisation, in addition to, contraction of stress fibres that exert a physical pulling force on the EC junctional membrane. Collectively, this leads to weakening of EC contacts and compromised junctional integrity, culminating in enhanced vascular permeability. Adapted from Azzi et al., 2013.

The role of the EC actin cytoskeleton is a growing area of interest. Apart from loosening EC contacts during inflammation, these structures can support the formation of endothelial *fenestrae* that permit greater vascular leakage and are commonly found in specialised organs, e.g. organs that require rapid transport of hormones such as glandular tissue, liver, pancreas and kidneys (Caruso et al., 2001). Fenestrae consist of circular pores that form in extremely thin, attenuated regions of ECs. There is some evidence to suggest that these structures may also form in capillaries of the cremaster muscle and the skin following VEGF (but interestingly, not histamine) stimulation (Roberts and Palade, 1995). Despite these observations, endothelial fenestration in the

cremasteric vasculature (as is relevant to this thesis) is seldom reported and hence is not expected to significantly contribute to vascular permeability in acute inflammation.

1.4.3. Impact of neutrophils on vascular leakage during acute inflammation

Vascular permeability and neutrophil migration are key elements of acute inflammation. Although, these phenomena have predominantly been identified to occur independently, as supported by distinct molecular pathways (Vestweber, 2015) (as discussed in Chapter 3), once recruited to the site of inflammation, activated neutrophils can contribute to the induction of enhanced microvascular leakage (Wedmore and Williams, 1981; DiStasi and Ley, 2009). In this regard, several studies have reported that neutrophils can generate and release vasoactive mediators such as ROS (Segal and Jones, 1978), VEGF (Scapini et al., 2004), LTA_4 (DiStasi and Ley, 2009), HBP (Kenne et al., 2019) and TNF (Finsterbusch et al., 2014), at the site of their transmigration. Some of these mediators are preformed and stored in intracellular neutrophil granules (Beil et al., 1995; Borregaard et al., 1996) and hence can be rapidly mobilised to the cell membrane for release upon priming/activation. Other factors, such as ROS for example, are exclusively synthesised *de novo* and released by neutrophils upon their adhesion to the endothelium where it is then taken up by ECs leading to downstream activation of pro-permeability signalling pathways (Di et al., 2016). The majority of neutrophil-derived pro-permeability mediators require ligation to their cognate receptors to directly and/or indirectly induce complementary signalling pathways. Of note, the mechanism and role of neutrophil-derived TNF is not completely understood, an issue addressed and discussed in Chapter 6. Better understood pathways include the role of the lipid LTA_4. Specifically, following neutrophil activation post adhesion to the EC surface, LTA_4 is released by neutrophils where it can be converted to LTB_4 by neutrophils (autocrine) or LTC_4 by ECs (paracrine) (Folco and Murphy, 2006; Di Gennaro et al., 2009). Whilst LTC_4 acts directly on ECs to induce endothelial permeability *via* a Rho kinase-dependent build-up of ROS and Ca^{2+} influx (leading to EC contractility) (Duah et al., 2013), LTB_4 acts indirectly in a neutrophil-dependent manner (Bjork et al., 1982). Here, ligation of LTB_4 to its cognate receptor on the neutrophil surface initiates the release of HBP, a critical mediator of neutrophil-induced permeability (Gautam et al., 2001), from secretory

granules. In the blood, HBP binds to EC surface proteoglycans and becomes internalised where it proceeds (*via* unknown signalling pathways) to induce an influx of Ca^{2+} and actomyosin contractility (Di Gennaro et al., 2009).

The interplay between vascular leakage and neutrophil migration remains a subject of keen interest. However, whilst there is ample evidence identifying neutrophil-mediated mechanisms of vascular leakage, the impact of microvascular leakage on leukocyte migration has been minimally investigated. For instance, histamine, a mediator classically defined by its function to induce vascular permeability, has been suggested to promote neutrophil adhesion and TEM (Massena, 2015). This however remains contentious, as many reports have shown histamine only impacts neutrophil rolling following mobilisation of preformed P-selectin from Weibel-Palade bodies (WPBs) to the EC surface, a key molecule implicated in leukocyte rolling (Jones et al., 1993; Ley, 1994; Yamaki et al., 1998). Similarly, mice deficient in Akt1, a vital serine/threonine protein kinase implicated in enhancing endothelial permeability, exhibited both a reduction in vascular permeability and neutrophil infiltration (Di Lorenzo et al., 2009), supporting the concept that vascular leakage may impact neutrophil migration. Hence, our understanding as whether microvascular leakage itself could impact neutrophil behaviour requires further exploration. This subject underpins the direction of this thesis, and hence requires an appreciation of the mechanisms of neutrophil recruitment and migration during inflammation.

1.5. The Leukocyte adhesion cascade

Under homeostatic conditions ECs maintain the integrity of the EC barrier *via* strict regulation in the expression and distribution of endothelial surface and junctional molecules (i.e. adhesion molecules) that are known to facilitate leukocyte recruitment and TEM. Following tissue damage or infection, DAMPs or PAMPs respectively, trigger downstream signalling to induce generation and/or release of cytokines and chemoattractants such as chemokines (e.g. CXCL1) by resident tissue and immune cells (Table 1.1), and elicit expression of EC surface adhesion molecules (Zindel and Kubes,

2020) (Table 1.2). Collectively these events lead to the recruitment of leukocytes from the blood circulation (Kolaczkowska and Kubes, 2013).

Table 1.1. Chemokines and cytokines involved in neutrophil recruitment and tissue infiltration during inflammation in the murine system (non-exhaustive list).

Molecule	Cell Source	Complementary Receptor	Functions	Reference
CXCL1	Pericytes, ECs, macrophages	CXCR2, GAGs, ACKR1	Mediates neutrophil adhesion and crawling	(Pruenster et al., 2009; Novitzky-Basso and Rot, 2012; Thiriot et al., 2017; Girbl et al., 2018)
CXCL2	Macrophages, monocytes, and neutrophils	CXCR2, GAGs, ACKR1	Mediates neutrophil TEM	(Pruenster et al., 2009; Novitzky-Basso and Rot, 2012; Thiriot et al., 2017; Girbl et al., 2018)
CXCL3	Platelets	CXCR2	Regulates bioavailability of CXCL1 and CXCL2 *via* competitive binding to ACKR1 and GAGs. Mediates neutrophil tissue infiltration during viral infection	(Sokulsky et al., 2020)
CXCL5	Platelets, Epithelial cells (in the lung)	CXCR2, GAGs, ACKR1	Regulates bioavailability of CXCL1 and CXCL2 *via* competitive binding to ACKR1 and GAGs. Mediates neutrophil tissue infiltration, particularly in the lungs	(Koltsova and Ley, 2010; Newton and Dixit, 2012; Su and Richmond, 2015)
CCL2	Macrophages, monocytes and dendritic cells	CCR2	Indirectly mediates neutrophil recruitment by inducing synthesis of chemoattractants such as LTB_4	(Reichel et al., 2009; Newton and Dixit, 2012; Su and Richmond, 2015)
CCL5 (RANTES)	Platelets, neutrophils	CCR5	Mediates neutrophil recruitment and activation	Tecchio et al., 2014; Yu et al., 2016; Pitchford et al., 2017)

TNF	Macrophages, monocytes, T-cells, neutrophils and ECs	TNFRI & TNFRII	In the acute phase, TNF induces the NF-kB pathway, particularly in ECs, resulting in upregulation of pro-inflammatory mediators including: ICAM-1, VCAM-1 and E-selectin, LTB_4, IL-1β, IL-6, CXCL1, CXCL2, CCL5 and nitric oxide. The net result is enhanced leukocyte recruitment, migration and vasodilation	(Carswell et al., 1975; Yang, 2005; Zhou et al., 2008; Flemming et al., 2015)
IL-1β	Macrophages, ECs	IL-1R	Pro-inflammatory mediator and potent inducer of NF-kB pathway. Induces neutrophil recruitment and neutrophil activation at the site of inflammation	(Prince et al., 2004; Biondo et al., 2014; Dinarello, 2018; Fahey and Doyle, 2019)
IL-6	ECs, neutrophils	IL-6Rα & gp130	Pro-inflammatory cytokine that indirectly mediates during TEM *via* induction of CXCL1 synthesis	(Fielding et al., 2008; Dinarello, 2018; Fahey and Doyle, 2019)

Once attracted to the site of insult, leukocytes undergo several steps, collectively described by the leukocyte adhesion cascade that culminates in leukocyte TEM into the tissue (**Fig. 1.7**) (Ley et al., 2007; Muller, 2013). As the focus of this thesis is on neutrophil trafficking, the steps involved in neutrophil breaching of venular walls are described below.

The leukocyte adhesion cascade is a tightly regulated process whereby neutrophils exhibit a number of luminal interactions with activated ECs, beginning with tethering and rolling of the neutrophils along the luminal surface of the endothelium. This is followed by neutrophil crawling, arrest and eventually TEM to exit the venular lumen. Beyond the endothelium, neutrophils exhibit abluminal motility and passage through the basement membrane and the pericyte layer prior to their entry into the interstitial tissue (**Fig. 1.7**). Over the past decade, our understanding of the leukocyte adhesion cascade has been accelerated in part due to development of confocal and fluorescent

microscopy techniques utilising reporter mice expressing EGFP specifically in neutrophils (Clausen et al., 1999; Stackowicz et al., 2020).

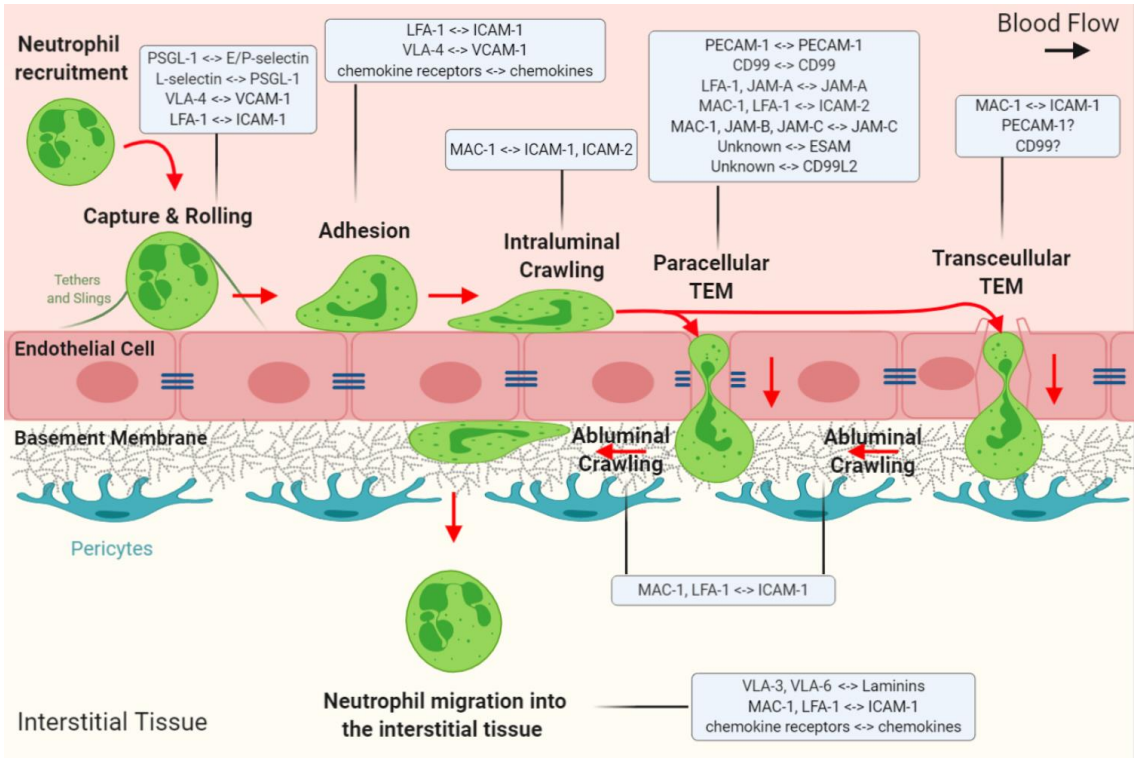

Figure 1.7. The leukocyte adhesion cascade. The cascade constitutes several key steps: leukocyte capture, rolling, adhesion (strengthening and spreading), intraluminal crawling and TEM. During neutrophil capture and rolling, tethers and slings operate to facilitate selectin-mediated weak and temporary holds on the EC surface. Integrins and chemokines mediate the transition towards neutrophil adhesion and crawling, before EC junctional molecules facilitate neutrophils to migrate through the EC barrier in either a para- or transcellular manner. Neutrophils then crawl on the abluminal EC surface before migrating through the basement membrane and pericyte layer to reach the inflamed site in the interstitial tissue. Key molecules involved at each step are depicted in boxes. '?' indicate molecules with suspected but unproven involvement. Adapted from Ley et al., 2007, Voisin et al., 2013 and Vestweber et al., 2015.

Table 1.2. Key endothelial cell adhesion receptors involved in the neutrophil adhesion cascade (Table adapted from Vestweber et al., 2015)*

Receptor/ Molecule	Neutrophil Ligand(s)	Endothelial Ligand(s)	Functions	Reference
E-selectin	PSGL-1, HCAM, ESL-1	None	Capture and rolling of neutrophils, and triggering integrin activation	(McEver, 2015; Vestweber and Blanks, 1999; Abram and Lowell, 2013; Kotovuori et al., 1993; Hidalgo et al., 2007)
P-selectin	PSGL-1, HCAM	None	Capture and rolling of neutrophils, and	(McEver, 2015; Vestweber and Blanks,

			triggering integrin activation	1999; Abram and Lowell, 2013)
PSGL-1	L-selectin	None	Capture and rolling of neutrophils, and triggering integrin activation	(Rosen, 2004; Martins et al., 2007)
ICAM-1	LFA-1, MAC-1	None	Rolling, adhesion and crawling of neutrophils, and triggering VE-cadherin phosphorylation	(Van Buul et al., 2007; Barreiro et al., 2002; Carman and Springer, 2004)
ICAM-2	LFA-1, MAC-1	None	Neutrophil crawling and initiation of diapedesis	(Halai et al., 2014; Woodfin et al., 2009)
VCAM-1	VLA-4	None	Rolling, adhesion and crawling of neutrophils, and triggering VE-cadherin phosphorylation	(Van Buul et al., 2007; Barreiro et al., 2002; Carman and Springer, 2004)
JAM-A	LFA-1	JAM-A	Neutrophil diapedesis	(Nourshargh et al., 2006; Ostermann et al., 2002; Martìn-Padura et al., 1998; Schmitt et al., 2014)
JAM-B	VLA-4 (in combination with JAM-C)	JAM-B, JAM-C	Unknown	(Cunningham et al., 2002; Aurrand-Lions et al., 2005)
JAM-C	MAC-1	JAM-B, JAM-C	Prevents reverse transmigration of neutrophils	(Woodfin et al., 2011; Aurrand-Lions et al., 2005; Colom et al., 2015)
ESAM	Unknown	ESAM	Neutrophil diapedesis and supporting the induction of increased permeability	(Wegmann et al., 2006; Nasdala et al., 2002)
PECAM-1	PECAM-1	PECAM-1	Triggering the LBRC in ECs; supports disconnection of neutrophils from ECs and their passage through the basement membrane	(Muller, 1995; Nourshargh et al., 2006; Mamdouh et al., 2003)
CD99	CD99	CD99	Triggering the LBRC in ECs; supports disconnection of neutrophils from ECs and their passage through	(Schenkel et al., 2002; Bixel et al., 2007; Lou et al., 2007; Dufour et al., 2008)

			the basement membrane	
CD99L2	Possibly CD99L2	CD99L2	Supports neutrophil disconnection from ECs and passage through the basement membrane	(Bixel et al., 2007; Schenkel et al., 2007; Seelige et al., 2013)
VE-cadherin	None	VE-cadherin	EC junctional barrier and prevention of neutrophils diapedesis	(Gotsch et al., 1997; Schulte et al., 2011; Wessel et al., 2014)

*Neutrophil transmigration is a highly complex process and this table does not represent an exhaustive list of the relevant receptor/ligand pairs.

1.5.1. Neutrophil capture and rolling

The first stage of the leukocyte adhesion cascade following neutrophil recruitment is their capture and rolling along the endothelium. These responses are mediated by two key factors: the physical hydrodynamic forces exerted by the blood flow on the neutrophil and the surface molecules expressed by both neutrophils and on the apical EC membrane (see Table 1.2). Capture of neutrophils is predominately facilitated *via* the expression of various glycoproteins, principally selectins, including the highly conserved L- E- and P-selectins (Kansas, 1996), while rolling is mediated primarily by selectin- but also to a lesser extent, integrin-interactions.

L-selectin is mainly expressed by leukocytes and is the principal selectin required for their capture on ECs (Rosen, 2004). P-selectin can be both newly synthesised and mobilised to the EC surface from intracellular WPBs stores, upon pro-inflammatory stimulation (Huo et al., 2003; Hidalgo et al., 2007). E-selectin expression however, requires *de novo* synthesis by activated EC, a response that peaks after 4-6 hr.

Selectins predominantly interact with P-selectin glycoprotein ligand-1 (PSGL-1) that is expressed on ECs and neutrophils (Table 1.2). During inflammation, PSGL-1 undergoes post-translational modification known as glycosylation (Rosen, 2004; Martins et al., 2007; Sperandio et al., 2009) that appends the tetrasaccharide carbohydrate, sulphated-

siayl-Lewis^{x} region; an essential domain that enhances the binding capacity of PSGL-1 to the lectin-binding domain (LBD) of the selectin (Bevilacqua and Nelson, 1993; Zarbock et al., 2011). Of note, selectins can form additional interactions with homing cell adhesion molecule (HCAM, also known as CD44) and E-selectin ligand-1 (ESL-1) expressed by neutrophils (refer to Table 1.2). In the blood, these interactions are initiated by a pushing force exerted on neutrophils away from the centre of the vessel where the hydrodynamic velocity is greatest, and towards the vascular wall where the hydrodynamic velocity is lower. Here, under conditions of high shear stress (i.e. close to the EC wall), neutrophils extend cell membrane protrusions termed 'tethers', which contain PSGL-1 and L-selectin rich domains (Alon et al., 1997; Ramachandran et al., 2004). At the vascular wall, neutrophil PSGL-1-decorated membrane tethers caress the endothelial surface and bind EC expressed P- and E-selectin, while L-selectin expressed by neutrophils interacts with EC-bound PSGL-1 (Sundd et al., 2012, 2013). These tethers constitute a weak and temporary capture of the neutrophil to the endothelium. However, as the hydrodynamic velocity is greater nearer the luminal facing edge of the neutrophil (i.e. closest to the centre of the vascular lumen), a hydrodynamic 'drag' is generated which causes the neutrophil to roll along the endothelium in the direction of blood flow. This rolling behaviour manifests as a continuous breaking of 'backend' PSGL-1 – P-/E-/L-selectin tethers which then swing around to the 'front end' of the cell to form new sling-like interactions with the endothelium (Sundd et al., 2012, 2013).

The importance of selectins in mediating neutrophil rolling has been shown through the use of selectin KO mice. In the context of bacterial mediated inflammation, P- and E-selectin KO mice all exhibited poor rolling capabilities and consequently neutrophil extravasation and thus had a greater susceptibility to infection (Mayadas et al., 1993; Bullard et al., 1996; Frenette et al., 1996). Likewise, L-selectin null mice exhibited poor neutrophil recruitment and tissue infiltration responses (Arbonés et al., 1994; Tedder et al., 1995). Similar responses are presented in human disease, such as leukocyte adhesion deficiency II, where patients often suffer from recurring infections. This occurs due to a defect in fucosyl transferases (or other related enzymes) that leads to a reduced capacity to form the sulphated-siayl-Lewis^{x}, which renders the selectins non-functional (Becker and Lowe, 1999).

During rolling, selectin-PSGL-1 interactions also facilitate the establishment of integrin-mediated attachments that stabilise the rolling phase and extend the lifetime of selectin-ligand bonds. This occurs *via* upregulation of several signalling pathways e.g. activation of the intracellular neutrophil p38 mitogen-activated protein kinase (p38-MAPK) pathway, which leads to conformational changes in neutrophil surface expressed LFA-1, resulting in a higher-avidity for EC-expressed ICAM-1 (Sigal et al., 2000; Simon et al., 2000). Neutrophil rolling is further supported by additional interactions between neutrophil-derived integrins VLA-4 and LFA-1 and EC surface VCAM-1 and ICAM-1 (see Table 1.2) (Giagulli et al., 2006; Rullo et al., 2012). Both selectin and integrin interactions are concomitantly supported by flattening of leukocytes, which not only reduces the hydrodynamic forces exerted on the cell, but also increases the physical footprint of the cell, a phenomenon that further strengthens neutrophil-EC interactions (Sundd et al., 2012). Collectively, these interactions result in slower rolling of the neutrophil and facilitate the transition to firm adhesion as discussed in more detail below.

1.5.2. Neutrophil adhesion and luminal crawling

Neutrophil adhesion and crawling are fundamentally mediated by chemokine and integrin signalling. Cell flattening enhances the exposure of the neutrophil surface to EC-derived chemokines (Table 1.1) and integrins (Nourshargh and Alon, 2014). Chemokines play an essential role in transitioning a predominantly selectin mediated process to an integrin supported response. Specifically, CXC chemokines such as CXCL8 and its murine homologues CXCL1, 2 and 5 (defined by their glutamine-leucine-arginine (ELR) motif adjacent to the cysteine residue) are particularly important in mediating neutrophil firm adhesion and intra-luminal crawling. Neutrophils are able to detect these chemokines *via* surface G-protein coupled receptors (GPCR), primarily CXCR2 (Olson and Ley, 2002).

During an inflammatory insult, these chemokines are produced by a variety of tissue resident cells (e.g. macrophages, pericytes and ECs) and recruited leukocytes, including neutrophils. Activated ECs have the capacity to traffic chemokines originating from the interstitial tissue from their abluminal- to luminal-surface *via* transcytosis. For example, the atypical chemokine receptor 1 (ACKR1), known to be expressed by RBCs and ECs,

can actively bind, retain and transcytose chemokines across the EC body, where they are then presented to immune cells such as neutrophils (Rot, 2010). Together, chemokines are predominantly retained and presented to neutrophils by glycosaminoglycans (GAGs) of the endothelial glycocalyx, a hydrated continuous surface of carbohydrates on the luminal side of the blood vessel (Reitsma et al., 2007; Proudfoot et al., 2017; Uchimido et al., 2019) and by ACKR1 at EC junctions (Pruenster et al., 2009; Novitzky-Basso and Rot, 2012; Thiriot et al., 2017; Girbl et al., 2018). Precise presentation of chemokines in this manner facilitates neutrophil adhesion, intraluminal crawling and sensing of sites along the endothelium for TEM to occur (Proudfoot, 2015). How these chemokines are presented to leukocytes has been proposed *via* two distinct models, the 'bridge' and the 'cloud' model (Majumdar et al., 2014; Proudfoot, 2015).

The bridge model proposes that chemokines simultaneously bind to ECs by GAG chains and to their cognate leukocyte-expressed receptors. However, this model remains contentious as *in vitro* binding assays have shown that GAGs and GPCR receptors compete for chemokine binding (Proudfoot, 2015). This dynamic equilibrium could be dependent on the conformation and dimerization of chemokines. This concept has been demonstrated for the human chemokine, lymphotactin (XCL1), which has two structural forms: the classic form which has greater affinity for GAG-binding and the beta-sheet fold form which has greater affinity for receptor binding (Tuinstra et al., 2008). In addition, the CXCL12 receptor CXCR4, is able to avidly bind chemokine dimers but doing so prohibits additional binding to GAG chains due to spatial interference (Veldkamp et al., 2008). Thus, for these reasons, the bridge model is generally unfavoured, as chemokines seem to be limited to binding to GAGs or the receptors at any one time due to steric limitations.

The more recently proposed 'cloud' model propositions that newly released chemokines are retained within the glycocalyx, which acts as a reservoir of chemotactic molecules. The latter could provide directional cues for leukocytes while preventing the chemokine from being washed away by vascular shear flow. In this model, chemokines continuously associate and dissociate from GAGs, thus existing in a soluble phase within the hydrated aqueous layer of the glycocalyx ('cloud'). It is believed that such a microenvironment provides sufficient amount of free chemokine within the glycocalyx that facilitates stimulation of leukocyte cognate receptors. Additionally, this results in directed

penetration of the receptor bearing filopodia into the glycocalyx, thereby facilitating integrin interactions and hence firm adhesion (Middleton et al., 1997; Pruenster et al., 2009). The concept of free chemokine being the active form has been supported by Ab blockade experiments. For example, a study using Abs with differing affinities for soluble and bound forms of the chemokine CXCL10 (T-cell chemoattractant) provided evidence that targeting the soluble form of the molecule was more efficacious in the control of the pathogenesis associated with many diseases including diabetes (Bonvin et al., 2017). During chemokine-mediated activation of neutrophils, the response switches from a predominantly selectin- to an integrin- mediated reaction (Rot and von Andrian, 2004). Under homeostatic conditions, integrins are maintained in their non-active conformation, exhibiting low affinity towards adhesion molecules on the EC membrane (Kinashi and Katagiri, 2005). However, following ligation of specific chemokine/chemoattractants with their respective GPCR, a complex network of signalling pathways are activated resulting in integrin activation. This response often occurs within minutes, culminating in leukocyte arrest under conditions of shear-stress (Shamri et al., 2005). This process is more commonly known as 'inside-out' signalling (Ley et al., 2007). Through this process, integrins switch from a low- to an intermediate- and then high-affinity conformational state, whereby the ligand binding pocket is exposed allowing for strengthened neutrophil-EC binding (Kinashi and Katagiri, 2005; Arnaout et al., 2005). Integrin-mediated 'outside-in' signalling can also facilitate strengthening of leukocyte adhesion in addition to supporting other intracellular pathways that aid in cell motility, proliferation and apoptosis (**Fig. 1.8**) (Shattil, 2005; Giagulli et al., 2006; Shattil et al., 2010).

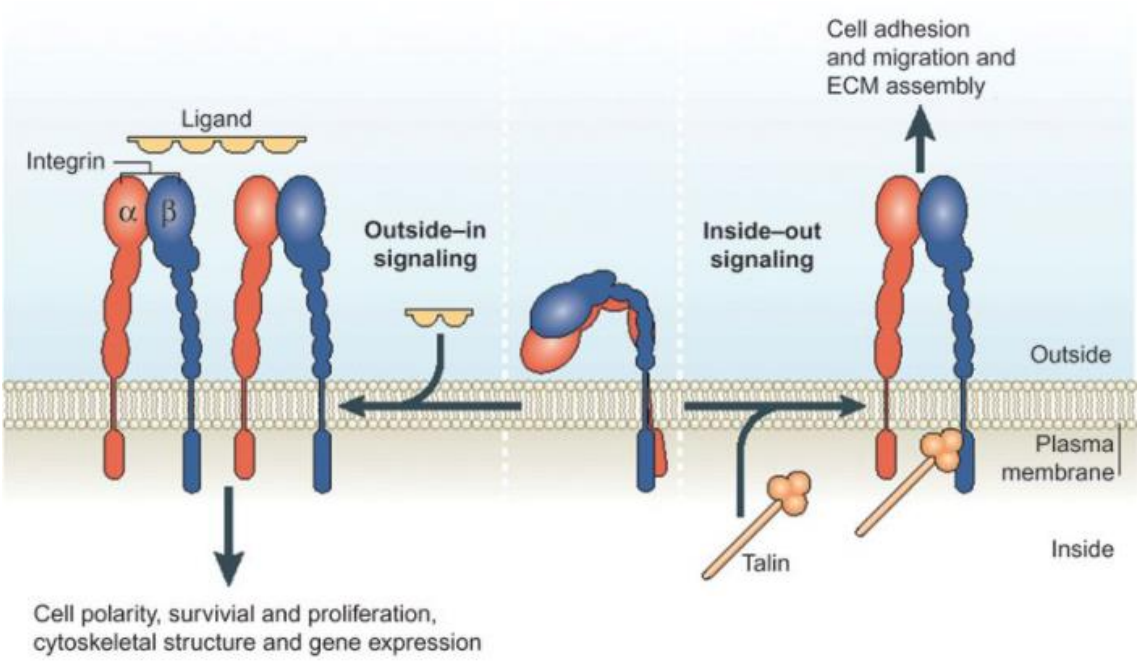

Figure 1.8. Regulation of integrin activation. The avidity of αβ-integrins for their ligands is defined by their affinity state and their valency. Right: Chemokine-triggered signalling *via* ligation to cell surface GCPRs (not shown, see text) induces complex intercellular signalling leading to the recruitment of cytoskeletal activators (e.g. talin) to the cytoplasmic domain of the integrin. This induces a conformational change in the ectoplasmic domain integrin, switching from a bent, low-ligand affinity conformation to a linear, high-affinity conformation. This process is known as 'inside-out' signalling and bolsters the ability of integrins support rearrangement of the neutrophil actin cytoskeleton and flattening of the cell; an essential part of neutrophil adhesion and crawling. Left: Integrin avidity is also supported by changes in the integrin valency, in which activated integrins form clusters, enabling multivalent interactions with their cognate ligands (e.g. ICAM-1, VCAM-1), more commonly referred to as 'outside-in' signalling. Consequentially, ligand-induced 'outside-in' signalling results in changes in cell polarity, survival, proliferation, gene activation and cytoskeletal rearrangement. Adapted from Shattil et al., 2010.

A change in integrin conformation is not the only factor influencing ligand avidity. For instance, valency of the integrins is also determined *via* lateral clustering of these receptors, allowing for greater receptor-ligand interactions (**Fig. 1.8**). Neutrophils express an array of integrins on their cell surface which are available to interact with their EC counterparts (see Table 1.2) (Muller, 2013; Nourshargh and Alon, 2014). Following integrin-mediated cell arrest on the endothelium, the neutrophil undergoes cytoskeletal rearrangements to facilitate leukocyte spreading mediated by 'inside-out' signalling mechanisms. The leukocyte can be seen to transition from a rounded morphology (as observed during leukocyte capture and rolling) to a flattened, more polarised morphology, in which the leukocyte develops a lamellipodium (leading edge)

and a uropod (trailing edge) (Nourshargh et al., 2010). F-actin polymerisation occurs at the lamellipodium, whereas actin-myosin contraction occurs at the uropod allowing for intra-luminal crawling along haptotactic gradients established by various chemoattractants (Phillipson et al., 2006). Neutrophil crawling is supported by integrins, principally interactions between MAC-1 with EC expressed ICAM-1. This is mediated *via* the formation of new bonds at the lamellipodium that are simultaneously broken at the uropod to enable neutrophil crawling across the endothelium, a response that ensures continuous contact between leukocytes and the endothelium, until a site of TEM is identified (Phillipson et al., 2006; Xu et al., 2011). At this point, it is vital that integrins are inactivated, for example, by the intracellular signalling molecule ARAP3 (McCormick et al., 2019), to allow neutrophils to deform and progress through the EC barrier.

1.5.3. Neutrophil transendothelial migration (TEM)

Neutrophil transmigration is a process whereby leukocytes penetrate the EC monolayer (i.e. exhibit TEM), while ensuring minimal disruption of the vascular barrier integrity to macromolecules. (as described in Chapter 3). TEM can occur through para- or trans-cellular routes, with the former being by far the most common mode (Schenkel et al., 2004; Phillipson et al., 2006; Woodfin et al., 2011) (**Fig. 1.9**). Both types of TEM rely on selective and tightly regulated interactions between the leukocyte and a multitude of adhesion molecules decorated on the endothelial membrane, including immunoglobin-like superfamily members PECAM-1, ICAM-1/2, JAM-A/B/C, VE-cadherin and ESAM and non-immunoglobulin-like CD99, as detailed in **Fig. 1.9** and section 1.5.3.1 (Muller, 2016). The contribution of each of these molecules to TEM can vary depending on the leukocyte subtype, the stage of leukocyte diapedesis and the stimulus used (Huang et al., 2006; Woodfin et al., 2007b, 2009). *In vitro*, neutrophil TEM is supported *via* the formation of endothelial adhesive platforms (EAP) exhibiting ICAM-1 and VCAM-1 enriched domains, which serve as docking structures (Phillipson et al., 2008). During TEM, these docking structures are believed to form a hermetic seal surrounding the neutrophil to maintain barrier function (i.e. non-permeable to plasma proteins). The formation of these docking structures requires Src-dependent phosphorylation of the actin binding protein, cortactin, which has been proposed to be induced by ICAM-1-MAC-1 interactions

(Muller, 2011). These defined docking structures form linear clusters of integrins on the surface of the endothelium in the direction of migration for both paracellular and transcellular TEM. Whilst the factors that determine the route of TEM remain largely unclear, one possibility is an effective crawling capability of cells prior to extravasation. For example, if crawling is halted due to insufficient interactions between MAC-1 and ICAM-1, then transcellular migration is favoured (Ley et al., 2007).

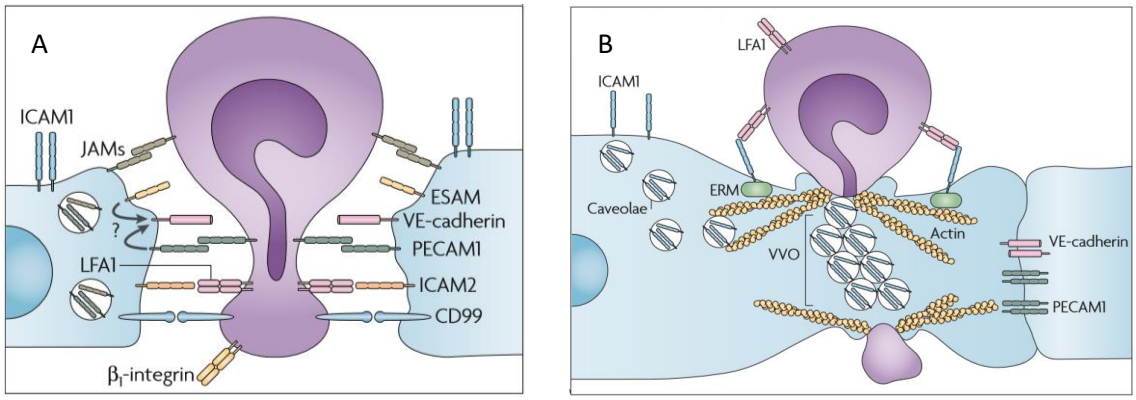

Figure 1.9. (A) Paracellular and (B) transcellular neutrophil TEM showing the important molecules involved for each mode of transmigration. Following neutrophil-EC adhesion *via* ICAM-1/MAC-1/LFA-1, neutrophils terminate crawling at the sight of transmigration. Paracellular migration is mediated by several junction-specific adhesion molecules including PECAM-1, CD99, ESAM and JAMs, in addition to dissociation of VE-cadherin intercellular dimers. Transcellular migration occurs in "thin" regions of the endothelium and involves translocation of ICAM-1 towards actin- and caveolin-rich domains. ICAM-1 containing VVOs form an intracellular pore that guides the neutrophil through the EC body. Figure adapted from Ley et al., 2007.

Neutrophil paracellular migration

In vivo, approximately 90% of neutrophils migrate through the EC barrier in a paracellular manner, i.e. through EC junctions (**Fig. 1.9A**). Paracellular neutrophil migration can be very rapid, typically requiring between 5-7 min to complete (Woodfin et al., 2011). Furthermore, during paracellular TEM, neutrophils typically migrate through tricellular EC junctions as these sites have 'looser' junctional integrity, and thus due to the reduced resistance, are more accommodating for neutrophils to migrate through (Sumagin and Sarelius, 2010).

Neutrophil paracellular TEM is a multifaceted process that requires EC junctional rearrangements as supported by intracellular RhoGTPase activation and increased Ca^{2+} influx, which results in activated MLC kinases and consequent EC contraction (Ley et al., 2007). Furthermore, this response is mediated either by the redistribution of certain junctional molecules away from the EC junction (e.g. VE-cadherin) (Shaw et al., 2001), or by targeted translocation of other junctional proteins towards the neutrophil (e.g. PECAM-1 and JAM-A). The latter enables the establishment of a "haptotactic gradient" of adhesion molecules that facilitate the movement of neutrophils toward EC junctions to extravasate (Muller, 2003). Under basal conditions, PECAM-1, JAM-A and CD99 shuttle between the EC surface and a cell-surface-connected vesicular compartment known as the lateral border recycling compartment (LBRC). During inflammation, the LBRC membrane is preferentially mobilised to the site of neutrophil diapedesis to promote TEM (Mamdouh et al., 2003). In addition, adherens molecules such as VE-cadherin dissociate from the membrane and are internalised resulting in reduced junctional integrity whilst maintaining tightly regulated passage of neutrophils (Schulte et al., 2011) (further details on key junctional molecules required for neutrophil TEM are described in section 1.5.3.1).

Of particular interest in the context of this thesis, specific adhesion molecules have been shown to mediate different stages of neutrophil TEM in a stimulus specific manner. For example, following IL-1β-stimulation, ICAM-2 has been shown to be particularly important in guiding neutrophils to EC junctions, whereas JAM-A and PECAM-1 mediated migration through the EC junction and basement membrane, respectively (Woodfin et al., 2009). However, neutrophil TEM induced by other stimuli such as fMLP, LTB_4 and TNF was independent of these junctional molecules (Huang et al., 2006; Nourshargh et al., 2006; Woodfin et al., 2007b) but was dependent on the integrins MAC-1 and LFA-1 (Sumagin et al., 2010).

Neutrophil transcellular migration

The least understood of the two routes, transcellular migration, is defined as translocation of a cell directly through the EC body and has predominantly been

observed within *in vitro* models and in the vasculature of the central nervous system (CNS) (**Fig. 1.9B**) (Engelhardt and Wolburg, 2004). This route of leukocyte migration appears to use much of the same molecular machinery to that employed by paracellular migration (Filippi, 2016). For example, PECAM-1, JAM-A and CD99 were observed around the site of neutrophil transcellular migration (Carman et al., 2007; Mamdouh et al., 2009), and blocking anti-PECAM-1 and anti-CD99 Abs arrested transcellular migration (Mamdouh et al., 2009). A key mechanistic distinction from paracellular TEM is that VVOs have been observed *in vivo* at the location of neutrophil firm adhesion where they have been suggested to play a role in facilitating transcellular TEM (Dvorak and Feng, 2001). Following ligand activation of EC ICAM-1 by neutrophil LFA-1, apical ICAM-1 is internalised and translocated to caveolae and F-actin rich domains. These ICAM-1-containing caveolae then fuse to form VVOs, thereby forming a transcellular pore (Millán et al., 2006; Nieminen et al., 2006). Structural support of these EC pores is further aided by the ezrin, radixin and moesin (ERM) complex that links the cytoskeleton to these ICAM-1 rich pores. This cascade of events results in EC 'thinning' facilitating neutrophil migration through the EC body (Feng et al., 1998).

1.5.3.1. Key endothelial junctional molecules involved in neutrophil TEM

As briefly introduced in section 1.4 and Table 1.2, EC junctional molecules play a vital role in mediating neutrophil TEM. This section aims to provide further insight into some of the key molecules involved in this response.

VE-cadherin

As discussed in section 1.4.3, neutrophils are able to induce vascular leakage through the release of a variety of pro-inflammatory factors. Several of these induce disruption of the EC barrier by stimulating phosphorylation and internalisation of VE-cadherin through the mechanisms discussed in section 1.4.2. More recently, Wessel and colleagues described a knock-in mouse model with a single point mutation in tyrosine 731 residue of VE-cadherin, VEC-Y731F (Wessel et al., 2014). In these mice, the Y731

residue can no longer be dephosphorylated and was shown to distinctly impact leukocyte migration independent of vascular permeability, whereby mice exhibited an approximate 50% reduction in neutrophil extravasation following IL-1β stimulation. Neutrophils were shown to trigger dephosphorylation of Y731 through a Src homology region 2 domain-containing phosphatase (SHP)-2-dependent mechanism, which enabled the binding of the adapter molecule activating protein (AP)-2 to VE-cadherin, resulting in its endocytosis.

JAMs

The JAMs are an immunoglobulin-like superfamily consisting of three key junctional molecules: JAM-A, -B and -C. JAMs are expressed on leukocytes, platelets, epithelial and ECs and play a vital role in mediating leukocyte migration and permeability. JAM protein expression can be upregulated under inflammatory, atherosclerotic and ischaemic conditions, which supports leukocyte adhesion *via* their redistribution away from the EC intercellular junctions to the apical cell surface (Weber et al., 2007). JAM-A is predominantly expressed and concentrated on EC boarders and engages primarily in homophilic interactions, but it can also interact with LFA-1 expressed on the surface of leukocytes to facilitate neutrophil TEM (Ostermann et al., 2002). Indeed, *in vivo* blockade of JAM-A results in inefficient neutrophil migration (Woodfin et al., 2009). JAM-C likewise is concentrated at EC borders and can engage in homophilic interactions but additionally in heterophilic interactions with JAM-B and MAC-1. JAM-C-JAM-B interactions have been shown to play a vital role in facilitating luminal-to-abluminal neutrophil migration *in vitro* and *in vivo* (Chavakis et al., 2004; Cunningham et al., 2002; Bradfield et al., 2007a; Woodfin et al., 2011). Additionally, JAM-C has been implicated in supporting vascular permeability, though this aspect of JAM-C biology remains contentious (see Chapter 3 & 4).

PECAM-1

PECAM-1 is a member of the immunoglobulin-like superfamily of proteins and expressed by platelets and a wide variety of cells including monocytes, neutrophils and ECs. With respect to ECs, PECAM-1 forms homodimers between adjacent cells and leukocytes to facilitate neutrophil migration during inflammation (Schenkel et al., 2004). PECAM-1 has also been shown to engage in heterophilic interactions with GAGs, CD38 and CD117 (DeLisser et al., 1993; Deaglio et al., 1998; Sachs et al., 2007). PECAM-1 function has been determined through a series of Ab blocking experiments or use of PECAM-1 deficient mice that display poor leukocyte migration responses into the peritoneum, mesentery and cremaster muscle during IL-1β-mediated inflammation. These effects were linked to both a reduction in penetration of EC junctions and an accumulation of leukocytes in the subendothelial space (Thompson et al., 2001; Dangerfield et al., 2002; Schenkel et al., 2006; Woodfin et al., 2007a; b). The latter effect was aligned with the ability of neutrophil PECAM-1 ligation to mobilise expression of the principal laminin receptor, integrin VLA-6, on the neutrophil surface (Dangerfield et al., 2002).

CD99

CD99 is another cell adhesion molecule that has been shown to play a role in paracellular neutrophil TEM (Bixel et al., 2007). Similar to PECAM-1, EC junctional CD99 forms homophilic interactions between adjacent ECs or leukocytes to facilitate their diapedesis into the interstitial tissue (Schenkel et al., 2002; Lou et al., 2007). Following IL-1β stimulation, CD99 has been shown to act sequentially after PECAM-1 to facilitate neutrophil TEM. Here, in HUVEC monolayers treated with an anti-CD99 blocking Ab, leukocytes exhibited only partial diapedesis through the endothelium, but once leukocytes reached this point, further progression through the EC junction could not be inhibited by the sequential application of an anti-PECAM-1 blocking Ab. However, PECAM-1 blockade resulted in enhanced leukocyte arrest on the apical EC surface with reduced diapedesis. Although, as discussed above, sequential blockade with an anti-PECAM-1 Ab may restrict progression through the pericyte layer. However, this does

suggests that PECAM-1 is one of the first interactions involved in neutrophil diapedesis through the EC junction (Schenkel et al., 2002; Dufour et al., 2008).

ICAMs

ICAM-1 and ICAM-2 have several functions during leukocyte TEM and are expressed by neutrophils and by ECs on their apical surface (ICAM-1 & ICAM-2) and at the junctions (ICAM-2) (Muller, 2016). Whilst ICAM-1 is primarily associated with the earlier stages of the leukocyte adhesion cascade, it appears that clusters of ICAM-1 near EC junctions direct adherent neutrophils towards sites of paracellular TEM (Shaw et al., 2004). ICAM-2 however plays a key role in mediating neutrophil migration through EC junctions (Huang et al., 2006; Halai et al., 2014) *via* interactions with LFA-1 and MAC-1 during IL-1β-, but not TNF-induced inflammation (Woodfin et al., 2009). Interestingly, despite its constitutive expression on ECs and neutrophils, the role of ICAM-2 in neutrophil migration is primarily governed by its EC, and not neutrophil, expression.

ESAM

ESAM is mainly limited to expression by ECs and platelets and has a similar molecular structure to JAMs, but with a longer cytoplasmic tail. Like JAMs and PECAM-1, ESAM expressed by ECs engages in homophilic interactions in trans with adjacent ECs (Nasdala et al., 2002). ESAM deficient mice exhibit a transient defect in neutrophil migration following peritoneal thioglycollate treatment. This is characterised by decreased TEM after 2 hr of stimulation that recovers at 4 hr post stimulation, though the mechanism of this effect is largely unknown (Wegmann et al., 2006). Of interest, ESAM has also been shown to be important in preventing endothelial permeability, whereby $ESAM^{KO}$ mice exhibited enhanced vascular leakage in a model of diabetic nephropathy (Hara et al., 2009).

1.5.4. Neutrophil migration through the venular basement membrane and pericyte sheath

After neutrophils migrate through the EC layer, they are then required to progress through the basement membrane and pericyte sheath before entering the interstitial space. The basement membrane is an extracellular matrix protein complex produced by both the ECs and pericytes (Jaffe et al., 1976; Davis and Senger, 2005; Stratman and Davis, 2012). This tight structure consists of two key networks of collagen and laminins (mainly collagen type IV and laminins 8 and 10) that are interconnected *via* smaller molecules such as heparin sulphate proteoglycans, perlecan and nidogen-2 (Hallmann et al., 2005). Neutrophil migration through the basement membrane and pericyte sheath takes much longer than TEM, lasting approximately 30-45 min (Ley et al., 2007; Woodfin et al., 2011; Proebstl et al., 2012).

During neutrophil migration, the basement membrane undergoes neutrophil-dependent remodelling. Under basal conditions 'low expression regions' (LERs) have been identified in the venular basement membrane, that are defined as sites with lower expression of certain matrix proteins (e.g. collagen type IV, laminin-8, laminin-10, nidogen, but not perlecan). The size of these regions enlarges during neutrophil TEM in a protease-dependent manner, providing evidence for the involvement of NE in neutrophil migration through the basement membrane. Furthermore, these weaker membrane regions correlate with pericyte gaps (Wang et al., 2006; Voisin et al., 2009, 2010; Proebstl et al., 2012) and as such, LERs may also allow the site to be more permeable to chemoattractants. Hence, although not yet proven, LERs could aid in the generation of chemotactic gradients that guide neutrophils to these regions (Ley et al., 2007). In addition, heparin sulphate GAGs on the abluminal surface of ECs and throughout the basement membrane have been shown to retain chemokines, which conceptually should be important for guiding neutrophil migration towards the interstitial tissue (Stoler-Barak et al., 2014; Monneau et al., 2016) (detailed in section 1.5.2). Finally, as mentioned above (section 1.5.3.1), the interaction of EC and neutrophil PECAM-1 results in upregulation of the neutrophil-derived integrin, VLA-6, which is the main receptor for laminins and has been shown to support neutrophil movement through the basement membrane (Dangerfield et al., 2002).

Pericytes are the second cellular layer of post-capillary venules that are also present on capillaries, lymphatics but to a lesser extent on veins and arteries. They surround the EC monolayer in a non-uniform manner resulting in a discontinuous EC coverage (Nourshargh and Alon, 2014). Pericytes are able to mediate the transition of neutrophils into the interstitial tissue through the expression of various receptors including TNF-receptor (TNFR)I/II, IL-1R, ICAM-1, VCAM-1 and secretion of chemokines (e.g. CXCL1). In particular, expression of ICAM-1 on pericytes supports neutrophil abluminal crawling in a MAC-1-dependent manner prior to breaching of the pericyte layer (Proebstl et al., 2012; Voisin and Nourshargh, 2013).

Collectively, through these tightly regulated interactions, neutrophils navigate through the venular basement membrane and the pericyte layer to egress from the vasculature into the interstitial tissue.

1.5.5. Interstitial neutrophil migration

Once in the interstitium, neutrophils respond to established chemotactic gradients to reach the core of the inflammatory insult. This migration is aided by precise, hierarchical and sequential presentation of various chemotactic molecules. fMLP and complement component 5a (C5a) are known as end-target chemoattracts towards which neutrophils migrate with greater preference over gradients established by secondary chemoattractants (e.g. LTB_4 and CXCL1) (Foxman et al., 1997). Indeed, fMLP is the most potent chemoattractant and sits at the top of the 'presentation hierarchy' (Heit et al., 2002). The nature of neutrophil responses to these mediators is governed *via* the regulation of specific intracellular pathways. LTB_4, for example, activates phosphoinositide 3-kinase (PI3K) signalling, whereas fMLP and C5a activate both PI3K and MAPK signalling that function to induce neutrophil polarisation and migration, respectively, towards the site of primary insult within the interstitial tissue. This process supports the formation of neutrophil swarms at the site of insult. Neutrophils have been observed to exhibit transient swarming, whereby they remain at the site for a few minutes, or persistent swarming whereby neutrophil presence at the site is more sustained. This neutrophil swarming behaviour has been suggested to be influenced by

several factors including the size of the initial tissue damage, the presence of pathogens, the volume of neutrophils recruited and the level of resulting cell death (Kienle and Lämmermann, 2016). Once at the core of the inflammatory trigger, neutrophils perform effector functions such as phagocytosis of microbes or dead cells, degranulation/intracellular killing and modulation of the immune response through the release of various pro-inflammatory and growth factors (described in section 1.3).

1.6. Neutrophil reverse migration

Following acute injury or infection it is vital that neutrophils are able to reach the area of insult quickly and efficiently. Typically, neutrophils migrate in a luminal-to-abluminal direction, however, there is now extensive evidence that during certain inflammatory reactions, a proportion of neutrophils can undergo reverse interstitial migration (rIM) and/or reverse transendothelial migration (rTEM). For example, during neutrophil rTEM, observed in post-capillary venules of the cremaster muscle, neutrophils breach the endothelium (~20-100% of their cell body) but never progress through the pericyte layer, before moving in an abluminal-to-luminal direction and returning back into the circulation (Woodfin et al., 2011; Colom et al., 2015). Incidences of leukocyte rTEM were initially identified *in vitro* by Randolph and Furie, who observed reverse migration of human derived monocytes through cultured endothelial monolayers (Randolph and Furie, 1996). A decade later, Buckley and colleagues reported that neutrophils undergo rTEM through cultured ECs *in vitro* (Buckley et al., 2006). However, it was not until 2011 that neutrophil rTEM was first observed *in vivo* in a mammalian system (Woodfin et al., 2011). Here, following IR-injury of the cremaster muscle, reverse motility of neutrophils was clearly observed and quantified at the level of the endothelium (Woodfin et al., 2011). Interestingly, this *in vivo* neutrophil rTEM response was noted to be stimulus specific, occurring in tissues stimulated with LTB_4 or IR-injury, but not following the application of IL-1β. The underlying cause of this phenomenon remains largely unknown but some possibilities are discussed in Chapter 4.

Neutrophils have also been observed to undergo rIM, whereby neutrophils fully migrate into the interstitial tissue before exhibiting reverse motility toward the blood vessel,

followed in some instances by rTEM back into the vascular lumen (Ellett et al., 2015; Wang et al., 2017). Neutrophil rIM was first observed in the zebrafish following sterile laser burn injury of the tail fin (Mathias et al., 2006; Yoo and Huttenlocher, 2011). Neutrophil swarming at the site of injury was observed to peak after 6 hr post injury, with neutrophils being observed to migrate away from the injured interstitial site as soon as 3 hr post injury (Mathias et al., 2006). Neutrophil rIM was later observed in murine models developed by Wang and colleagues using laser induced liver injury (Wang et al., 2017). The occurrence of neutrophil rIM in the liver raises the possibility of tissue/vasculature specific effects in determining the frequency of neutrophil rTEM and neutrophil rIM + rTEM.

1.6.1. Functional consequences of neutrophil rTEM

Our understanding of the (patho)physiological relevance of reverse neutrophil migration remains poor and thus far has only been indirectly linked to pathological outcomes. For example, reactions that induce neutrophil rTEM in the locally inflamed mouse cremaster muscle resulted in the development of distal lung oedema (Woodfin et al., 2011; Colom et al., 2015). However, if and how rTEM neutrophils can induce distant organ damage remained unclear and was indeed a key subject of this thesis (Chapter 5). Here, a principal hypothesis is that as neutrophils initiate diapedesis through the EC layer, they become primed/activated and as such their return into the circulation and potential dissemination to distant organs (e.g. lungs) could lead to distant organ injury. This notion is supported by the findings of Buckley et al., who identified that isolated rTEM neutrophils *in vitro* exhibited increased expression of ICAM-1 and generation of ROS. Furthermore, although indirect, they identified a population of ICAM-1^{high} neutrophils in the blood of patients suffering from rheumatoid arthritis (RA) (Buckley et al., 2006). This data is further supported by the findings of Woodfin et al., whereby neutrophils with an rTEM neutrophil phenotype (e.g. ICAM-1^{high} and ROS^{high}) were detected in murine lungs following local IR-injury (Woodfin et al., 2011). Collectively, as local inflammation can in some cases lead to systemic consequences (e.g. ALI) (Grace, 1994; Bartels et al., 2013), these data suggest that neutrophil rTEM could be of pathophysiological relevance in humans and provides an interesting avenue for further exploration.

1.6.2. Functional consequences of neutrophil rIM

Poznansky and colleagues were the first to propose that 'reverse' motility of neutrophils could be an important mechanism in providing inflammation resolution (Tharp et al., 2006). Here, they observed that neutrophils moved away from areas of high CXCL8 concentration, indicating a chemo-repulsive affect that they suggested could be the mechanism of down-regulating the inflammatory response. This concept was further supported by data published by Deng and colleagues demonstrating similar neutrophil behaviour at sites of inflammation in zebrafish embryos (Deng and Huttenlocher, 2012). Together, these findings indicate that actively recruited neutrophils can become unresponsive during the later phase of the inflammatory response, thus losing their ability to migrate towards the core of an inflammatory site. Numerous mechanisms could account for this. For example, the retrograde motility in the tissue could be due to receptor desensitisation on the neutrophil surface. The CXCL8-CXCR2 signalling axis has been shown to play an important role in rIM behaviour as CXCR2 null zebrafish have defective/delayed resolution of inflammation (Powell et al., 2017). Furthermore, following stabilisation of the hypoxia-inducible factor (HIF) pathway by genetic modification in zebrafish, the frequency of neutrophil rIM was reduced during sterile inflammation (Elks et al., 2011). Here, Elks et al., demonstrated that the reduced ability for neutrophils to reverse migrate coincided with delayed inflammation resolution, reduced cellular apoptosis and development of scar tissue. Although no direct mechanism of neutrophil rIM was explored, it is interesting that HIF-1α, an important mediator of the EC HIF pathway, mediates the expression of the chemorepellent, netrin-1. Whilst the function of netrin-1 remains largely unexplored, it is known to prevent neutrophil migration across epithelial cell layers in *vitro* (Rosenberger et al., 2009). Finally, following laser burn injury of the liver, and photoactivation of rIM + rTEM neutrophils at this site, Wang et al., identified a small population of these neutrophils in the lungs and BM, where they exhibited elevated surface expression of CXCR4. Here, this retrograde motility in the liver was reduced in a cathepsin-C KO ($Ctsc^{KO}$) mice, suggesting that either/both the rIM or TEM require the activity of serine proteases. The authors suggested that neutrophils having undergone rIM followed by rTEM in the liver microvasculature, upregulate CXCR4 expression in order to return to the BM to be

cleared, thus aiding the resolution of local inflammation (Wang et al., 2017). Collectively, it is postulated that rIM may provide an attractive therapeutic target to promote wound healing and to prevent the formation of undesirable scar tissue. Indeed, some progress has already been made in this context with the finding that tashinone IIa, a compound derived from the roots of *Salvia miltorrhiza* commonly used in Chinese medicine as a treatment of cardiovascular disease, accelerated inflammation resolution through promoting neutrophil apoptosis and reverse migration (Robertson et al., 2014).

In light of these recent discoveries regarding reverse migration of neutrophils (discussed in sections 1.6.1 and 1.6.2), there is a clear need to further explore the mechanisms driving the reverse motility of neutrophils, with a focus on rTEM in this thesis, and to determine the phenotypic changes and fate of these cells, which are discussed further in Chapters 4 and 5.

1.7. Hypothesis and aims of the thesis

There is extensive evidence in the literature supporting a role for neutrophils as inducers of vascular leakage *via* release of pro-permeability factors including VEGF, LTB_4, HBP, ROS and TNF during inflammation. However, there is minimal understanding of if and how microvascular leakage influences neutrophil behaviour. As such, the principal aim of this work was to explore the impact of vascular leakage on neutrophil-EC interactions *in vivo*. Here, since the primary effect of microvascular leakage we saw was that of induction of neutrophil rTEM, the second important aim of this thesis was to gain insight into the phenotype and fate of rTEM neutrophils. The points below highlight the approaches used to address the aims of this project.

1.7.1. Development of a confocal IVM methodology for simultaneous study of neutrophil migration and vascular leakage

In order to investigate the potential impact of microvascular leakage on neutrophil migration we developed a confocal IVM methodology for the simultaneous

quantification of both events in real-time. Our ability to concomitantly image and quantify vascular leakage and neutrophil TEM responses at high temporal and spatial resolutions was assessed using established models of acute inflammation, namely as induced by local IL-1β, LTB_4 and IR-injury. Initial works aimed to establish the temporal association between neutrophil migration and microvascular permeability responses.

1.7.2. Investigating the impact of vascular permeability induction on neutrophil migration

From the investigations conducted, as detailed in 1.7.1, we hypothesised that microvascular leakage can augment the directionality of neutrophil TEM. To directly investigate the impact of vascular permeability on neutrophil migration, the effects of two established potent pro-permeability agents, histamine and VEGF, were tested in WT mice and in a genetically modified (GM) mouse model that exhibits a selective defect in vascular leakage. Hypothesising that enhanced permeability disrupts the normal localisation of tissue chemokines, confocal IVM and complementary enzyme linked immunosorbent assays (ELISA) were used to assess this notion.

1.7.3. Development of a model to label and track rTEM neutrophils

As enhanced permeability promoted neutrophil rTEM, a key objective was to gain insight into the biology of this sub-set of cells. Of note, full understanding of the phenotype and fate of rTEM neutrophils has remained a challenging objective, in part due to the difficulty to exclusively label and track the fate of these cells. To address this important point, this thesis describes a novel *in vivo* labelling technique for tracking rTEM neutrophils that enabled phenotyping of this neutrophil subset and provided insight into their dissemination and fate. Here, we hypothesised with this new approach we could exclusively and more efficiently label rTEM neutrophils and demonstrate that these cells disseminate to the lungs where they exhibit a pro-inflammatory phenotype.

1.7.4. Investigating the role of the TNF/TNFR pathway in induction of vascular leakage and neutrophil TEM

Finally, to strengthen the link between vascular permeability and neutrophil rTEM, we sought to develop experimental models for future investigations of this novel association. Specifically, as previous works from our laboratory identified a role for neutrophil-derived TNF in induction of neutrophil-mediated vascular permeability (Finsterbusch et al., 2014), here we developed a novel mouse model with selective neutrophil-TNF deficiency (Neutro-TNF^{KO}). Furthermore, for mechanistic works, we established protocols for the generation of chimeric mice deficient in expression of TNFRI/II on haematopoietic cells. Overall, we hypothesised that neutrophil-derived TNF plays a fundamental role in the vascular leakage response *via* its action through TNFRs and can subsequently alter the directionality of neutrophil TEM. Whilst the model development element of these works was successfully achieved, due to time constraints and a lack of experimental mice, this Chapter represents a work in progress.

Chapter 2

Materials and Methods

This Chapter presents an overview of the experimental material/resources and core techniques employed for the investigations described in this thesis. The initial section provides a list of reagents, sources and additional details to help readers replicate the work. The latter section describes the murine models employed, and where relevant, how they were generated and treated along with details of data analysis techniques. Specialised protocols are detailed in relevant result chapters.

2.1. List of Reagents

Table 2.1. Anaesthetics

Reagent	Source	Details
Ketamine	Fort Dodge Animal Health Ltd, Southampton, UK	Ketaset® injection (Working Conc: 100 mg/ml)
Xylazine	Bayer plc, Newbury, UK	Rompun® 2 % (v/v in saline) (Working Conc: 20 mg/ml)
Isoflurane	Zoetis, London, UK	Isoflo® 100% (Working Conc: 100 %)

Table 2.2. General reagents

Reagent	Source	Details
123count eBeads	Thermofisher, Dartford, UK	Cat No.: 01-1234-42
ACK (Ammonium-Chloride-Potassium) red cell lysis buffer	Made in house	PBS containing 150 mM NH_4Cl, 1 mM $KHCO_3$, 0.1 mM EDTA
Baytril	Centaur, Castle Carey, UK	Working Conc: 0.08 % (v/v in water)
Bovine Serum Albumin (BSA)	Sigma Aldrich, Poole, Dorset, UK	Cat No.: A1933
Phosphate buffered saline (PBS) – modified without $CaCl_2$ and $MgCl_2$	Sigma Aldrich, Poole, Dorset, UK	Cat No.: D8537
Ethylenediaminetetraacetic acid (EDTA)	Sigma Aldrich, Poole, Dorset, UK	Cat No.: E5134

Ethanol	VWR International, Lutterworth, UK	Working Conc: 70 % (v/v in water)
Foetal Calf Serum (FCS)	Gibco/Thermofisher, Dartford, UK	Cat No.: 10500-064
GolgiPlug™ (Brefeldin-A)	BD Biosciences, California, USA	Cat No.: 555029. Working Conc: 1 µl/ml (flow cytometry)
Paraformaldehyde (PFA)	Sigma Aldrich, Poole, Dorset, UK	Working Conc: 4 % (w/v in PBS, pH 7.4)
Megamix-Blue PCR mastermix	Clent Life Science, UK	Cat No.: 2MMB-25
Halt Protease and Phosphatase Inhibitor cocktail	Thermofisher, Dartford, UK	Cat No.: 78441
Proteinase K	Bioline (Scientific Laboratory Supplies, Nottingham, UK)	Cat No.: BIO-37037
Sterile Saline	Baxter Healthcare, Northampton, UK	Cat No.: UKF7114, T2145
Smart Ladder SF	Eurogentec, Seraing, Belgium	Cat No.: 1800-04
Sodium Hydrogen Carbonate	Fisher Scientific, Dartford, UK	Cat No.: 10020510
Schwartz Micro Serrefine – Straight clamps (10 x 1.75 mm)	Fine Science Tools (FST), Heidelberg, Germany	Cat No.: 18555-01
Tetramethylrhodamine isothiocyanate-dextran (TRITC-dextran - 75 kDa)	Sigma Aldrich, Poole, Dorset, UK	Cat No.: 46944-F
Triton X-100	Sigma Aldrich, Poole, Dorset, UK	Cat No.: 9002-93-1
Tyrodes Salt Solution	Sigma Aldrich, Poole, Dorset, UK	Cat No.: T2145
Ultracomp eBeads	Thermofisher, Dartford, UK	Cat No.: 01-2222-42
Zombie Yellow Fixable *Via*bility Dye	Biolegend, London, UK	Cat No.: 77168

Table 2.3. PCR Primers (All purchased from Integrated DNA Technologies, Leuven, Belgium)

Primer	**Sequence**	**Application**
Tnf$^{f/f}$ Forward	5’ - TGAGTCTGTCTTAACTAACC - 3’	Genotyping

Tnf$^{f/f}$ Reverse	5’ - CCCTTCATTCTCAAGGCACA - 3’	
Mrp8-Cre Forward *Mrp8*-Cre Reverse	5’ - CTGGAAAATGCTTCTGTCCGTTTG - 3’ 5’ - ACGAACCTGGTCGAAATCAGTGCG - 3’	Genotyping

Table 2.4. List of primary antibodies (Staining antibody cocktails were incubated in a volume of 200 µl for flow cytometry application)

Antigen	**Source**	**Clone**	**Antibody**	**Isotype control (further detailed in Table 2.5)**	**Fluorophore**	**Working concentration/ route of administration (Application)**
CD11b	Biolegend, London, UK	M1/70	Rat monoclonal anti-mouse/ human	$IgG2b_{\kappa}$	Brilliant Violet-711 (BV711)	0.4 µg per 10^6 cells (flow cytometry)
CD16/CD32 (Fc block)	BD Biosciences, California, US	2.4G2	Rat monoclonal anti-mouse	N/A	None	1 µg per 10^6 cells (flow cytometry)
CD29 (Integrin-β1)	Biolegend, London, UK	HMβ1-1	Armenian hamster monoclonal anti-mouse	IgG	Phycoerythrin-Cyanine®7 (PE-Cy7)	1 µg per 10^6 cells (flow cytometry)
CD31 (PECAM-1)	Thermofisher, Waltham, MA, USA	390	Purified, functional grade rat monoclonal anti-mouse	N/A	Conjugated to Alexa Fluor® 647 (AF647) or 555 (AF555) in house with a Life Technologies Alexa Fluor® antibody labelling kit to a stock conc of 1 mg/ml	4 µg in 400 µl PBS (intrascrotal, i.s.) (confocal intravital microscopy, IVM)

CD45	Biolegend, London, UK	30-F11	Rat monoclonal rat anti-mouse	$IgG2b_{\kappa}$	Pacific Blue (PB)	0.25 µg per 10^6 cells (flow cytometry)
CD54 (ICAM-1)	Biolegend, London, UK	YN1/1.7.4	Rat monoclonal anti-mouse	$IgG2b_{\kappa}$	Phycoerythrin-Dazzle^{TM}594 (PE-Dazzle594)	0.125 µg per 10^6 cells (flow cytometry)
CD62L (L-selectin)	Biolegend, London, UK	MEL-14	Rat monoclonal anti-mouse	$IgG2a_{\kappa}$	Brilliant Violet 605 (BV605)	0.25 µg per 10^6 cells (flow cytometry)
CD102	Biolegend, London, UK	3C4 MIC2/4	Rat monoclonal anti-mouse	$IgG2a_{\kappa}$	AF488	0.25 µg per 10^6 cells (flow cytometry)
CD115	Biolegend, London, UK	AFS98	Rat monoclonal anti-mouse	$IgG2a_{\kappa}$	AF488 or Allophycocyanin-Cyanine®7 (APC-Cy7)	1 or 0.25 µg per 10^6 cells (flow cytometry)
CD120a (TNFRI/TNFRSF1A)	R&D Systems, Abingdon, UK	-	Goat polyclonal anti-mouse	Goat IgG	None	2.5 µg per 10^6 cells (flow cytometry)
CD184 (CXCR4)	Thermofisher, Waltham, MA, USA	2B11	Rat monoclonal anti-mouse	IgG2b	PE	0.5 µg per 10^6 cells (flow cytometry
CXCL1	R&D Systems, Abingdon, UK	48415	Rat monoclonal anti-mouse	IgG2a	None	1 mg/kg of mouse weight (intravenous, i.v.) (confocal IVM)
F4/80	Biolegend, London, UK	BM8	Rat monoclonal anti-mouse	$IgG2a_{\kappa}$	AF647	1 µg per 10^6 cells (flow cytometry)

Ly6G	Biolegend, London, UK	1A8	Rat monoclonal anti-mouse	$IgG2a_{\kappa}$	PB or PE or APC-Cy7	1/0.25 µg per 10^6 cells respectively (flow cytometry)
Ly6G and Ly6C (Gr-1)	Biolegend, London, UK	RB6-8C5	Rat monoclonal anti-mouse	$IgG2b_{\kappa}$	PB or AF488	1 µg per 10^6 cells (flow cytometry)
Ly6G-Biotin	Biolegend, London, UK	1A8	Rat monoclonal anti-mouse	N/A	None	2 µg/150 µl i.v. (*in vivo* labelling/ flow cytometry)
MRP14	Generated and provided by Dr. Nancy Hogg, The Francis Crick Institute, UK	2B10	Rat monoclonal anti-mouse	N/A	Conjugated to AF647 or AF488 in house with a Life Technologies Alexa Fluor antibody labelling kit to a stock conc of 1 mg/ml	5 µg/ml (immunofluorescence (IF) tissue staining)
Neutrophil Elastase (NE)	Abcam, Cambridge, UK	ab68672	Rabbit polyclonal anti-mouse	IgG	Conjugated to AF594 in house with a Life Technologies Alexa Fluor antibody labelling kit to a stock conc of 1 mg/ml	1 µg per 10^6 cells (flow cytometry)
Tumour necrosis factor (TNF)	Biolegend, London, UK	MP6-XT22	Rat monoclonal anti-mouse	$IgG1_{\kappa}$	APC	0.25 µg per 10^6 cells (flow cytometry)
Vascular Endothelial Protein Tyrosine Phosphata	Generated and provided by Prof. Dietmar Vestweber	NA	Rabbit polyclonal anti-mouse	IgG	None	100 - 200 µg/mouse i.v. (confocal IVM and ELISA)

se (VE-PTP)	, Max Plank Institute, Munster, Germany					

Table 2.5. Isotype control and secondary antibodies (Staining antibody cocktails were incubated in a volume of 200 µl for flow cytometry application)

Antibody	**Source**	**Species (clone)**	**Fluorophore**	**Working concentration/ route of administration (Application)**
IgG	R&D Systems, Abington, UK	Goat polyclonal	None	2.5 µg per 10^6 cells (flow cytometry)
IgG2a	R&D Systems, Abington, UK	Rat monoclonal, raised against the immunogen keyhole limpet hemocyanin (KLH) (#54447)	None	1 mg/kg i.v. (confocal IVM)
IgG	Thermofisher, Waltham, MA, USA	Rabbit polyclonal	None	100 - 200 µg/mouse i.v. (confocal IVM) or 200 µg/400 µl i.s. (ELISA)
$IgG1_K$	Biolegend, London, UK	Rat monoclonal, raised against the immunogen KLH + Trinitrophenol (RTK2071)	APC	0.25 µg per 10^6 cells (flow cytometry)
IgG	Biolegend, London, UK	Armenian hamster monoclonal, raised against the immunogen KLH + Trinitrophenol (HTK888)	PE-Cy7	1 µg per 10^6 cells (flow cytometry)
$IgG2b_K$	Biolegend, London, UK	Rat monoclonal, raised against the immunogen KLH + Trinitrophenol (RTK4530)	PE-Dazzle594	0.125 µg per 10^6 cells (flow cytometry)
$IgG2b_K$	Biolegend, London, UK	Rat monoclonal, raised against the immunogen KLH + Trinitrophenol (RTK4530)	AF488	1 µg per 10^6 cells (flow cytometry)

$IgG2b_K$	Biolegend, London, UK	Rat monoclonal, raised against the immunogen KLH + Trinitrophenol (RTK4530)	BV711	0.125 µg per 10^6 cells (flow cytometry)
$IgG2b_K$	Biolegend, London, UK	Rat monoclonal, raised against the immunogen KLH + Trinitrophenol (RTK4530)	PB	1 or 0.125 µg per 10^6 cells (flow cytometry)
$IgG2a_K$	Biolegend, London, UK	Rat monoclonal, raised against the immunogen KLH + Trinitrophenol (RTK2758)	BV605	0.25 µg per 10^6 cells (flow cytometry)
$IgG2a_K$	Biolegend, London, UK	Rat monoclonal, raised against the immunogen KLH + Trinitrophenol (RTK2758)	AF488	0.25 µg or 1 µg per 10^6 cells (flow cytometry)
$IgG2a_K$	Biolegend, London, UK	Rat monoclonal, raised against the immunogen KLH + Trinitrophenol (RTK2758)	APC-Cy7	0.25 µg per 10^6 cells (flow cytometry)
$IgG2a_K$	Biolegend, London, UK	Rat monoclonal, raised against the immunogen KLH + Trinitrophenol (RTK2758)	PB	1 µg per 10^6 cells (flow cytometry)
$IgG2a_K$	Biolegend, London, UK	Rat monoclonal, raised against the immunogen KLH + Trinitrophenol (RTK2758)	PE	0.25 µg per 10^6 cells (flow cytometry)
$IgG2a_K$	Biolegend, London, UK	Rat monoclonal, raised against the immunogen KLH + Trinitrophenol (RTK2758)	AF647	1 µg per 10^6 cells (flow cytometry)
IgG2b	Thermofisher, Waltham, MA, USA	Rat monoclonal, immunogen raised against is proprietary information (eB149/10H5)	PE	0.5 µg per 10^6 cells (flow cytometry)
IgG	Thermofisher, Waltham, MA, USA	Goat polyclonal	Biotin	1 µg per 10^6 cells (flow cytometry)
IgG	Abcam, Cambridge, UK	Rabbit polyclonal	AF594	1 µg per 10^6 cells (flow cytometry)

Table 2.6. Streptavidin and Alexa-Fluor™ conjugates

Reagents	Source	Fluorophore	Working concentration (Application)
Streptavidin	Thermofisher, Waltham, MA, USA	AF647	1 µg/ml (confocal IVM and flow cytometry)
Alexa Fluor® labelling kit	Thermofisher, Waltham, MA, USA	AF488 or AF555 or AF594 or AF647	Conjugated to 100 µg of primary antibody according to manufactures instructions

Table 2.7. Inflammatory stimuli

Stimulus	Source	Cat No.	Working concentration/dose (route of administration)
Histamine	Sigma Aldrich, Poole, Dorset, UK	H7250	30 µM, (topical) at 1 ml/min, or i.s. 400 µl
Leukotriene B4 (LTB_4)	Cambridge Bioscience Ltd, Cambridge, UK	20110	300 ng/400 µl (i.s.)
Recombinant Mouse Interleukin-1β (IL-1β) /IL-1F2	R&D Systems, Abingdon, UK	401-ML-005/CF	50 ng/400 µl (i.s.)
Recombinant Vascular Endothelial Growth Factor 164 (VEGF)	R&D Systems, Abingdon, UK	493-MV-025	4 µg/100 µl (i.v.)
Lipopolysaccharide (LPS) E.coli O111:64	Sigma Aldrich, Poole, Dorset, UK	L4391	500 ng/ml (*ex vivo*)

Table 2.8. ELISA and RNA Isolation kits

Kit	Source	Cat No.
Mouse CXCL1 DuoSet ELISA kit	R&D Systems, Abington, UK.	DY453-05

2.2. Animals

All *in vivo* experiments were conducted under the UK legislation according to the Animal Scientific Procedures Act 1986, with the animals humanely sacrificed *via* cervical dislocation at the end of experiments in accordance with UK Home Office regulations. Animals were housed in individually ventilated cages and provided with food and water ad libitum, with a 12 hr light-dark cycle maintained throughout. All mice used were over the age of 8 weeks and weighed between 25 - 30 g.

Table 2.9. Mouse strains

Strain/Gene Nomenclature (Abbre*via*tion used in thesis)	**Description**	**Origin**	**Reference**
C57BL/6 (WT)	Wild-type black mouse.	Charles River, Margate, UK.	https://www.criver.com/products-services/find-model/c57bl6-mouse?region=3671
LysM-EGFP$^{ki/ki}$	EGFP gene 'knock in' into the *LysM* gene, resulting in a homozygous EGFP expression in monocytes+ and granulocytes++. These mice were used to generate *LysM-EGFP* heterozygous (*LysM-EGFP*$^{ki/+}$) mice as detailed in section 2.2.2.	Commercially available (Jackson Laboratory), provided by Dr. Thomas Graf, Centre for Genomic Regulation, Barcelona, Spain and provided by Dr. Markus Sperandio (Ludwig-Maximillians University, Germany).	(Faust et al., 2000)
Tnfrsf1a$^{-/-}$ *;Tnfrsf1B*$^{-/-}$ (*TNFRI/II*^{KO})	Global knock out. Mice deficient in both the *Tnfrsf1a* (p55) and *Tnfrsf1b* (p75) genes as detailed in section 2.2.3.	Commercially available (Jackson Laboratory), donated by Dr. J. Peschon, Amgen, Department of Molecular Immunology, Immunex Corp., Seattle, USA.	(Peschon et al., 1998)
Cdh5^{tm5Dvst} (*VEC-Y685F*) and Cdh5$^{tm2(Cdh5)Dvst}$ (*VEC-WT*)	Targeted 'knock in' inserted into the *Cdh5* (VE-cadherin) gene as detailed in section 2.2.4.	Donated by Prof. Dietmar Vestweber, Max-Planck-Institute for Molecular Biomedicine, Münster, Germany.	(Wessel et al., 2014)
Mrp8-Cre-IRES-EGFP, (Mrp8-Cre)	Transgenic. Cre recombinase inserted downstream of the MRP8 promotor. Mice were used to generated neutrophil-TNF knock out mice as detailed in section 2.2.6 and Chapter 6.	Commercially available (Jackson Laboratory), donated by Dr. E. Passegue (Institute of Cancer and Stem Cell Biology and Medicine, Stanford University, USA).	(Passegué et al., 2004)
Tnf$^{flox/flox}$	Targeted gene modification ('knock in') creating a floxed allele in the *Tnf* gene. Mice were used to generate neutrophil-TNF knock out mice as detailed in section 2.2.6 and Chapter 6.	Bred in house following permission from Prof. S. Nedospasov, Molecular Immunology, Russian Academy of Sciences, Moscow, Russia) and provided by the laboratory of Prof. F. Balkwill (Barts Cancer Institute, QMUL, UK).	(Grivennikov et al., 2005)

2.2.1. Wild-type mice

Commercially purchased male wild-type (WT) C57BL/6 mice were allowed to acclimatise for one week prior to experimental use.

2.2.2. *LysM-EGFP*$^{ki/+}$ mice

LysM-EGFP$^{ki/+}$ mice exhibit fluorescently labelled myelomonocytic cells in which mature monocytes express EGFP at low levels and mature neutrophils at much higher levels (Woodfin et al., 2011). In brief, *LysM-EGFP*$^{ki/ki}$ mice were generated by knocking-in EGFP cDNA into the lysozyme M (*LysM*) locus, containing the coding part of exon 1 (including the start codon) and parts of intron 1. Mice were backcrossed for a minimum of 8 generations with WT mice (Faust et al., 2000). In-house experimental heterozygous *LysM-EGFP*$^{ki/+}$ mice were generated by crossing *LysM-EGFP*$^{ki/ki}$ mice with WT mice.

2.2.3. TNFRI/II^{KO} mice

TNF receptor I (TNFRI) and II (TNFRII) double receptor knockout (*TNFRI/II*^{KO}) mice, back crossed onto a WT background for a minimum of 8 generations, were acquired from Jackson Laboratory. These mice were generated by Peschon and colleagues *via* the intercrossing of singly receptor deficient mice (*Tnfrs1a* $^{tm1/mx}$ *x Tnfrsf1b* $^{tm1/mx}$) (Peschon et al., 1998). Once imported, *TNFRI/II*^{KO} mice were then successively intercrossed in house to maintain the colony.

2.2.4. VE-cadherin-Y685F (*VEC-Y685F*) and control VE-cadherin-WT (*VEC-WT*) mice

VEC-Y685F and *VEC-WT* mutant mice were provided by Prof. Dietmar Vestweber (Max Plank Institute, Munster, Germany). *VEC-Y685F* mice were engineered to encode a single amino acid substitution, converting a tyrosine amino acid to phenylalanine, *via* substitution of a Y to F codon at position 685 of the VE-cadherin receptor (*VEC-Y685F*).

As a control, the locus encoding VE-cadherin was targeted with cDNA encoding WT VE-cadherin (*VEC-WT*) (Wessel et al., 2014). *VEC-Y685F* mice have been shown to have no effect on leukocyte migration but have a defect in vascular permeability (Wessel et al., 2014). Mice were irradiated and reconstituted with bone marrow from *LysM-EGFP*$^{ki/+}$ mice as detailed below in section 2.2.5.1 by our collaborators. This allowed for the visualisation of neutrophils by confocal intravital microscopy (confocal IVM) for experiments conducted in-house, aimed at analysing neutrophil transendothelial migration (TEM) dynamics in inflamed tissues.

2.2.5. Generation of chimeric mice

All donor and recipient mice intended for the generation of chimeras were treated as follows: 7 days prior to irradiation all recipient animals were placed on sterile tap water supplemented with 0.08% Baytril (enrofloxacin), a broad-spectrum fluoroquinolone antibiotic commonly used for the management of bacterial diseases in dogs and cats. The purpose of this treatment was to reduce the risk of the irradiated mice developing bacterial infections during the recovery period.

2.2.5.1. Generation of LysM-EGFP$^{ki/+}$ - VEC-Y685F or VEC-WT chimeras

VEC-Y685F and littermate control (*VEC-WT*) mice were irradiated with 2 doses of 5 Gy, 4 hr apart using a RadSource-2000 irradiator and placed in fresh cages provided with wet mash diet. 24 hr post irradiation, the mice were injected i.v. with freshly isolated *LysM-EGFP*$^{ki/+}$ bone marrow. In brief, the donor mouse was culled and swabbed with 70% ethanol and the hind legs were removed, cutting at the ball of the hip joint to leave the femur intact. The skin and muscle tissue were removed, and in a laminar flow hood, the bones were briefly soaked in 70% ethanol and then washed in sterile PBS. The bone marrow (BM) was flushed out from both the femur and tibia bones with 10 ml/leg of cold-sterile PBS. Afterwards, the cells were filtered through a 100 µm nylon mesh filter and centrifuged at 300 g for 5 min and the cell pellet resuspended in ACK lysis buffer (150 mM NH_4Cl, 1 mM $KHCO_3$, 0.1 mM EDTA) for 5 - 7 min at room temperature to lyse the erythrocytes. The cell suspension was centrifuged again as above, resuspended in

PBS and counted using a haemocytometer. The cell density was then adjusted to 7.5 x 10^6 cells/ml and 200 µl injected i.v. into each recipient mouse. Reconstitution of *VEC-WT* or *VEC-Y685F* recipients with *LysM-EGFP*$^{ki/+}$ BM was assessed by flow cytometry as detailed in section 2.2.5.3.

2.2.5.2. Generation of haematopoietic-derived cell (HDC)-TNFRI/II^{KO} and WT chimeras

In a similar series of experiments, WT or *LysM-EGFP*$^{ki/+}$ recipient mice were irradiated and then reconstituted with BM from WT or *TNFRI/II*^{KO} donor mice as described above. This resulted in the generation of chimeric mice exhibiting WT HDCs (WT-BM->-WT) or *TNFRI/II*^{KO} null HDCs (TNFRI/II KO-BM->-WT), respectively. Reconstitution of WT recipients with *TNFRI/II*^{KO} or WT BM was assessed by flow cytometry as detailed in section 2.2.5.3.

2.2.5.3. Flow cytometry to assess haematopoietic reconstitution of chimeric animals

Flow Cytometry was employed to assess the reconstitution of WT or *LysM-EGFP*$^{ki/+}$ mice with BM of *TNFRI/II*^{KO}- or WT control- mice, and in an alternate series of experiments, in *VEC-WT* and *VEC-Y685F* mice with BM from *LysM-EGFP*$^{ki/+}$ mice. 4-6 weeks after BM transfer, reconstitution of the haematopoietic system in all recipient mice was assessed by flow cytometry as follows: 10 µl of blood was collected in 50 µl of PBS with 5 mM ETDA *via* a tail vein bleed. Samples were then centrifuged at 400 g for 5 min and the cell pellet was re-suspended in ACK lysis buffer for 5 min at room temperature. 20 µl of counting eBeads were added post blood collection for the *TNFRI/II*$^{KO/WT}$ experimental mice and just after the ACK lysis steps for the *VEC-Y865F/WT* mice. The cell suspension was then centrifuged again as above and the pellet washed 3 times with sorting buffer (SB, 2.5 mM EDTA, 0.5% BSA in PBS). Samples were washed again and pre-incubated with anti-CD16/-CD32 (Fc-block) for 10 min followed by incubation with fluorescently conjugated primary antibodies for 40 min at 4^{o}C in the dark. For the detection of *LysM-EGFP*$^{ki/+}$ or *TNFRI/II*^{KO} neutrophils, CD45-PB and Ly6G-PE antibodies or CD45-PB and Ly6G-PE antibodies in combination with an unconjugated goat anti-mouse TNFRI antibody were used, respectively. Samples were then washed 3 times with SB buffer and

the latter further incubated with an anti-goat IgG biotin antibody for 30 min at 4°C in the dark, washed 3 times with SB buffer and then incubated with strept-AF647 as above. In all cases, after a further 3 washes with SB buffer, samples were resuspended in 200 µl of SB buffer and analysed using an LSR Fortessa flow cytometer (Becton Dickinson) and quantified offline using FlowJo software (TreeStar). A minimum of 10,000 neutrophils were recorded. Doublets were first excluded and neutrophils were gated using the markers expressed by the donor populations to quantify the reconstitution efficiency against any remaining host cell populations. Reconstitution was assessed using the following gating strategy, CD45-PB^{+}, Ly6G-PE^{+}, EGFP^{high} or CD45-PB^{+}, Ly6G-PE^{+}, TNFRI-biotin-strept-AF647$^{+/-}$ for *LysM-EGFP*$^{ki/+}$ or *TNFRI/II*^{KO} transfer experiments, respectively. Peripheral neutrophil counts are presented in Chapter 4, section 4.2.2 for *LysM-EGFP*$^{ki/+}$ or Chapter 6, section 6.2.4 for *TNFRI/II*^{KO} null transfer experiments.

2.2.6. Generation of *Mrp8-Cre*;*Tnf*$^{flox/flox}$;*LysM-EGF*$^{ki/+}$ (Neutro-TNF^{KO}) mice

To generate *Mrp8-Cre*;*Tnf*$^{flox/flox}$ mice, *Tnf*$^{flox/flox}$ mice (Grivennikov et al., 2005) were intercrossed with *Mrp8-Cre-IRES-GFP* (Mrp8-Cre) transgenic mice (Passegué et al., 2004), in which the Cre recombinase cDNA is inserted downstream of the *Mrp8* promoter. Myeloid-related protein-8 (MRP8) is an inflammatory protein which has been shown to upregulate expression of pro-inflammatory cytokines such as TNF and contribute to the development of toxic shock syndrome (Vogl et al., 2007). MRP8 is expressed primarily by neutrophils and by approximately 20% of monocytes, allowing for conditional deletion of floxed alleles in these 2 cell populations (Abram et al., 2014). In-house, these mice were crossed with *Tnf*$^{flox/flox}$;*LysM-EGFP*$^{ki/ki}$ mice to generate experimental *Mrp8-Cre*;*Tnf*$^{flox/flox}$;*LysM-EGF*$^{ki/+}$ (Neutro-TNF^{KO}) or *Tnf*$^{flox/flox}$;*LysM-EGF*$^{ki/+}$ (Neutro-TNF^{WT}) mice as depicted in Chapter 6, section 6.2.1. The resultant mice selectively expressed neutrophils that were conditionally deficient in TNF. In addition, through the expression of EGFP, neutrophils and monocytes could be tracked by confocal IVM.

2.2.6.1. Genotyping methods

For genotyping of the animals, ear notch biopsies were taken after weaning and stored at -20°C. Subsequent processing was carried out by Dr. Matthew Golding. In brief, ear notch samples were lysed in 100 µl of DirectPCR lysis reagent (*Via*gen Biotech), containing 200 µg/ml proteinase K overnight at 55°C. The samples were then heated at 85°C for 45 min in order to denature the protease K enzyme rendering it inactive. Subsequently, samples were centrifuged briefly to sediment insoluble material and the crude lysate was stored at 4°C prior to PCR analysis.

The $Tnf^{flox/flox}$, $Tnf^{KO/KO}$ and *MRP8-Cre* transgene sequences were amplified in separate PCR reactions using their respective primer pairs detailed in Table 2.3, and using the reaction constituents detailed in Table 2.10. DNA was amplified in a thermocycler (DNAEngine® Peltier Thermal cycler, Bio-Rad, Hemel Hempstead, UK) using reaction conditions detailed in Table 2.11. Briefly, 4 µl (Flox product) or 4 µl (Cre product) was loaded onto a 2.5% agarose gel and 1.5 µl of SmartLadder SF in adjacent wells. The gel was run at 135 V for 30 min and PCR products visualised under UV light and photographed (data presented in Chapter 6, section 6.2.2). Expected PCR products were then determined according to Table 2.12.

Table 2.10. PCR master mix

Reagent	Volume per sample	Concentration
Forward primer (stock 100 µM)	0.08 µl	0.8 µM
Reverse primer (stock 100 µM)	0.08 µl	0.8 µM
DirectPCR Lysis Reagent crude lysate	0.1 µl	-
Megamix Blue PCR mastermix	10 µl	-
Total	10.26 µl	-

Table 2.11. PCR reaction conditions

PCR programme		
Initial denaturation	94°C for 3 min	1 cycle
Denaturation	94°C for 30 sec	30 cycles
Annealing	60°C for 30 sec	
Elongation	72°C for 30 sec	
Final extension	72°C for 3 min	1 cycle
Hold sample	10°C	-

Table 2.12. Expected PCR products

Product	Molecular Weight
Tnf$^{flox/flox}$ allele	450 bp
Cre transgene	325 bp

2.2.6.2. TNF protein expression analysis using flow cytometry

Flow cytometry was used to assess total TNF protein expression of neutrophils and monocytes in order to validate *Mrp8*-Cre mediated *Tnf* deletion efficiency in the Neutro-TNF^{KO} mouse model. Experimental details can be found in Chapter 6, section 6.2.3.

2.4. Confocal intravital microscopy on the mouse cremaster muscle

To investigate hallmarks of acute inflammation such as neutrophil-EC interactions and vascular leakage overtime, a confocal IVM platform was developed for simultaneous visualisation and quantification of these two phenomena *via* confocal microscopy *in vivo*. In this section, the core methodology enabling investigations into neutrophil-EC interactions is detailed in accordance to Woodfin et al., 2011, while further specialised methodology details are described in their relevant result chapters. This includes details of imaging and quantification of vascular leakage that is reported in Chapter 3.

Under isoflurane (intranasal) anaesthesia, male *LysM-EGFP*$^{ki/+}$ mice, which exhibit green fluorescent neutrophils, received an i.s. injection of PBS (400 µl) containing 4 µg of the non-blocking anti-CD31-AF647 or AF555 antibody in order to fluorescently label endothelial cell junctions and in some cases together with IL-1β (50 ng) or LTB_4 (300 ng) to elicit an inflammatory response. These animals were then allowed to recover for 2 hr or 30 min, respectively. 30 min prior to tissue exteriorisation, the mouse was subjected to terminal anaesthesia by intraperitoneal injection of ketamine (100 mg/kg) and xylazine (10 mg/kg). The animals were kept fully anaesthetized and maintained on a heated custom-built Perspex® microscope stage throughout the entire imaging period. To maintain deep anaesthesia, mice were subjected to additional periodic intramuscular (i.m.) administration of 1 ml/kg anaesthetic mix (40 mg ketamine and 2 mg xylazine in saline) approximately every 20-30 min. The depth of anaesthesia was monitored every 10-15 min using the pedal reflex to ensure the animals felt no discomfort at any time.

Cremaster muscles were prepared for intravital imaging as previously described (Woodfin et al., 2011; Colom et al., 2015). Briefly, one testis was gently exteriorised by making an incision at the base of the skin of the scrotum. The cremaster muscle around the testis was incised longitudinally (avoiding cutting through major arteries and veins/large venules) and laterally pinned out over the optical window of a custom-made microscope stage. The tissue was kept warm and superfused with pre-warmed Tyrode's balanced salt solution. The vasculature integrity in the tissue was assessed to ensure there was good blood flow in approximately 90% of all vessels before leukocyte responses were quantified by IVM over a 1.5 - 2 hr period. In some experiments, the mice were subjected to acute IR-injury of the cremaster muscle prior to confocal imaging. For this purpose, vessels of the cremaster muscle were occluded using two overlapping non-crushing Schwartz Micro Serrefine clamps which were used to occlude the blood supply to the cremaster muscle (**Fig. 2.1**). The effectiveness of this procedure was validated by viewing the cremaster muscle under brightfield illumination to confirm that blood flow had stopped. The cremaster muscle was consistently superfused with warm Tyrode's solution throughout this ischaemic phase (maximum of 40 min). The clamps were then removed to initiate the reperfusion phase and the return of adequate blood flow was verified by brightfield microscopy. The tissue was allowed to reperfuse for 2 hr during which leukocyte-vessel wall interactions were imaged. Sham operated

mice underwent an identical surgical procedure with the exception of placement of the clamps. Z-stack images of 'straight walled' post-capillary venules measuring 20–40 µm in diameter were imaged to record leukocyte–vessel wall interactions using Leica SP5 or SP8 confocal microscopes incorporating a 20x water-dipping objective (NA 1.0). Images were acquired every minute with sequential scanning of different channels at a resolution of 1024 x 450 pixels, corresponding to a voxel size of approximately 0.25 x 0.25 x 0.69 µm in the x-y-z planes. Z-stacks comprised of approximately 60 optical sections. Each stack routinely took 40 seconds to acquire on the SP8 platform using the 8,000 Hz resonance scanner, thus enabling high temporal and spatial resolution of leukocyte behaviour. At the end of the procedure, all animals were culled *via* cervical dislocation or *via* exsanguination according to UK Home Office regulations.

Figure 2.1. Photograph showing IR-injury of the cremaster muscle. The cremaster muscle (highlighted with a red arrow) is flat-mounted and pinned over an optical window of a custom made microscope stage. Two serrefine clamps (highlighted with black arrows) are placed at the anterior aspect of the of the cremaster muscle to occlude the afferent blood supply, thus inducing ischaemia.

2.5. IMARIS analysis of neutrophil migration

IMARIS software (Bitplane, Oxford Instruments, Zurich, Switzerland) enabled the off-line analysis of confocal image sequences to visualise and quantify neutrophil-EC interactions and vascular leakage in high temporal and spatial resolution overtime. Lif files generated on the Leica confocal microscopes were then opened in IMARIS Bitplane

software and saved as an Ims file. For visualisation purposes, anti-CD31 staining was underwent thresholding to a point in which predominantly only junctional staining was visible to allow for greater ease when quantifying neutrophil TEM at EC junctions. Images were all processed for image smoothing using a median filter on the anti-CD31 staining and neutrophil EGFP fluorescence. Subsequently for sequential images (i.e. those that generated timecourses) underwent an additional step to facilitate drift correction to minimise the amount of autonomous drift of the vessel from its original location. Here, using an IMARIS spots tool, a spot was placed in the same location (i.e. picking a unique recognisable vessel reference point) and was subsequently placed on the same location over all frames. The software then can correct for translational and rotational drift.

Numerous neutrophil responses were quantified. Most notably, normal neutrophil TEM was classified as a response in which the cells migrated through EC junctions in a luminal-to-abluminal direction without pausing. In contrast, neutrophils exhibiting reverse TEM (rTEM) were defined as cells that moved in an abluminal-to-luminal direction through EC junctions as previously described (Woodfin et al., 2011; Colom et al., 2015). This included cells that fully or partially breached the endothelium from the vascular lumen before exhibiting reverse motility through EC junctions and re-entering the blood circulation (**Fig. 2.2**).

In some experiments, the duration of neutrophil migration was measured from the timepoint at which the neutrophil initiated breaching of the endothelium through an endothelial pore until the time point at which the neutrophil had fully migrated and was in the sub-endothelial space. To assess interstitial motility, IMARIS software was used to generate tracks that followed the movement of the neutrophil within the interstitial tissue. This was achieved *via* the placement of a tracking dot at the centre of the neutrophil from the timepoint it exits the pericyte layer for a minimum of 7 min. IMARIS software then generates a value based on the placement of the track to determine the interstitial velocity of the neutrophil. For neutrophil duration and interstitial velocity an average of 10 neutrophils/mouse were assessed with data presented as the average neutrophil- TEM duration (min) or interstitial speed (μm/min) per mouse, respectively. Additionally, the temporal nature of the extravascular leakage response was analysed as described in Chapter 3, section 3.2.1.

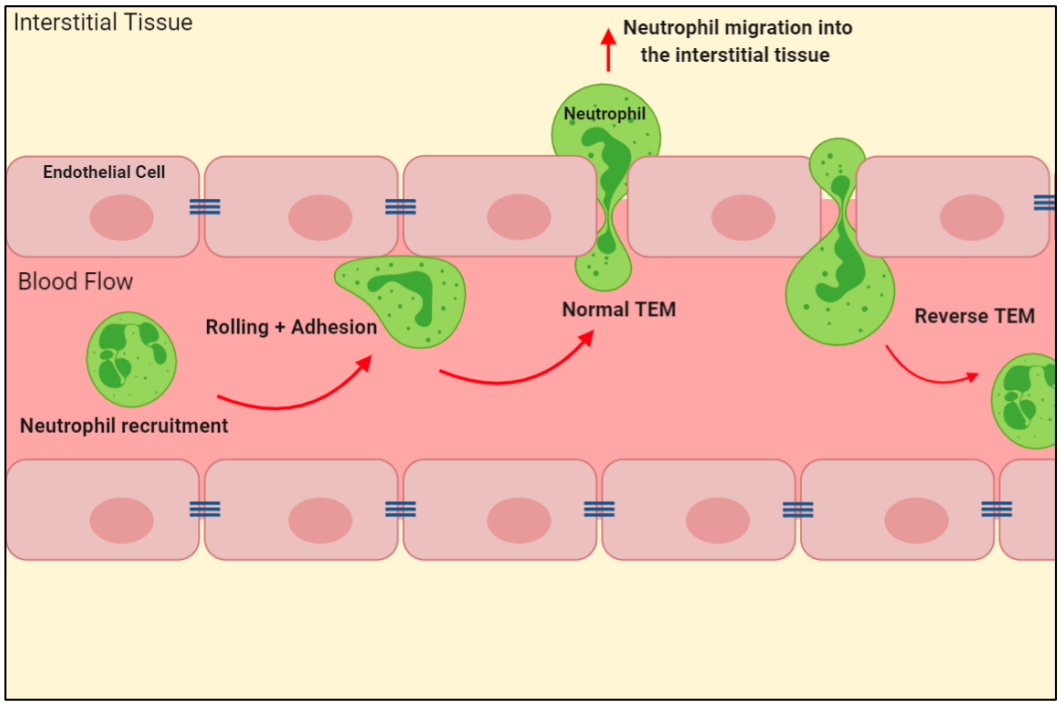

Figure 2.2. Schematic representation depicting normal and reverse modes of neutrophil transendothelial migration (TEM) in a post-capillary venule.

2.6. Acquisition and quantification of total neutrophil extravasation

To quantify the total number of extravasated EGFP$^+$ neutrophils from *LysM-EGFP$^{ki/+}$* mice in the extravascular space, 4-6 representative still confocal images of post-capillary venules measuring 300 µm x 300 µm were acquired. Each image consisted of ~60 - 75 individual steps, each measuring 0.69 µm, at the end of the confocal IVM experiment. These images were then analysed using IMARIS software, which identified extravascular EGFP$^+$ neutrophils that had fully transmigrated through the endothelial layer (**Fig. 2.3**). Fully extravasated neutrophils in the interstitial tissue were identified as those that had returned to a more spherical as opposed to the flattened morphology that is characteristic of neutrophils within the sub-endothelial space. In experiments using mice that did not possess EGFP$^+$ neutrophils, post real-time imaging, tissues were fixed and immunostained for the neutrophil marker MRP14, using established protocols (Woodfin et al., 2011; Colom et al., 2015). Briefly, cremaster muscles were fixed in ice-cold PFA (4% in PBS) for 40 min, blocked and permeabilised at room temperature for 4 hr in PBS containing 25% FCS and 0.5% Triton X-100, and then incubated overnight at 4°C with a rat AF647 or AF488 conjugated anti-MRP14 mAb diluted in PBS containing

10% FCS. Tissues were then washed 3 times in PBS and flat mounted under a coverslip using a Leica SP5 or SP8 confocal microscope as detailed previously. Post-acquisition, images were analysed off-line using IMARIS software. All total neutrophil extravasation quantification was presented as the total number of extravasated neutrophils per mm^3 of tissue.

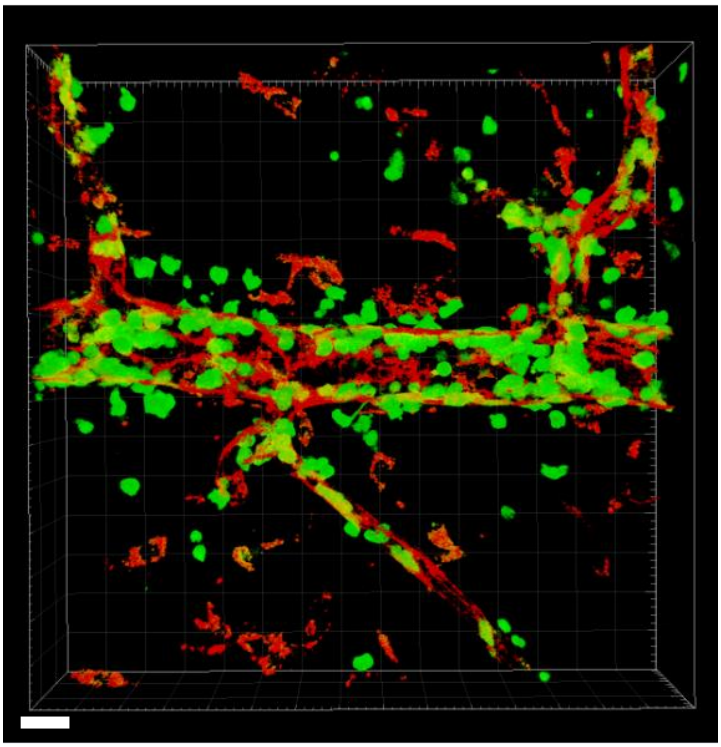

Figure 2.3. Representative 3D image reconstruction of a postcapillary venule from a *LysM-EGFP*$^{ki/+}$ mouse using IMARIS software to quantifiy total neutrophil extravasation into the surrounding tissue. The image displays EGFP$^+$ neutrophils (green) and fluorescently labelled PECAM-1 on endothelial cells (red). Scale Bar: 20 µm.

2.7. Quantification of plasma and tissue CXCL1 levels

Plasma and tissue levels of CXCL1 post-treatment with IL-1β + histamine or following IR-injury (as detailed in section 2.4), were analysed by ELISA in collaboration with Dr. Régis Joulia.

Mouse plasma and cremaster muscle tissues were collected after 40 min of ischaemia and 30 min of reperfusion or alternatively after 2 hr of locally injected IL-1β (50 ng in 200 µl PBS, i.s.) followed by 30 min of locally injected histamine (200 µl of a 30 µM

solution, i.s.) or PBS control (200 µl). In some experiments, anti-VE-PTP (100 - 200 µg) or rabbit IgG control (200 µg) antibodies were injected i.v. 90 min after IL-1β injection in 100 µl of PBS and blood samples were collected at the end of the confocal IVM acquisition (1 hr post histamine). Whole blood was collected from the ascending vena cava and decanted into 50 µl of a 50 mM EDTA-PBS solution, immediately centrifuged for 10 min at 2000 g and the plasma was collected. Cremaster muscles were weighed and then homogenized in 500 µl PBS containing 0.1% Triton and 1% Halt Protease and Phosphatase Inhibitor Cocktail (ThermoFisher) using the Precellys24 bead-beating system (Bertin Technologies, France). Tissue samples were then centrifuged for 5 min at 10,000 g and the supernatant collected to determine CXCL1 content in parallel with the plasma samples from above. All samples were snap frozen in liquid N_2 prior to their thawing and analysis by ELISA, using a commercial kit as per manufacturer's instructions. Data obtained from plasma was presented as picogram (pg) of CXCL1 per ml of plasma and for tissue as pg of CXCL1/mg of protein.

2.8. Statistics

All data were analysed using GraphPad Prism 8 software (GraphPad, San Diego, CA, USA) and are expressed as mean ± standard error of the mean (SEM). As the experiments conducted in this thesis have been utilised in our lab and were previously identified to exhibit a normal distribution, we assumed our data sets exhibit a normal distribution and thus we applied the corresponding tests. Statistical significance between two groups was assessed by an unpaired student t-test. To determine significance between multiple groups (e.g. different stimuli treatment groups) a one-way analysis of variance (ANOVA) or two-way ANOVA was used followed by a Bonferroni post hoc test as appropriate. P values < 0.05 were considered significant.

Chapter 3

Development and application of a confocal intravital microscopy method for simultaneous analysis of microvascular leakage and neutrophil TEM

3.1. Introduction

Inflammation is a physiological response that develops rapidly following sterile or non-sterile insults such as tissue damage (e.g. IR-injury) or infection. Principal hallmarks of this critical response are leukocyte infiltration of tissues and tissue oedema as the result of enhanced/abnormal vascular permeability. Both phenomena typically occur acutely following stimulation and are essential in mediating the pro-inflammatory response. Furthermore, both phenomena are critical in ensuring efficient host defence, providing rapid resolution and tissue repair, essential processes for our survival. However, excessive or dysregulated infiltration of pro-inflammatory leukocytes and tissue oedema can lead to the development of acute and chronic inflammation as illustrated by pathologies such as acute lung injury, myocardial infarction, arthritis or multiple organ failure (Park-Windhol and D'Amore, 2016; Chen et al., 2018).

Fundamentally, both vascular leakage and trafficking of leukocytes from the blood circulation into the surrounding tissues are governed by the integrity of the vessel wall, and in particular the endothelium. Composed of a monolayer of ECs, the endothelium is the first cellular barrier between the lumen and the extravascular space, composed by the presence of specific intercellular molecular complexes between adjacent cells. These complexes form junctional structures known as tight junctions (composed of claudins, occludins and JAMs) and adherens junctions (composed of nectins and cadherins), which are connected to the cytoskeleton of the ECs and collectively maintain the junctional barrier to macromolecules and immune cells (Dejana, 2004; Dejana et al., 2008; Chistiakov et al., 2015). Under basal conditions, EC junctions allow minimal plasma protein leakage into the tissue that primarily occurs through the paracellular route. However, under inflammatory conditions the EC junctional barrier is disrupted by two significant mechanisms. Firstly, ligation of pro-inflammatory molecules (e.g. histamine and VEGF) to their respective GPCRs induces a build-up of intracellular Ca^{2+} and the activation of intracellular protein kinases (Vestweber et al., 2014). This in turn leads to actinomyosin-based contractions and dissolution of radical stress fibres which together results in the exertion of pulling forces on ECs and destabilisation of EC junctional contacts (Bates, 2010; Frye et al., 2015). Secondly, this ligation can perturb the function of key stabilising junctional adhesion molecules, such as VE-cadherin, by inducing their

internalisation and therefore loss of their corresponding intercellular tethers (Guo et al., 2008; Sun et al., 2012). Collectively, these events disrupt the endothelial integrity that results in a rapid increase in luminal-to-abluminal leakage of plasma fluids, solutes and proteins (e.g. complement proteins and antibodies) into injured or infected tissues to aid bacterial recognition/removal and hence promote tissue repair. Furthermore, EC junctional integrity also plays a vital role in facilitating controlled entry of leukocytes across the EC barrier, a process predominately mediated by paracellular breaching of EC junctions.

Neutrophil migration through the endothelium is a multifaceted and highly regulated process. Once recruited to the vasculature near the site of injury or infection, commonly in response to locally generated DAMPs and PAMPs, neutrophils interact with ECs as described by the leukocyte adhesion cascade (see Chapter 1, section 1.5). This response begins with capture and rolling of free-flowing neutrophils along the endothelium, followed by firm arrest, luminal crawling and ultimately transendothelial migration (TEM); all of which are mediated by various adhesion molecules. Neutrophil TEM itself is mediated by several key EC junctional molecules (Nourshargh and Alon, 2014; Muller, 2016) in addition to chemotactic directional cues across the endothelium. Chemotaxis of neutrophils to the site of damaged or infected tissue is governed by the presence and levels of chemokines such as CXCL1 and CXCL2 that are released by ECs, pericytes and resident tissue cells such as mast cells and macrophages (Jin, 2013; Girbl et al., 2018; Majumdar et al., 2016). These directional cues are further enhanced by the secretion of secondary chemotactic agents such as LTB_4, generated by neutrophils, that act in an autocrine and paracrine manner to prime and activate neighbouring neutrophils (Majumdar et al., 2016). Response to these chemotactic directional cues are governed by transmembrane GPCRs, which are uniformly distributed on the neutrophil cell surface, and that link to, and dissociate from heterotrimeric G-proteins. These G-proteins induce intracellular signalling that leads to continuous growth of the actin cytoskeleton towards the sensing-edge of the cell, resulting in a polarised morphology consisting of a leading and trailing edge (Xu et al., 2005; Janetopoulos and Firtel, 2008); ultimately leading to neutrophil diapedesis and tissue infiltration.

The distinct mechanisms underpinning vascular leakage and neutrophil migration have been widely reported in the literature. For example, early investigations from Hurley *et*

al., identified that following histamine treatment, endothelial gaps that supported microvascular leakage were not associated with sites of neutrophil migration in rat skin (Hurley, 1963). Subsequently, Baluk *et al*., reported that allergen-induced leukocyte migration and vascular leakage occurred at distinct locations from each other in post-capillary venules of the rat trachea (Baluk et al., 1998). Furthermore, neutrophil migration has been shown to occur independently of vascular leakage as supported by the formation of an F-actin-rich contractile endothelial pore, which prevented vascular leakage occurring at the site of leukocyte migration (Heemskerk et al., 2016). In another important example, VE-cadherin is known to play a vital role in controlling vascular leakage and neutrophil migration (Broermann et al., 2011; Vestweber, 2012) (see Chapter 1, section 1.4.2 & 1.7.1 for details). To further elucidate the function of VE-cadherin, additional formative studies have been conducted by Wessel et al., using a knock-in mouse model expressing specific point mutations within the VE-cadherin complex at either Tyr685 (*VEC-Y685F*) or Tyr731 (*VEC-Y731F*). Here, it was identified that phosphorylation of these distinct residues was essential for vascular leakage and leukocyte migration, respectively. Furthermore, phosphorylation of Tyr685 was detected in venules but not arterioles following treatment with histamine, whereas the action of VEGF was even more restricted and only induced phosphorylation in a sub-population of capillaries (Wessel et al., 2014).

Despite these seminal observations, recent studies have demonstrated a potential interplay between these two phenomena culminating in the general consensus that adhered and transmigrating neutrophils in vasculature can impact microvascular leakage through the direct secretion of vasoactive mediators. These include ROS (Segal and Jones, 1978; Smith, 1994), HBP (Kenne et al., 2019), TNF (Djeu et al., 1990; Finsterbusch et al., 2014), VEGF (Scapini et al., 2004) and LTA_4, the precursor for the generation of LTB_4 (Wedmore and Williams, 1981; DiStasi and Ley, 2009). Nevertheless, whether microvascular permeability can impact neutrophil TEM dynamics is a subject that remains poorly understood and provides the basis of this Chapter (**Fig. 3.1**).

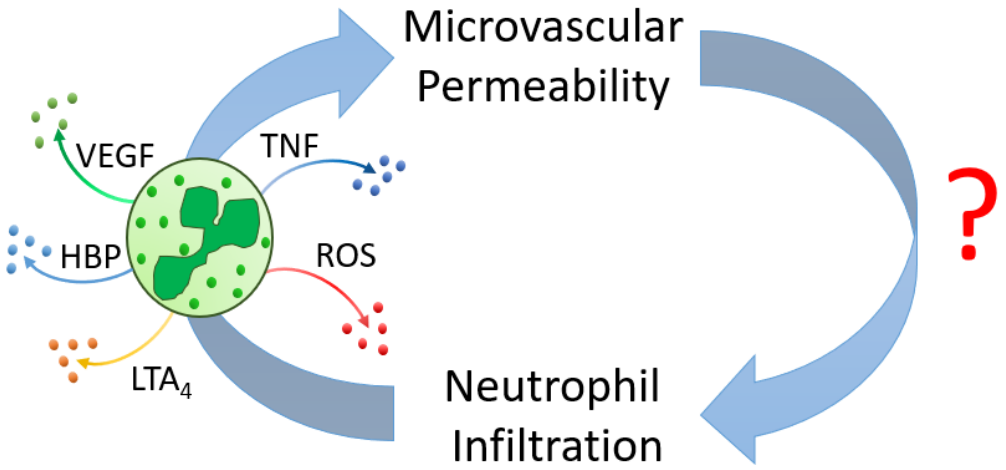

Figure 3.1. Investigating the role of microvascular leakage on neutrophil dynamics. Investigation into the interplay between microvascular leakage and neutrophil infiltration has provided extensive understanding and identification of the factor's neutrophils generate and release to induce vascular leakage (ROS, VEGF, HBP, TNF, LTA_4). Although not shown in Fig 3.1, a number of cells (e.g. macrophages, ECs, monocytes and mast cells) are also able to secrete factors capable of inducing changes in microvascular permeability in addition neutrophils. However, what role microvascular leakage has on neutrophil migration dynamics remains poorly understood and contentious offering a novel direction for scientific investigations and provides the basis on this thesis.

3.1.1. Scope of the Chapter

This Chapter sought to investigate the potential inter-play between enhanced vascular permeability and neutrophil TEM as investigated by confocal IVM. To this end, the key aims of this Chapter were as follows:

- To establish a reliable intravital microscopy-based experimental approach for the simultaneous visualisation of neutrophil TEM and vascular leakage.
- To develop rigorous quantification methods to measure neutrophil TEM and vascular leakage in defined models of acute inflammation.
- To analyse potential temporal relationships of neutrophil TEM and enhanced vascular leakage.

3.2. Results

3.2.1. Development of a confocal intravital microscopy methodology for simultaneous analysis of neutrophil transendothelial migration and vascular leakage

In order to simultaneously visualise and quantify neutrophil migration and vascular leakage in real time, experiments were conducted using *LysM-EGFP*$^{ki/+}$ mice that express high levels of enhanced GFP (EGFP) in neutrophils, and to a lesser extent, in monocytes/macrophages. In addition, we injected locally a fluorescently-labelled anti-CD31 antibody to label the endothelial vasculature, thus enabling examination of neutrophil-EC interactions as previously described (Huang et al., 2006; Woodfin et al., 2009; Colom et al., 2015; Woodfin et al., 2016). To concomitantly visualise vascular leakage, fluorescently (i.e. TRITC)-labelled dextran, a branched polysaccharide with good solubility and low *in vivo* toxicity, was used. This methodology was applied to an experimental model of IR-injury that has previously been shown to elicit both neutrophil migration and vascular leakage (Woodfin et al., 2011; Voisin et al., 2019), making it an ideal test-bed for validation of the approach.

Briefly, male mice received an i.s. injection of a non-blocking anti-CD31 mAb conjugated to AF647 in a vehicle solution (PBS) for 30 min to label ECs. The cremaster muscle was then exteriorised, and ischaemia of the tissue was induced *via* the placement of clamps at the base of the cremaster muscle for 40 min. Upon their removal, reperfusion was initiated and imaging acquisition by confocal IVM began (further detailed in Chapter 2, section 2.4). At the point of image acquisition, all mice were subjected to an i.v. injection of fluorescent TRITC-dextran (75 kDa, 40 mg/kg in 100 µl of PBS). Three lasers were used to activate and detect the fluorescence emitted by the EGFP (Argon 488 laser), anti-CD31-AF647 (HeNe 633 laser) and TRITC-dextran (DPSS 561 laser). The 488 and 647 were run on one scan and the TRITC was detected on a second sequential scan, over the period of 1 min, to avoid spectral overlap from the different fluorescent channels.

Offline analysis of the 4D image sequences was subsequently performed using IMARIS Bitplane software. Images were first processed for IMARIS analysis as described in

section 2.5. Additionally, enhanced vascular leakage was analysed by generating 6-8 regions of interest (ROI, **Fig. 3.2**) along the periphery of the vessel reaching up to 30 µm away into the interstitial tissue. The fluorescent signal in each ROI was smoothed and thresholding was set to the absolute intensity (i.e. set to 0). This ensures the entire signal was being quantified within each ROI. Of note, it was important to switch off the TRITC-dextran channel on IMARIS to prevent bias when placing the ROIs. After placement, the channel was switched back on to ensure there was no overlap with perivascular immune cells (i.e. macrophages that phagocytose the TRITC-dextran). This placement was then applied to each time-point, enabling quantification of the vascular leakage response over time. Mean fluorescence intensity (MFI) values were obtained from the ROIs within the TRITC-dextran channel and an average intensity was calculated to provide a mean value for the vessel segment for each min. To account for variation between animals and depth of the vessel in the tissue, which could impact fluorescence intensity values, the relative mean fluorescence intensity (rMFI) was obtained by normalizing the data set per vessel over the mean of the first two baseline time-point measurements.

Implementation of this experimental approach to IR-stimulated tissues illustrated the method's ability to simultaneously detect and quantify neutrophil migration and vascular leakage over time (**Fig. 3.2 and video 1**). Of note, perivascular cells were observed to accumulate the TRITC-Dextran over time. Therefore, it was essential to exclude those cells from ROI position along the vessel wall to prevent false measurement of the vascular leakage response. Specifically, in IR-stimulated cremaster muscles, a rapid and transient leakage response was observed during the reperfusion period. This initiated within the first few min post reperfusion, peaking at 9 min and returning to basal levels by 60 min (**Fig. 3.2 and video 1**).

Collectively, this model enabled simultaneous detection of vascular leakage and neutrophil migration *in vivo*, providing a means for deciphering the relationship between these two responses in a wider range of inflammatory models.

Visualisation of neutrophil TEM and vascular leakage using confocal intravital microscopy following IR-injury

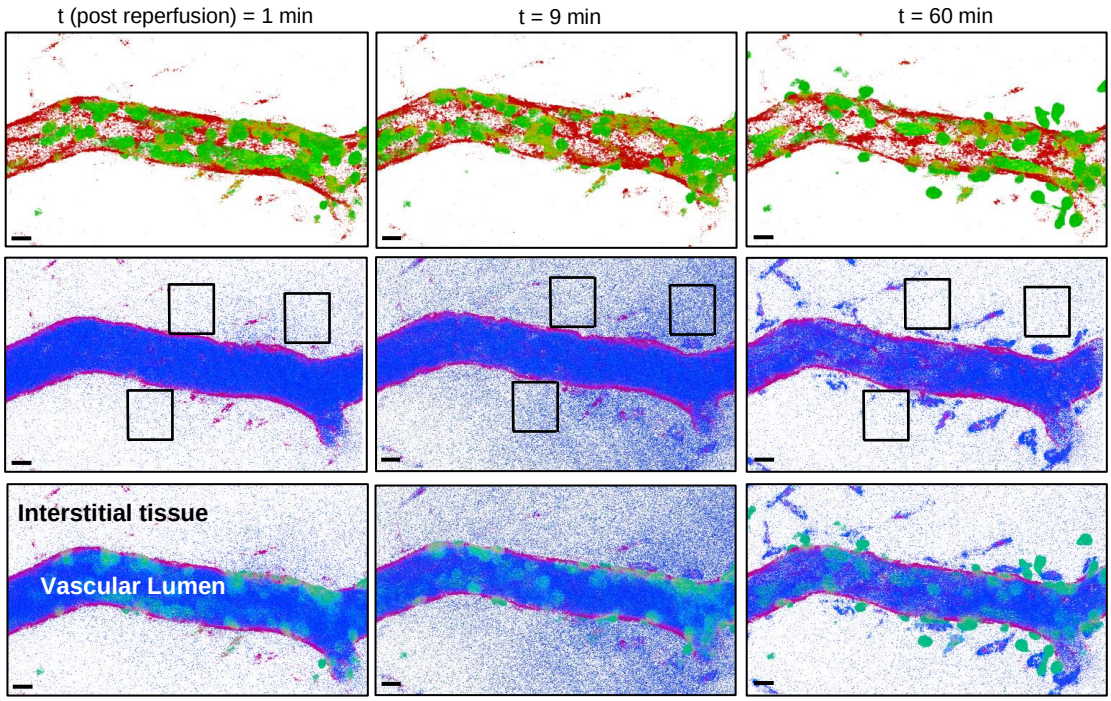

Figure 3.2. Validation of a confocal IVM platform for simultaneous and real-time investigation of vascular leakage and neutrophil-EC interactions in the mouse cremaster muscle. *LysM-EGFP*$^{ki/+}$ mice received an i.s. injection of a fluorescently (AF647)-labelled anti-CD31 mAb (4 µg) 30 min prior to exteriorisation to label EC junctions. Following exteriorisation of the cremaster tissue, mice were subjected to IR-injury (40 min ischaemia followed by 2 hr of reperfusion). In addition, all mice received i.v. injection of TRITC-dextran (75 kDa) at the beginning of confocal IVM image acquisition. (**A**) Representative confocal images at t = 1, 9 and 60 min after the start of the image acquisition period of a mouse cremasteric post-capillary venule from IR-stimulated tissues. Images show neutrophils (green) and ECs (red, top row) and corresponding venules with ECs (red) and dextran extravasation (blue) with the black boxes showing examples of defined ROIs for the measurement of vascular leakage (middle row), and all three parameters merged (bottom row). Images are representatives of at least seven independent experiments. Scale bar (black) = 15 µm.

3.2.2. Stimulation of cremaster muscles with IL-1β, LTB_4 and IR-injury elicited comparable total neutrophil extravasation responses

To investigate associations between neutrophil TEM dynamics and microvascular permeability the confocal IVM methodology detailed above was applied to other established models of inflammation. Specifically, mouse cremaster muscles were stimulated with IL-1β (Woodfin et al., 2011), LTB_4 (Finsterbusch et al., 2014; Colom et al., 2015), or were subjected to our pathophysiological model of IR-injury (Woodfin et al., 2011; Colom et al., 2015; Voisin et al., 2019).

In brief, *LysM-EGFP*$^{ki/+}$ mice were injected i.s. with a fluorescently (AF647)-labelled anti-CD31 mAb to visualize EC junctions in combination with PBS or inflammatory stimuli LTB_4 or IL-1β, 30 min or 2 hr prior to exteriorisation of the cremaster muscle, respectively. Subsequently, to facilitate quantification of vascular leakage, the mice were injected with i.v. TRITC-dextran as previously described (Chapter 2, section 2.5.4). In addition, for all reactions, the total number of neutrophils that had fully migrated through the endothelial and pericyte layer, and thus appearing in the extravascular tissue, was quantified at the final time-point of image acquisition, corresponding to 2 hr post reperfusion, 2.5 hr post LTB_4 or 4 hr post IL-1β (experimental timeline depicted in Appendix 3, section 9.3.1 & 9.3.2).

Analysis of neutrophil responses in the cremaster tissue revealed that locally administered IL-1β and LTB_4 and IR-injury elicited significant neutrophil extravasation as compared to control PBS-treated mice. All reactions induced comparable responses, resulting in ~7000 neutrophils/mm^3 of tissue at the final time-point of acquisition (**Fig. 3.3A-B**).

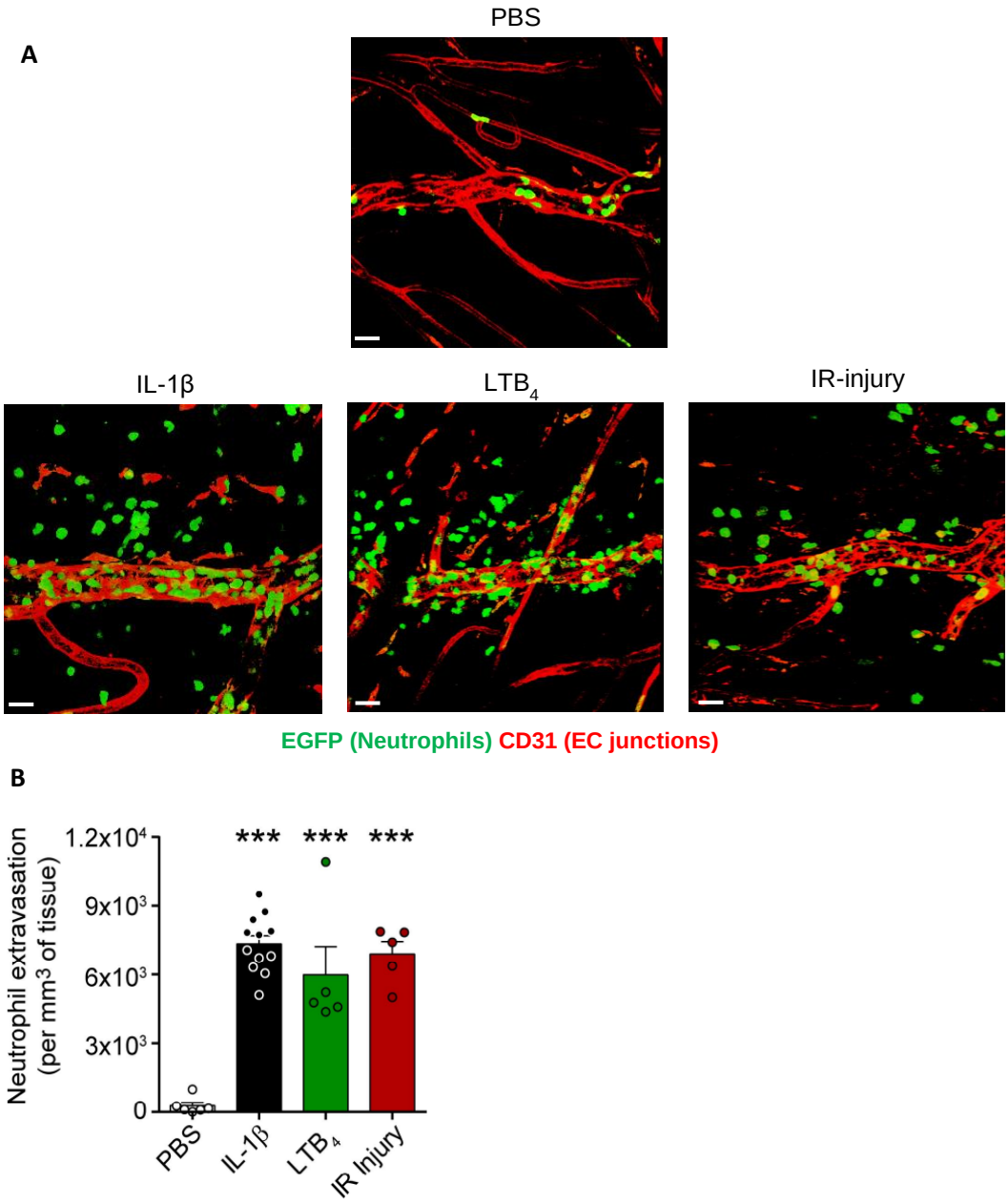

Figure 3.3. Locally injected IL-1β, LTB_4 and IR-injury induced comparable levels of neutrophil extravasation in the mouse cremaster muscle. *LysM-EGFP*$^{ki/+}$ mice received an i.s. injection of fluorescently (AF647) labelled anti-CD31 mAb (4 µg) to label EC junctions, in combination with either PBS (2 hr or 30 min), IL-1β (50 ng, 2 hr) or LTB_4 (300 ng, 30 min). Alternatively, 30 min post i.s. of anti-CD31, mice were subjected to IR-injury (40 min ischaemia followed by 2 hr of reperfusion). In addition, all mice were subjected to an i.v. injection of TRITC-dextran (75 kDa) at the start of image acquisition using confocal IVM. (**A**) Representative confocal IVM images and (**B**) quantification of total neutrophil extravasation responses taken at the final time-point of image acquisition (2 hr post reperfusion, 2.5 hr post LTB_4 or 4 hr post IL-1β, n = 5-12 mice/group). Data are represented as mean ± SEM (each dot represents one mouse and one independent experiment). Statistically significant differences from PBS (**B**) treated mice are indicated by ***p<0.001, as analysed by one-way ANOVA followed by Bonferroni's post hoc test. Scale bar (white) = 30 µm.

3.2.3. Local LTB_4 and IR-injury, but not IL-1β, elicited enhanced vascular leakage

Having assessed the neutrophil infiltration response induced by LTB_4, IR-injury and IL-1β, we next sought to quantify vascular leakage in these inflammatory reactions. Time-course of dextran leakage into the interstitial tissue, as described in sections 3.2.1 & 3.2.2, showed that both IR-injury and LTB_4 induced rapid but transient leakage of dextran into the extravascular space (**Fig. 3.4A**). In both reactions, vascular leakage peaked at 9 min, reaching approximately a 3-fold increase over basal levels ($p<0.0001$ relative to PBS and IL-1β) (**Fig. 3.4B**), before returning close to baseline level after 60 min. In contrast, IL-1β-induced inflammation showed a modest, but non-significant, enhanced dextran leakage, reaching a 1.3x increase as compared to the baseline value ($p>0.05$ relative to PBS) (**Fig. 3.4B**).

Following the characterisation of their vascular leakage and neutrophil extravasation responses, the dynamics and mode of neutrophil TEM in each reaction was evaluated.

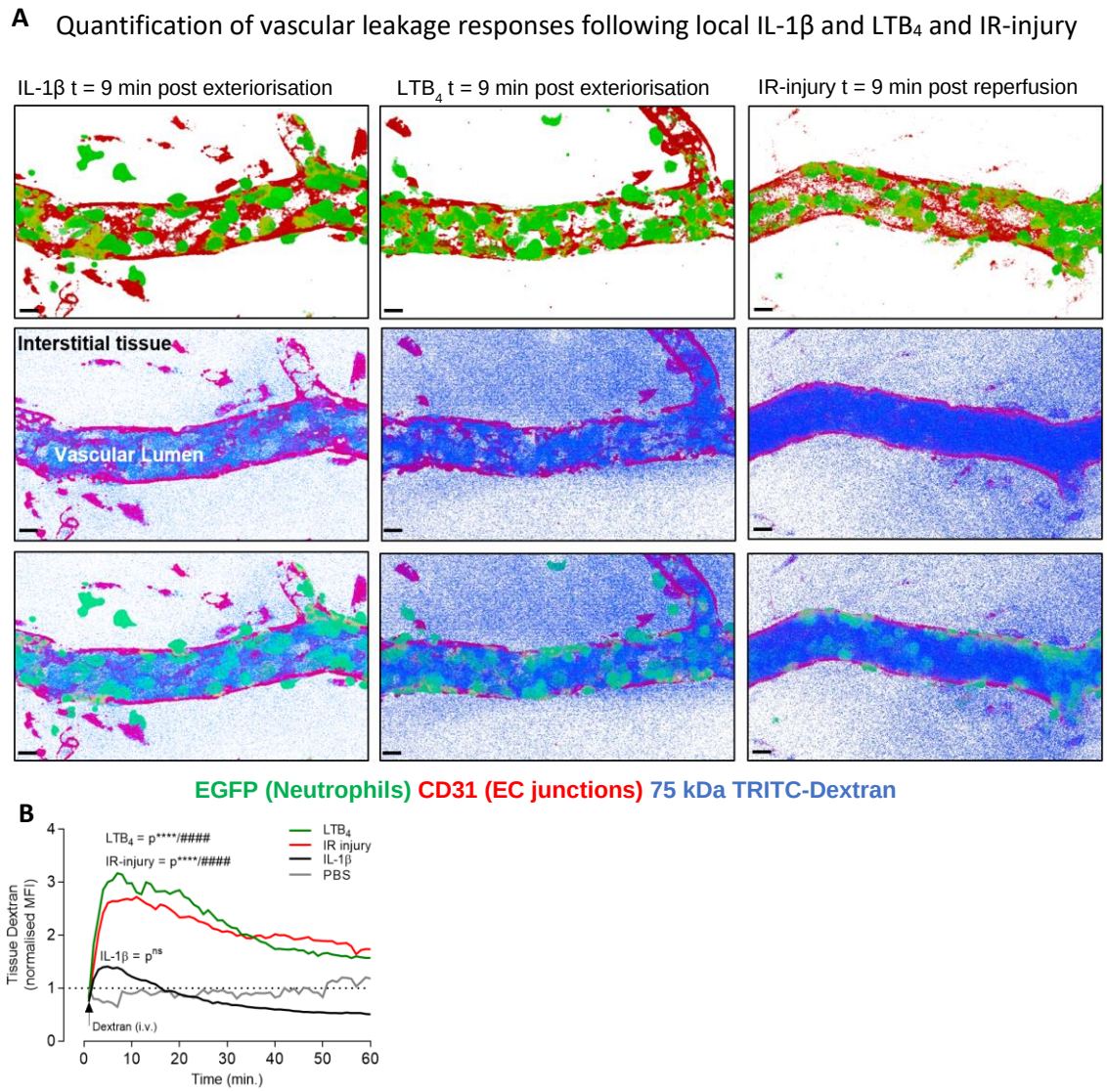

Figure 3.4. IR-injury and LTB_4 stimulation induced rapid vascular leakage responses, whereas IL-1β did not. *LysM-EGFP*$^{ki/+}$ mice received an i.s. injection of a fluorescently (AF647) labelled anti-CD31 mAb (4 µg) to label endothelial junctions in combination with either vehicle (PBS, 2 hr or 30 min) IL-1β (50 ng, 2 hr) or LTB_4 (300 ng, 30 min) prior to exteriorisation. Alternatively, 30 min post i.s. of anti-CD31, mice were subjected to IR-injury (40 min ischaemia followed by 2 hr of reperfusion). In addition, all mice were subjected to an i.v. injection of TRITC-dextran (75 kDa) at the start of confocal IVM image acquisition. (**A**) Representative images of cremasteric venules following IL-1β-, LTB_4-stimulation or IR-injury. Images show neutrophils (green) and ECs (red) and corresponding venules with ECs and dextran extravasation (blue) (middle row), and the final row shows all three parameters merged at t = 9 min (maximal vascular leakage timepoint) after the start of the image acquisition. Images are representatives of at least five independent experiments. (**B**) Time-course of dextran accumulation in the perivascular region of a selected post-capillary venule, represented as relative MFI (normalised to the first 2 time-points post dextran i.v., mean of n = 3-10 mice/group). Error bars are not shown for clarity but the SEM at the peak timepoint was within 0.047 and 0.347. Statistically significant differences from PBS (****p<0.0001) or IL-1β (####p<0.0001) treated mice are indicated, as analysed by two-way ANOVA followed by Bonferroni's post hoc test. (ns = not significant). Scale bar (black)=15 µm.

3.2.4. Hyper-permeability inflammatory reactions were associated with dysregulated neutrophil TEM

Having characterised the vascular leakage profiles of IR-injury, LTB_4 and IL-1β-mediated acute inflammatory responses, the dynamics of neutrophil TEM in these reactions was next analysed.

Quantification of neutrophil TEM dynamics was performed by observing neutrophil motility through EC junctions by confocal IVM over the 2 hr imaging period. This analysis showed that the majority of neutrophils breaching the endothelium migrated in a luminal-to-abluminal direction through EC junctions, a response termed normal neutrophil TEM (**Fig. 3.5A and video 2**). Interestingly however, in response to local LTB_4 and IR-injury, a significant portion of neutrophils exhibited an aberrant behaviour whereby cells that had initiated breaching of the endothelium, exhibited reverse motility in an abluminal-to-luminal direction and re-entered the blood circulation (**Fig. 3.5B and video 3**). This response, which we have previously termed neutrophil reverse transendothelial migration (rTEM) (Woodfin et al., 2011; Colom et al., 2015), accounted for ~15% and ~25% of total neutrophil TEM events in LTB_4- and IR-stimulated tissues, respectively (**Fig. 3.4C**). In contrast, local IL-1β induced very little neutrophil rTEM, accounting for less than 5% of the total quantified TEM events.

As reactions exhibiting increased levels of neutrophil rTEM featured strong vascular leakage responses, we hypothesised a causal effect, prompting us to look at both phenomena concomitantly over time.

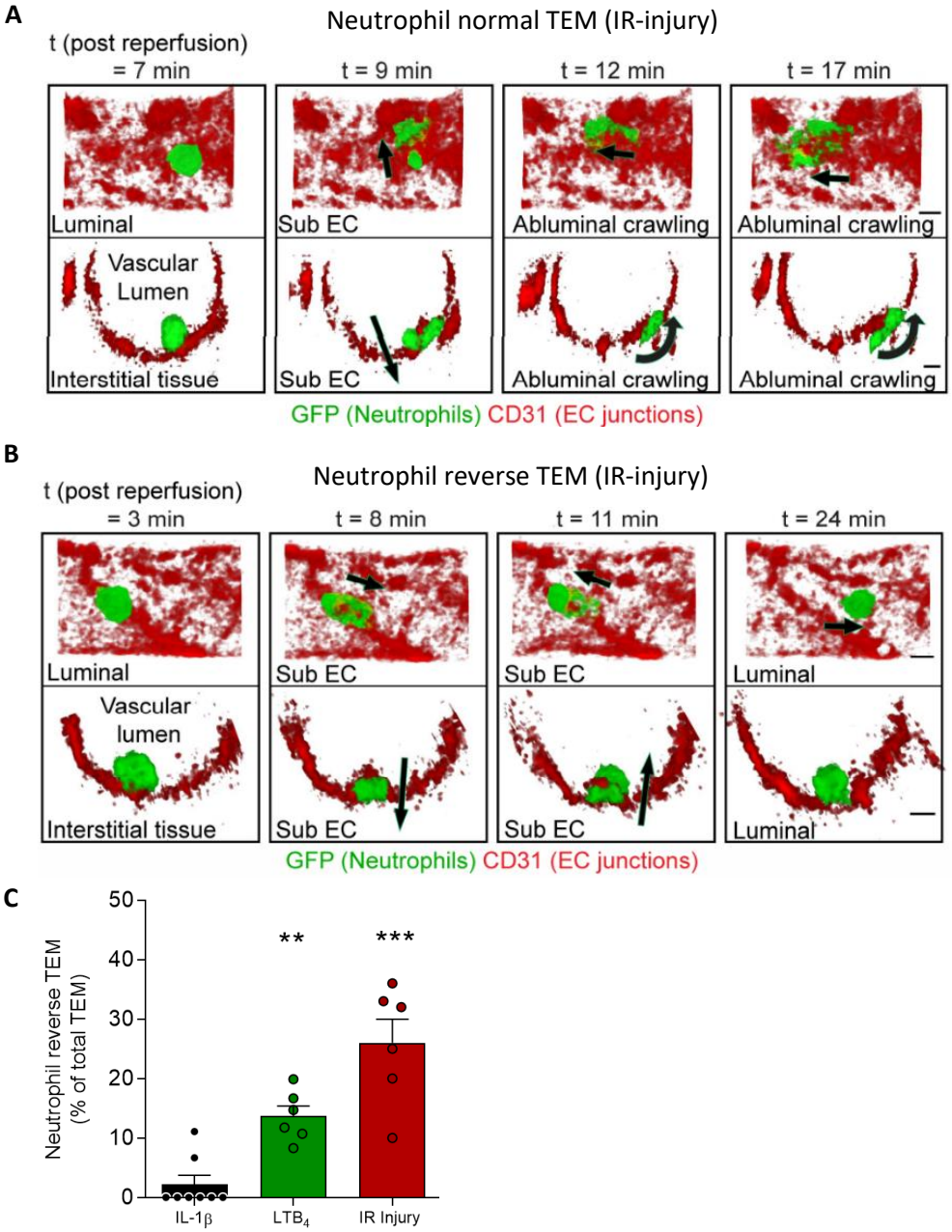

Figure 3.5. IR-injury and LTB_4 stimulation, but not IL-1β, were associated with enhanced levels of neutrophil rTEM. *LysM-EGFP*$^{ki/+}$ mice received an i.s. injection of a fluorescently (AF647) labelled anti-CD31 mAb (4 µg) to label EC junctions, in combination with IL-1β (50 ng, 2 hr) or LTB_4 (300 ng, 30 min). Alternatively, 30 min post i.s. of anti-CD31, mice were subjected to IR-injury (40 min ischaemia followed by 2 hr of reperfusion). (**A-B**) Representative confocal IVM images of an IR-stimulated cremasteric post-capillary venule at different time-points post reperfusion illustrating an example of a normal neutrophil TEM event (**A**) and a rTEM event (**B**). Luminal (top panels) and cross-sectional (bottom panels) views are shown with the arrows (black) signifying the direction of motility of the indicated neutrophil. (**C**) Frequency of neutrophil rTEM events (n = 6-8 mice/group). Data are represented as mean ± SEM (each dot represents one independent experiment). Statistically significant differences from IL-1β treated mice are indicated by **p<0.01, ***p<0.001, as analysed by one-way ANOVA followed by Bonferroni's post hoc test. Scale bar (black) = 5 µm.

3.2.5. Microvascular leakage and neutrophil rTEM were temporally aligned

Following the observation that vascular hyperpermeability and enhanced neutrophil rTEM occurred in the same inflammatory reactions, we next considered the temporal association of the two phenomena. Specifically, we analysed the time-course of neutrophil rTEM induction in relation to the time-course of enhanced microvascular leakage.

Analysis of the temporal relationship between TRITC-dextran leakage and neutrophil rTEM events during IR-injury and LTB_4 indicated a rapid increase in microvascular leakage within the first few min post reperfusion or exteriorisation. Interestingly, permeability induction was closely followed by rapidly enhanced frequency of neutrophil rTEM. Indeed, ~90% of all neutrophil rTEM events occurred within the first 20 min of reperfusion (**Fig. 3.6A**), or with respect to LTB_4, post tissue exteriorisation (**Fig. 3.6B**). Occurrences of neutrophil rTEM plateaued at 30 min, coinciding with the decline of the vascular leakage response. Of interest, mice treated with IL-1β alone exhibit minimal leakage which coincided with a poor neutrophil rTEM response (**Fig. 3.6C**). Collectively, these results demonstrate a previously unappreciated association between microvascular permeability and aberrant neutrophil TEM; a notion that was further explored in the following Chapters.

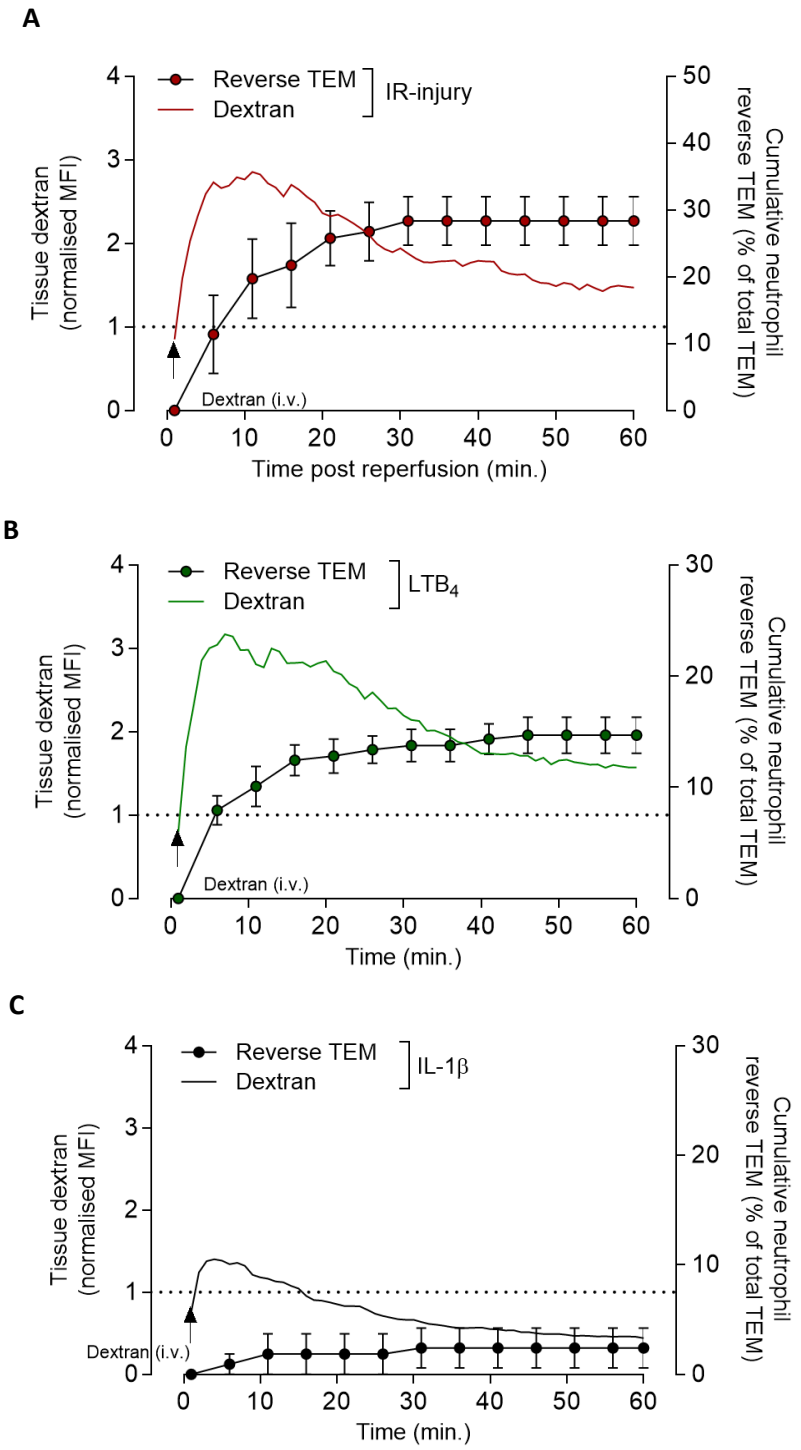

Figure 3.6. Temporal association between neutrophil rTEM and microvascular leakage in inflammatory models of IR-injury and local LTB$_4$. *LysM-EGFP$^{ki/+}$* mice received an i.s. injection of a fluorescently (AF647) labelled anti-CD31 mAb (4 µg) to label EC junctions in combination with IL-1β (50 ng, 2 hrs) or LTB$_4$ (300 ng, 30 min). Alternatively, 30 min post i.s. of anti-CD31, mice were subjected to IR-injury (40 min ischaemia followed by 2 hr of reperfusion). In addition, all mice received i.v. fluorescent TRITC-dextran (75 kDa) at the beginning of the confocal IVM image acquisition. Temporal association of dextran leakage and cumulative mean (± SEM) frequency of neutrophil rTEM following (**A**) IR-injury or (**B**) LTB$_4$ or (**C**) IL-1β stimulation (n = 4-6 mice).

3.3. Discussion

Investigations surrounding the interplay between microvascular leakage and neutrophil migration remain poorly developed in part due our limited ability to visualise these two phenomena spatially, temporally and simultaneously. To overcome this limitation, we successfully extended our existing confocal IVM platform that has been optimised for high resolution tracking of neutrophil TEM (Woodfin et al., 2011; Colom et al., 2015; Girbl et al., 2018) for simultaneous analysis of vascular permeability. Hence, alongside our established methodology for quantifying neutrophil TEM, we utilised TRITC-dextran as a fluorescent tracer of vascular leakage into the extravascular tissue of the cremaster muscle in real-time. By doing so, our investigations into the acute inflammatory responses as mediated by IL-1β, LTB_4 and IR-injury revealed that despite induction of comparable neutrophil extravasation by the different stimuli at the end of the respective reactions, a rapid and transient vascular leakage was observed only following LTB_4 and IR-injury. In addition, inflammatory reactions induced by LTB_4 and IR-injury were associated with enhanced levels of neutrophil rTEM, a response temporally aligned with the onset of vascular leakage.

To extend our confocal IVM platform for concomitant analysis of neutrophil TEM and vascular permeability, we opted to use fluorescently labelled (TRITC-)dextran (75 kDa) as a plasma protein marker. This branched polysaccharide is classically characterised by its good solubility and low toxicity *in vivo*. This particular fluorophore-tracer was chosen compared to other examples, such as FITC-dextran (Pink *et al*., 2012), for a number of reasons. For example, whilst FITC-dextran exhibits a high quantum yield and good aqueous solubility, it suffers from rapid photo bleaching after excitation. Consequently, this would render the FITC-dextran invisible over time by confocal IVM. TRITC-dextran is a great alternative that makes reasonable compromises on aqueous solubility and quantum yield but offers excellent photo-stability (Reeves *et al*., 2012). Hence, it is more suitable for the relatively long-term monitoring required for time-course studies *via* confocal IVM.

Similar to our experimental approach, a recent study by Park and colleagues developed a model for concomitant visualisation of vascular leakage and neutrophil extravasation using two-photon confocal IVM imaging (Park *et al*., 2018). In this study, *LysM-EGFP*$^{ki/+}$

mice received an i.v. injection of Texas-Red labelled Dextran (70 kDa) to label the blood flow prior to exteriorisation of the cremaster tissue, which was followed by superfusion of fMLP, a potent neutrophil chemoattractant. Using this protocol, the authors quantified the fluorescence intensity of Texas-Red-dextran as a measure of vascular leakage with two large defined ROIs covering interstitial tissue but also both the vessel and extravascular resident tissue cells such as macrophages. Whilst they normalised their data as percentage change over a vessel section without leakage, their quantification method suffers from a lack of scientific rigour as the accumulation of dextran over time within the interstitial macrophages and within the lumen of blood vessels would negatively influence the MFI detected in the ROIs. In contrast, in our model, the ROIs were positioned as to avoid vessel dextran and resident tissue cells such that only measurements of the interstitial tissue contributed to the detected fluorescence intensity. In addition, whilst using *LysM-EGFP*$^{ki/+}$ mice, the group did not discuss neutrophil migration dynamics but concluded the model would be sufficient to do so (Park *et al*., 2018). This model is therefore complementary to the one discussed in this Chapter, which aims to provide novelty in the form of simultaneous analysis of neutrophil dynamics and vascular leakage.

Our methodology for the simultaneous quantification of microvascular leakage and neutrophil migration was implemented for the evaluation of these responses in three established inflammatory reactions, as induced by IL-1β, LTB_4, or following a pathophysiological model of IR-injury. Here, we observed a marked and rapid increase in vascular leakage following IR-injury or stimulation of tissues with local LTB_4. In both cases, the majority of vascular leakage occurred within the first 20 min after exteriorisation or post reperfusion of the mouse cremaster muscle. These findings are in line with previous reports indicating that IR-injury (Voisin et al., 2019) and LTB_4-stimulated (Finsterbusch *et al*., 2014) cremaster muscles exhibit enhanced vascular leakage, as detected by the Miles assay. In contrast, using our methodology, we were able to determine that IL-1β-induced inflammation was not characterised by a significant enhancement of vascular leakage. Interestingly, the role of IL-1β on vascular permeability in the literature is controversial, with only scarce examples examining this point directly (Fahey and Doyle, 2019). Firstly, investigations on the impact of IL-1β on EC monolayers *in vitro* showed loss of β-catenin and VE-cadherin at EC borders leading

to the formation of gaps between adjacent ECs and an increase in endothelial leakage, as measured by transendothelial electrical resistance (TEER) (Wong et al., 2004; Skaria et al., 2017). Studies looking directly at the effects IL-1β *in vivo* are limited to mouse intestinal models that investigated the effect of IL-1β on intestinal permeability (Al-Sadi et al., 2012). In this study, modest increases in permeability were observed in a dose-dependent manner after 24 hr, a response that was hypothesised to occur through a myosin-light chain kinase (MLCK)-mediated pathway within enterocytes (Al-Sadi *et al*., 2012). MLCKs are also involved in mediating EC contractility, however we observed only minimal vascular leakage in our model of IL-1β. This may highlight tissue-specific differences between ECs and enterocytes, whereby IL-1β does not result in endothelial contractility in our model. More likely however, the cause of this disparity is due to the difference in time-points at which permeability is measured (2 hr vs. 24 hr+), and the size of the dextran (75 vs. 10 kDa) whereby the latter employed in the comparative study would be more susceptible to passive diffusion (Al-Sadi et al., 2012; Claesson-Welsh, 2015). Therefore, it can be concluded that between 2 – 4 hr post IL-1β administration there is minimal vascular leakage, however, we may observe more significant changes after 24 hr, outside our experimental window of interest.

Having established the vascular permeability profiles of our inflammatory models, we looked at the associated neutrophil migration responses. Here, compared to PBS-treated mice, treatment with LTB_4 or IL-1β and following IR-injury elicited significant and comparable levels of neutrophil extravasation into the tissue; an observation that is in line with previously published studies (Woodfin et al., 2009, 2011; Finsterbusch et al., 2014; Voisin et al., 2019). In combination with the present findings on vascular permeability discussed above, these results confirm that neutrophil infiltration by itself is not sufficient for eliciting neutrophil-dependent microvascular leakage, complimentary to previous findings (DiStasi and Ley, 2009; He, 2010).

Furthermore, using our confocal IVM and 3D-imaging platform, we carefully evaluated neutrophil migration dynamics. Interestingly, whilst in all inflammatory reactions tested neutrophil TEM was predominantly in the expected luminal-to-abluminal manner (termed normal TEM), a large proportion of the TEM detected following IR-injury and stimulation of tissues with LTB_4 was in the reverse mode, i.e. reverse (r)TEM. This incomplete, aberrant mode of neutrophil TEM accounted for ~25% and 15% of all TEM

events driven by IR-injury and LTB_4, respectively, but was rarely seen in IL-1β-stimulated tissues where rTEM events accounted for less than 5% of total TEM events. Complementary to these findings, Woodfin et al., observed that approximately 15% of total neutrophil migration events following IR-injury were rTEM (Woodfin *et al*., 2011). The slightly reduced overall level of neutrophil rTEM reported by Woodfin *et al*., may be accounted for by their use of a shorter 30 min period of ischaemia, compared to the 40 min period used in the present work. However, whether the duration of ischaemia correlates to the frequency of neutrophil rTEM requires further exploration. In addition, Colom *et al*., observed that approximately 20% of neutrophils undergo rTEM following LTB_4 stimulation of tissues (Colom *et al*., 2015), findings that are comparable to the present results.

Following the observation that neutrophil rTEM events occurred in reactions that exhibited higher levels of microvascular leakage, a time-course comparison of the two responses demonstrated that microvascular leakage and neutrophil rTEM had a close temporal association. Furthermore, the majority of this aberrant neutrophil TEM occurred during the peak of hyperpermeability induction, a response which ceased following the decline of vascular leakage. Taken together, these findings indicate that microvascular leakage may directly influence neutrophil TEM dynamics. Thus, to explore this idea further, in the subsequent Chapter we sought to investigate the effect of direct permeability inducing agents such as histamine and VEGF on neutrophil TEM dynamics. This approach enabled manipulation of the vascular leakage response in a more controlled manner and hence directly provided a means of investigating the impact of vascular leakage on neutrophil TEM.

3.4. Conclusion

The development of the confocal IVM platform to enable the simultaneous quantification of neutrophil trafficking and vascular leakage in real-time, allowed for spatiotemporal investigations of these events within acute inflammatory responses. *Via* this approach, we identified that acute inflammatory reactions (mediated by LTB_4 and IR-injury) characterized by marked vascular leakage, exhibited an increased frequency of neutrophil rTEM. Further insights into these models included the findings that a rapid

and transient vascular leakage response was closely followed by enhanced levels of neutrophil rTEM. These data led to the formulation of a novel hypothesis that microvascular leakage could directly impact the dynamics of neutrophil migration through EC junctions and mandated further exploration.

Chapter 4

Acute vascular leakage promotes neutrophil reverse transendothelial migration

4.1. Introduction

In Chapter 3, we extended our confocal IVM platform to investigate both neutrophil migration and vascular leakage simultaneously using established models of acute inflammation, as elicited by locally administered IL-1β and LTB_4 or following IR-injury. Of particular interest, only the last two models induced both vascular leakage and increased the levels of neutrophil rTEM, whilst IL-1β exhibited minimal vascular leakage and neutrophil rTEM. Intrigued by these findings, we explored the hypothesis that 'microvascular leakage drives neutrophil rTEM'. To address this, we used exogenous pro-permeability agents and employed a GM mouse model that exhibits reduced vascular leakage. In addition, we investigated the mechanism supporting this phenomenon.

Neutrophil TEM is a multifaceted, tightly regulated process, involving a complex array of mediators and mechanical endothelial alterations, as described in Chapter 1, section 1.5 & 1.6 and Chapter 3, section 3.1. Fundamental to this process is a reduction in EC junctional integrity and the sequential interactions between neutrophils and EC junctional molecules, including PECAM-1, JAMs, ESAM, ICAM-2 and CD99 (Vestweber, 2015). Simultaneously, neutrophil directional motility through the EC wall is guided by presentation and ligation of specific chemoattractants including C5a, LTB_4, or chemokines such as CXCL8, its murine homologue CXCL1, CXCL2 and CXCL5, (Koltsova and Ley, 2010; Newton and Dixit, 2012), whereby neutrophils migrate towards higher chemotactic concentrations (Jin, 2013). Our current understanding of leukocyte TEM is the product of several decades of research, however, neutrophil rTEM is a relatively recent observation. rTEM was first noted by Randolph and Furie, who observed reverse migration of human derived monocytes through EC monolayers *in vitro* (Randolph and Furie, 1996). Bradfield et al., extended this observation *in vivo* additionally finding that blockade of JAM-C enhanced the frequency of monocyte rTEM (Bradfield et al., 2007b). Later, Buckley and colleagues identified that neutrophils could also exhibit rTEM through cultured ECs in response to TNF or fMLP (Buckley et al., 2006). This finding has since been extended into murine *in vivo* inflammatory settings (Woodfin et al., 2011) and explorations into the underlying mechanisms and pathological significance of neutrophil rTEM has been the subject of several papers from our group (Woodfin et al., 2011; Girbl et al., 2018; Owen-Woods et al., 2020) and beyond (Wu et al., 2016; Wang et al., 2017).

Pioneering *in vivo* investigations on neutrophil rTEM by Woodfin et al., first identified that its frequency is stimulus-dependent, with the highest occurrence being observed in tissues stimulated with LTB_4 (approximately 25% of total TEM) and IR-injury (approximately 15% of total TEM) with minimal neutrophil rTEM occurring in IL-1β-stimulated tissues (Woodfin et al., 2011). This study also identified that similar to neutrophil TEM, the majority of neutrophil rTEM occurred in a paracellular (as opposed to transcellular) manner (i.e. between EC junctions). Mechanistically, the increased frequency of neutrophil rTEM was associated with loss of EC junctional JAM-C, which was required for unidirectional migration of neutrophils (Woodfin et al., 2011). This study provided the first evidence of neutrophil rTEM being induced by disrupted molecular changes in the venular wall. Intriguingly, Woodfin and colleagues also observed that conditions promoting neutrophil rTEM also induced significantly higher plasma protein leakage and promoted elevated numbers of ICAM-1^{high} and ROS^{high} neutrophils in the pulmonary vasculature (Woodfin et al., 2011). This is of particular interest as increased leukocyte migration and vascular leakage in the lungs are both characteristics of pathologies such as ALI (Johnson and Matthay, 2010). Similar results have been found following analysis of human blood samples taken from patients with systemic inflammation (Buckley et al., 2006) and those suffering from acute pancreatitis (Wu et al., 2016). Collectively, these findings suggest a pathophysiological role for neutrophil rTEM in human disease.

These findings were subsequently extended by Colom et al., where it was determined that during an LTB_4 driven inflammatory reaction, JAM-C cleavage and subsequent induction of neutrophil rTEM was promoted by release of NE upon neutrophil degranulation. The latter was presented to EC JAM-C by the neutrophil surface pro-adhesion molecule, CD11b (Colom et al., 2015). The authors also demonstrated that JAM-C loss at the endothelium was a characteristic of IR-injury, implying that LTB_4-NE axis is a key mediator of IR-injury induced neutrophil rTEM. Furthermore, Colom *et al*., identified an elevated presence of neutrophil retention and plasma protein leakage in the lung vasculature, complementary to the findings of Woodfin *et al*. This response was effectively abolished following inhibition of NE (Colom et al., 2015). Indeed, Colom et al., further discovered that human patients suffering from ARDS exhibited elevated levels of soluble JAM-C relative to healthy patients. As increased NE expression in the

lung is a known risk factor towards the development of lung pathologies (Polverino et al., 2017), the combined findings of Colom et al., and Woodfin et al., comprised compelling evidence to mandate further investigations into the mechanisms that promote neutrophil rTEM.

Chemokines are essential in mediating neutrophil recruitment and provide directional cues into damaged or infected tissues *via* establishment of chemotactic gradients (Furze and Rankin, 2008; Massena et al., 2010). In part, chemokines such as CXCL1 and CXCL2 interact with neutrophils following their presentation by GAGs and receptors such as ACKR1 expressed on the surface of ECs (Proudfoot et al., 2003; Novitzky-Basso and Rot, 2012; David and Kubes, 2019). Initially, investigations by Girbl et al., identified that the sequential presentation of CXCL1 and CXCL2 was required to facilitate TNF-induced neutrophil crawling and TEM, respectively. Of particular interest, they identified that the frequency of neutrophil rTEM was increased by disruption of chemokine presentation at EC junctions. More specifically, retention of neutrophil-derived CXCL2 at EC junctions by ACKR1 was required for facilitating unidirectional neutrophil TEM. This was demonstrated by pharmacological blockade of CXCL2 and use of *ACKR1*^{KO} mice; experimental strategies that enhanced the frequency of neutrophil rTEM. This study thereby highlighted that the correct and sequential presentation of specific chemokines is essential in facilitating luminal-to-abluminal neutrophil TEM (Girbl et al., 2018). However, as yet, how these findings relate to our observations in Chapter 3, whereby the onset of enhanced vascular leakage coincided with an enhanced frequency of neutrophil rTEM was unknown and provides the basis of this Chapter.

4.1.1. Scope of the chapter

As Chapter 3 identified that models of vascular leakage exhibited enhanced levels of neutrophil rTEM, the aim of this Chapter was to gain direct insight into the impact of microvascular leakage on neutrophil TEM directionality. To this end, the key aims of this Chapter were as follows:

- To investigate the impact of direct vasoactive agents on neutrophil TEM.
- To explore the underlying mechanisms governing vascular leakage-mediated neutrophil rTEM.

4.2. Results

4.2.1. Pro-permeability agents promote neutrophil rTEM in IL-1β-stimulated tissues

To directly investigate the impact of vascular leakage on neutrophil migration dynamics *in vivo*, we investigated the effect of the pro-permeability agents histamine (Benly, 2015) and VEGF (Bates, 2010) in IL-1β-stimulated murine cremaster tissues. As previously determined in Chapter 3, IL-1β (Dinarello, 2018) promotes neutrophil extravasation but not significant vascular leakage (Chapter 3, section 3.2.2 & 3.2.3). As such, this model was chosen for investigating the effect of vascular leakage inducing agents on the quantity and profile of neutrophil TEM.

In brief, *LysM-EGFP*$^{ki/+}$ mice were injected i.s. with IL-1β for 2 hr followed by exteriorisation of the cremaster muscle (refer to Chapter 2, section 2.4.2). Histamine (30 µM, at a drip rate of 1 ml/min) or vehicle control was then topically applied to the tissue over a period of 2 hr during image acquisition using our extended confocal IVM platform. Alternatively, VEGF (4 µg) was injected i.v. at the start of acquisition period. Furthermore, to visualise vascular leakage, TRITC-dextran was injected i.v. 2 min prior to the application of histamine/VEGF. Both vascular permeability and neutrophil extravasation were quantified using IMARIS software as detailed in Chapter 3, section 3.2.1 and Chapter 2, section 2.7, respectively. Lastly, at the final time-point (2 hr post histamine or VEGF application) still images of random post-capillary venules (n = 4-8/mouse) were taken to determine total neutrophil extravasation as detailed in Chapter 2, section 2.6 (experimental timeline depicted in Appendix 3, section 9.3.3).

Firstly, we confirmed that histamine or VEGF did not impact total neutrophil extravasation when used on their own (data not shown) (Owen-Woods et al., 2020) or in IL-1β-stimulated cremaster tissues (**Fig. 4.1B**). However, as expected, time-course analysis of confocal image sequences revealed that the addition histamine or VEGF induced strong and significant leakage of TRITC-dextran into the extravascular tissue, whereas IL-1β or PBS (control)-treated mice showed minimal leakage responses (**Fig. 4.1A & C**). Interestingly, the leakage responses following histamine or VEGF application

were very rapid and transient, occurring within the first few min and peaked after 15 and 7 min, respectively and in both cases returned close to the baseline by 60 min (**Fig. 4.1A & C and video 4**). Of note, the leakage induced following i.v. VEGF was significantly lower than that observed following topical histamine (~2.8-fold vs. ~4-fold, at 10 min post histamine/VEGF application, respectively), possibly due to the different doses used and/or the differing route of administration of the agents.

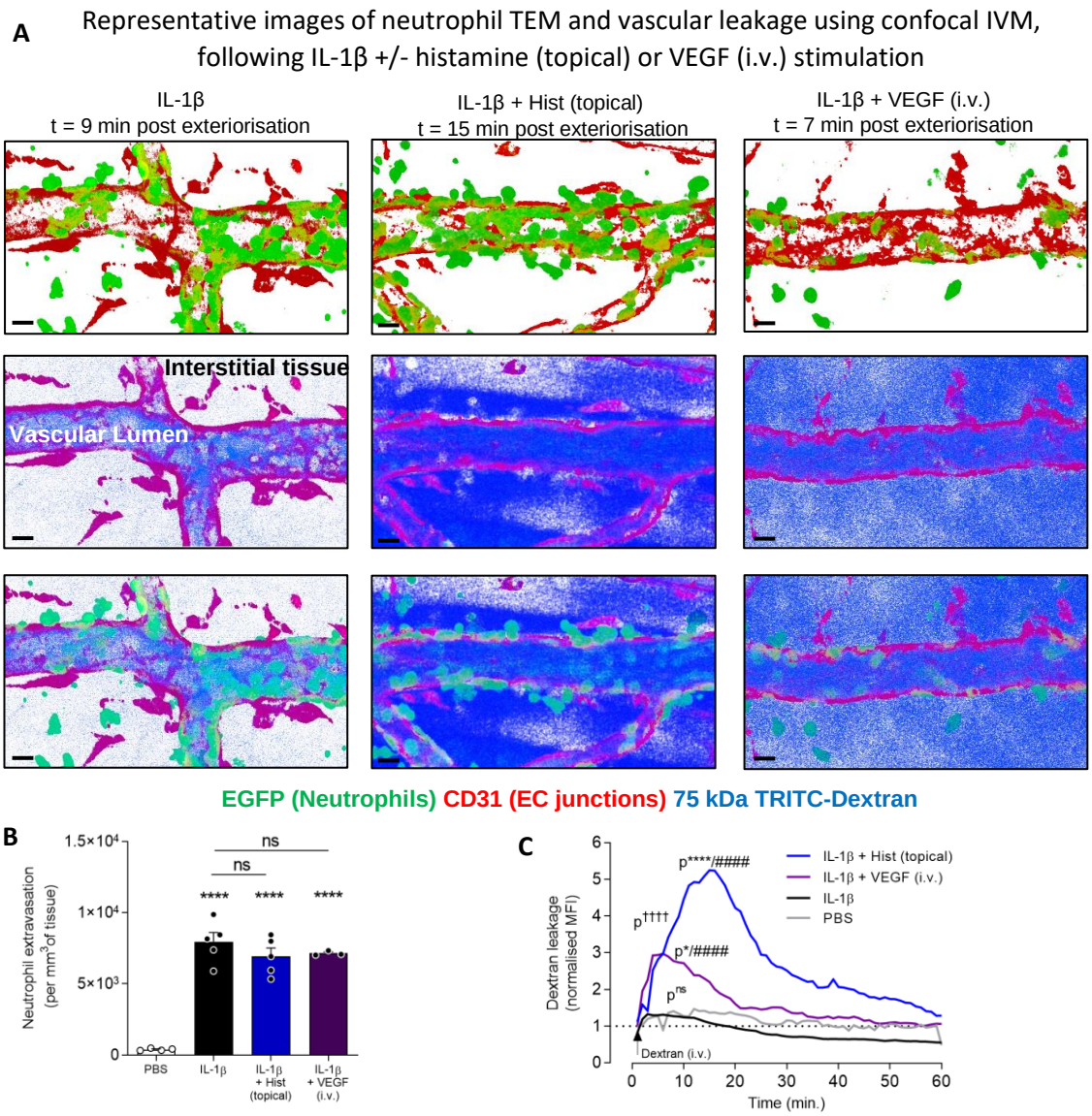

Figure 4.1. Histamine and VEGF had no impact on neutrophil extravasation induced by IL-1β. *LysM-EGFP*$^{ki/+}$ mice received an i.s. injection of an anti-CD31 mAb (4 µg) to label EC junctions for 2 hr in combination with either PBS or IL-1β (50 ng). Cremaster muscles were then exteriorised and the mice were treated with histamine (30 µM, topical), VEGF (4 µg, i.v) or control vehicle solution (Tyrode's topical and/or PBS i.v.) and neutrophil migration and vascular leakage responses were quantified by confocal IVM. In addition, all the mice were subjected to an i.v. injection of fluorescent TRITC-dextran at the start of the image acquisition period. (**A**) Representative confocal IVM images illustrating neutrophil TEM and dextran leakage responses from a post-capillary venule segment subjected to IL-1β alone, IL-1β + histamine or VEGF stimulation. Images are representative of the peak of the vascular leakage response. Scale bars (black) = 15 µm. (**B**) Total neutrophil extravasation (n = 3-5 mice/group). (**C**) Dextran leakage extravasation normalised to the value of the first 2 min in control (grey), IL-1β (black), IL-1β + histamine (blue) or IL-1β + VEGF (purple) stimulated tissues (n = 3-9 mice/group). Error bars are not shown for clarity but the SEM at the peak timepoint was within 0.195 and 1.736. Statistically significant differences from (**B & C**) PBS-treated (indicated by *p<0.05 or ****p<0.0001) or (**C**) IL-1β-treated (indicated by ####p<0.0001) or IL-1β + VEGF-treated (indicated by ††††p<0.0001) mice, as analysed by a (**B**) one-way ANOVA or (**C**) two-way ANOVA followed by Bonferroni's post hoc test, (ns = not significant).

Next, we assessed whether the addition of pro-permeability agents could impact the mode of neutrophil transmigration and in particular the directionality of neutrophil TEM (**Fig. 4.2A & B**). As expected, treatment with IL-1β alone induced almost exclusively luminal-to-abluminal migration through EC junctions (i.e. 97% of normal TEM vs. 3% of reverse TEM). In contrast, in mice treated with IL-1β + histamine or VEGF, neutrophil rTEM events rose to 25% (**Fig. 4.2C and video 4**). Interestingly, the permeability response in the IL-1β + histamine reaction occurred very rapidly (i.e. within the first 10 min of histamine application) and was promptly followed by an increase in the frequency of neutrophil rTEM (79% of neutrophil rTEM events occurred within 30 min post topical histamine). Furthermore, once the vascular leakage declined, the neutrophil rTEM response ceased (**Fig. 4.2D**). Collectively, these findings suggested a temporal association between vascular leakage and neutrophil rTEM.

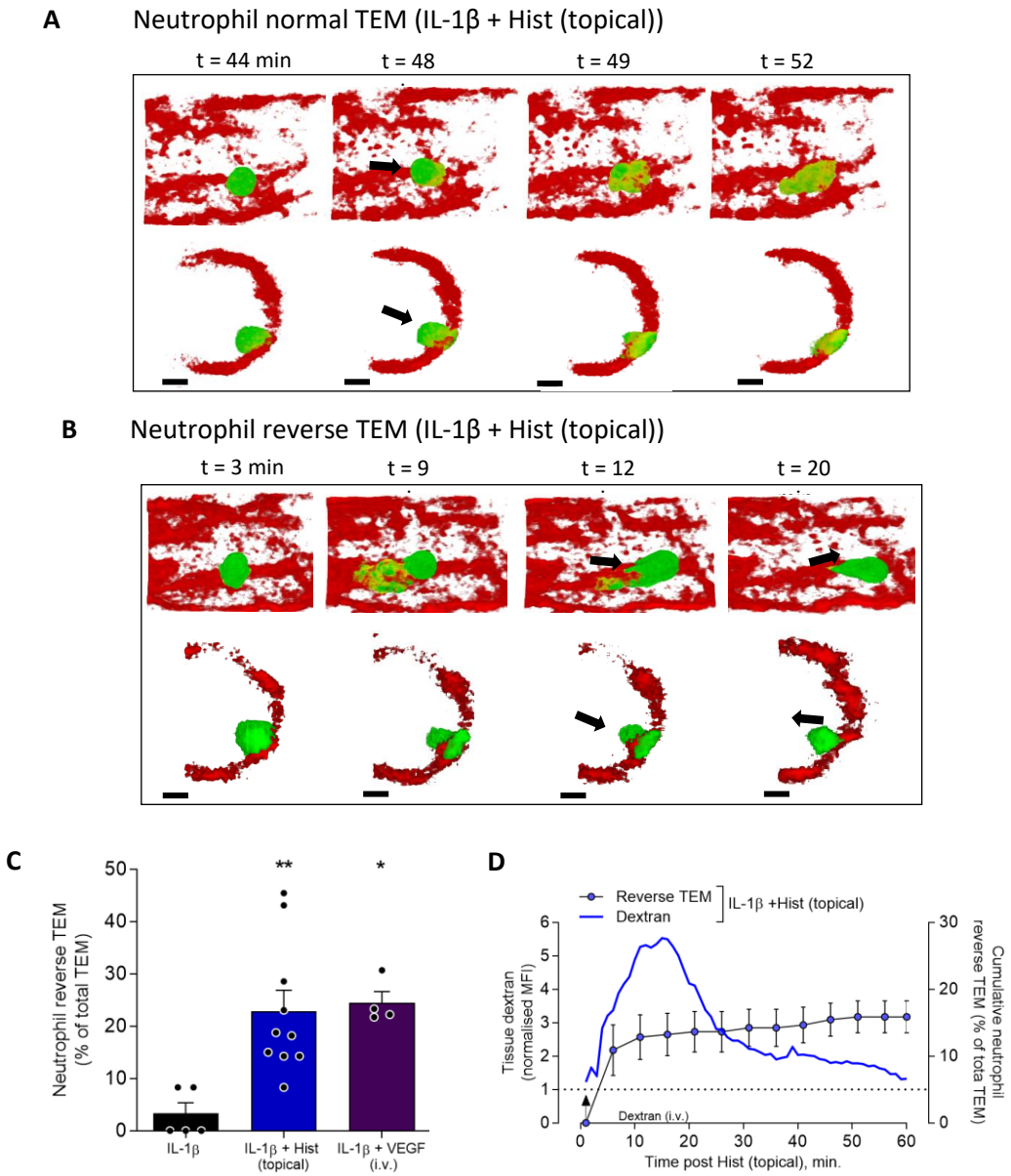

Figure 4.2. Pro-permeability agents promote neutrophil rTEM in IL-1β-stimulated tissues. *LysM-EGFP*$^{ki/+}$ mice received an i.s. injection of an anti-CD31 mAb (4 µg) to label EC junctions for 2 hr in combination with either PBS or IL-1β (50 ng). Cremaster muscles were then exteriorised and the mice were treated with histamine (30 µM, topical), VEGF (4 µg, i.v) or control vehicle solution (Tyrode's topical and/or PBS i.v.) and neutrophil migration and vascular leakage responses were quantified by confocal IVM. In addition, all the mice were subjected to an i.v. injection of fluorescent TRITC-dextran at the beginning of the image acquisition period and prior to the addition of histamine or VEGF. (**A & B**) Representative images of an IL-1β + histamine-stimulated post-capillary venule at different time-points, illustrating a normal neutrophil TEM (top) and a reverse TEM (bottom) event. Luminal and cross-sectional views with arrows indicating the direction of motility of the indicated neutrophil. Scale bars (black) = 5 µm. (**C**) Frequency of neutrophil rTEM events in IL-1β or IL-1β + histamine or VEGF stimulated tissues (n = 4-10 mice/group). (**D**) Temporal association between dextran leakage and frequency of neutrophil rTEM shown as an accumulated frequency over time (n = 7 mice/group). Statistically significant differences from (**C**) IL-1β-treated mice are indicated by *p<0.05 or **p<0.01, as analysed by a one-way ANOVA followed by Bonferroni's post hoc test.

4.2.2. Mice exhibiting defective vascular permeability showed reduced neutrophil rTEM

VE-cadherin is a vital EC junctional adhesion molecule that is intricately involved in the regulation of vascular permeability and neutrophil TEM. To gain conclusive evidence for the ability of microvascular permeability to impact neutrophil TEM dynamics, the IL-1β + histamine reaction was investigated in a genetically modified knock-in mouse model that exhibits reduced vascular permeability induction (e.g. a 33% reduction in histamine-induced vascular leakage) (Wessel et al., 2014). This mouse strain is characterised by the presence of a single point mutation in the VE-cadherin gene sequence leading to the specific replacement of a tyrosine residue in position 685 of the peptide sequence by a phenylalanine residue (*VEC-Y685F*).

In order to analyse the dynamics of both vascular leakage and neutrophil responses in these mice concomitantly, *VEC-Y685F* mice and control littermates (*VEC-WT*) were sub-lethally irradiated and reconstituted with BM cells from *LysM-EGFP*$^{ki/+}$ (**Fig. 4.3A & B**), as described in Chapter 2, section 2.2.5.1. Acute inflammation was induced using our aforementioned IL-1β + histamine protocol and vascular leakage and neutrophil time-course responses were analysed by confocal IVM (experimental timeline depicted in Appendix 3, section 9.3.3).

Engraftment efficiency was evaluated 4 weeks post BM transplant and was assessed by flow cytometry as detailed in section 2.2.5.3. Here, both chimeras exhibited comparable peripheral neutrophil counts (**Fig. 4.3A & B**). In line with investigations from Wessel *et al.*, we found that in our model, the *VEC-Y685F* chimeric mice showed a significantly reduced microvascular leakage response when exposed to histamine stimulation corresponding to an approximate 30% inhibition at the peak of the reaction (i.e. 15 min post topical histamine application) as compared to *VEC-WT* control littermates (**Fig. 4.3C & D**). In addition, analysis of neutrophil TEM dynamics identified that whilst no significant differences in total neutrophil extravasation could be observed during the IL-1β + histamine-mediated reaction (**Fig. 4.3E**), *VEC-Y658F* mice exhibited a significant 50% inhibition in the frequency of neutrophil rTEM as compared to *VEC-WT* (**Fig. 4.3F**). Collectively these data strongly support the concept that vascular leakage promotes aberrant modes of neutrophil TEM.

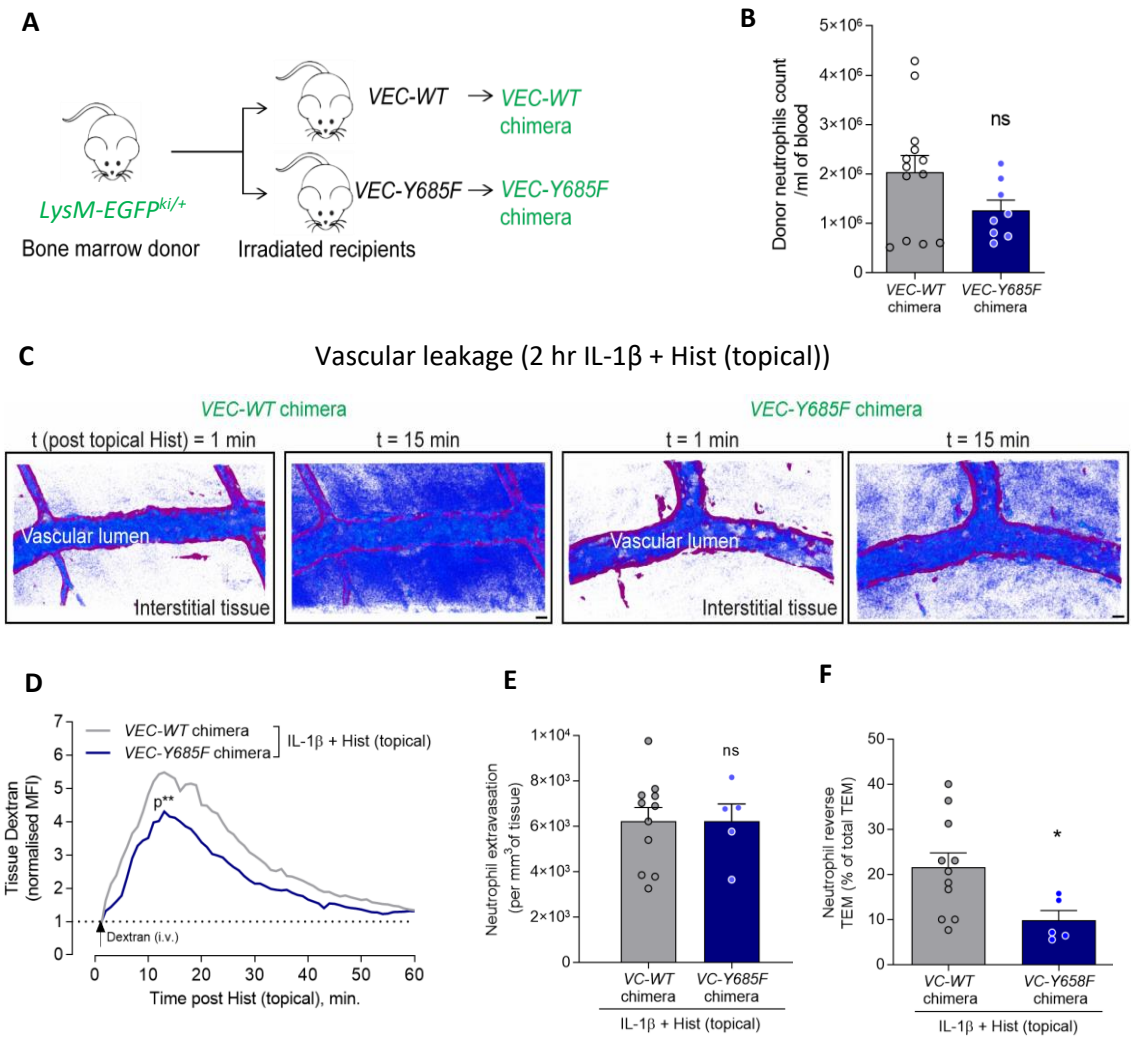

Figure 4.3. Chimeric VEC-Y658F mice exhibit reduced microvascular leakage induction and neutrophil rTEM. (**A**) Schematic diagram illustrating the generation of chimeric mice exhibiting LysM-EGFP$^{ki/+}$ HSCs within VEC-WT or VEC-Y658F recipients. Recipient mice (VEC-WT or VEC-Y658F) mice were irradiated and reconstituted with BM from LysM-EGFP$^{ki/+}$ donor mice as described in Chapter 2, section 2.2.5.3. This resulted in the generation of chimeric mice exhibiting LysM-EGFP$^{ki/+}$ monocytes (+) and neutrophils (++). (**B**) 4 weeks after reconstitution, both chimeras exhibited comparable neutrophil counts (>99% LysM-EGFP-positive neutrophils). (n = 8-13 mice/group). (**C**) Representative confocal IVM images of post-capillary venular segments (stained with anti-CD31; red) subjected to IL-1β + histamine stimulation at two time-points post application of histamine in chimeric VEC-WT and VEC-Y658F mice, illustrating dextran leakage (blue pseudocolour intensity). Scale bars (black) = 10 µm. (**D**) Time-course of dextran accumulation in the perivascular region of selected IL-1β-stimulated post-capillary venules in VEC-WT and VEC-Y658F chimeric mice post topical application of histamine. Tissue dextran accumulation is represented as MFI normalised to the first 2 time-points post i.v. dextran injection (n = 6-12 mice/group). Error bars are not shown for clarity but the SEM at the peak timepoint was within 0.782 and 1.013. (**E**) Total neutrophil extravasation (n = 5-11 mice/group). (**F**) Frequency of neutrophil rTEM events (n = 5-11 mice/group). Data are represented as mean ± SEM (each dot represents one mouse and one independent experiment). Indicated statistical differences are shown by *p<0.05 or **p<0.01, unpaired student t-test, (ns = not significant).

4.2.3. Enhanced vascular leakage promotes redistribution of CXCL1 from tissues to the vascular lumen

The next series of experiments aimed to investigate the molecular mechanism by which microvascular leakage influenced neutrophil migration dynamics. As previous investigations have demonstrated the importance of chemokines, specifically CXCL1 & CXCL2 in unidirectional neutrophil TEM (Girbl et al., 2018), we hypothesised that models of hyper-permeability could disrupt the established chemotactic gradient across the venular wall, thus impacting the ability of neutrophils to migrate in a strictly luminal-to-abluminal direction before reaching the tissue. In particular, as IL-1β effectively induces expression of the potent neutrophil chemoattractant, CXCL1, (Ribaux et al., 2007; Biondo et al., 2014), we sought to investigate whether the tissue distribution of CXCL1 was disrupted. To address this, in collaboration with Dr. Régis Joulia, we analysed the expression of CXCL1 in plasma and tissue by ELISA, following IL-1β +/- histamine-treatment or IR-injury of the cremaster tissue, according to Chapter 2, section 2.4.2. In brief, for IR-injury, WT mice were subjected to 40 min of ischaemia prior to reperfusion. Alternatively, WT mice were subjected to a local injection of IL-1β (200 µl of a 50 ng solution, i.s.) 2 hr prior to a local injection of histamine (200 µl of a 30 µM solution, i.s.) or PBS control (200 µl). Plasma and cremaster tissue samples were then collected after the peak of vascular leakage in each reaction i.e. following 30 min post reperfusion (**Fig. 3.4B**) or 30 min post topical histamine treatment (**Fig. 4.1C**) and processed for ELISA as detailed in Chapter 2, section 2.7.

Quantitative analysis of chemokine concentrations (kindly provided by Dr. Régis Joulia) revealed that tissue levels of CXCL1 were significantly increased in mice treated with IL-1β or IL-1β + histamine as compared to unstimulated (PBS) or histamine alone-treated mice (**Fig. 4.4A**). Of particular interest, mice treated with IL-1β + histamine had enhanced levels of CXCL1 in their plasma (1.3-fold increase) as compared to IL-1β-treated mice (**Fig. 4.4B**). Similarly, mice subjected to IR-injury had increased tissue and plasma CXCL1 levels relative to PBS-treated control animals (**Fig. 4.4C & D**). These findings suggest that microvascular leakage modifies the levels of CXCL1 between tissue and lumen/plasma; thus, disrupting the chemotactic gradient across the inflamed venular wall.

To further investigate the link between microvascular leakage induction and enhanced plasma CXCL1, we sought to inhibit histamine-dependent permeability. *In vivo*, vascular permeability is determined by the strength of intercellular interactions, which are themselves mediated by several pathways. In particular, the activity of Tie2, a tyrosine-protein kinase receptor known to be important for bolstering EC junctional integrity, is dependent on its dissociation from VE-PTP (Winderlich et al., 2009; Frye et al., 2015). Thus, we opted to use an anti-VE-PTP blocking Ab previously known to partially inhibit histamine- and VEGF-dependent vascular leakage in murine skin by inhibiting association of VE-PTP with Tie2 (Broermann et al., 2011; Frye et al., 2015).

In a first set of control experiments, we investigated if VE-PTP blockade inhibits vascular leakage in our IL-1β + histamine model in the cremaster muscle. For this purpose, WT mice received an i.v. injection of an anti-VE-PTP Ab (100-200 µg/mouse) 90 min post IL-1β stimulation. Alternatively, control mice were treated with an isotype matched control Ab or PBS (rabbit IgG 100-200 µg/mouse - no differences were observed between the PBS and the isotype control Ab). The cremaster muscle tissue was then exteriorised and processed to measure histamine-dependent vascular leakage as detailed in section 4.2.1 (experimental timeline depicted in Appendix 3, section 9.3.4). Alternatively, IL-1β treated mice received a local injection of histamine as described above for subsequent analysis of CXCL1 by ELISA. Plasma was collected from all mice 1 hr post application of histamine and were analysed by Dr. Régis Joulia to determine CXCL1 levels by ELISA.

Mice injected with the anti-VE-PTP Ab exhibited a 37% reduction in histamine-induced vascular leakage relative to treatment with PBS or the control IgG rabbit Ab (**Fig. 4.4E**). Furthermore, a 36% decrease in the plasma CXCL1 levels was noted in mice treated with the anti-VE-PTP Ab (**Fig. 4.4F**).

Collectively, the increase in plasma CXCL1 levels is at least partly governed by VE-cadherin-dependent vascular leakage.

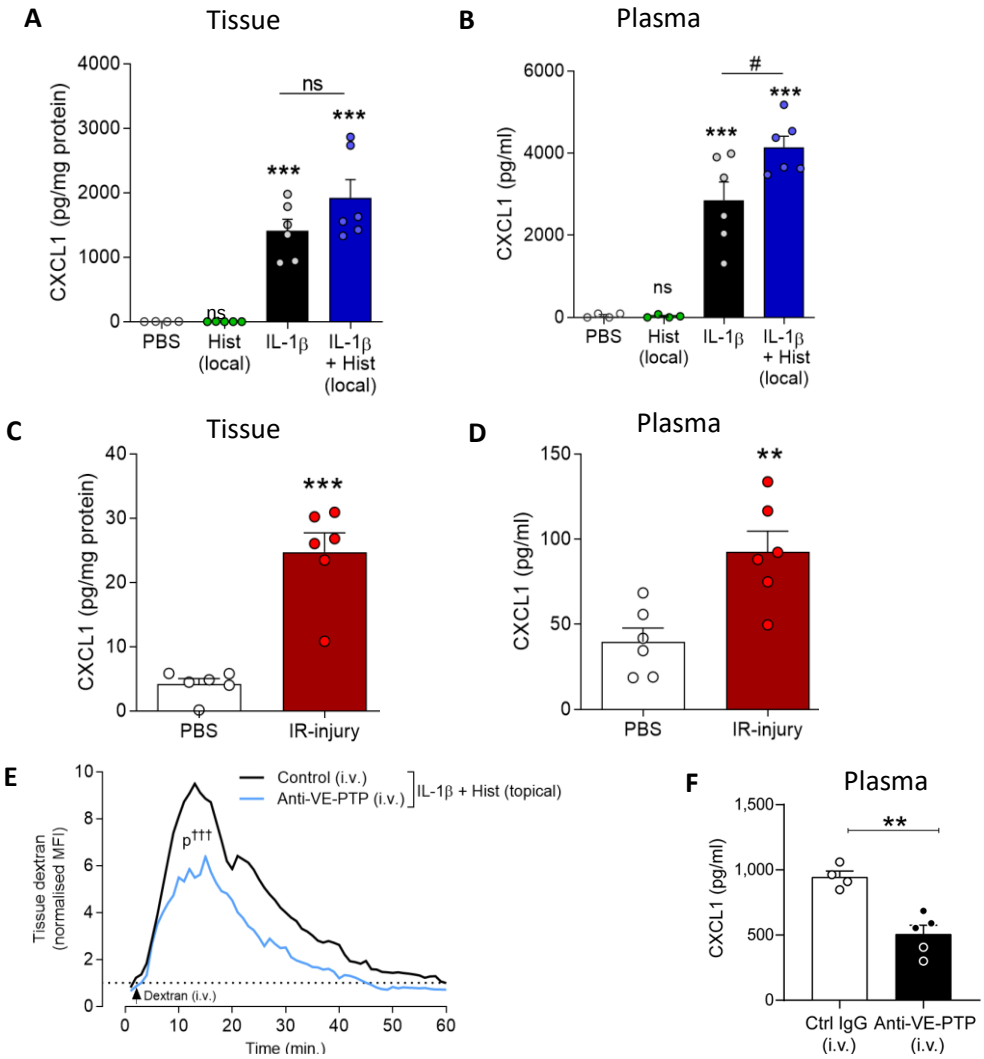

Figure 4.4. Histamine-induced vascular leakage enhanced translocation of tissue generated CXCL1 into the blood. (**A-F**) Cremaster muscles of WT mice were subjected to 40 min of ischaemia and 30 min of reperfusion or alternatively after 2 hr of locally injected IL-1β (200 µl of a 50 ng solution, i.s.) followed by 30 min of locally injected histamine (200 µl of a 30 µM solution, i.s.) or PBS control (200 µl). In some experiments, fluorescently labelled anti-CD31 mAb (4 µg) was injected i.s. 30 min prior to exteriorisation (IR-injury experiments) or in combination with PBS/IL-1β (IL-1β + Histamine experiments). Some mice were also injected i.v. with an anti-VE-PTP Ab or IgG rabbit control Ab 90 min post local IL-1β. In addition, some mice received an i.v. injection of 75 kDa TRITC-dextran at the start of the image acquisition period. In some experiments plasma and tissue samples were isolated 30 min post reperfusion or local application of histamine and processed for CXCL1 quantification as analysed by ELISA. (**A & C**) Tissue or (**B & D**) Plasma CXCL1 analysis (n = 4-6 mice/group). (**E**) Time-course of dextran accumulation in the perivascular region of a post-capillary venule, represented as relative MFI (n = 3-4 mice/group). Error bars are not shown for clarity but the SEM at the peak timepoint was within 2.668 and 2.207. (**F**) Plasma CXCL1 as analysed by ELISA, 1 hr post histamine +/-anti-VE-PTP (100-200 µg) (n = 4-5 mice/group). Data are represented as mean ± SEM (each dot represents one mouse/independent experiment). Statistically significant differences from (**A-D + F**) PBS-treated (indicated by **p<0.01, ***p<0.001) or (**A & B**) IL-1β (indicated by #p<0.05) or (**E**) anti-VE-PTP Ab treated (indicated by †††p<0.001) mice, as analysed by an (**A & B**) one-way ANOVA followed by Bonferroni's post-hoc test or (**C-F**) unpaired student t-test, (ns = not significant). Data obtained in collaboration with Dr. Régis Joulia.

4.2.4. Blockade of systemic CXCL1 reduced the frequency of neutrophil rTEM

As previous experiments provided evidence that vascular leakage induction leads to a disrupted distribution of tissue CXCL1, we considered that this excess plasma CXCL1 could drive transmigrating neutrophils back into the vascular lumen and hence promote rTEM. To this end, the next series of experiments were aimed at investigating the effect of systemic blockade of CXCL1, using an anti-CXCL1 blocking Ab (Girbl et al., 2018), in our models of IL-1β + histamine and IR-injury.

Briefly, 2 hr post-stimulation of tissues with IL-1β, mice were injected i.v. with an anti-CXCL1 blocking Ab (1 mg/kg) at a dose determined by colleagues (data not shown) not to block total neutrophil recruitment. Control animals received the same dose of an isotype matched control Ab. Alternatively, mice were subjected to IR-injury, as described in Chapter 2, section 2.4.2. and were additionally, injected i.v. with an anti-CXCL1 antibody at the point of reperfusion of the cremaster muscle. In the IL-1β + histamine studies, TRITC-dextran was injected i.v. at the start of the 2 hr confocal image acquisition period (experimental timeline depicted in Appendix 3, section 9.3.5 & 9.3.6). Neutrophil migratory behaviour and vascular leakage were then analysed offline with IMARIS software as detailed in Chapter 2, section 2.6 and Chapter 3, section 3.2.1, respectively.

Analysis of confocal image sequences revealed that at the dose and time employed, systemic administration of anti-CXCL1 Ab had no impact on plasma protein leakage (**Fig. 4.5A**) or total neutrophil extravasation into the surrounding tissue (**Fig. 4.5B & D**). However, the frequency of neutrophil rTEM events was significantly reduced by approximately 60 % as compared to mice injected with a control Ab (**Fig. 4.5C & E**).

Collectively, these data strongly suggest that inflammatory reactions characterised by a rapid increase in vascular leakage also lead to enhanced levels of plasma CXCL1, which in turn, disrupts chemotactic directional cues, a response that drives neutrophil rTEM.

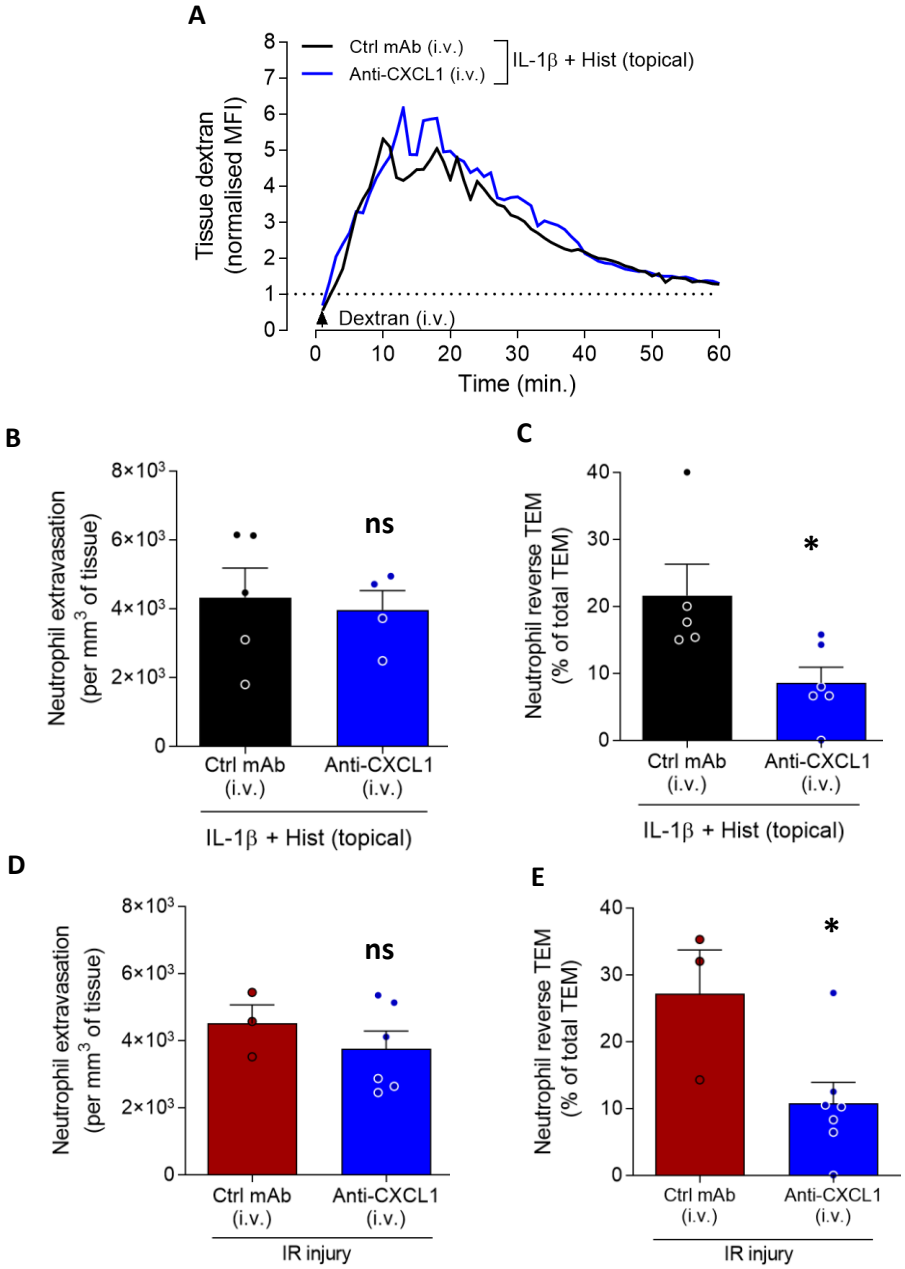

Figure 4.5. Systemic CXCL1 blockade reduces the frequency of neutrophil rTEM. Cremaster muscles of *LysM-EGFP*$^{ki/+}$ mice were stimulated with IL-1β (50 ng for 2 hr) followed by topical superfusion of histamine (30 µM) onto an exteriorised cremaster tissue. Alternatively, mice were subjected to 40 min ischaemia and 2 hr of reperfusion. Blocking anti-CXCL1 Ab (1 mg/kg), or control IgG Ab was injected i.v. immediately prior to exteriorisation of the cremaster tissue or at the point of reperfusion. Fluorescently labelled anti-CD31 mAb (4 µg) was injected i.s. to visualise EC junctions and in some experiments, 75 kDa TRITC-dextran was injected i.v. at the start of the image acquisition period. (**A**) Time-course of dextran accumulation in the perivascular region of a post-capillary venule, represented as relative MFI (n = 4-6 mice/group). Error bars are not shown for clarity but the SEM at the peak timepoint was within 0.499 and 1.213. (**B & D**) Total neutrophil extravasation (n = 3-6 mice/group). (**C & E**) Frequency of neutrophil rTEM events. (n = 3-7 mice/group). Data are represented as mean ± SEM (each dot represents one mouse and one independent experiment). (**B-E**) Statistically significant differences from control Ab-treated groups is shown by *p<0.05 as determined by an unpaired student t-test, (ns = not significant).

4.3. Discussion

Vascular hyper-permeability and leukocyte recruitment are key hallmarks of the innate immune system that occur during the development of acute inflammatory reactions. Whilst these two events have largely been studied independently, there is ample evidence for neutrophil activation and transmigration to alter the barrier functions of blood vessel walls. More specifically, there is now extensive evidence that neutrophils can promote vascular leakage in the very preliminary stages of the inflammatory process through the secretion of a variety of factors, including TNF (Djeu et al., 1990; Finsterbusch et al., 2014), VEGF (Scapini et al., 2004) and LTA_4 (Wedmore and Williams, 1981; DiStasi and Ley, 2009). However, it is not yet understood whether vascular leakage itself can impact neutrophil trafficking. Therefore, experiments were conducted to investigate the interplay of these two fundamental components in models of acute inflammation. The present work provides evidence for the first time that microvascular hyper-permeability induction can lead to disruption of neutrophil TEM, whereby a significant proportion of neutrophils (20-25%) migrate in an abluminal-to-luminal direction, known as neutrophil rTEM. Mechanistically, this response was mediated by a permeability-dependent disruption of chemokine distribution, namely CXCL1, across the endothelium. Collectively, these findings extend our current knowledge of how vascular leakage and neutrophil TEM are interlinked during acute inflammatory reactions.

In this Chapter, our extended confocal IVM platform (as established in Chapter 3) was utilised to further investigate the impact of vascular leakage on neutrophil TEM dynamics in real time. Here, application of pro-permeability agents (histamine or VEGF) to IL-1β stimulated cremaster muscles resulted in rapid and transient but potent vascular leakage responses. This was associated with enhanced levels of neutrophil rTEM within the first 30 min, whilst all treatment groups exhibited comparable levels of total neutrophil extravasation at the end of the imaging acquisition period (2 hr post histamine/VEGF). Overall, this suggested a causal link whereby the onset of microvascular leakage results in enhanced levels of neutrophil rTEM.

To explore this concept further, we sought to manipulate the vascular leakage response. Our investigations focused on VE-cadherin, a vital EC junctional adherens molecule and

mediator of histamine-induced vascular permeability (Winter et al., 2004). In collaboration with Prof. Dietmar Vestweber, we utilised a mutant VE-cadherin mouse model which has been shown to exhibit reduced vascular leakage induction following histamine treatment, but with no effect on total neutrophil extravasation following IL-1β-stimulation of the cremaster tissue, as analysed by confocal IVM (Wessel et al., 2014). In the present study, histamine-dependent vascular leakage was similarly decreased by ~30% in *VEC-Y685F* mice, relative to *VEC-WT* mice. Importantly, while this inhibition of vascular leakage did not affect total neutrophil extravasation, the frequency of neutrophil rTEM was partially decreased (~30%), providing direct evidence that microvascular leakage can impact the directionality of neutrophil TEM.

Next, we investigated mechanistically how enhanced microvascular leakage could lead to augmented neutrophil rTEM. Firstly, we considered previous publications identifying the mechanisms regulating neutrophil rTEM (Woodfin et al., 2011; Colom et al., 2015). In these previous studies, the NE-dependent cleavage of JAM-C at EC junctions results in enhanced neutrophil rTEM during IR-injury and LTB_4 treatment (Woodfin et al., 2011; Colom et al., 2015). Whilst we initially considered this mechanism in our model of IL-1β + histamine, a review of the relevant literature revealed that findings regarding the distribution of JAM-C during vascular permeability is conflicting. While investigations by Orlova *et al.,* observed that loss of JAM-C resulted in reduced vascular permeability compared to control groups following histamine or VEGF stimulation, investigations by Imhof and colleagues found opposing observations in a parasitic infection model of Leishmania major in which loss of JAM-C increased vascular permeability by 15% (Ballet et al., 2014). As such, the role of JAM-C in vascular leakage remains ambiguous and requires exploration in our model of IL-1β + histamine. To assess whether loss of EC JAM-C can impact vascular permeability and subsequently the rTEM response in our acute inflammatory model, Dr. Régis Joulia performed experiments that identified no difference in junctional JAM-C expression following histamine alone, IL-1β alone or IL-1β + histamine (Owen-Woods et al., 2020). Therefore, other avenues needed to be explored to elucidate the mechanism driving permeability-mediated neutrophil rTEM.

To this end, we considered the potential disruption of chemokine expression/localisation, essential aspects of the neutrophil transmigration cascade. Chemotactic directional cues are governed by the establishment of a concentration

gradient as determined by the localisation and expression of chemoattractants such as LTB_4 and CXCL1 (Janetopoulos and Firtel, 2008; McDonald et al., 2010; Jin, 2013). The importance of chemotactic directional cues has also recently been demonstrated in the context of neutrophil TEM (Girbl et al., 2018). This work showed that neutrophils require sequential interactions with the chemokines CXCL1 followed by CXCL2, as potentially presented by EC surface GAGs (Proudfoot et al., 2017; Uchimido et al., 2019) and EC junctional ACKR1 (Pruenster et al., 2009; Novitzky-Basso and Rot, 2012; Thiriot et al., 2017; Girbl et al., 2018), to mediate neutrophil crawling and unidirectional paracellular TEM, respectively. Based on our current understanding of neutrophil directional motility towards a chemotactic gradient, we hypothesised that enhanced microvascular leakage could disrupt the correct localisation of directional cues, and in turn, lead to abnormal neutrophil TEM. As IL-1β is known to be a potent inducer of CXCL1 expression (Ribaux et al., 2007; Biondo et al., 2014), our investigations focused on this chemokine. In collaboration with Dr. Régis Joulia, we observed that IL-1β induced production and release of CXCL1 in the tissue and plasma. However, following IL-1β + histamine treatment, CXCL1 levels were significantly increased (1.3-fold increase) in the plasma as compared to control IL-1β-treated mice. This could suggest that tissue generated CXCL1 may be translocated/transported through the disrupted EC junctions into the plasma following enhanced vascular leakage, thus reversing the chemotactic gradient of this chemokine. Indeed, the interstitial tissue contains many cellular sources of CXCL1, including pericytes (Girbl et al., 2018), ECs (Goebeler et al., 1997; Girbl et al., 2018) and macrophages (Becker et al., 1994). However, if true, this would require CXCL1 to move against the luminal-to-abluminal hydraulic flux, which would be greater in scenarios of enhanced vascular leakage.

To test the veracity of this hypothesis, mathematical modelling was initially developed in collaboration with the group of Prof. David Bates from the University of Nottingham, which simulated venule and tissue exchange dynamics of our inflammatory reaction (Owen-Woods et al., 2020). Under basal conditions, passage of molecules across the endothelium is minimal, but under conditions of hyper-permeability the EC junctions widen/loosen and enable transendothelial movement of blood and tissue bound molecules. In our mathematical model, movement across the endothelium of molecule of interest, such as CXCL1, is related to the Péclet number (*Pe*). This number is a ratio of

the opposing transendothelial diffusive flux (i.e. abluminal-to-luminal movement) and advective flux (i.e. luminal-to-abluminal movement), whereby lower or higher numbers indicate dominating advective or diffusive flux, respectively. These factors are determined by four underpinning major factors: the hydraulic velocity of fluids and solutes from the blood into the tissue, the chemokine diffusion distance, diameter of the EC junctional pore and finally the size of the molecule of interest, in this case 10 kDa. The hydraulic velocity depends on hydrostatic/oncotic pressures exerted by the blood and tissue, as well as the overall endothelial permeability. These factors were determined using known data available in the literature and adapted to simulate scenarios of minimal and enhanced vascular permeability, whereby in the latter hydraulic velocity is reduced. Through this approach, our mathematical model predicted that molecules such as CXCL1 would have a *Pe* number of 0.8 under homeostatic control conditions, which decreased to 0.3 under enhanced vascular permeability. This indicated that the diffusion of CXCL1 from tissue into plasma was feasible in our inflammatory reaction as induced by IL-1β + histamine. These predictions were thus experimentally tested by Dr. Régis Joulia using a small fluorescently labelled 10 kDa dextran topically applied to the cremaster tissue prior to the topical application of histamine- or vehicle control solution. The experimental data successfully demonstrated trafficking of the 10 kDa dextran from the tissue into the blood (as detected by fluorospectrometry of plasma samples) following topical application of histamine, but minimally in vehicle control treated mice (Owen-Woods et al., 2020).

To further explore the hypothesis that vascular permeability can promote the translocation of tissue-generated chemokines into the vascular lumen, we sought to block the vascular leakage response. This was accomplished using an anti-VE-PTP blocking Ab previously shown to partially inhibit histamine- and VEGF-dependent vascular leakage in a model of skin inflammation through a Tie2 dependent mechanism (Frye et al., 2015; Winderlich et al., 2009). *In vivo*, Tie2 functionally attenuates vascular leakage by activating the GTPase, Rac1, which is turn blocks the activation of RhoA and prevents the induction of contractile forces of actinomyosin stress fibres. This not only helps to prevent the formation of EC junctional gaps but also acts to prevent internalisation of VE-cadherin (Braun et al., 2019). Indeed, in our study at the dose employed, blockade with anti-VE-PTP Ab partially reduced (~30 %) the vascular leakage

response as induced by IL-1β + histamine. Furthermore, plasma CXCL1 levels were also reduced, supporting the hypothesis that vascular permeability drives enhanced translocation of tissue generated CXCL1 into the plasma.

Finally, the impact of increased plasma CXCL1 on neutrophil dynamics was directly assessed. Here, mice received an i.v. injection of a blocking anti-CXCL1 Ab at a dose known not to interfere with the neutrophil extravasation response (data not shown) prior to the topical application of histamine on IL-1β stimulated tissues or following IR injury. In this context, mice treated with the anti-CXCL1 Ab exhibited a reduced frequency of neutrophil rTEM in both inflammatory reactions. Here, we provide evidence that chemotactic cues are critical for neutrophil luminal-to-abluminal migration across the EC wall. This result is consistent with previous investigations from Girbl *et al.,* showing that CXCL1 and CXCL2 sequentially interact with neutrophil expressed-CXCR2 to ensure effective neutrophil crawling and luminal-to-abluminal TEM, respectively, following TNF stimulation (Girbl et al., 2018).

In the context of our study, increased detection of CXCL1 in the plasma following histamine application may be indicative of augmented retention and presentation of the chemokine CXCL1 at EC junctions, which subsequently disrupts the sequential steps required for neutrophil migration. Increased passage of CXCL1 through EC junctions in an abluminal-to-luminal direction could result in excessive retention and therefore presentation at the junction of CXCL1 by ACKR1, which has been shown to bind CXCL1 (Pruenster et al., 2009; Novitzky-Basso and Rot, 2012). This could consequently either saturate neutrophil-expressed CXCR2 and thus not allow for sufficient binding of CXCL2, previously shown to mediate neutrophil TEM (Girbl et al., 2018). Alternatively, this could lead to desensitisation and internalisation of CXCR2, thus resulting in the inability for CXCL2 to bind. In both cases, the resultant effect could be ineffective signalling to mediate normal TEM and hence could lead to neutrophil rTEM. This hypothesis requires further exploration to determine the specific contribution of chemokines governing neutrophil rTEM, as discussed in Chapter 7.

4.4. Conclusion

This Chapter provided direct evidence for the ability of vascular leakage to impact the directionality of neutrophil TEM *in vivo*. Here, and as supported by the relevant literature and detailed in our recent publication (Owen-Woods *et al.,* 2020; see appendix 1), we identified a novel mechanistic pathway whereby vascular leakage results in disruption of the CXCL1 chemotactic gradient across the endothelium. This response was subsequently found to enhance the occurrence of neutrophil rTEM (**Fig. 4.6**). Previous studies investigating this phenomenon have reported that during inflammatory reactions that exhibit local neutrophil rTEM, enhanced levels of lung permeability are also observed (Woodfin et al., 2011; Colom et al., 2015). Thus, it has been hypothesised that rTEM neutrophils disseminate to distant organs where they have a pathological consequence. Hence, in the next Chapter, we sought to eludicate the potential pathophysiological relevance of this abnormal mode of neutrophil TEM.

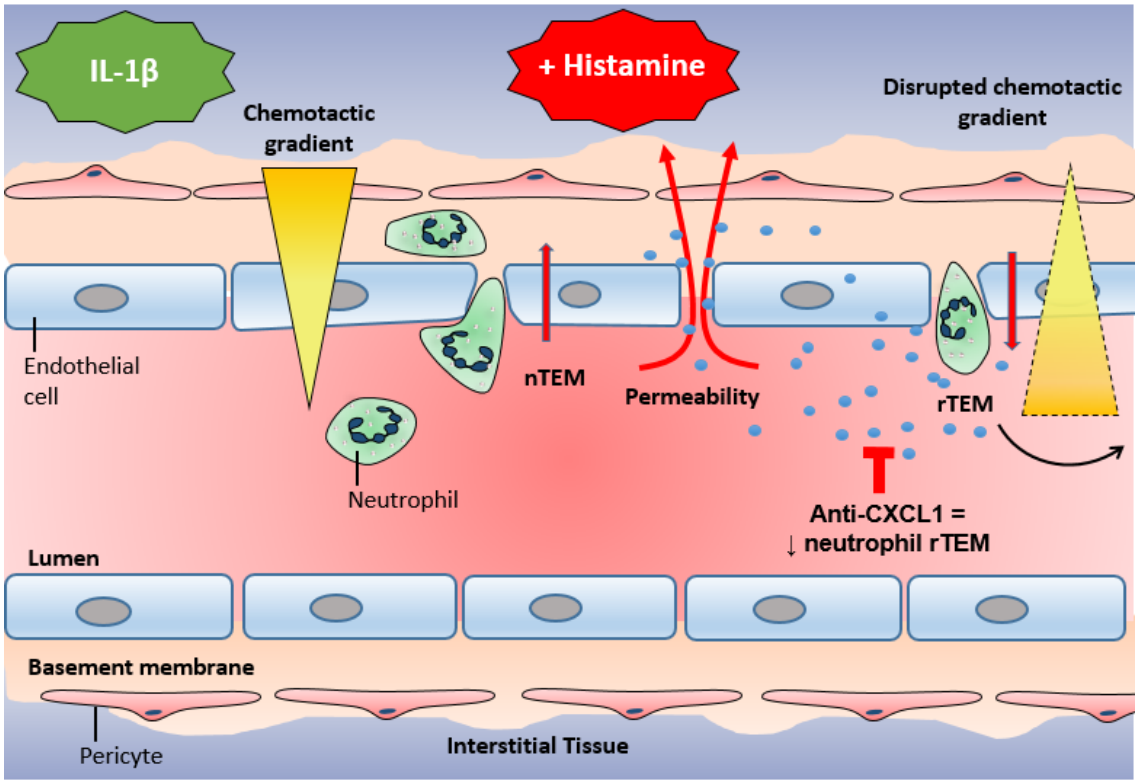

Figure 4.6. Microvascular leakage disrupts chemotactic cues and promotes neutrophil rTEM. Following local IL-1β stimulation of the mouse cremaster muscle, a chemotactic gradient across the endothelium is established, one such chemokine being CXCL1, resulting in the rapid recruitment of neutrophils to the site of inflammation, where they then adhere and undergo normal TEM. However, under conditions of hyper-permeability such as those seen following IR-injury or following the addition of the exogenous pro-permeability agent, histamine, the chemotactic gradient is disrupted resulting in elevated plasma CXCL1 levels. This augmentation of CXCL1 supported enhanced neutrophil rTEM. Following systemic blockade of CXCL1 the gradient is rebalanced and the frequency of neutrophil rTEM is reduced.

Chapter 5

Tracking and phenotypic analysis of reverse transmigrating neutrophils

5.1. Introduction

Our understanding that neutrophils can undergo rTEM is well established (Buckley et al., 2006; Woodfin et al., 2011; Colom et al., 2015; Girbl et al., 2018; Owen-Woods et al., 2020), but the phenotype, fate and (patho)physiological role of reverse transmigrating neutrophils remains poorly understood. Primarily, this lies in the difficulty to exclusively target, track and isolate this sub-set of neutrophils. An early *in vivo* attempt to understand the phenotype of rTEM neutrophils was carried out by our team (Woodfin et al., 2011). Following a model of local IR-injury of the hind limb, the group observed an increased frequency of neutrophil rTEM and further identified a population of activated neutrophils in the lung vasculature expressing high levels of ICAM-1 and ROS (Woodfin et al., 2011). This small population of pro-inflammatory neutrophils were hypothesised to be reverse migrating neutrophils that had disseminated from the local injured area. However, to conclusively demonstrate this hypothesis, a method to directly track and phenotype reverse transmigrating neutrophils was required.

One of the first studies aiming to directly track reverse transmigrating neutrophils employed a model of sterile injury in a transgenic zebrafish that expressed the photoconvertible fluorescent reporter Dendra2 in leukocytes (Yoo and Huttenlocher, 2011). Following wounding of the tail fin, neutrophils that had reached the site of inflammation in the interstitial tissue were laser-targeted for photoconversion (PC). Here, over the course of a few days, a small proportion of extravasated photoconverted neutrophils where observed to migrate back into the vasculature lumen (Yoo and Huttenlocher, 2011). The interstitial reverse migration element of this response was later termed reverse interstitial migration (rIM) (Nourshargh et al., 2016). While the approach employed allowed for differentiation of neutrophils undergoing rIM and rTEM, the authors did not isolate the neutrophils for phenotypic analysis (Yoo and Huttenlocher, 2011). More recently, Wang et al., utilised a similar approach by employing laser-photoactivation (PA) of neutrophils to enable tracking of cells that underwent a combined rIM and rTEM response in injured murine livers (see Chapter 1, section 1.6) (Wang et al., 2017). Specifically, *Ly6G-PA-GFP* mice that specifically express photoactivatable GFP exclusively in mature neutrophils, were subjected to surface liver burn injury. Cell PA was conducted 14 hr post injury of neutrophils located within the

extravascular tissue and close to the injured site. With this approach, only neutrophils that had undergone migration into the interstitium were photoactivated, whilst neutrophils in the vasculature remained inactivated. The authors then observed that a proportion of these photoactivated neutrophils undergo rIM followed by rTEM into the murine liver microcirculation and thus were able to definitively label and track a proportion of these cells. The group then extended their investigations to track these reverse migrating neutrophils. Subsequently, the group identified a small population of photoactivated (and therefore assumedly) reverse migrated neutrophils in the lungs and BM of the mice 24 hr post induction of liver injury. Furthermore, at both sites, Ly6G-PA-GFP^{+} cells had elevated surface expression levels of CXCR4, whilst those exclusively in the BM also exhibited elevated surface expression of annexin V, suggesting these cells homed to the BM to be cleared. Collectively, these two cited studies indicated that neutrophil rIM may serve as a physiological clearance mechanism for neutrophils, thus contributing to local resolution of the inflammatory response and wound healing (Yoo and Huttenlocher, 2011; Wang et al., 2017).

Comparison of investigations by Woodfin et al., Yoo & Huttenlocher and Wang et al., reveals a conflict between the fate of reverse migrating neutrophils, which may be attributed to two key factors. Firstly, the type of reverse migration under consideration (rTEM by the former and rIM + rTEM by the latter studies) and secondly, the timepoint post injury at which Woodfin et al., and Wang et al., conducted phenotypic analysis (at 1 hr or 24 hr, respectively), among other factors as further detailed in the discussion (section 5.3). However, a comprehensive comparison is difficult without direct phenotypic analysis of rTEM neutrophils in these reactions. Although the aforementioned PC/PA techniques have advanced our understanding of reverse migrating neutrophils, they remain impractical for analysis of rTEM neutrophils. For instance, laser PA only allows for selected regions of interest to be targeted and therefore only provides a snapshot of the overall response. This severely limits the number of cells tracked and thus reduces the reliability of any observed phenotype change. In addition, while these approaches are suitable for targeting reversing neutrophils that have migrated deep into the tissue (i.e. rIM), they do not possess the precision to target rTEM neutrophils, in which reversing cells are limited to breaching of the thin endothelium only. Hence, a new technique was required to improve the number

of reversing neutrophils tracked, and more importantly, to selectively track rTEM neutrophils that only breach the endothelium and do not enter the interstitial tissue.

5.1.3. Scope of the Chapter

This Chapter details a novel methodology for the exclusive labelling and tracking of rTEM neutrophils and thus provides insight into their phenotype and fate. To this end, the aims of this Chapter are as follows:

- Establish an effective immuno-labelling protocol for the tracking of neutrophils exhibiting rTEM.
- To validate the methodology.
- To provide insight into the phenotype and fate of reverse migrating neutrophils.

5.2. Results

5.2.1. Strategy for the exclusive labelling and tracking of rTEM neutrophils

In order to specifically target rTEM neutrophils (and not intraluminal cells), a two-step immuno-labelling approach was added to our IVM protocol. As the objective was to track rTEM neutrophils, the new labelling strategy was applied to analysis of tissues stimulated with the combination of IL-1β + histamine, an inflammatory reaction that caused a significant rTEM response (see Chapter 4 & Chapter 2, section 2.4 for the details of the IVM protocol). Since neutrophil rTEM is a rapid response during which neutrophils do not migrate beyond the pericyte layer, it was essential that the labelling occurred immediately and irreversibly upon engagement of the neutrophils within EC junctions.

To this end, we sought to exploit the high affinity between biotin and streptavidin, which when bound, exhibits one of the strongest known non-covalent interactions (dissociation constant, $K_D \approx 10^{-15}$ mol/L) (Green, 1975; Weber et al., 1989). Thus, we elected to inject biotinylated anti-Ly6G Ab (anti-Ly6G-biotin – 2 µg) i.v., 30 min prior to cremaster exteriorisation, to target the glycoprotein, Ly6G (exclusively expressed by mature neutrophils in the blood) to label all peripheral neutrophils (Lee et al., 2013). In addition, streptavidin (fluorescently labelled, strept-AF647 – 1 µg/ml) was applied topically to the cremaster tissue. Based on its molecular weight (e.g. 60 kDa; see the mathematical modelling discussed in Chapter 4), we envisaged minimal diffusion of strept-AF647 into the vascular lumen.

Through this methodology, only neutrophils that breached the endothelium (extravascular and rTEM) became labelled with strept-AF647 (**Fig. 5.1**). Thus, in the circulation, rTEM neutrophils could be identified as Ly6G-biotin-Strept-AF647$^+$ (strept-AF647$^+$) by both confocal IVM and flow cytometry. Firstly however, it was important to validate this approach as detailed in section 5.2.2.

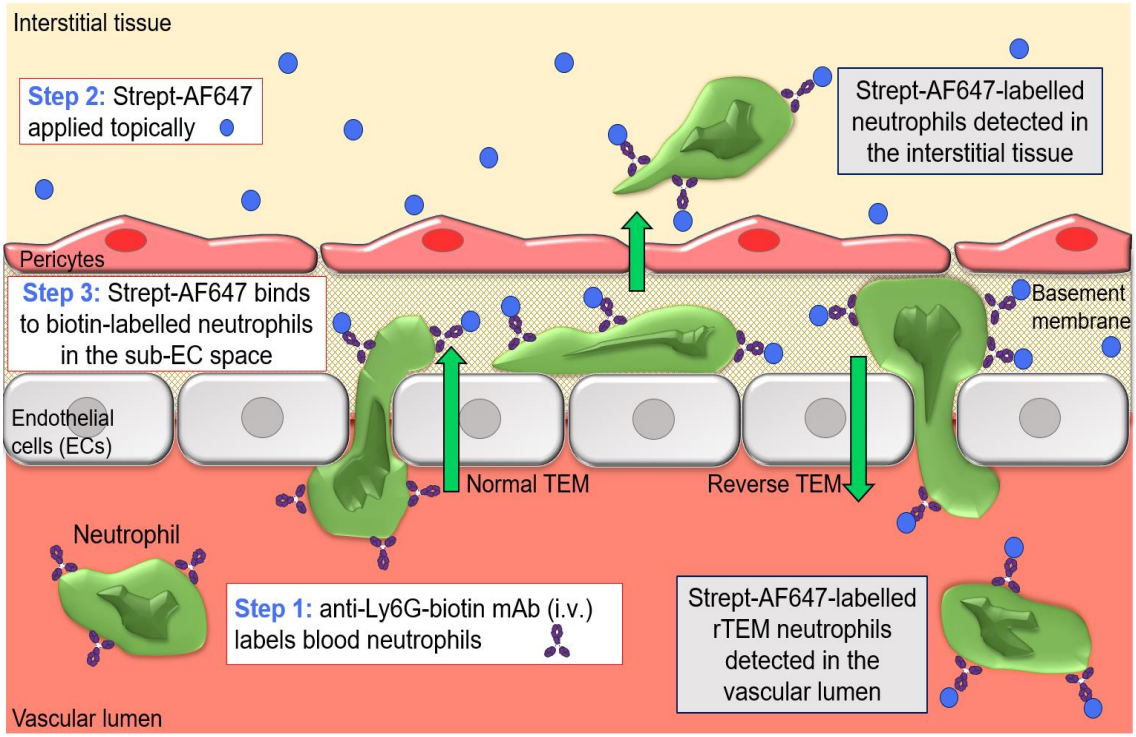

Figure 5.1. Schematic demonstrating the novel labelling strategy developed for exclusive targeting of rTEM neutrophils. *LysM-EGFP*$^{ki/+}$ mice received an i.v. injection of anti-Ly6G-biotin Ab (2 µg) for 30 min. Cremaster muscles were then exteriorised and strept-AF647 (1 µg/ml) was topically applied for up to 2 hr. Reproduced from Owen-Woods et al., 2020.

5.2.2. Experimental validation of the methodology

Before fully assessing the efficacy of the protocol in labelling rTEM neutrophils, we conducted a number of validation steps. Firstly, we assessed whether the anti-Ly6G-biotin Ab, at the dose employed, labelled all peripheral neutrophils with high efficacy and specificity. Secondly and crucially, to assess the selectivity of the technique for labelling rTEM neutrophils, we analysed the potential diffusion of topically applied strept-AF647 from the tissue into the blood. Naturally, such an effect would lead to undesirable labelling of blood circulating Ly6G-biotin^{+} neutrophils and hence confound conclusions drawn in the context of rTEM neutrophils.

To address the efficacy and specificity of the anti-Ly6G Ab staining *in vivo*, *LysM-EGFP*$^{ki/+}$ mice were treated locally with IL-1β and subsequently injected i.v. with anti-Ly6G-biotin, as described in section 5.2.1. Blood samples were then collected *via* the tail vein every 30 min up to 150 min. Samples were then processed for flow cytometry as detailed in Chapter 2, section 2.2.5.3. Distinctly, samples were incubated *in vitro* with exogenous strept-AF647 (1 µg/ml) or vehicle solution in combination with anti-CD45 and anti-GR1-PE mAb to discriminate between neutrophils (CD45-PB^{+}, Gr1-PE^{high} and EGFP^{high}) and inflammatory monocytes (CD45-PB^{+}, Gr1-PE^{low} and EGFP^{low}). The data showed that 2 µg of anti-Ly6G-biotin was sufficient to label >99% of all circulating neutrophils for up to 150 min post injection of anti-Ly6G-biotin, whilst monocytes remained negative for Ly6G staining throughout (**Fig. 5.2A & B**).

For assessment of strept-AF647 diffusion into the circulation, *LysM-EGFP*$^{ki/+}$ mice received an i.v. injection of anti-Ly6G-biotin for 30 min. The cremaster muscle was then exteriorised and subjected to topical application of strept-AF647 (1 µg/ml) ± histamine for 2 hr. Blood samples were collected from the ascending vena cava and processed for flow cytometry as detailed in Chapter 2, section 2.2.5.3. Samples were incubated with fluorescently labelled anti-CD45 and anti-Gr1 mAbs. Our analysis showed that topical application of strept-AF647 in the presence and absence of histamine for 2 hr led to very low numbers of strept-AF647^{+} neutrophils (<0.17%) in the blood (**Fig. 5.2C**).

Collectively, we established that at the doses employed, i.v. anti-Ly6G-biotin was suitable for specific and efficient labelling of blood neutrophils and that topically applied strept-AF647 exhibited minimal intraluminal diffusion, even under conditions of

enhanced vascular leakage as induced by local histamine. With these findings in hand, we next assessed if this strategy was sufficient to label migrating neutrophils.

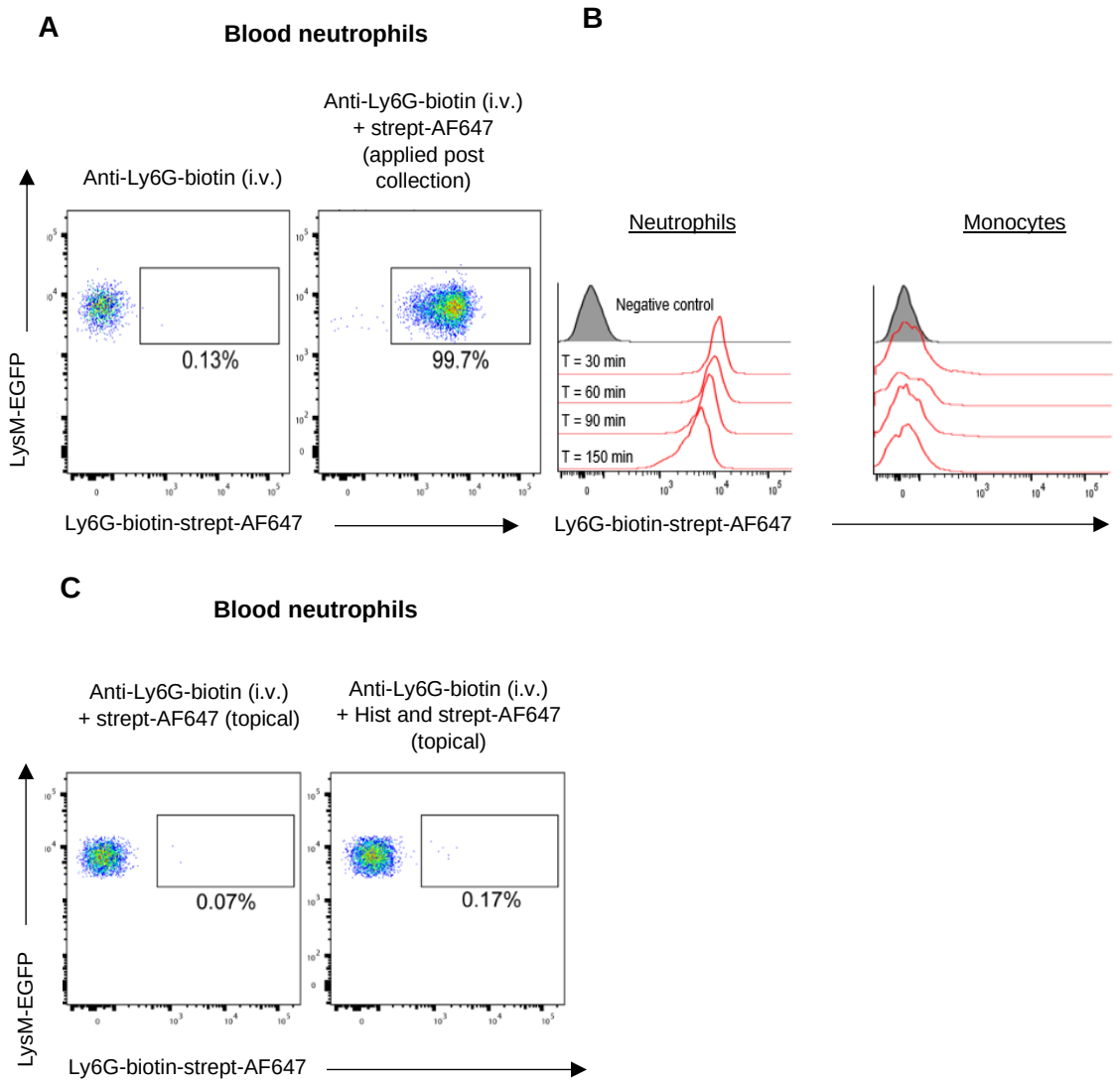

Figure 5.2. Anti-Ly6G-biotin efficiently and specifically labelled neutrophils, while topical strept-AF647 exhibited minimal diffusion into the blood. (**A-B**) *LysM-EGFP*$^{ki/+}$ mice received an i.s. injection of IL-1β (50 ng) for 1.5 hr followed by an i.v. injection of anti-Ly6G-biotin Ab (2 µg). Blood was then taken every 30 min up to 150 min post anti-Ly6G-biotin injection and treated with exogenous strept-AF647 (1 µg/ml). (**A**) Validation of anti-Ly6G-biotin dose efficacy and (**B**) assessment of the specificity of anti-Ly6G-biotin binding to selectively label neutrophils overtime (30-150 min post i.v. anti-Ly6G-biotin). (**C**) Alternatively, *LysM-EGFP*$^{ki/+}$ mice were injected i.v. with anti-Ly6G-biotin mAb for 30 min. The dot plot histograms show the assessment of strept-AF647 diffusion into the circulation under basal condition or following histamine-induced vascular leakage as determined by flow cytometry. Representative of (**A-B**) 5 and (**C**) 3 independent experiments. Experiments were carried out in collaboration with Dr. Loïc Rolas.

For this purpose, we assessed the capacity of this protocol to label neutrophils that undergo diapedesis in IL-1β-stimulated tissues, as analysed by confocal microscopy.

Here, *LysM-EGFP*$^{ki/+}$ mice were treated with local IL-1β (50 ng) in combination with anti-CD31-AF555 (2 µg) for 1.5 hr, after which, anti-Ly6G-biotin (2 µg) was administered i.v. After 30 min the cremaster tissue was exteriorised and topically applied with strept-AF647 (1 µg/ml) for 2 hr, as described in section 5.2.1. Tissues were then collected and fixed as detailed in Chapter 2, section 2.6 and imaged on a confocal microscope in collaboration with Dr. Loïc Rolas, as described in **Fig. 5.3**. Fixed tissue images showed/indicated that luminal EGFP^{+} neutrophils, i.e. those that had not breached the endothelium, were strept-AF647^{-} following topical application of strept-AF647. In contrast, EGFP^{+} neutrophils in the interstitial tissue, but most importantly, in the sub-EC space were clearly strept-AF647^{+} (**Fig. 5.3**).

These results further confirmed that strept-AF647 was retained on the abluminal side of the endothelial wall and only labelled neutrophils that had undergone TEM. With these encouraging findings at hand, we next investigated the potential impact of the labelling protocol on neutrophil behaviour, including their capacity to exhibit rTEM.

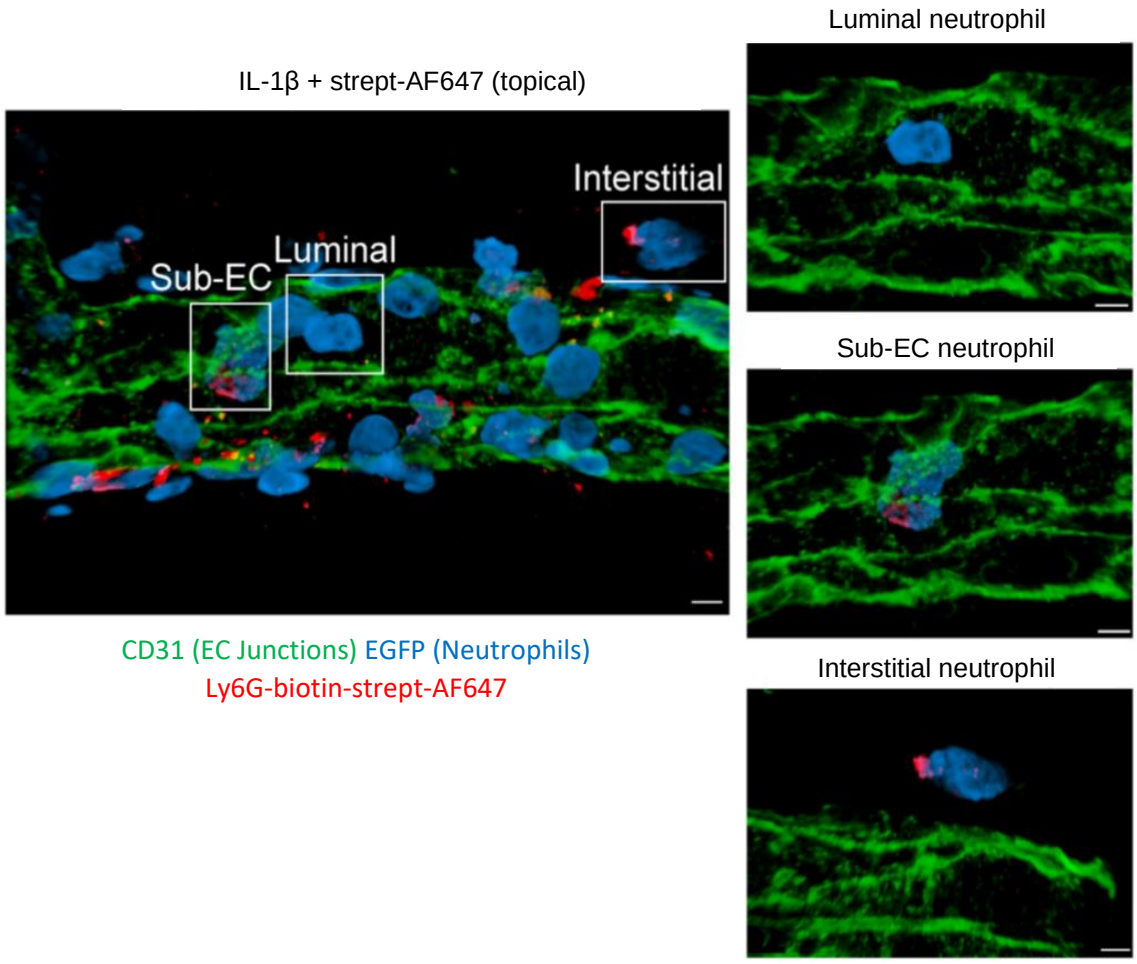

Figure 5.3. Topical strept-AF647 only labels neutrophils that have breached the endothelial layer. *LysM-EGFP*$^{ki/+}$ mice received an i.s. injection of an anti-CD31-AF555 mAb (4 µg) to label EC junctions for 2 hr in combination with IL-1β (50 ng). After 1.5 hr an anti-Ly6G-biotin Ab (2 µg) was injected i.v. Cremaster muscles were then exteriorised and treated with topical strept-AF647 (1 µg/ml) for 2 hr. The tissue was then dissected away, fixed with 4% paraformaldehyde for 30 min and visualised in collaboration with Dr. Loïc Rolas using an inverted Zeiss LSM 800 confocal laser scanning microscope with a 40 x (1.3 numerical aperture, NA) or 63 x (1.4 NA) oil dipping objective in a single-track scanning mode. Images measuring 160 µm x 85 µm were acquired with a Z-step of 0.25 µm (30-70 individual steps, dependent on the size of the blood vessel). Post-acquisition, images were analysed off-line using IMARIS software. All quantification was determined from 4-8 images/tissue and expressed total number of extravasated neutrophils per mm^3 of tissue. The left panel shows a representative confocal image of an IL-1β–stimulated postcapillary venule illustrating the extent of AF647-streptavidin labelling of neutrophils at different stages of trafficking. Right panels show enlarged images of the boxed regions and demonstrate that both sub-EC and interstitial neutrophils are strept-AF647$^+$ whilst luminal cells are strept-AF647$^-$. Scale bars, 5 µm.

For this purpose, we compared neutrophil responses in tissues stimulated with IL-1β + histamine by confocal IVM in mice subjected to the labelling strategy or not (experimental timeline depicted in Appendix 3, section 9.3.7). Neutrophil- extravasation, rTEM, TEM duration and interstitial speed migration parameters were quantified using IMARIS software as detailed in Chapter 2, sections 2.5-2.6. The data revealed that in mice treated with the labelling methodology, neutrophils exhibited comparable levels of migration into tissues (~8 x 10^3 neutrophils/mm^3 of tissue) and frequency of rTEM (~25%) (**Fig. 5.4A & B**), as compared to mice not exposed to the labelling protocol (shown in Chapter 4, section 4.2.1). Furthermore, the labelling of cells did not affect the duration of neutrophil TEM or neutrophil interstitial motility (**Fig. 5.4C & D**).

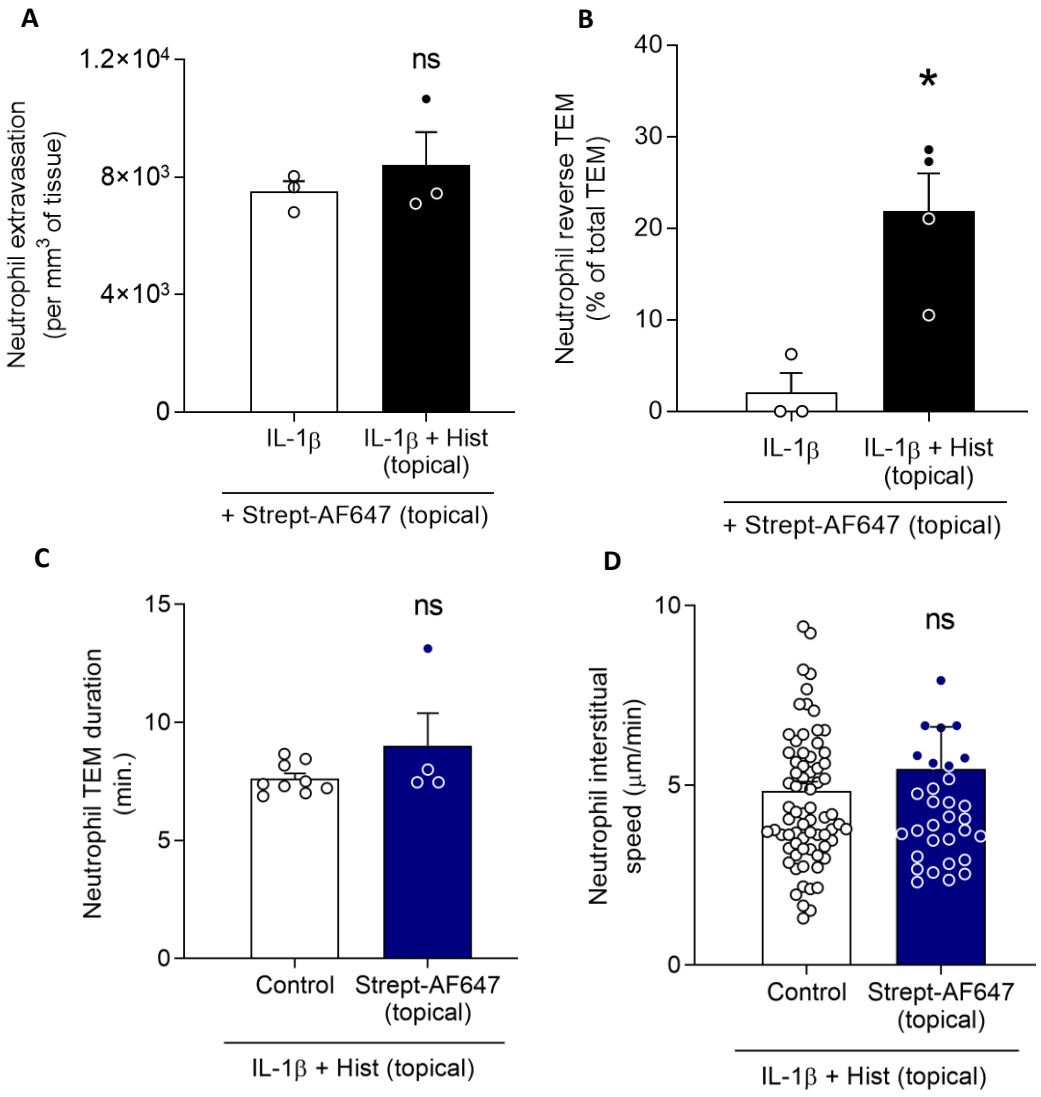

Figure 5.4. Labelling of neutrophils did not impact neutrophil migration behaviour. (**A-D**) *LysM-EGFP*$^{ki/+}$ mice received an i.s. injection of an anti-CD31 mAb (4 µg) to label EC junctions for 2 hr in combination with IL-1β (50 ng). After 1.5 hr an anti-Ly6G-biotin Ab (2 µg) was injected i.v. The cremaster muscle was then exteriorised and treated with topical histamine (30 µM) in combination with strept-AF647 (1 µg/ml). (**A**) Total neutrophil extravasation (n = 3 mice/group) and (**B**) frequency of neutrophil rTEM (n = 3-4 mice/group) show similar levels compared to reactions quantified in mice not subjected to the labelling strategy (shown in Chapter 4, section 4.2.1). (**C** and **D**) Mice subjected to the anti-Ly6G-biotin and strept-AF647 labelling strategy and unlabeled mice (not subjected to anti-Ly6G-biotin or strept-AF647 application) exhibited similar neutrophil TEM duration (**C**, n = 4-9 mice/group) and neutrophil interstitial migration speed (**D**, n = 32-74 neutrophils/group, across 4-8 mice) in cremaster muscles following local stimulation with IL-1β + histamine. Data are represented as mean ± SEM (**A-C**) each point represents one mouse, (**D**) each dot represents one neutrophil across 4-8 mice. Statistically significant differences from (**A-B**) IL-1β or (**C-D**) without strept-AF647 application are shown by *p<0.05, unpaired student t-test, (ns = not significant).

Having established that our labelling strategy did not disrupt neutrophil migratory behaviour, we next directly analysed the efficacy of the method in labelling and tracking rTEM neutrophils. For this purpose, using the IL-1β + histamine reaction, mice were treated- and data was acquired by confocal IVM- as described in section 5.2.1., with strept-AF647 labelling quantification being determined using IMARIS software. To allow for distinction of 'true' neutrophil-associated strept-AF647 signal, in each mouse we obtained a background value prior to the application of topical strept-AF647. This was achieved by creating a surface on a total of 20 neutrophils/mouse (10 representative neutrophils in the interstitium and 10 in the luminal space), a step that provided an MFI value for each neutrophil. In each experiment, the average background neutrophil MFI was subtracted from the MFI values obtained from neutrophils categorised as "luminal", "interstitial" and "rTEM". The strept-AF647 MFI values were similarly attained following the creation of a surface on luminal and interstitial neutrophils, 2 hr post topical strept-AF647 treatment. Strept-AF647 MFI values for rTEM neutrophils were quantified immediately prior to their detachment from the vascular wall. The average MFI of all quantified neutrophils were presented as a mean/mouse in each defined category, once again demonstrating the efficacy of the labelling method for tracking all neutrophils that had breached the endothelium, including most importantly, rTEM neutrophils (**Fig. 5.5B**). Indeed, time-course analysis of our confocal IVM sequences revealed that rTEM neutrophils rapidly became strept-AF647^{+} (**Fig. 5.5A and video 5**) to a similar extent to that observed with fully extravasated cells (**Fig. 5.5B**). In contrast, no significant labelling of (non-rTEM) luminal neutrophils could be detected.

Collectively, these results showed that only cells that breached the endothelium (i.e. fully extravasated or exhibited reverse TEM) were labelled with locally applied strept-AF647. With the method fully validated, we extended the investigations to analysis of the fate and phenotype of rTEM neutrophils.

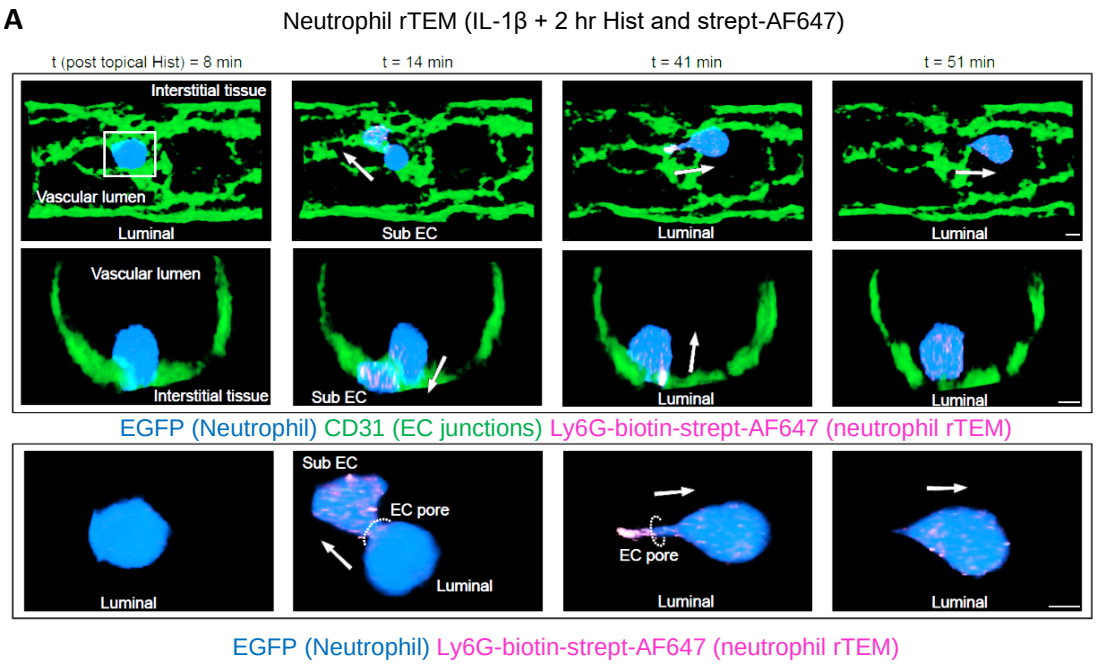

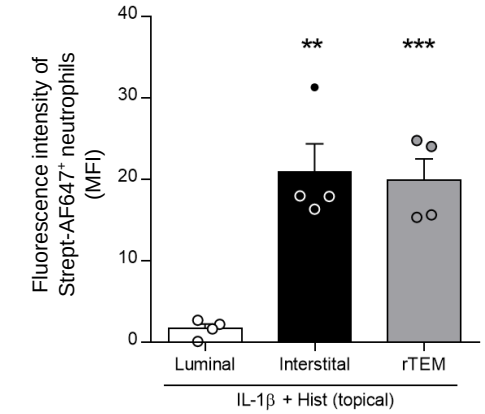

Figure 5.5. rTEM neutrophils were efficiently labelled with strept-AF647. (**A-B**) *LysM-EGFP*$^{ki/+}$ mice received an i.s. injection of an anti-CD31 mAb (4 µg) to label EC junctions for 2 hr in combination with IL-1β (50 ng). After 1.5 hr an anti-Ly6G-biotin Ab (2 µg) was injected i.v. Cremaster muscles were then exteriorised and treated with topical histamine (30 µM) in combination with strept-AF647 (1 µg/ml). (**A**) Representative confocal IVM images of a tissue stimulated with IL-1β + histamine illustrating the effective labelling of an rTEM event. The exemplified neutrophil shows that once the cell has breached an EC junction, the leading body part in the sub-EC space rapidly becomes strept-AF647^{+} whilst the luminal body segment remains strept-AF647^{-}. Luminal and cross-sectional views are shown with the arrows indicating the direction of motility for the indicated neutrophil. Scale bars, 3 µm. (**B**) Fluorescence intensity of strept-AF647 on neutrophils in the venular lumen, tissue and cells exhibiting rTEM (n = 4 mice/group). Data are represented as mean ± SEM (Each dot represents an average of 1-4 neutrophils for rTEM and 10 neutrophils for luminal and interstitial/300 µm vessel segment/mouse). Statistically significant differences from luminal neutrophils is shown by **p<0.01, ***p<0.001, one-way ANOVA followed by Bonferroni's post-hoc test.

5.2.3. rTEM neutrophils were detected in the blood and lung vascular washout (LVWO)

Having validated our novel cell labelling technique, we next sought to determine the fate of rTEM neutrophils following local IL-1β + histamine. Since our confocal IVM works showed that following completion of rTEM neutrophils detach from the venular wall and re-enter the circulation, we first examined the presence of rTEM neutrophils in the peripheral blood.

In brief, *LysM-EGFP*$^{ki/+}$ mice were treated with local IL-1β (50 ng) for 1.5 hr, after which, anti-Ly6G-biotin (2 μg) was administered i.v. After 30 min the cremaster tissue was exteriorised and topically applied with strept-AF647 (1 μg/ml) for 2 hr, as described in section 5.2.1. Blood was then collected from the ascending vena cava 2 hr post local application of histamine + strept-AF647 application, immunostained *ex vivo* with anti-Gr1 and anti-CD115 mAbs and analysed by flow cytometry as detailed in Chapter 2, section 2.2.5.3. Neutrophils were gated as EGFP^{high}, Gr1-PE^{high} and CD45-PB^{+} (**Fig. 5.6A**). With this approach, we found that in the absence of histamine, only 0.1% (equivalent to 800 cells/ml of blood) of the circulating neutrophils were strept-AF647^{+}. In contrast, following histamine-induced vascular leakage, the frequency of strept-AF647^{+} neutrophil rose to ~0.5% (~5-fold increase), corresponding to ~2,800 strept-AF647^{+} neutrophils/ml of blood (**Fig. 5.6B & C**). These results were consistent with the approximately 5-fold increase in the frequency of neutrophil rTEM events between IL-1β alone and IL-1β + histamine treated mice (see section 5.2.3). Collectively, these results strongly indicated that rTEM neutrophils recirculate through the blood/systemic circulation.

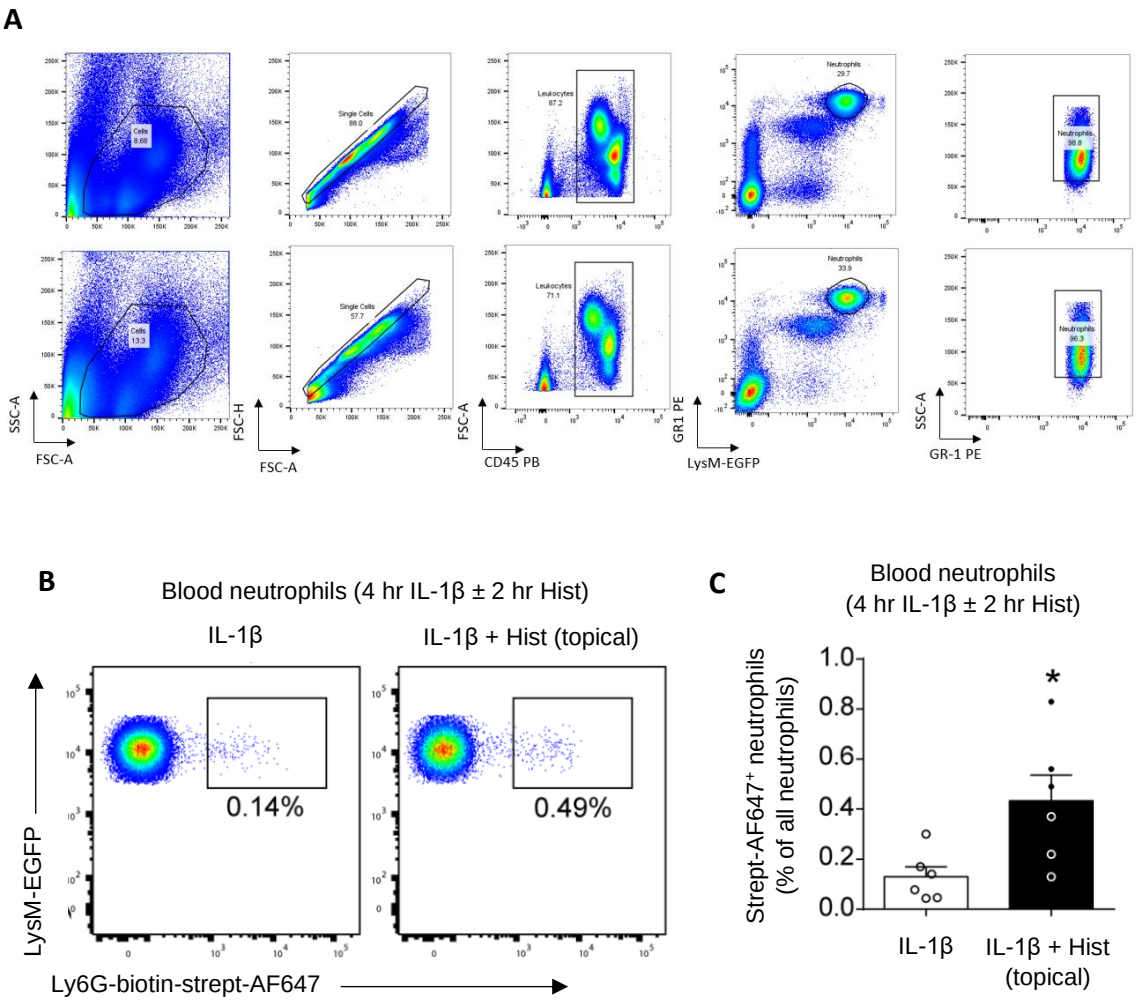

Figure 5.6. Strept-AF647^{+} neutrophils were detected in the blood of IL-1β + histamine-treated mice. (**A-C**) *LysM-EGFP$^{ki/+}$* mice received an i.s. injection of an anti-CD31 mAb (4 µg) to label EC junctions for 2 hr in combination with IL-1β (50 ng). After 1.5 hr an anti-Ly6G-biotin Ab (2 µg) was injected i.v. Cremaster muscles were exteriorised and treated with topical histamine (30 µM) in combination with strept-AF647 (1 µg/ml). (**A**) Representative gating strategy (**B**) Representative flow cytometry profiles and (**C**) frequency of strept-AF647^{+} neutrophils (EGFP^{high}, Gr1-PE^{high} and CD45-PB^{+}), (n = 6 mice/group). Data are represented as mean ± SEM (each dot represents one mouse/independent experiment). (**C**) Statistically significant differences from IL-1β is shown by *p<0.05, using an unpaired student t-test.

Next, we sought to determine if strept-AF647^{+} neutrophils disseminated into other organs. This hypothesis is supported by previous publications that reported an association between rTEM neutrophils stemming from inflamed cremaster muscles and increased lung permeability (Woodfin et al., 2011; Colom et al., 2015). To investigate this directly, we harvested the lung vascular washout (LVWO) from mice exposed to different treatment groups, namely PBS, histamine and IL-1β ± histamine. For these studies, our inflammatory and labelling protocol was slightly modified.

In brief, WT mice were treated with IL-1β (50 ng, i.s.) for 1.5 hr after which mice were injected i.v. with anti-Ly6G-biotin Ab (2 µg) for 30 min. Mice then received an i.s. injection of strept-AF647 (400 ng) co-administered with histamine (200 µl of 30 µM solution) or PBS for 2 hr to stimulate both cremaster muscles, as opposed to the previous protocol of topical application onto one exteriorised tissue. This adaptation was confirmed by Dr. Régis Joulia to exclusively label neutrophils that breached the endothelium, while non-transmigrating luminal neutrophils remained strept-AF647^{-} (data not shown, Owen-Woods et al., 2020). At the end of the stimulation period, and in collaboration with Dr. Régis Joulia, animals were terminally anaesthetised, and the peripheral blood was removed to minimise contamination of the LVWOs. A thoracotomy was then performed to expose the heart and lungs and the vena cava and aortic arch were clamped to isolate the pulmonary vasculature. 5 ml of ice-cold PBS containing heparin (20 U/ml) and EDTA (5 mM) was injected into the right ventricle at a perfusion rate of 1 ml/min using a syringe pump. LVWO was then collected from the left ventricle. Samples were then processed with the relevant fluorescently labelled antibodies (described in section 5.2.3) and analysed by flow cytometry (as detailed in Chapter 2, section 2.2.5.3). Neutrophils were gated as Gr1-PB^{high} and CD115-AF488^{-}.

Here, a marginal number of strept-AF647^{+} neutrophils were detected in the LVWO (~0.2%, corresponding to ~120 strept-AF647^{+}/LVWO) in PBS, histamine or IL-1β alone conditions, reactions characterised by negligible levels neutrophil rTEM. However, following local IL-1β + histamine, a 4-fold increase of strept-AF647^{+} neutrophils were detected in the LVWO (~0.8%, corresponding to ~1100 strept-AF647^{+}/LVWO) (**Fig. 5.7A & B**).

Collectively, these data indicated that upon local inflammation associated with acute vascular permeability, rTEM neutrophils recirculating in the blood trafficked to the lungs.

In the next series of investigations, the phenotype of rTEM neutrophils in the blood and LVWO was analysed.

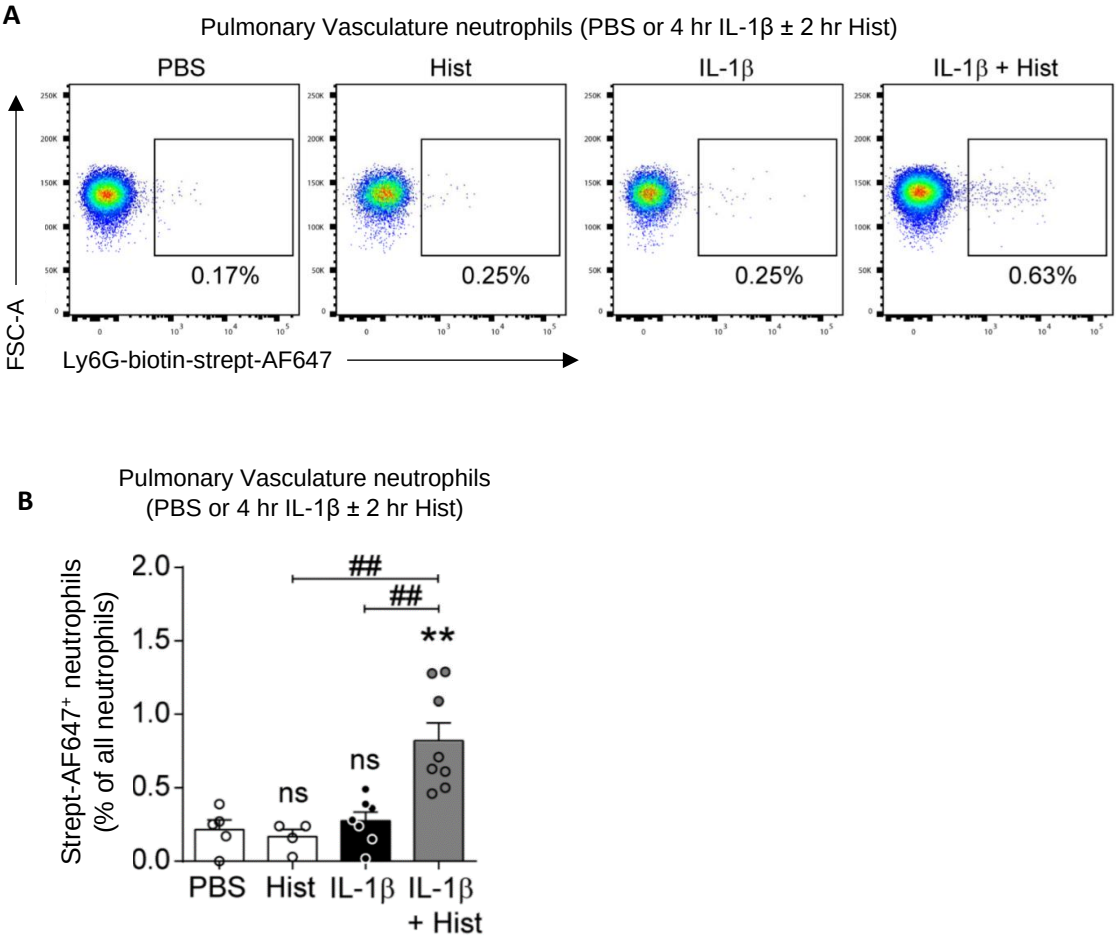

Figure 5.7. Strept-AF647^{+} neutrophils accumulated in the lung vasculature. (**A-B**) WT mice received an i.s. injection of IL-1β (50 ng). After 1.5 hr, mice were injected i.v. with anti-Ly6G-biotin Ab (2 µg) for 30 min. Mice then received an i.s. injection of strept-AF647 (400 ng) co-administered with histamine (200 µl of 30 µM solution) or PBS for 2 hr. (**A**) Representative flow cytometry profiles and (**B**) frequency of strept-AF647^{+} neutrophils (Gr1-PB^{high}, CD115-488^{-}) (n = 4-8 mice/group). Data are represented as mean ± SEM (each dot represents one mouse/independent experiment). Statistically significant differences from PBS are shown by **p<0.01 or by indicated comparisons ##p<0.01, one-way ANOVA followed by Bonferroni's post-hoc test, (ns = not significant).

5.2.4. rTEM neutrophils in the blood and LVWO exhibited a pro-inflammatory phenotype

As the identification of rTEM neutrophils was facilitated by the Ly6G-biotin-strept-AF647 labelling protocol, we next compared the phenotype of strept-AF647^{+} and strept-AF647^{-} neutrophils present in the blood and lung vasculature by flow cytometry.

In brief, in collaboration with Dr. Régis Joulia, blood and LVWO were collected as described in section 5.2.3. Samples were then processed as detailed in Chapter 2, section 2.2.5.3 and were immunostained uniquely with fluorescently labelled antibodies raised against Gr1 and CD115 to identify neutrophil populations, in addition to CXCR4, CD62L (L-selectin), CD11b, ICAM-2 (CD102), ICAM-1 (CD54), β1-integrin (CD29) and/or NE to evaluate surface markers of activation. Neutrophils were gated as Gr1-PB^{high}, CD115-APC-Cy7^{-} and strept-AF647$^{+/-}$.

We noted that as compared to strept-AF647^{-} neutrophils, strept-AF647^{+} neutrophils in the blood exhibited no significant change in the expression of CD62L, β1-integrins, ICAM-2, NE, or CXCR4. However, these neutrophils exhibited significantly increased surface levels of CD11b and to a lesser extent ICAM-1 (**Fig. 5.8A**) as compared to strept-AF647^{-} neutrophils. Interestingly, strept-AF647^{+} neutrophils from the LVWO exhibited increased expression of β1-integrins, NE and CXCR4 in addition of CD11b and ICAM-1, whilst no significant change in expression of CD62L and ICAM-2 were detected. Thus, suggesting that this activated phenotype is further exacerbated once they reach the lung vasculature (**Fig. 5.8B**). Of note, strept-AF647^{-} neutrophils collected from the blood and LVWO of IL-1β + histamine-treated mice exhibited a comparable phenotype to PBS, histamine or IL-1β only-treated mice (data not shown, Owen-Woods et al., 2020).

Collectively, the activated phenotype of rTEM neutrophils indicates a pro-inflammatory state of these cells that may contribute to the development of pathogenicities in distant organs.

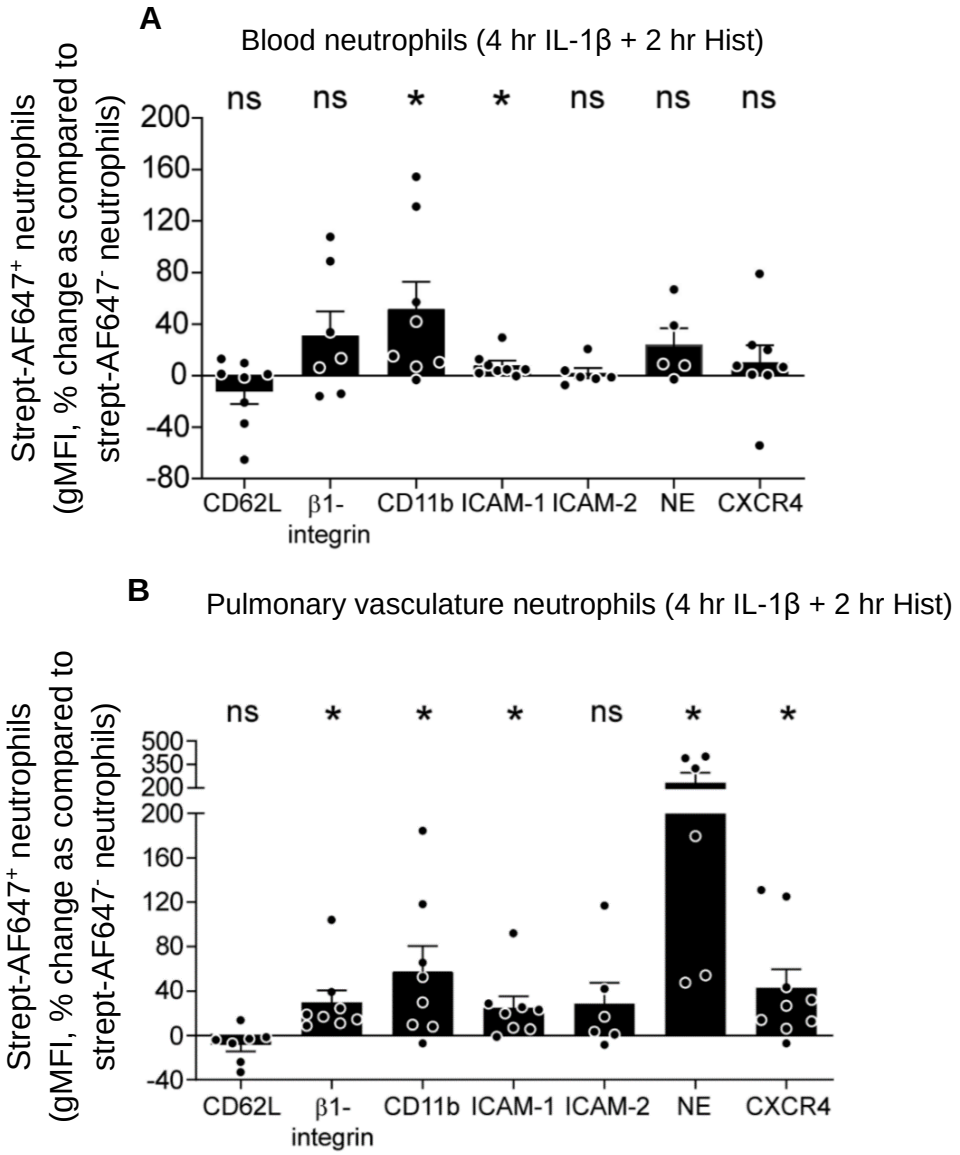

Figure 5.8. Labelled rTEM neutrophils exhibit an activated phenotype in the blood and LVWO. (**A-B**) WT mice were subjected to local cremaster muscle stimulation with IL-1β (50 ng, 2 hr) and an i.v. injection of anti-Ly6G-biotin Ab (2 µg) after 1.5 hr. Mice then received an i.s. injection of strept-AF647 (400 ng) co-administered with histamine (200 µl of 30 µM solution) or PBS for 2 hr. Peripheral blood and LVWO samples were analysed by FACS. (**A-B**) Expression of indicated markers on strept-AF647^{+} neutrophils (gated: Gr1-PB^{high}, CD115-APC-Cy7^{-}, strept-AF647$^{+/-}$) relative to levels on strept-AF647^{-} neutrophils in (**A**) blood or (**B**) LVWO samples collected from mice subjected to IL-1β (4 hr) + histamine (2 hr), as measured by geometric MFI (gMFI) (**A**) n = 5-8 mice/group (**B**) n = 6-9 mice/group. Data are represented as mean ± SEM (each dot represents one mouse/independent experiment). Statistically significant differences from gMFI of indicated markers of blood (**A**) or LVWO (**B**) strept-AF647 labelled neutrophils. Statistical significance is shown by *p<0.05, paired student's t-test, (ns = not significant).

5.3. Discussion

Reverse migration of neutrophils through EC junctions is a recently established phenomenon observed in various models of sterile inflammatory reactions such as IR-injury, (Woodfin et al., 2011; Colom et al., 2015), burn injury, (Yoo and Huttenlocher, 2011; Wang et al., 2017) and more recently hyper-permeability associated reactions (Colom et al., 2015; Owen-Woods et al., 2020). However, despite these advancements in the field, understanding the fate and phenotype of these cells has proven difficult. This lack of understanding resided mainly in our inability to exclusively target and efficiently label neutrophils that exhibit rTEM.

In this Chapter, tracking of rTEM neutrophils has been comprehensively addressed by establishing an effective immunolabelling method of rTEM neutrophils. In brief, as the glycoprotein Ly6G is highly and exclusively expressed on the surface of mature neutrophils (Lee et al., 2013), biotinylated anti-Ly6G Ab was used to tag blood neutrophils when injected i.v. Furthermore, we exploited the high affinity binding of biotin and streptavidin by applying fluorescent strept-AF647 topically onto the exteriorised cremaster tissue so as to label anti-Ly6G-biotin^{+} neutrophils that had exclusively breached the EC layer during diapedesis. With this approach, extravascular and reverse migrating neutrophils became rapidly strept-AF647^{+} whilst luminal non-migrating neutrophils remained strept-AF647^{-}. Furthermore, strept-AF647^{+} reverse migrating neutrophils could be detected in the circulation but also within the pulmonary vasculature where they exhibited an activated phenotype. These results provide the first direct evidence that rTEM neutrophils exhibit an activated phenotype and establish a platform for future *in vivo* investigations into the function and pathological consequences of these cells.

In the literature, tracking of reverse migrating neutrophils has previously been explored in zebrafish that express the photoconvertible fluorescent reporter, Dendra2 in leukocytes, or using genetically modified *Ly6G-PA-GFP* mice. However, these methods have limitations in the sense that tracking of neutrophils is restricted to the laser-accessible microscopic field-of-view outside the vasculature and beyond the pericyte layer (Yoo and Huttenlocher, 2011; Wang et al., 2017). Inevitably, such a targeted method restricts the number of reversing neutrophils that can be tracked. In addition, UV/visible

lasers used for photoconversion with single-photon confocal microscopy penetrate the whole depth of tissues, thus increasing the risk of converting cells that that may not have undergone rIM or rTEM. Additionally, this technique lacks the level of precision required for targeting rTEM neutrophils that do not migrate beyond the pericyte layer of the vessel wall. To this end, we developed a novel tracking technique as described in section 5.2.1. Overall, this was proven to be an effective strategy, whereby a low dose (2 µg) of anti-Ly6G-biotin was sufficient to label >99% of all circulating neutrophils, while other myeloid cells (e.g. monocytes) remained strept-AF647^{-}. Furthermore, in the absence of rTEM induction, nominal fluorescence of strept-AF647 was detected on the surface of circulating anti-Ly6G-biotin-labelled neutrophils, with or without local histamine, demonstrating a lack of abluminal-to-luminal diffusion of topically applied strept-AF647. Histamine most likely does not affect strept-AF647 retention, because with a size similar to albumin, i.e. 60 kDa, (Kuzuya et al., 2008), streptavidin would not be susceptible to tissue-to-blood diffusion under conditions of hyper-permeability as discussed in Chapter 4 (*Pe* = ~4). Similarly, our observation that non-migrating luminal neutrophils were largely strept-AF647^{-} demonstrates minimal drainage *via* the tissue lymphatics at the time-points analysed, which could otherwise lead to undesirable entry of strept-AF647 into the blood stream.

Next, as part of our model validation, we observed that the experimental labelling conditions did not induce any diminution of neutrophil extravasation, interstitial migration velocity, duration of TEM or the frequency of rTEM. Collectively, these validations were crucial as previous *in vitro* studies have shown that pre-treatment of EC monolayers with streptavidin-biotin complexes resulted in reduced neutrophil-EC adhesion under conditions of shear flow (Chan et al., 2004). Such effects have been proposed to be mediated by streptavidin binding to, and blocking of pro-adhesive cell surface integrins (Alon et al., 1993). However, to-date there have been no reports on the influence of streptavidin-biotin on neutrophil-EC interactions *in vivo*. In addition, Ab binding can lead to enhanced cell activation or cell death through antibody-dependent cellular cytotoxicity (ADCC) or complement-dependent cytotoxicity (CDC) leading to cellular depletion (Pitsillides et al., 2011). Regarding *in vivo* treatment with anti-Ly6G Ab, this occurs at relatively high doses (>200 µg) (Pollenus et al., 2019), whilst at lower doses (1-40 µg) the impact of anti-Ly6G Ab on neutrophil migration remains contentious. For

instance, Wang et al., suggested that neutrophil migration was reduced following i.p. injection of doses between 5 – 50 μg in arthritic mice, which they hypothesised to occur *via* disruption of β2-integrin-dependent ICAM-1 adhesion (Wang et al., 2012; Cunin et al., 2019). However, a rebuttal report by Yipp and Kubes, details no significant effect on neutrophil migratory behaviour at doses up to 40 μg i.v. in an *in vivo* model of *staphylococcus aureus*-infection of the mouse skin (Yipp and Kubes, 2013). Therefore, our results are in accordance with the latter study, whereby a low dose of anti-Ly6G Ab has no impact on neutrophil migration. Lastly, during our investigations we also observed that rTEM neutrophils exhibited a comparable degree of labelling to those that had fully migrated. This may be mediated by persistent Ly6G rearrangement on the cell membrane as seen in **Fig. 5.6 and video 5**. Overall, these results form a robust validation and are an ideal basis upon which to assess the fate and phenotype of rTEM neutrophils in different inflammatory contexts.

In the first instance, as neutrophils move away from their site of rTEM into the direction of blood flow, we sought to determine if we could detect strept-AF647^{+} cells in the systemic circulation. Indeed, we observed ~2,800 strept-AF647^{+} neutrophils/ml in mice subjected to cremasteric inflammation through local application of IL-1β + histamine, a reaction that caused significant frequency of neutrophil rTEM. In contrast, mice treated with just IL-1β, exhibited only ~800 strept-AF647^{+} neutrophils/ml of blood. This ~5-fold change aligns closely with the difference observed in the frequency of neutrophil rTEM for each of these reactions and supports the notion that strept-AF647^{+} represent rTEM neutrophils. Comparatively, Wang et al., identified ~300 PA-GFP^{+} neutrophils/ml blood (Wang et al., 2017) following liver burn injury compared to the negligible count of PA-GFP^{+} neutrophils/ml blood detected in sham-operated mice. In both cases labelling occurred just prior to the peak of reverse transmigration suggesting that our approach may be more efficacious for labelling of reverse migrating neutrophils. However, a more comprehensive comparison is difficult as each scenario consists of different inflammatory reactions (IL-1β + histamine vs. sterile burn injury), type of reverse migration (rTEM vs. rIM), type of organ (cremaster muscle vs. liver) and time-points of the reaction (4 hr post IL-1β + 2 hr post histamine vs. 16-24 hr post burn injury). In any case, the present work provides the first report of rTEM neutrophils being effectively

labelled and tracked and thus opens up opportunities for explorations of the fate and phenotype of these cells.

Next, as previous publications have shown an association between locally reverse-migrating neutrophils and increased distal lung permeability (Woodfin et al., 2011; Colom et al., 2015), we sought to assess the presence of rTEM neutrophils in the pulmonary vasculature. LVWOs from mice treated locally with IL-1β + histamine exhibited a significantly higher frequency of strept-AF647^{+} neutrophils, consistent with a higher frequency of neutrophil rTEM, compared to PBS-, IL-1β-, or histamine-alone treated mice. Of interest, this observation reveals some similarity to the behaviour of neutrophils that underwent rIM + rTEM, whereby these cells accumulated in the lung 24 hr post sterile injury of the liver (Wang et al., 2017).

Finally, we sought to determine the phenotype of rTEM neutrophils in the blood and those reaching the lung vasculature to provide insight into their function. Here, we showed that strept-AF647^{+} neutrophils in the blood exhibited a typically activated phenotype characterised by elevated surface expression of the pro-adhesion molecules CD11b and ICAM-1, as compared to strept-AF647^{-} neutrophils. In addition, strept-AF647^{+} neutrophils within LVWO exhibited an exacerbated activated phenotype with significantly increased surface expression of CD11b, ICAM-1, β1-integrins, the chemokine receptor CXCR4 and the serine protease NE. Neutrophil ICAM-1, CD11b and β1-integrin are markers of neutrophil activation and aid in neutrophil adhesion and migration (Sumagin et al., 2010; Nourshargh and Alon, 2014). Of particular interest, our finding of ICAM-1^{+} strept-AF647^{+} neutrophils in the lung vasculature is complementary to investigations by Buckley et al., and Woodfin et al., who both proposed links between neutrophil rTEM and distant organ damage (Buckley et al., 2006; Woodfin et al., 2011). Buckley et al., identified *in vitro* that rTEM neutrophils were ICAM-1^{high} and could be detected in the blood of patients suffering with chronic inflammatory disorders. Here they suggested that the reason these patients have a greater risk of developing distal organ damage e.g. post-surgery, may be due to the increased prevalence of rTEM neutrophils (Buckley et al., 2006). Furthermore, investigations by Woodfin et al., identified a population of ICAM-1^{high} neutrophils in the mouse lung vasculature, following local IR-induced rTEM, which were further hypothesised to represent rTEM neutrophils (Woodfin et al., 2011). Collectively, the findings of the discussed literature

and those presented in this Chapter, demonstrate that rTEM neutrophils in various inflammatory conditions are ICAM$^{high/+}$ and thus may prove a reliable biomarker to assess patient prognosis and risk of developing distal organ injury. Of interest however, Woodfin et al., identified approximately 300 ICAM-1^{high} neutrophils in the lung 1 hr post local IR-injury of the mouse hide limb, in contrast to the ~1100 strept-AF647^{+} neutrophils observed in our study (4 hr IL-1β + 2 hr histamine). Whilst this discrepancy may be explained by differing inflammatory conditions, it may also highlight that gating on an ICAM-1^{high} sub-population of neutrophils may not account for all rTEM neutrophils. The presence and importance of neutrophil sub-populations is a currently developing concept (Rosales, 2018), and may provide an exciting avenue for further study.

Of particular interest, strept-AF647^{+} cells were found to be closely associated with sites of pulmonary vascular leakage, a finding that was only observed following our local IL-1β + histamine reaction (data not shown, Owen-Woods et al., 2020). Our initial phenotypic findings provide some insight as to how rTEM neutrophils may drive this vascular leakage response. For example, ICAM-1-mediated signalling in neutrophils has been shown to support generation of ROS (Woodfin et al., 2016). In combination with the fact that activated neutrophils release TNF in close proximity to ECs (Finsterbusch et al., 2014), increased ability to generate ROS may contribute to the ability of rTEM neutrophils to induce lung vascular leakage. Of particular interest however, is the increased expression of NE by strept-AF647^{+} neutrophils. NE is a destructive serine protease enzyme secreted by activated neutrophils following degranulation of azurophilic (primary) granules or release of neutrophil extracellular traps (NETs) (Cowland and Borregaard, 2016). The increased detection of NE suggests that these cells undergo degranulation. This is further supported by the concomitantly enhanced expression of CD11b and β1-integrin, which are known to be stored in pre-formed granules, the former being a surface ligand for the enzyme (Roussel and Gingras, 1997; Cowland and Borregaard, 2016). Once released, NE facilitates the breakdown of the extracellular matrix and cleaves endothelial junctional molecules causing compromised endothelial barriers and subsequent vascular leakage (Chua and Laurent, 2006; Taylor et al., 2018; Voisin et al., 2019). Indeed, elevated expression of NE has been strongly associated with various lung diseases such as ALI and ARDs in humans (Polverino et al.,

2017). Collectively, the elevated surface expression of NE in our study may indicate that rTEM neutrophils are capable of contributing to the development of lung pathologies.

At first glance, this predominately pro-inflammatory phenotype of rTEM neutrophils shown in this Chapter, contrasts with the pro-resolution role of rIM neutrophils suggested by Wang *et al.* (Wang et al., 2017). Indeed, whilst neutrophil rTEM and rIM are distinct forms of reverse migration, these findings may be complementary, when considered sequentially. Recent investigations by Wang et al., observed increased CXCR4 expression on Ly6G-PA-GFP^{+} (i.e. rIM) neutrophils in the lung and BM, 16 – 24 hr post local liver injury (Wang et al., 2017). Furthermore, increased expression of CXCR4 in aged neutrophils has been associated with a neutrophil's capacity to migrate/home back to the BM at the end of their life cycle (Martin et al., 2003; Furze and Rankin, 2008), whilst the CXCL12/CXCR4 axis, has also been shown to mediate neutrophil margination in the lung (Devi et al., 2013). We now report that rTEM neutrophils as induced by local IL-1β + histamine reaction are retained in the lung vasculature after 2 hr, a response that slightly reduced after 4 hr (data not shown, Owen-Woods et al., 2020). Consistent with the findings of Wang et al., we observed increased surface expression of CXCR4. In addition, after 4 hr a significant number of strept-AF647^{+} neutrophils were detected in the BM suggesting that neutrophils that previously resided in the lungs, later relocated to the BM (data not shown, Owen-Woods et al., 2020), consistent with findings of Furze and Rankin. Hence, we propose that during the acute phase of the inflammatory reaction, reverse migrated neutrophils exhibit a typically pro-inflammatory/pro-permeability phenotype and are capable of inducing distant organ damage. Then, during the increased retention time in the lung, neutrophils undergo modifications altering their phenotype and begin expressing CXCR4 before trafficking back to the BM, thereby shifting from an inflammatory to pro-resolution phenotype. This hypothesis is further supported by experiments that analysed vascular leakage in the lung at both time points. Although very different inflammatory reactions are at play, Wang et al., stated an absence of any significant permeability in the lungs 11 hr after the peak of reverse migration in the liver (24 hr post injury). However, experiments conducted by Dr. Régis Joulia using our model showed increased vascular leakage in lung alveoli 2 hr after the peak of reverse migration (4 hr post IL-1β + 2 hr post histamine) (data not shown, Owen-Woods et al., 2020). Together, these results are indicative of reverse migrating

neutrophils switching phenotypes in the lung over time, a concept that would require further investigations.

Lastly, we found striking similaries between the phenotype of reverse transmigrating neutrophils in our model and 'aged' netrophils (so called, due to their phenotype). Aged neutrophils have been shown to have increased expression of CXCR4, ICAM-1, CD11b and decreased expression of CD62L (Rosales, 2018). This is largely consistent with the findings of this chapter. In addition, aged neutrophils exhibit CXCR2 downregulation and VLA-4 upregulation (Rosales, 2018), markers that were not evaluated in this thesis. Of particular interest, Adrover and colleagues have recently shown that neutrophil aging is induced by activation of CXCR2 (Adrover et al., 2019). As suggested in Chapter 4, following enhanced vascular leakage, excessive diffusion of CXCL1 through paracellular junctions could potentially result in hyper-activation of CXCR2, leading to its internalisation and the stated aged phenotype. Collectively, this would suggest that rTEM neutrophils acquire an accelerated "aged" phenotype. Further studies are needed to assess deep phenotyping of these cell types, investigating key cell surface markers such as CXCR2 expression.

5.4. Conclusion

In conclusion, we have established a novel cell labelling technique that enables direct tracking of reverse TEM neutrophils *in vivo* (**Fig. 5.9**). For the first time, through application of this methodology, rTEM neutrophils were found to be enriched in the lung vasculature where they exhibited a typically pro-inflammatory phenotype and were associated with sites of induced vascular leakage. These findings strongly suggest that the link between local trauma and distant organ damage, may be mediated to some extent by rTEM neutrophils (Owen-Woods et al., 2020). In the future, this approach will facilitate further explorative studies into the phenotype, fate and pathophysiological relevance of rTEM neutrophils.

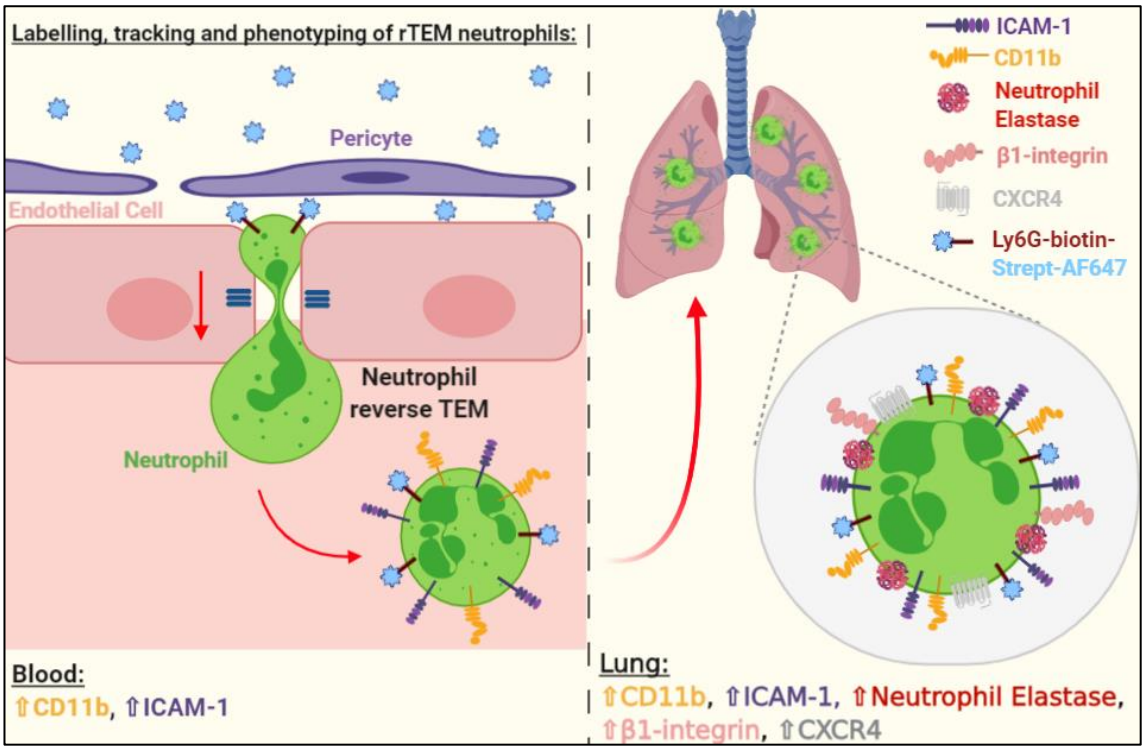

Figure 5.9. Representative schematic displaying labelling, tracking and phenotyping of rTEM neutrophils. Strept-AF647^{+} cells were identified in blood samples following local IL-1β + histamine- induced inflammation where they presented an activated phenotype as shown by enhanced surface expression of CD11b and ICAM-1, relative to strept-AF647^{-} neutrophils. Furthermore, an enrichment of strept-AF647^{+} neutrophils was identified in LVWO, where they exhibited a pro-inflammatory phenotype as identified by further increased expression of CD11b and ICAM-1, in addition to increased NE, β1-integrin and CXCR4, relative to strept-AF647^{-} neutrophils.

Chapter 6

Investigations into the role of TNF/TNFR pathway in the regulation of vascular leakage and neutrophil TEM

6.1. Introduction

The previous Chapters (see Chapters 3 – 5) demonstrated for the first time that vascular leakage supports an aberrant mode of leukocyte diapedesis during acute inflammatory responses, namely neutrophil rTEM. Here, we sought to further elucidate the causal link between neutrophil TEM and vascular permeability by exploring the role of the TNF pathway in these events. Our interest in this cytokine extends from previous investigations within our group demonstrating for the first time that neutrophil-derived TNF is a fundamental mediator of vascular leakage in tissues stimulated by chemotactic agents (Finsterbusch et al., 2014).

TNF is a prototypical pro-inflammatory cytokine produced by an array of cells including monocytes, macrophages, T-cells, ECs and neutrophils. First discovered for its potent anti-tumour activity in animal models (Carswell et al., 1975; Bradley, 2008; Josephs et al., 2018), TNF plays a crucial role in our immune system by maintaining lymphoid organ structure, activating blood vasculature and inducing acute and chronic inflammatory responses (Pfeffer et al., 1993; Rothe et al., 1993; Pasparakis et al., 1996; Flynn et al., 1995). Specifically, TNF induces EC upregulation of a range of pro-inflammatory mediators, including surface pro-adhesion molecules ICAM-1, VCAM-1 and E-selectin, cytokines such as IL-1β, IL-6, chemokines CXCL8 & RANTES (CCL5) and promotes generation of nitric oxide (Zhou et al., 2008). Overall, these factors can result in enhanced leukocyte recruitment, migration, and vasodilation (Yang, 2005). TNF also induces vascular permeability by activating p38-MAPK, leading to internalisation of EC junctional VE-cadherin (Flemming et al., 2015), and contraction of actin stress fibres, reducing EC junctional integrity (Nwariaku et al., 2003). Our group has previously demonstrated that ablation of the TNF pathway by genetic deficiency or pharmacological blockade using *TNFRI/II*^{KO} mice or an anti-TNF-blocking Ab, respectively, inhibited/suppressed neutrophil-dependent vascular permeability (Finsterbusch et al., 2014). Specifically, it was shown that neutrophils released pre-formed TNF in response to LTB_4, CXCL1 and C5a when the leukocytes adhere to ECs *via* ICAM-1 and ICAM-2 but also that TNF could be detected on the neutrophil cell surface prior to- and during- neutrophil TEM (Finsterbusch et al., 2014).

TNF exists in two active forms, soluble TNF (sTNF) and transmembrane TNF (mTNF). The former moiety is generated from cleavage of mTNF from the cell surface by the matrix metalloprotease enzyme, TNF-alpha converting enzyme (TACE). Both sTNF and mTNF consist of homotrimers and act through two transmembrane receptors, TNFRI/p55 and TNFRII/p75, which together mediate the effects of TNF during inflammation. While TNFRI is expressed ubiquitously, TNFRII is more restrictively expressed by ECs, pericytes and leukocytes, including neutrophils (Dopp et al., 2002; Futosi et al., 2013; Proebstl et al., 2012). Both TNFRI and TNFRII form homotrimers with cysteine-rich motifs in the extracellular space and can also be cleaved by TACE to yield sTNFRI and sTNFRII. Knowledge on the function of sTNFRs is lacking at present but it is thought that at lower concentrations, sTNFRs enhance the function of TNF by stabilising the active homotrimeric structure of TNF; whilst at higher concentrations they inhibit and clear TNF. The latter discovery led to the development of pharmaceuticals based on sTNFRs to treat chronic inflammatory disorders associated with high levels of pro-inflammatory sTNF such as idiopathic pulmonary fibrosis (Koga et al., 2000; Barash et al., 2003; Raghu et al., 2008; Carlsson et al., 2014; Cui et al., 2018).

The key distinction between TNFRI and TNFRII lies in their different intracellular domains and signalling pathways which determine their respective effector functions (Wu and Hymowitz, 2010). Generally, TNFRI supports a pro-inflammatory outcome while TNFRII is considered to support pro-resolution responses (Carpentier et al., 2004; Cabal-Hierro and Lazo, 2012). However, these receptors exhibit ample signalling crosstalk through activation of nuclear factor-kappa B (NF-κB) and mitogen-activated protein kinase (MAPK) transcription pathways. Hence, both receptors have been implicated to have anti- and pro-inflammatory functions (Naudé et al., 2011; Bouwmeester et al., 2004). Signalling crosstalk occurs despite the receptors having distinct intracellular domains. For example, the cytoplasmic tail of TNFRI contains a death domain (DD) and recruits TNFR-associated death domain (TRADD) which in turn recruits TNFR-associated factor 2 (TRAF2). By contrast, TNFRII does not have a DD and instead recruits TRAF2 directly. Fundamentally, TNFRI signalling can mediate EC contractility and apoptosis mediated cell death *via* the activation of TRAF2/NF-κB, MAPK/C-Jun and caspase/ signalling and apoptotic pathways, respectively. TNFRII signalling mediates pro-survival effects by the activation of PI3K/Akt and pro-angiogenic pathways, while also being able to activate

NF-κB (**Fig. 6.1**) (Baud et al., 2001; Cicha and Urschel, 2015). Ultimately, the prevailing response (pro-apoptosis vs. pro-survival) depends on the inflammatory stimulus, cell type, activation status of the cell and state of the microenvironment (Cabal-Hierro and Lazo, 2012; Holbrook et al., 2019). Adding to this complexity, negative and positive feedback loops are common features of TNF signalling and can be supported by both paracrine and autocrine mechanisms. In particular, NF-κB positive feedback loops are often operational during inflammatory responses, to amplify the production of pro-inflammatory mediators (Blasi et al., 1994; Caldwell et al., 2014; Gane et al., 2016).

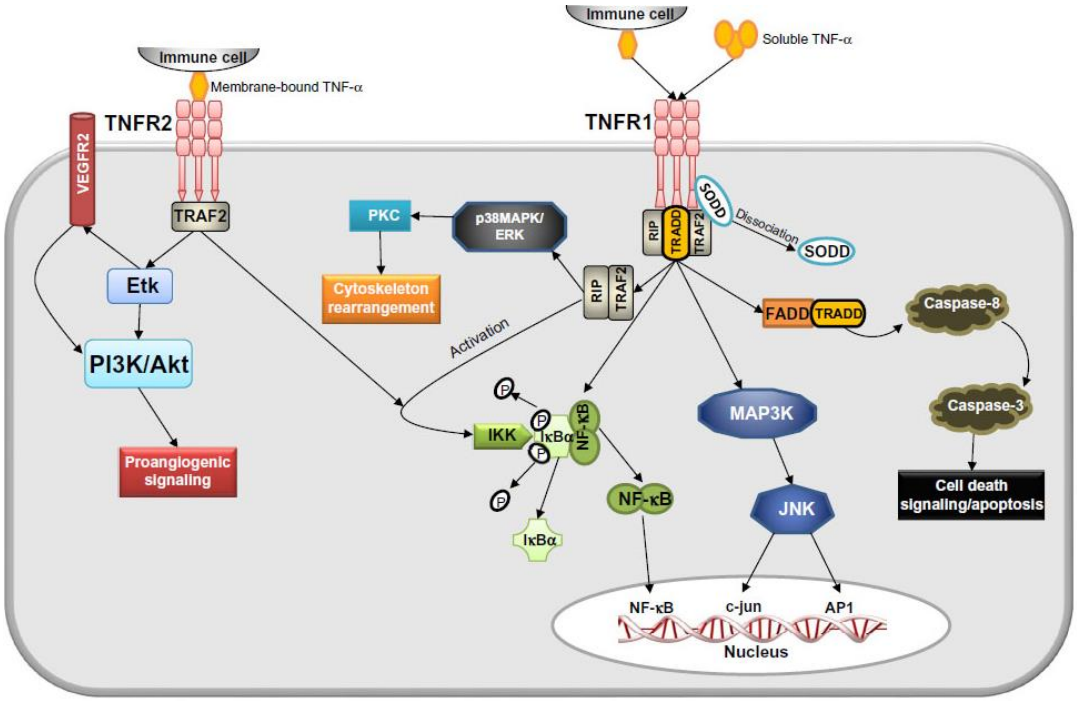

Figure 6.1. Summary of the signalling pathways following TNF ligation through EC-bound TNFRI or TNFRII. TNF exists in two active forms, soluble TNF (sTNF) and transmembrane TNF (mTNF) that act through two main transmembrane receptors, TNFRI and TNFRII, respectively. TNF-TNFRI interactions initiate recruitment of two distinct adaptor molecules (TRAF2 and TRADD) at the intracellular DD. This ultimately leads to the activation of three major signalling pathways, NF-κB-, MAPK/C-Jun- and caspase/apoptotic- signalling. Alternatively, TNF-TNFRII interactions lead to activation of the PI3K/Akt- and pro-angiogenic (e.g. VEGF-VEGFR2) pathways, while also being able to interfere with NF-κB mediated signalling. It is through these pathways that TNFRI signalling can mediate EC contractility and apoptosis mediated cell death and TNFRII signalling mediates pro-angiogenic/survival effects. Reproduced from Urschel and Cicha et al., 2015.

Both the source and target of TNF can lead to different effector functions. For example, in leukocytes, TNF signalling promotes monopoiesis, survival, and differentiation of monocytes into macrophages and dendritic cells (Wolf et al., 2017; Chomarat et al., 2003). Macrophage-derived TNF can act in an autocrine-manner to mediate enhanced phagocytosis and killing of pathogens and removal of apoptotic neutrophils; the latter being an essential step in the resolution of inflammation (Michlewska et al., 2009). In a particularly relevant example reported by Bowers et al., granulocyte-derived TNF was shown to be essential for successful HSC transplantation following irradiation, by promoting blood vessel regeneration and haematopoietic repopulation (Bowers et al., 2018). Using chimeric animals exhibiting *Tnf knock out* (*TNF*^{KO}) donor granulocytes in WT host mice or WT donor granulocytes *in TNFRI/II knock out* (*TNFRI/II*^{KO}) mice, the authors demonstrated these affects were governed by granulocyte-derived TNF acting on EC-TNFRs in the BM. The authors further proposed the existence of a positive feedback loop *via* the neutrophil-TNF/EC-TNFR signalling axis. Here, EC regeneration (and return of the stromal niche) drives haematopoietic-progenitor expansion; including generation of neutrophils (e.g. stem cell factor, G-CSF, granulocyte-macrophage-CSF and IL-6), thus supporting further vessel regeneration (Bowers et al., 2018; Kim et al., 2019).

In this Chapter, we sought to continue previous investigations by Finsterbusch et al., on the role of the TNF/TNFR axis on neutrophil migration and vascular leakage in a more pathophysiologically relevant model of acute inflammation, namely IR-injury. This model emulates scenarios commonly encountered following a period of blood vessel occlusion such as during transplantation surgery or myocardial infarction (Grace, 1994). IR-injury is also considered a risk factor for the development of ALI, and if left unresolved, may develop into ARDS (Mukhopadhyay et al., 2006). As shown in Chapter 3, IR-injury is characterised by a robust neutrophil migration and vascular leakage response, with an enhanced frequency of neutrophil rTEM. In Chapter 5, we confirmed that rTEM neutrophils exhibiting a pro-inflammatory phenotype, accumulated in the lung vasculature, and were associated with pulmonary vascular damage, which may be a contributing factor to the development of ALI (Owen-Woods et al., 2020). Similar observations were noted by Woodfin et al., and Colom et al., who identified increased vascular permeability in the lung following IR-injury and LTB_4 induced inflammatory reactions that exhibited enhanced levels of local neutrophil rTEM (Woodfin et al., 2011;

Colom et al., 2015). Therefore, we asked the question: Could neutrophil TNF-mediated vascular permeability induce neutrophil rTEM in IR-injury, as inferred by Finsterbusch and colleagues? Addressing this question would lay the groundwork for future works, investigating how enhanced levels of neutrophil rTEM could contribute to IR-injury as a risk factor for ALI and assess the therapeutic value of targeting TNF/TNFRs in such conditions.

6.1.1. Scope of the Chapter

This Chapter describes investigations aimed at addressing the contribution of neutrophil-derived TNF in vascular leakage and neutrophil migration responses. Due to time constraints and limited availability of experimental mice, this chapter represents work in progress, and presents the groundwork for future investigations.

Specific aims:

- To devise and validate a novel mouse strain exhibiting a selective deficiency in neutrophil-derived TNF (Neutro-TNF^{KO}).
- To generate and validate a mouse chimeric model, consisting of *TNFRI/II*^{KO} haematopoietic derived cells (HDCs) and WT vasculature.
- To investigate the impact of HDC-*TNFRI/II*^{KO} on vascular leakage and neutrophil TEM.

6.2. Results

6.2.1. Generation of a neutrophil-TNF deficient mouse model

We have previously demonstrated that acute microvascular leakage as induced by inflammatory mediators LTB_4, C5a or CXCL1 in mouse cremaster muscles or dorsal skin was dependent on endogenous TNF (Finsterbusch et al., 2014). However, whilst experiments using neutrophil depletion or chimeric animals exhibiting TNF deficiency in HDCs suggested a role for neutrophil-derived TNF in this response, conclusive and direct evidence needed to be established. Therefore, a new GM mouse strain exhibiting a neutrophil-specific TNF-deficiency was generated as depicted in **Fig. 6.2**.

In brief, these mice were generated *via* Cre-lox mediated functional deletion of the $Tnf^{flox/flox}$ allele leading to formation of a $Tnf^{KO/KO}$ allele. Here, we utilised a myeloid specific Cre-driver expressed from the myeloid-related protein 8 (MRP8)-promoter. MRP8 is a protein highly expressed by mature neutrophils and a small percentage of monocytes, thus controlling and restricting the expression of the Cre-transgene to these HDCs only.

To this end, we imported and inter-crossed *Mrp8-Cre* (Passegué et al., 2004) with $Tnf^{flox/flox}$ (Grivennikov et al., 2005) mice as previously described in Chapter 2, section 2.2.6. These mice were further inter-crossed with the $LysM\text{-}EGFP^{ki/ki}$ mice to enable the tracking of neutrophils by confocal IVM. $Mrp8\text{-}Cre;Tnf^{flox/flox};LysM\text{-}EGFP^{ki/+}$ (Neutro-TNF^{KO}) or $Tnf^{flox/flox};LysM\text{-}EGFP^{ki/+}$ (Neutro-TNF^{WT}) littermate controls were used for our investigations (**Fig. 6.2**).

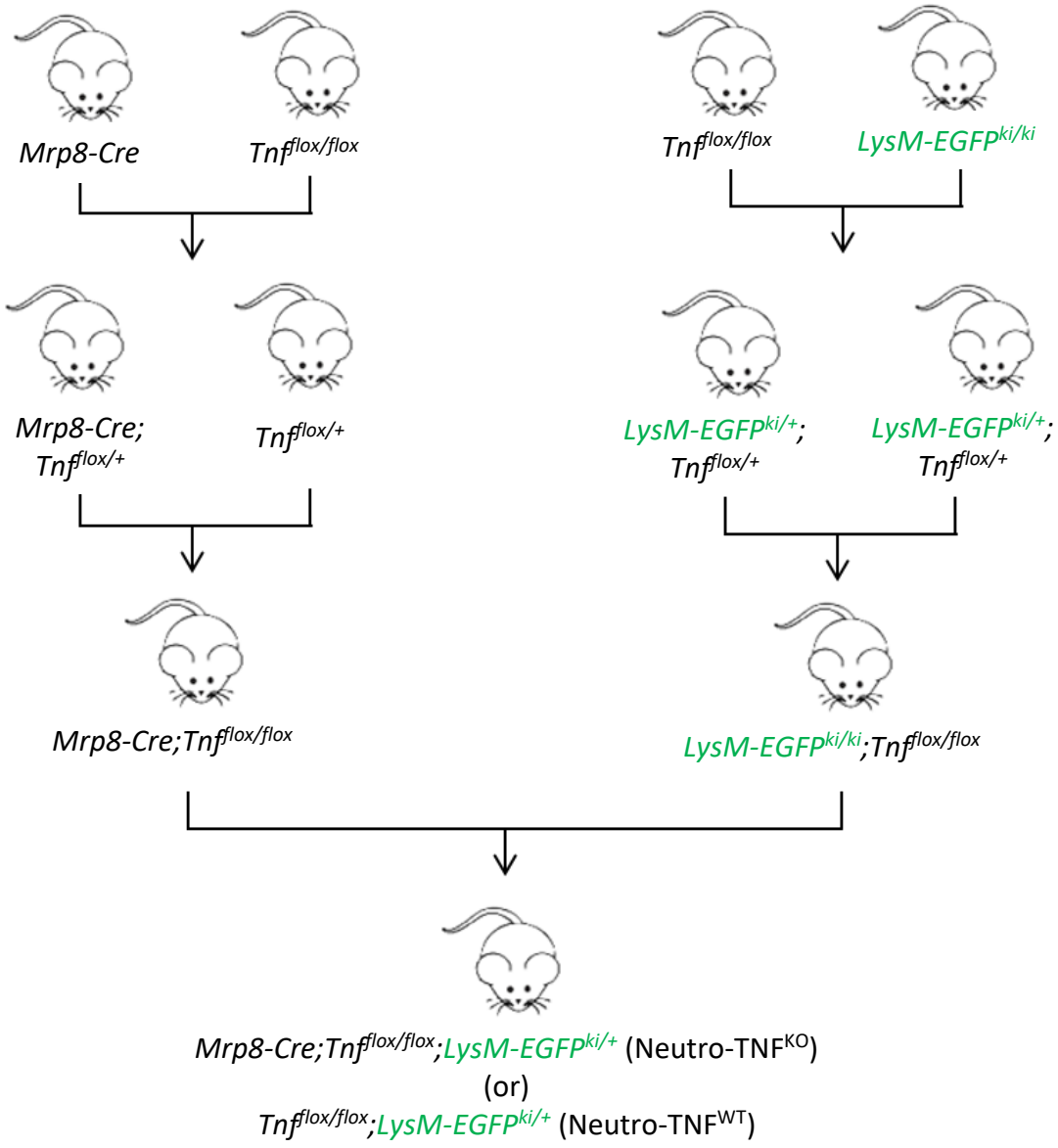

Figure 6.2. Generation of neutrophil-TNF deficient mice. To generate *Mrp8-Cre;Tnf*$^{flox/flox}$ mice, *Tnf*$^{flox/flox}$ mice (Grivennikov et al., 2005) were inter-crossed with Mrp8-Cre-IRES-GFP (Mrp8-Cre) transgenic mice (Passegué et al., 2004), in which the Cre recombinase cDNA is inserted downstream of the Mrp8 promoter. MRP8 is an inflammatory protein expressed primarily by neutrophils and by approximately 20% of monocytes, allowing for conditional deletion of floxed alleles in these cells (Abram et al., 2014). In-house, these mice were crossed with *Tnf*$^{flox/flox}$*;LysM-EGFP*$^{ki/ki}$ mice to generate experimental *Mrp8-Cre;Tnf*$^{flox/flox}$*;LysM-EGF*$^{ki/}$ (Neutro-TNF^{KO}) or *Tnf*$^{flox/flox}$*;LysM-EGF*$^{ki/+}$ (Neutro-TNF^{WT}).

6.2.2. Genomic validation of specific neutrophil-TNF deletion

With help from Dr. Matthew Golding, genomic PCR was initially conducted to assess the genotype of the mice generated from the inter-crossing described above. Briefly, ear notch samples were collected and processed for isolation of genomic DNA, followed by amplification using PCR and run on an agarose gel as detailed in Chapter 2, section 2.2.6.1. Specifically, two genomic amplifications were performed independently to detect the presence or absence of both the *Mrp8-Cre* transgene and the fully functional *Tnf*$^{flox/flox}$ allele. All samples returned the *Tnf*$^{flox/flox}$ allele due to the pluricellular nature of ear notches and Neutro-TNF^{KO} also return an amplified band for Cre-transgene, while those that returned only the full length *Tnf*$^{flox/flox}$ were identified as Neutro-TNF^{WT} (**Fig. 6.3A-B**).

A

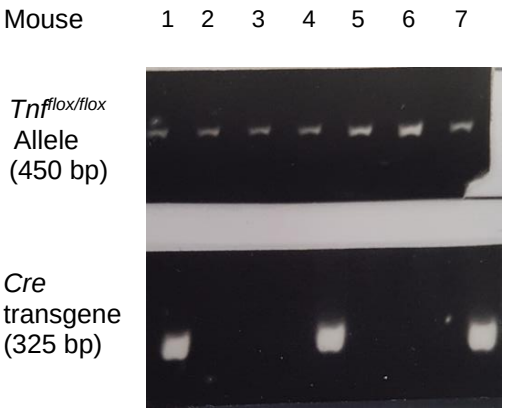

B

Mouse ID	Genotype	Acronym
1	*Mrp8-Cre;Tnf*$^{flox/flox}$	Neutro-TNF^{KO}
2	*Tnf*$^{flox/flox}$	Neutro-TNF^{WT}
3	*Tnf*$^{flox/flox}$	Neutro-TNF^{WT}
4	*Mrp8-Cre;Tnf*$^{flox/flox}$	Neutro-TNF^{KO}
5	*Tnf*$^{flox/flox}$	Neutro-TNF^{WT}
6	*Tnf*$^{flox/flox}$	Neutro-TNF^{WT}
7	*Mrp8-Cre;Tnf*$^{flox/flox}$	Neutro-TNF^{KO}

Figure 6.3. Validating neutrophil specific deletion of TNF using PCR. (**A**) Detection of PCR fragments on a 2.5% agarose gel. Band were visualised under UV light and the expected molecular weight for each band was determined. (**B**) Represents the genotype concluded for each mouse based on the representation observed in (**A**).

6.2.3. Protein validation of specific neutrophil-TNF deletion

Due to the inherent mixed cell population of ear notch samples and to fully validate the selectivity of the TNF deletion in neutrophils, we sought to assess TNF protein levels in neutrophils by flow cytometry. For these investigations, leukocytes from Neutro-TNF^{KO} mice and their littermate controls were initially stimulated *in vitro* with LPS, a potent inducer of TNF synthesis. As such, whole blood was collected from the ascending vena cava of naïve Neutro-TNF^{KO} mice and Neutro-TNF^{WT} littermates and processed for red cell lysis as detailed in Chapter 2, section 2.2.5.3. Following red blood cell lysis, samples were incubated with GolgiPlug^{TM} (1:1000) for 10 min at 37^{o}C to prevent the release of endogenous cellular TNF. LPS (500 ng/ml) was then added directly for 4 hr at 37^{o}C. Samples were then processed for Ab staining as described in Chapter 2, section 2.2.5.3. Distinctly, samples were incubated with fluorescently conjugated antibodies targeting the cell surface proteins CD45 and Ly6G. Samples were then fixed/permeabilised according to the BD cytofix/cytoperm^{TM} kit and immunostained with an anti-TNF-APC conjugate or isotype control and resuspended in SB buffer prior to LSR Fortessa flow cytometry analysis (Becton Dickinson). Data was quantified offline using FlowJo software (TreeStar).

Neutrophils were gated as LysM-EGFP^{high}/Ly6G-PE^{pos}/CD45-PB^{pos} and monocytes were gated as LysM-EGFP^{low}/Ly6G-PE^{neg}/ CD45-PB^{pos}. TNF-APC positivity was determined for cells gated outside the control population immunostained with an isotype Ab. Data showed that ~20% of Neutro-TNF^{WT} neutrophils upon *in vitro* stimulation were TNF positive whilst only ~2% of neutrophils derived from Neutro-TNF^{KO} mice were positive, suggesting a 90% reduction in neutrophil-derived TNF expression in *Mrp8-Cre* expressing mice (**Fig. 6.4A-B**). In addition, we noted ~20% reduction in the number of TNF expressing monocytes in Neutro-TNF^{KO} compared to Neutro-TNF^{WT} mice (**Fig. 6.4C**).

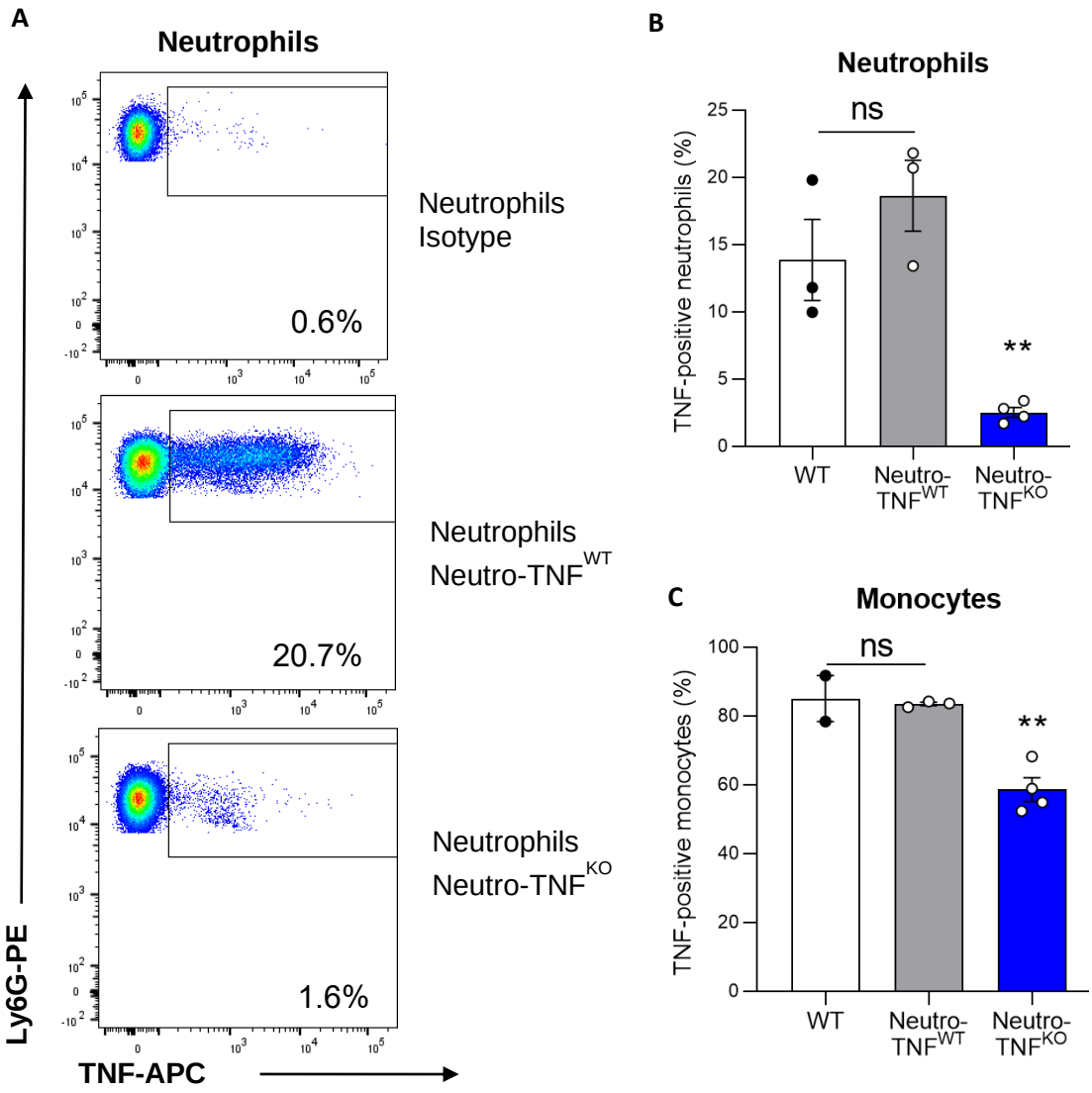

Figure 6.4. Validation of neutrophil TNF deletion using flow cytometry. (**A-C**) Whole blood was collected from WT, Neutro-TNF^{WT} or Neutro-TNF^{KO} and stimulated *in vitro* with LPS to induce TNF protein synthesis. As assessed by flow cytometry, neutrophils were gated as LysM-EGFP^{high}/Ly6G-PE^{pos}/CD45-PB^{neg} and monocytes were gated as LysM-EGFP^{low}/Ly6G-PE^{neg}/CD45-PB^{pos}. (**A**) Determination of TNF-APC positive cells was established over the isotype control antibody. (**B**) Total number of gated TNF-positive neutrophils (n = 3-4 mice/group). (**C**) Total number of gated TNF-positive monocytes (n = 2-4 mice/group). Statistically significant differences are relative to Neutro-TNF^{WT} mice (**B-C**). Data are represented as mean ± SEM (each dot represents one mouse and one independent experiment). Indicated statistical differences are shown by **p<0.01 as analysed by a one-way ANOVA followed by a Bonferroni post-hoc test (ns = not significant).

Although we successfully established a novel Neutro-TNF^{KO} mouse model, due to time restrictions and limited supply of experimental Neutro-TNF^{KO} mice, no functional studies were conducted as part of the present work.

6.2.4. Generation and validation of chimeric animals with *TNFRI/II^{KO}* HDCs

To build upon a previous study from our lab that demonstrated *TNFRI/II^{KO}* mice exhibited reduced LTB_4-induced vascular permeability (Finsterbusch et al., 2014), we extended these investigations to further explore the TNF pathway and its receptors in acute inflammatory responses. Specifically, we sought to elucidate the distinct contribution of both HDC-derived TNFRs in vascular permeability induction and neutrophil migration in a model of IR-injury. To address this, chimeric animals were generated, whereby BM from *TNFRI/II^{KO}* or WT control mice were isolated and injected into lethally irradiated WT or *LysM-EGFP$^{ki/+}$* (herein, collectively referred to as WT) recipients as detailed in Chapter 2, section 2.2.5. This strategy led to the generation of mice with TNFRI/II null myeloid and lymphoid cells (TNFRI/II KO-BM->-WT) while maintaining the expression of these receptors on other cell types such as ECs and pericytes (**Fig. 6.5A**).

Flow cytometry was first employed to assess the reconstitution of recipient mice with TNFRI/II^{KO}- or WT- donor BM as described in Chapter 2, section 2.2.5.3. Neutrophils were gated as CD45$^+$ and Ly6G$^+$ (i.e. all neutrophils) and the level of TNFRI surface expression by these cells was determined by their fluorescence intensity (**Fig. 6.5B**). TNFRI$^+$ from TNFRI$^-$ expressing cells were first distinguished by the use of an isotype control Ab or a global *TNFRI/II^{KO}* mouse. Furthermore, the total neutrophil count was calculated as the number of CD45$^+$ and Ly6G$^+$ cells (**Fig. 6.5C**).

Our analysis showed that blood neutrophils from TNFRI/II KO-BM->-WT chimeric mice had no detectable TNFRI or GFP expression (>98% negative), similar to global *TNFRI/II^{KO}* or *LysM-EGFP$^{ki/+}$* mice, respectively (**Fig. 6.5B**). Together, these results confirmed complete ablation of *LysM-EGFP$^{ki/+}$* and/or WT HDCs from the host animals. Furthermore, mice injected with WT BM cells (WT-BM->-WT) had detectable and comparable TNFRI expression (MFIs) to control WT or *LysM-EGFP$^{ki/+}$* mice, indicating that these chimeric mice would serve as a suitable TNFRI/II positive control (**Fig. 6.5B**). Importantly, both chimeric groups exhibited comparable neutrophil counts with approximately 3.5 x 10^6 neutrophils/ml of blood (**Fig. 6.5C**), suggesting a comparable level of BM reconstitution.

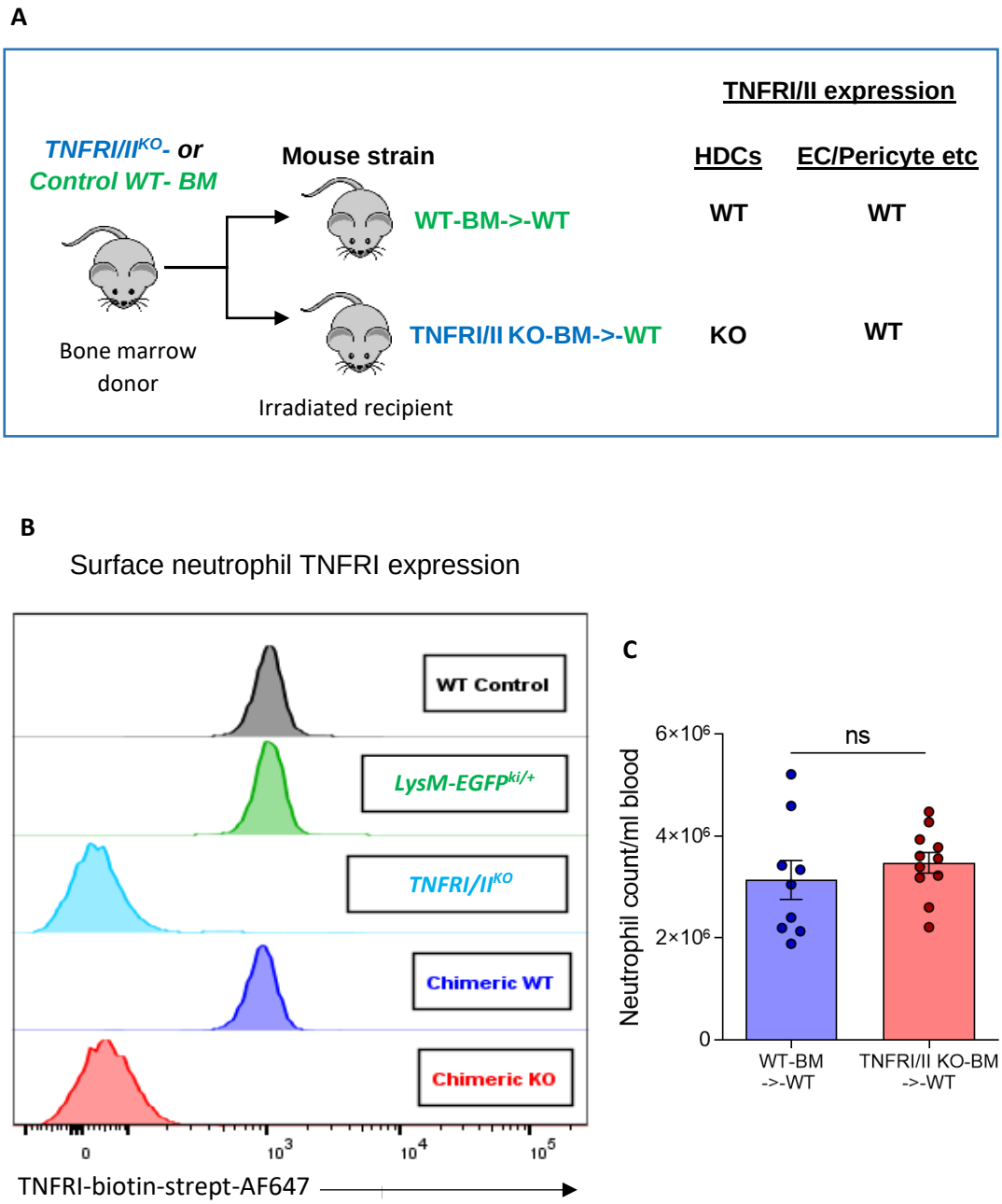

Figure 6.5. Generation of chimeric mice with TNFRI/II^{KO} HDCs. (**A-C**) Recipient mice (*LysM-EGFP$^{ki/+}$*or WT) mice were irradiated and reconstituted with BM from WT or TNFRI/II^{KO} donor mice as described in Chapter 2, section 2.2.5.3. This resulted in the generation of chimeric mice exhibiting WT HDCs (WT-BM->-WT) or TNFRI/II^{KO} HDCs (TNFRI/II KO-BM->-WT), respectively. (**B**) Representative histogram of TNFRI surface expression on neutrophils, from each representative mouse strain/chimera. 6 weeks after reconstitution, *LysM-EGFP$^{ki/+}$* or WT recipients with TNFRI/II^{KO} BM exhibited >98% of circulating donor derived neutrophils. (**C**) Both chimeras exhibited comparable neutrophil counts (n = 9-11 mice/group). Data are represented as mean ± SEM (each dot represents one mouse and one independent experiment). Statistical differences were analysed using an unpaired t-test (ns = not significant).

6.2.5. HDC-derived TNFRI/II support neutrophil tissue infiltration and vascular leakage

Upon generation and validation of the chimeric mice described in the previous section, we sought to assess vascular leakage and neutrophil extravasation responses following IR-injury in both WT-BM->-WT and TNFRI/II KO-BM->-WT chimeric animals by confocal IVM.

Briefly, mice received an i.s. injection of a fluorescently (AF647)-labelled anti-CD31 mAb to label ECs, 2 hr prior to exteriorisation of the cremaster tissue. Following exteriorisation, mice were subjected to IR-injury (40 min ischaemia followed by 2 hr of reperfusion) as described in Chapter 3, section 3.2.2. Control animals (sham) were not subjected to IR-injury but the cremaster was exteriorised. In addition, all mice received an i.v. injection of fluorescent TRITC-dextran (75 kDa) at the beginning of the confocal IVM image acquisition period. Vascular leakage responses were then quantified as previously described in section 3.2.1. Furthermore, neutrophil counts in the extravascular tissue were assessed post mortem by confocal microscopy in fixed cremaster tissues collected 2 hr post reperfusion as detailed in Chapter 2, section 2.6 (experimental timeline depicted in Appendix 3, section 9.3.2).

Our data revealed a rapid vascular leakage response upon reperfusion in WT-BM->-WT (**Fig. 6.6A**). Interestingly, whilst the peak of leakage was reached within 20 min, the leakage response was sustained, decreasing slowly without returning to basal level up by 60 min post reperfusion. In contrast, in TNFRI/II KO-BM->-WT chimeras the vascular leakage response was comparable to sham operated animals. Furthermore, quantification of tissue-infiltrated neutrophils demonstrated that in TNFRI/II KO-BM->-WT chimeric mice the neutrophil migration extravasation response was reduced by 40% as compared to WT-BM->-WT animals (**Fig. 6.6B-C**).

In conclusion, these data suggest that HDC-TNFR's play a fundamental role in IR-induced vascular leakage and neutrophil TEM.

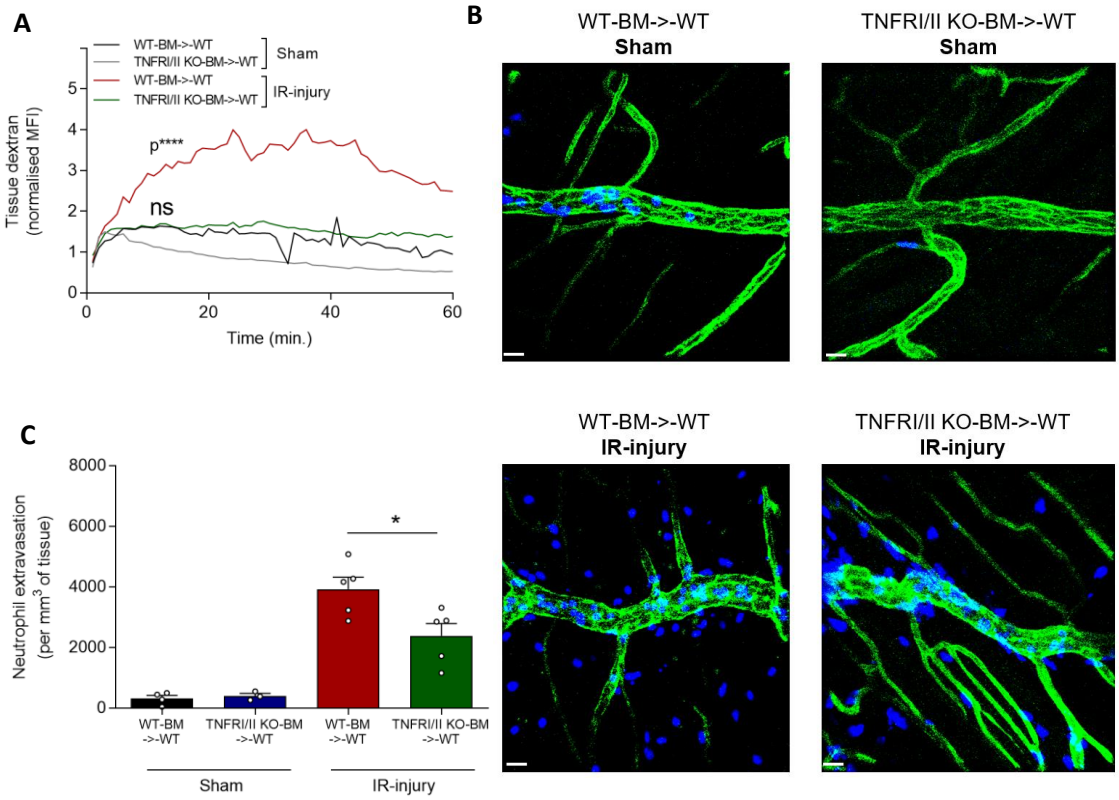

Figure 6.6. HDC-derived TNFRI/II mediated both enhanced vascular leakage and neutrophil transmigration following IR injury. Mice received an i.s. injection of a fluorescently (AF647) conjugated anti-CD31 mAb (4 µg) to label EC junctions, 2 hr prior to exteriorisation of the cremaster tissue. Following exteriorisation, mice were subjected to IR-injury (40 min ischaemia followed by 2 hr of reperfusion). Control animals (sham) were not subjected to IR-injury but the cremaster was exteriorised. In addition, all mice were subjected to an i.v. injection of fluorescent dextran (75 kDa) at the beginning of confocal IVM image acquisition. (**A**) Time-course of dextran accumulation in the perivascular region of a post-capillary venule, quantified as relative MFI (normalised to the first 2 time-points post dextran i.v., (n = 2-5 mice/group). Error bars are not shown for clarity but the SEM at the peak timepoint was within 0.157 and 1.223. (**B**) Representative confocal images of post-capillary venular segments (stained with anti-CD31; green and MRP14-AF647; blue) and (**C**) quantification of total neutrophil extravasation after 2 hr reperfusion (n = 3-5 mice/group). Data are represented as mean ± SEM (each dot represents one mouse and one independent experiment). (**A**) Statistically significant differences of TNFRI/II KO-BM->-WT mice are indicated, relative to WT-BM->-WT Sham ($^{ns}p>0.05$) or WT-BM->-WT IR (****$p<0.0001$) treated mice, as analysed by two way ANOVA followed by Bonferroni's post hoc test (**C**) or significant differences are indicated are indicated (*$p<0.05$) as analysed using a one-way ANOVA followed by a Bonferroni post hoc test. (ns = not significant).

6.3. Discussion

In this Chapter, we sought to understand how neutrophil-derived TNF impacts vascular leakage and neutrophil migration during IR-injury, a pathophysiological model of acute inflammation. To this aim, we successfully developed a novel GM mouse strain, selectively deficient in neutrophil-derived TNF. Furthermore, to enhance our understanding of the signalling pathways by which TNF mediates the inflammation response, we generated chimeric animals deficient in TNFRI/II for HDCs exclusively. In these mice, vascular leakage following IR-injury was abolished and neutrophil extravasation was significantly reduced as compared to control (WT-HDC) animals.

During acute inflammation, TNF is released from tissue macrophages, dendritic cells, ECs and neutrophils (Kany et al., 2019). However, as suggested by Finsterbusch et al., the onset of vascular leakage is fundamentally driven by neutrophil-derived TNF (Finsterbusch et al., 2014). TNF is known to act on EC-expressed TNFRI/II, leading to activation of the NF-kB pathway and the production of a variety of additional pro-inflammatory mediators such as IL-1β, CXCL1 and VEGF (Madge and Pober, 2001; Chen and Goeddel, 2002; Bian et al., 2017; Zhou et al., 2017). Another vital component of this signalling in ECs is the induction of Rac-dependent activation of various ROS-producing enzymes, such as NADPH oxidase, xanthine oxidase and nitric oxide synthase (Gao et al., 2015). ROS activity then leads to additional stimulation of the NF-κB pathway, and activates Src kinase which is responsible for the phosphorylation and subsequent internalisation of VE-cadherin (Naikawadi et al., 2012). Independently, ROS also leads to an influx of Ca^{2+}, resulting in stimulation of actin stress fibres and EC contractility. In conjunction with VE-cadherin internalisation, this results in compromised EC junctional integrity and the formation of 'micro-pores' between ECs, thus facilitating the passage of plasma proteins and solutes into the surrounding tissue (Szocs, 2004; Kumar et al., 2009; Claesson-Welsh, 2015). However, in response to pro-inflammatory mediators, neutrophils can augment the permeability response through the release of TNF-independent mediators, including ROS, VEGF (Gong and Koh, 2010), LTA_4 (which is metabolised by neutrophils to yield LTB_4 and ECs to yield LTC_4) and HBP (DiStasi and Ley, 2009) (**Fig. 6.7**). Similar to ROS, most of these mediators' act to induce contractility of ECs. It is rather remarkable then, that this ostensible plethora of pro-permeability

mediators requires, at least in the early acute phase, the release of neutrophil-derived TNF.

To facilitate future investigations into the impact of neutrophil-derived TNF, we developed a neutrophil-TNF deficient mouse model (Neutro-TNF^{KO}). Genomic PCR was successfully used to assess deletion/truncation of the *Tnf* gene (*Tnf*$^{KO/KO}$ allele) in neutrophils, which was further validated by evaluation of LPS-induced TNF protein expression by flow cytometry. Here, compared to Neutro-TNF^{WT} mice, neutrophils from Neutro-TNF^{KO} mice exhibited an almost complete loss of neutrophil-derived TNF expression thus validating the robustness of the genetic targeting strategy used. As expected, the majority of monocytes in Neutro-TNF^{KO} mice retained TNF expression. To generate this Neutro-TNF^{KO} mouse strain, we used a myeloid specific Cre-driver expressed from the MRP8 promoter. As MRP8, an essential component of the anti-bacterial protein calprotectin, is restrictively expressed by mature neutrophils and a small percentage of monocytes, we were able to restrict the expression of the Cre-transgene (and thus TNF deletion) to these cells only. Our strategy of using MRP8-Cre to conditionally delete floxed alleles has been reported previously to induce selective neutrophil knock-outs of Caspase recruitment domain-containing protein 9 (CARD9) (Németh et al., 2016), Syk tyrosine kinase (Elliott et al., 2011), and Mcl-1 (Csepregi et al., 2018). Furthermore, its effectiveness as a cell-specific deletion tool was comprehensively assessed by Abram and colleagues (Abram et al., 2014) whereby MRP8-Cre mice were crossed with R26-stop-enhanced yellow fluorescent protein (ROSA-EYFP) lineage trace reporter mice. Here, ROSA comprises a stop codon which controls the expression of the EYFP gene. Hence, any cell that expressed MRP8-Cre at any time during its lifetime would excise the stop codon and thereafter constitutively express EYFP (Abram et al., 2014). This study confirmed that approximately 85% of neutrophils isolated from peripheral blood, spleen and BM were EYFP-positive (Abram et al., 2014). We can now extend this finding to our Neutro-TNF^{KO} mice, which exhibited a similar level of floxed allele (*Tnf*) deletion in that only 2% of circulating neutrophils expressed TNF in Neutro-TNF^{KO} mice, compared to 20% identified as TNF^{+} from Neutro-TNF^{WT} mice. Overall, this equates to a 90% reduction in neutrophil-derived TNF expression. Furthermore, Abram et al., also identified that approximately 20% of peripheral blood and 8% of tissue resident monocytes exhibited EYFP expression, and

hence had expressed MRP8-Cre at some point during ontogeny (Abram et al., 2014). Similar findings were confirmed by Elliot et al., following MRP8-Cre induced Syk deletion (Elliott et al., 2011) and are also consistent with our findings where approximately 20% of circulating monocytes exhibited a TNF-deficient phenotype. It is difficult to suggest an improved method of selectively targeting neutrophils for TNF deletion, as to our knowledge, no gene has yet been identified to be exclusively expressed by neutrophils. Overall, we take these findings as a positive validation for a selective deficiency in neutrophil-derived TNF. As such, we anticipate that these experimental mice will be a useful tool for future investigations into the role of neutrophil-derived TNF in mediating acute inflammatory responses.

Due to time constraints and a lack of experimental Neutro-TNF^{KO} mice, we concomitantly sought to investigate the contribution of both TNFRI & TNFRII on vascular leakage and neutrophil extravasation during a model of acute sterile inflammation as elicited by IR-injury. Specifically, a series of experiments were conducted to investigate the contribution of HDC-TNFRs on vascular leakage and neutrophil extravasation. This direction follows a growing number of reports that TNF may act in an autocrine manner, where it initiates and amplifies the synthesis/release of pro-inflammatory mediators within a variety of cell types, including neutrophils (Cassatella et al., 1993; Yarilina et al., 2008; Pękalski et al., 2013; Tecchio et al., 2014). To this end, chimeric animals were generated in which BM from global *TNFRI/II*^{KO} or respective WT control mice was injected i.v. into irradiated *LysM-EGFP*$^{ki/+}$ or WT recipient mice. In both cases, haematopoietic regeneration was successful and chimeric mice containing *TNFRI/II*^{KO} and WT BM exhibited comparable neutrophil counts in the blood. Subsequently, these mice were used to investigate the role of HDC-TNFRs in response to IR-injury of the cremaster muscles. This was the model of choice as TNF has previously been shown to play a key role in the induction of vascular leakage and leukocyte migration responses during IR-injury (Gao et al., 2015; Wu et al., 2018).

Here, whilst mice receiving WT BM elicited a very rapid vascular leakage response, mice receiving *TNFRI/II*^{KO} BM did not. This result was a rather surprising finding, as ECs are the 'gatekeepers' that regulate leakage into the interstitial tissue and in such it was expected that EC-TNFRs, and not HDC-TNFRs, would be more important in mediating enhanced endothelial permeability. This finding was complimentary to that of

Finsterbusch *et al*., whereby LTB_4-induced vascular leakage in global *TNFRI/II*^{KO}-, neutrophil depleted- or chimeric HDC-*TNF*^{KO}-mice, was abolished (Finsterbusch et al., 2014). Taken together, these results demonstrate that induction of vascular leakage may require a reservoir of pre-formed neutrophil-TNF and HDC-TNFRI/II to indirectly mediate the response. This also suggests that the initial release of pre-formed neutrophil-TNF may not be sufficient to induce enhanced endothelial permeability and that TNF acts indirectly through an autocrine pathway, but would require further experimental investigation to definitively address this hypothesis. Nevertheless, it is surprising that other pro-permeability mediators that are generated during IR-injury, are not sufficient to induce permeability. Therefore, we hypothesise the presence of a permeability "threshold" during inflammation, which must be overcome before vascular leakage can occur. Pivotal to surpassing of this threshold is the requirement of early HDC-TNFRI/II signalling as initiated by the release of preformed intracellular TNF. Thus, based on our findings and those in the literature, we propose the following series of events: following neutrophil adhesion to ECs, intracellular neutrophil TNF is released and acts in an autocrine manner. Subsequently, this amplifies the synthesis and release of TNF in addition to other pro-inflammatory/permeability factors, such as LTB_4, VEGF and HBP (DiStasi and Ley, 2009), resulting in the amplification of the inflammatory/permeability response and surpassing of the permeability threshold (**Fig. 6.7**).

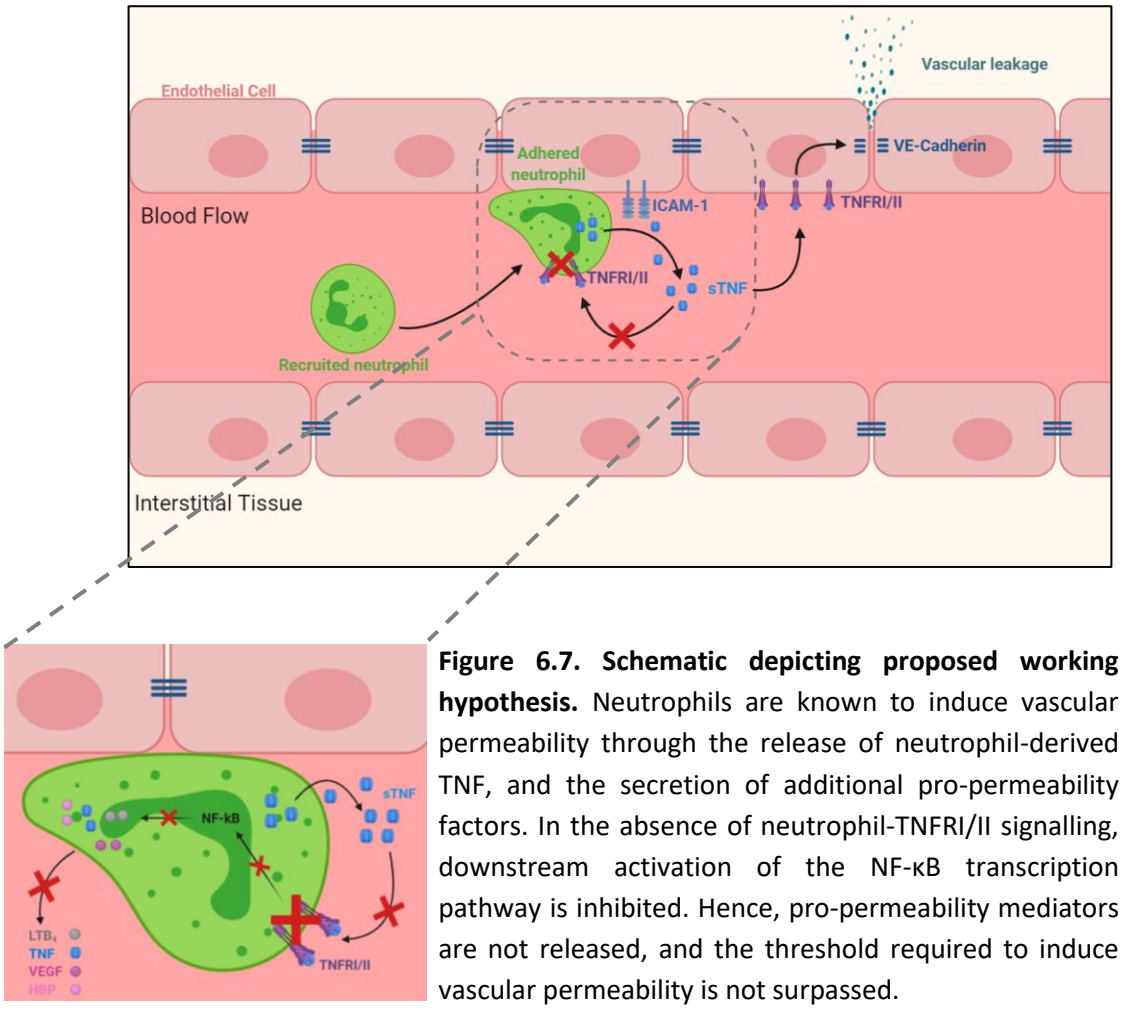

Figure 6.7. Schematic depicting proposed working hypothesis. Neutrophils are known to induce vascular permeability through the release of neutrophil-derived TNF, and the secretion of additional pro-permeability factors. In the absence of neutrophil-TNFRI/II signalling, downstream activation of the NF-κB transcription pathway is inhibited. Hence, pro-permeability mediators are not released, and the threshold required to induce vascular permeability is not surpassed.

Finally, we also observed that TNFRI/II KO-BM->-WT mice exhibited reduced neutrophil extravasation as compared to WT-BM->-WT mice. Interestingly, this would constitute further evidence that neutrophil migration can occur independently of vascular leakage (DiStasi and Ley, 2009). Here, the observed partial defect in neutrophil extravasation could also be the consequence of downregulation of CD11b and LFA-1, both of which mediate TNF-induced leukocyte crawling and migration (Sumagin et al., 2010). Instead, neutrophil migration in IR has been previously shown to be mediated by PECAM-1, ICAM-2 and JAM-A, whilst these junctional adhesion molecules are not involved in neutrophil TEM upon TNF stimulation (Nourshargh et al., 2006; Huang et al., 2006; Woodfin et al., 2007b, 2009). Overall, whilst shedding novel insight into the role and mechanism of action of TNF/TNFR pathway in regulation of neutrophil migration and vascular leakage, primarily the present findings provide a platform for future works as discussed in Chapter 7.

6.4. Conclusion

This Chapter provides preliminary insights into the contribution of TNFRs expressed by different cell types, whereby HDC-TNFRs play a fundamental role in mediating an IR-dependent vascular leakage response in addition to partially mediating neutrophil migration into the extravascular tissue. While these findings suggest intriguing underlying mechanisms, further experimentations are required to definitively understand the observed phenotypes (see Chapter 7, future works). Lastly, to exclusively investigate the role of neutrophil-derived TNF in models of acute inflammation, a selective neutrophil TNF 'knock out' mouse was generated and successfully validated. Collectively, the present work provides the basis of future studies currently beyond the scope of this thesis.

Chapter 7

General Discussion

7.1. Project overview

Microvascular permeability and neutrophil TEM are key hallmarks of the immune response that are essential for survival and recovery following sterile (e.g. IR-injury) or non-sterile (i.e. infection) acute inflammatory reactions and tissue injury. However, our understanding of the interplay between these phenomena is limited and has historically focused on how neutrophils hinder endothelial integrity and vascular barrier functions. The aim of this thesis was to advance our understanding of the impact of microvascular permeability on neutrophil TEM *in vivo*. Overall, whilst increased vascular permeability did not appear to grossly influence neutrophil infiltration into tissues, we provide strong evidence for enhanced vascular leakage supporting an aberrant mode of neutrophil migration known as neutrophil rTEM. Mechanistically, this was caused by augmented abluminal-to-luminal translocation of the endogenously generated chemokine CXCL1. Furthermore, through the development of a novel tracking method, rTEM neutrophils were found to disseminate rapidly to the lung, where they exhibited an activated phenotype and were associated with sites of lung tissue damage. The project also began investigations into the roles of TNFRI/II in the induction of vascular leakage and neutrophil migration following IR-injury. This Chapter collectively discusses and critiques the findings of this thesis and suggests future directions to extend these investigations.

7.1.1. Enhanced microvascular leakage supports neutrophil rTEM

Microvascular leakage and neutrophil migration occur independently, as supported by distinct molecular pathways (Ley et al., 2007; Vestweber, 2007; DiStasi and Ley, 2009; Vestweber, 2012; Frye et al., 2015). For instance, vascular leakage can occur at local luminal sites separate from those supporting neutrophil migration (Baluk et al., 1998) and each phenomenon is mediated by phosphorylation of distinct VE-cadherin residues at EC junctions (Wessel et al., 2014). However, direct evidence showing that migrating neutrophils can induce vascular permeability suggested an interplay between these phenomena (Wedmore and Williams, 1981; DiStasi and Ley, 2009). Nevertheless, the

direct impact of vascular permeability on neutrophil TEM dynamics has not previously been studied and formed the focus of the present research.

Using our extended confocal IVM platform optimised for imaging the mouse cremaster muscle (described in Chapter 3), we observed that reactions featuring enhanced vascular leakage, namely as induced by local LTB_4 and IR-injury, exhibited an enhanced frequency of neutrophil rTEM (**Fig. 3.5C**), without affecting total neutrophil extravasation (**Fig. 3.2B**). Although neutrophil rTEM in these reactions was previously reported (Woodfin et al., 2011; Colom et al., 2015), the novel observation of a temporal association between increased vascular leakage and rTEM led to the hypothesis of a direct link between these two responses.

To investigate directly the effect of vascular permeability on neutrophil TEM, the project studied the impact of vasoactive mediators (i.e. histamine and VEGF) on neutrophil TEM induced by locally applied IL-1β. With this approach, we demonstrated that histamine-induced vascular leakage resulted in enhanced neutrophil rTEM (**Fig. 4.2D**) without affecting total neutrophil extravasation (**Fig. 4.1B**). Furthermore, VEGF, a well-established alternative pro-permeability factor (Ferrara, 2004) elicited the same effect (**Fig. 4.2C**). Crucially, a GM mouse strain characterised by a defect in vascular permeability induction (**Fig. 4.3D**) (Wessel et al., 2014), exhibited reduced levels of neutrophil rTEM in tissues stimulated with IL-1β + histamine (**Fig. 4.3F**). Overall, these results comprehensively established a causative link between vascular permeability and the incidence of neutrophil rTEM. However, as vasoconstriction can lead to a decrease in blood flow rate, which has been shown to impact neutrophil migration parameters such as adhesion, we cannot directly rule out the potential impact that histamine, a vasoconstrictor, may have on neutrophil rTEM (Majno et al., 1969; Ebeigbe Anthony and Talabi Olufunke, 2014; Ashina et al., 2015). Nevertheless, as compared to IL-1β alone, additional administration of histamine did not affect neutrophil adhesion or extravasation parameters as measured by brightfield IVM (data not shown). In addition, stimulation with VEGF, a known vasodilator that increases blood flow rate (Ashrafpour et al., 2004; Ferrara, 2004), induced a similar frequency of neutrophil rTEM compared to histamine. To conclusively examine potential changes in blood flow rate in the inflammatory models used, measurements in single post-capillary venules would be required. Blood flow rate in the cremaster tissue could be measured using full field laser

perfusion doppler imaging (Ye et al., 2020), or measured and calculated for single post-capillary venules using a dual photodiode and brightfield video analysis (Lipowsky and Zweifach, 1978; Lindner et al., 2000; Ortiz et al., 2014).

Next, we considered how hyper-permeability could lead to augmented aberrant neutrophil migration. Previous investigations from our group have identified NE-dependent cleavage of JAM-C in EC junctions as a key regulator of neutrophil rTEM during LTB_4- and IR-injury-induced inflammation (Woodfin et al., 2011; Colom et al., 2015). This was complementary to findings by Bradfield et al., who demonstrated that maintenance of JAM-C at EC junctions was vital for unidirectional monocyte TEM (Bradfield et al., 2007b). These observations raised the question as to whether loss of junctional JAM-C could drive vascular leakage-dependent neutrophil rTEM. Indeed, JAM-C has been shown to be involved in the regulation of vascular permeability. Works by Orlova et al., observed that loss of JAM-C resulted in reduced histamine- or VEGF-dependent vascular permeability induction by stabilisation of EC junctional VE-cadherin (Orlova et al., 2006). On the other hand, investigations by Imhof and colleagues found opposing observations in a bacterial infection model of Leishmania major, wherein loss of JAM-C increased vascular permeability induction by 15% (Ballet et al., 2014). As such, the role of JAM-C in vascular leakage remains contentious and may be reaction-specific. To determine the contribution of JAM-C in our model, Dr. Régis Joulia, within our group, analysed EC junctional JAM-C expression and found no difference following treatment of tissues with histamine, IL-1β alone, or IL-1β + histamine. This suggested the presence of a novel mechanism, independent of JAM-C loss, in driving permeability-mediated rTEM (Owen-Woods et al., 2020). This hypothesis is consistent with findings from Colom *et al.,* 2015 who observed only a partial reduction (~50%) in the neutrophil rTEM response following LTB_4-stimulation in a full *Elane*^{KO} (NE^{KO}) mouse model (Colom et al., 2015).

7.1.2. Enhanced vascular leakage leads to augmented tissue-to-blood translocation of CXCL1

Neutrophil TEM is fundamentally orchestrated by sequential molecular interactions and directional chemotaxis as mediated by chemotactic cues/chemokines such as CXCL1 and

CXCL2 (Janetopoulos and Firtel, 2008; McDonald et al., 2010; Jin, 2013). The importance of these interactions in neutrophil TEM was recently demonstrated by Girbl et al., in a murine model of TNF-induced acute inflammation (Girbl et al., 2018). This work demonstrated that unidirectional neutrophil migration across the vessel wall requires consecutive interactions with CXCL1 and CXCL2. These mediators were potentially presented at the EC-surface on GAGs (Proudfoot et al., 2017; Uchimido et al., 2019) and at EC junctions by ACKR1 (Pruenster et al., 2009; Novitzky-Basso and Rot, 2012; Thiriot et al., 2017; Girbl et al., 2018), where they mediated crawling and TEM, respectively (Girbl et al., 2018). To this end, we hypothesised that under conditions of hyper-permeability, chemokine expression/localisation may be disrupted leading to a loss of directional cues, which consequently facilitates augmented levels of neutrophil rTEM. As CXCL1 is known to be highly upregulated following IL-1β stimulation (Ribaux et al., 2007; Biondo et al., 2014), we focused our investigations on this chemokine.

Here we identified that IL-1β induced generation of CXCL1 in both the tissue and plasma (**Fig. 4.4A-D**). Chemokines are known to be released by various resident-tissue cells such as pericytes, ECs, mast cells and macrophages (Becker et al., 1994; Griffin et al., 2012; De Filippo et al., 2008; Girbl et al., 2018), where they usually form a chemotactic gradient to direct neutrophils to the site of insult (McDonald et al., 2010). Interestingly, in samples isolated from inflammatory reactions associated with acute vascular leakage and neutrophil rTEM, (e.g. IL-1β + histamine and IR-injury), CXCL1 levels significantly increased in the plasma as compared to IL-1β-treated mice (~1.4-fold) or PBS-treated mice (~2.3-fold), respectively (**Fig. 4.4B & D**). This suggested that tissue generated CXCL1 may be rapidly translocated through loose EC junctions into the bloodstream following induction of vascular leakage. In support of this concept, pharmacological blockade of histamine-induced vascular permeability using an Ab against VE-PTP, a phosphatase vital in controlling EC junctional barrier function, resulted in a partial reduction of CXCL1 in the plasma (**Fig. 4.4F**). We therefore hypothesised that during scenarios of enhanced permeability (i.e. histamine-induced leakage), tissue-generated CXCL1 is able to overcome the advective flux and diffuse through EC junctions into the bloodstream. This idea was first supported by mathematical modelling that simulated fluid flow across the endothelium (data not shown, Owen-Woods et al., 2020) and was then experimentally tested *in vivo* by Dr. Régis Joulia. In both cases, it was shown that a small 10 kDa molecule

(such as CXCL1) could feasibly diffuse from the tissue into the blood under conditions of enhanced vascular permeability. Lastly, we directly assessed if this disruption of CXCL1 localisation was responsible for the enhanced frequency of neutrophil rTEM. Indeed, inhibition of CXCL1 using an anti-CXCL1 Ab reduced the frequency of neutrophil rTEM (**Fig. 4.5C & E**). Of consideration, whilst detection of CXCL1 in the plasma upon inflammation could also result from lymphatic drainage, our study clearly showed VE-PTP blockade resulted in reduced CXCL1 blood levels, suggesting that the increase observed following acute hyperpermeability reactions is directly associated with EC junctional translocation of CXCL1. Collectively, these investigations provide evidence for the first time that enhanced microvascular leakage disrupts the directional chemotactic cues required to govern unidirectional neutrophil TEM, resulting in enhanced neutrophil rTEM. However, precisely how this augmented localisation of CXCL1 leads to aberrant neutrophil migration provides scope for postulation and is further summarised in **Fig. 7.1**.

Perhaps the most intuitive hypothesis would be that excessive CXCL1 specifically in the blood might lead to disrupted neutrophil migration. However, this assumption is contrary to the fact that both the IR-injury and IL-1β + histamine reactions exhibited very different levels of plasma CXCL1, but had comparable frequencies (~20%) and number (~4/300 μm vessel segment/2 hr) of neutrophil rTEM events. While this may be partially explained by the fact that neutrophil rTEM is additionally mediated by JAM-C cleavage in IR-injury (but not in response to IL-1β + histamine) (Woodfin et al., 2011), this does not account for the similar reduction in neutrophil rTEM upon administration of an anti-CXCL1 Ab. In addition, at the timepoints analysed, mice treated with IL-1β alone exhibited a higher concentration of plasma CXCL1 than IR-injury and yet demonstrated minimal neutrophil rTEM. Furthermore, of consideration, chemokines are prone to proteolytic degradation and would wash away in the blood from the site of inflammation. Lastly, under inflammatory conditions the plasma concentration of chemokines, such as CXCL1, is usually buffered by ACKR1 that is expressed not only by ECs, but also on circulating RBCs. This “sink” of chemokine modulates their bioavailability and prevents excessive changes in plasma chemokine concentrations (Darbonne et al., 1991; Bonecchi and Graham, 2016). Collectively, a plausible explanation may be that vascular leakage induces an augmented localisation of CXCL1

specifically at the junction as opposed to the increased CXCL1 level in the blood; the latter acting more as a reservoir for excess unbound CXCL1. Indeed, as suggested by Girbl et al., it is conceivable that within the confines of the EC junction, where chemokines are physically retained, proteolytic degradation and dilution that is noted in the blood will be attenuated (Girbl et al., 2018). Consequently, excessive presentation of CXCL1 at EC junctions could result in overstimulation and possibly internalisation of neutrophil-derived CXCR2, leading to a loss of regulated chemokine sensing/signalling by the neutrophil, promoting augmented neutrophil rTEM. This hypothesis is supported by findings from Wiekowski et al., who identified desensitisation of neutrophil-derived CXCR2 in a conditional transgenic mouse model that overexpresses CXCL1, resulting in poor neutrophil migration responses (Wiekowski et al., 2001). In addition, CXCR2 internalisation was observed by Carlos and colleagues to lead to poor neutrophil migration, whereby elevated blood levels of histamine in a model of sepsis resulted in upregulation of GRK2 causing reduced surface expression of CXCR2 (Carlos et al., 2013). Furthermore, Girbl *et al.*, identified CXCL2, another ligand for CXCR2, as the chemokine that supports luminal-to-abluminal neutrophil TEM (Girbl et al., 2018). Thus, excessive presentation of CXCL1 to CXCR2 may prevent CXCL2 from interacting with its shared receptor, either by occupying the physically space or following internalisation of CXCR2.

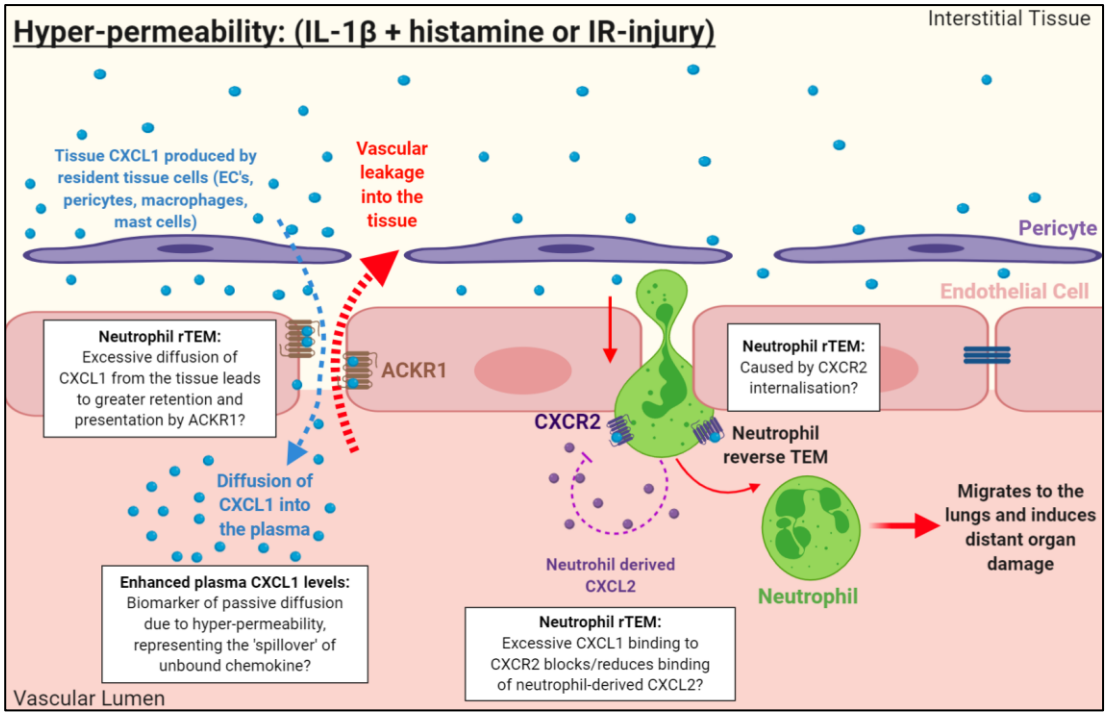

Figure 7.1. Schematic presenting the proposed mechanisms of how microvascular leakage-induced CXCL1 redistribution facilitates neutrophil rTEM. IL-1β is a potent stimulator of synthesis and release of CXCL1 from a variety of cells including ECs, pericytes, macrophages and mast cells. Following reactions exhibiting hyper-permeability (e.g. IL-1β + histamine or IR-injury), CXCL1 passively diffuses through EC junctions. Here, we hypothesise that excessive diffusion of CXCL1 from the tissue to the blood may result in overstimulation and internalisation of its respective receptor, CXCR2, either by disproportionate presention by ACKR1 and/or direct binding of CXCL1 to CXCR2 within the confines of the junction during neutrophil diapedesis. Alternatively, excessive availabilty of CXCL1 may saturate CXCR2 leading to an inability for neutrophil-derived CXCL2 to bind and facilite unidirectional neutrophil TEM.

Lastly, although we have substantial evidence to support enhanced diffusion of CXCL1 through EC junctions, we cannot necessarily rule out the possibility that CXCL1 could be actively transported across the endothelium by ACKR1. Indeed, overexpression of ACKR1 has been shown to support neutrophil trafficking by internalising and transporting chemokine from the basolateral to apical membrane *in vitro*. Here, the chemokine is presented and was found to enhance adhesion of neutrophils to the luminal EC surface *in vivo* (Lee et al., 2003; Pruenster et al., 2009). In addition, temporal investigations into ACKR1 transcytosis have shown that trafficking of the chemokine, CCL2, across Madin-Darby Canine Kidney (MDCK) cells takes approximately 30 – 120 min (Pruenster et al., 2009). If we make the assumption that transcytosis of ACKR1 occurs at similar rates in ECs (equivalent data not available), it would seem unlikely that ACRK1-mediated chemokine transcytosis contributes to the changes in CXCL1 distribution that

drives neutrophil rTEM, the majority of which occurs within 30 min post-histamine/VEGF treatment or reperfusion. To definitively assess this, experiments would need to be conducted *in vitro* using HUVECs or *in vivo* using *ACKR1*^{KO} mice. In addition, chemokines can also be retained by GAGs to facilitate neutrophil migration. Thus, potential changes in the GAG retention capacity or cleavage, known to occur during inflammation due the presence of MMPs and other enzymes such as heparanase (Massena et al., 2010; Thompson et al., 2017), could lead to elevated plasma CXCL1. However, as neutrophil adhesion was not affected in our IL-1β + histamine reaction (data not shown), where CXCL1 presentation on GAGs is key, contributions from GAG disruption is less plausible. Overall, to ascertain the direct regulation, expression and presentation of CXCL1 dynamics would require further investigations (see section 7.2.1).

7.1.3. Activated rTEM neutrophils disseminate to the lungs and induce damage

Reverse migration of neutrophils through the endothelium occurs in a variety of sterile inflammatory reactions including IR-injury, (Woodfin et al., 2011; Colom et al., 2015), burn injury (Yoo and Huttenlocher, 2011; Wang et al., 2017), and more recently, hyper-permeability associated reactions (Owen-Woods et al., 2020). Although advancements have been made to target, track and phenotype neutrophils that undergo rIM followed by rTEM (i.e. neutrophils that return to the vasculature from the interstitial tissue), our understanding of neutrophils that undergo rTEM exclusively is limited. The main reason for this resides in fundamental limitations of these photoconversion (PC)/photoactivation (PA) tracking methods, in the sense that targeting of neutrophils is restricted to the laser-accessible microscopic field-of-view outside the vasculature and beyond the pericyte layer (Yoo and Huttenlocher, 2011; Wang et al., 2017). Thus, in our model, as rTEM neutrophils only partially breach the endothelium, these approaches are impractical. In addition, PC/PA only allows for select numbers of neutrophils to be targeted within defined ROIs (i.e. not all reverse migrating cells are tagged), thus limiting the frequency of trackable reverse migrating cells.

To overcome these limitations, we developed a novel fluorescent labelling approach to exclusively label rTEM neutrophils. This methodology, applied to the inflammatory reaction as induced by IL-1β + histamine, utilised the natural high affinity between biotin

and streptavidin through i.v. administration of anti-Ly6G-biotin and locally applied strept-AF647, as described in Chapter 5 (**Fig. 5.1**). *Via* this approach, we were able to 'tag' interstitial but also rTEM neutrophils whilst non-migrating neutrophils (i.e. free-flowing, rolling or adherent cells) and other immune cells (e.g. monocytes) remained unlabelled (**Fig. 5.2B**). Related to this approach, the use of an anti-Ly6G Ab to label circulating neutrophils without affecting their migration required addressing due to mixed literature reports. Specifically, whilst Nigrovic and colleagues had observed defects in neutrophil migration with doses of anti-Ly6G Ab between 5 – 50 µg (i.p.) (Wang et al., 2012; Cunin et al., 2019), Yipp and Kubes have reported no such effects up to the dose of 40 µg (i.v.) of the Ab (Yipp and Kubes, 2013). The latter finding is consistent with our data showing that anti-Ly6G labelling of neutrophils *in vivo* has no impact on their migratory behaviour (**Fig. 5.4A-D**).

Following induction of vascular permeability, a ~5-fold increase in the number of strept-AF647^{+} neutrophils was detected in the blood as compared to levels detected in mice treated with IL-1β alone (**Fig. 5.6A & B**). This aligned closely with the observed change in the frequency of neutrophil rTEM. Further, these data strongly supported the notion that strept-AF647^{+} cells are indeed rTEM neutrophils. Application of our novel tracking method to the IL-1β + histamine reaction enabled the detection of ~2,800 strept-AF647^{+} neutrophils/ml of blood, compared to the ~300 PA-GFP^{+} (i.e. rIM + rTEM) neutrophils/ml blood detected using the PA approach (Wang et al., 2017). Hence, our model may offer the ability to track a larger number of reversing cells as compared to the alternative PA approach. However, a definite comparison of each technique is limited by fundamental differences including: the inflammatory reactions employed (IL-1β + histamine vs. sterile burn injury), types of reverse migration studied (rTEM vs. rIM), type of organ (cremaster muscle vs. liver), time-points of the reaction (4 hr post IL-1β + 2 hr histamine vs. 16-24 hr post sterile burn injury) and the labelling duration used (continuous topical application of strept-AF647 vs. single laser pulse PA). Nevertheless, our advancement allowed us to directly explore the phenotype and fate of rTEM neutrophils for the first time.

Previous *in vitro* studies from Buckley et al., discovered that neutrophils that underwent rTEM through a monolayer of ECs expressed higher levels of the surface molecule, ICAM-1 (Buckley et al., 2006). Interestingly, *in vivo*, an ICAM-1^{high} neutrophil population could

be detected in the lung vasculature in reactions characterised by a high frequency of reversing neutrophils, which were hypothesised to be local rTEM cells that disseminated to secondary organs (Woodfin et al., 2011). Furthermore, Colom et al., observed increased pulmonary vascular leakage following local LTB_4 stimulation of the cremaster muscle, suggesting that rTEM neutrophils may contribute towards the onset of secondary organ injury (Colom et al., 2015). Therefore, through our direct tracking method we sought to determine if our labelled rTEM neutrophils indeed relocated to the lungs. We identified an increased population of strept-AF647$^+$ neutrophils in lung vascular washout (LVWO) and in the bone marrow (BM) at 2 hr and 4 hr post histamine, respectively (Owen-Woods et al., 2020). Similar to our study, Wang et al., observed increased retention of rIM neutrophils in the lungs and BM post local sterile inflammation, albeit at 24 hr and 48 hr, respectively (Wang et al., 2017). As return of neutrophils to the BM is associated with resolution of inflammation (Furze and Rankin, 2008), Wang et al., postulated that neutrophils that undergo rIM + rTEM support a pro-resolutory pathway.

Due to the limited understanding of the fate of reverse migrating leukocytes, it was vital to assess the phenotype of tracked rTEM neutrophils in the blood and LVWO. Here, Ly6G-strept-AF647-tagged rTEM neutrophils in the blood exhibited an activated phenotype (increased ICAM-1 and CD11b) (**Fig. 5.8A**) and were further detected in the lung vasculature where they presented an exacerbated pro-inflammatory phenotype (increased CD11b, ICAM-1, β1-integrin, NE and CXCR4) (**Fig. 5.8B**). Increased expression of ICAM-1 and of integrin subunits (e.g. CD11b and β1-integrin) are established markers of neutrophil activation that could explain their retention in the lung vasculature (Sumagin et al., 2010; Nourshargh and Alon, 2014). Furthermore, expression of CXCR4 on the surface of leukocytes can mediate neutrophil margination in the lung (Devi et al., 2013). Lastly, we observed that strept-AFT647$^+$ neutrophils correlated with sites of vascular leakage (data not shown, Owen-Woods et al., 2020), a finding consistent with the results of Colom et al., suggesting a pro-inflammatory role for rTEM neutrophils. This is supported by the increased expression of NE by rTEM neutrophils in the lung vasculature which could be responsible for the observed increase in vascular leakage. NE is a destructive serine protease enzyme secreted from azurophil (primary) granules or released in NETs (Cowland and Borregaard, 2016). NE can facilitate the breakdown of the

extracellular matrix and cleave essential EC junctional molecules such as JAMs (Colom et al., 2015), ICAM-1 (Champagne et al., 1998) and VE-cadherin (Carden et al., 1998), thus resulting in reduced stability of the endothelial barrier (Chua and Laurent, 2006; Taylor et al., 2018; Voisin et al., 2019). Of particular importance, increased NE expression can induce tissue damage and has been strongly associated with various lung diseases including ALI and ARDs (Polverino et al., 2017). The identification of elevated NE surface expression on rTEM neutrophils reported in this thesis may indicate that these neutrophils are indeed capable of contributing to the development of lung pathologies. However, neutrophils have the capacity to induce vascular leakage through the release of a variety of other factors, such as ROS, TNF, VEGF and HBP (DiStasi and Ley, 2009). Of particular interest, ICAM-1 expression by neutrophils enhances their phagocytic activity, and more importantly, generation of ROS (Woodfin et al., 2016). To assess the potential contribution of these factors in the tissue destructive capability of rTEM neutrophils would require further investigations (section 7.2.2.1). Of consideration, the increased levels of CXCL1 in the plasma detected following the topical application of histamine to IL-1β stimulated cremaster tissues, may also play a role in the observed lung vasculature dysfunction. Indeed, injection of CXCL1 i.v. can induce vascular leakage and increase neutrophil accumulation in rabbit lungs (Rot, 1991). However, although a different animal species is used in our model, the dose of CXCL1 employed in the former study (100 µg i.v.) was far higher than the increase observed in this thesis between IL-1β and IL-1β + histamine-treated mice (0.01 µg increase following histamine application). Furthermore, although in our studies we observed lung vascular dysfunction, total local (**Fig. 4.1B**) and remote (data collected by Dr Régis Joulia, not shown) organ neutrophil accumulation was similar between IL-1β +/- histamine-treated groups. Therefore, the increased plasma level of CXCL1 following IL-1β + histamine is unlikely to be the cause of vascular leakage in the lung. However, to definitively investigate the contribution of plasma CXCL1 in our model, a dose response of injected recombinant CXCL1 (i.v.) experiment, followed by assessment of the lung vascular leakage would be required. Additionally, adoptive cell transfer experiments could be conducted, whereby isolated strept-AF647^{+} or strept-AF647^{-} neutrophils could be injected into naïve mice followed by subsequent analysis of the pulmonary vascular leakage response.

Lastly, we found striking similarities between the phenotype of rTEM neutrophils within the pulmonary vasculature and “aged” neutrophils, whereby both exhibit enhanced suface expression of CXCR4, ICAM-1 and CD11b (Rosales, 2018), with the exception of CD62L where only a trend towards reduction was observed. Aged neutrophils also reportedly exhibit upregulation of VLA-4 and downregulation of CXCR2, which could provide potential markers for future characterisations. Furthermore, Androver and colleagues have recently shown that activation of CXCR2 induces cell aging, which they suggest favours neutrophil clearance from the tissue into the circulation (Adrover et al., 2019). This could be consistent with our proposed mechanism for neutrophil rTEM, involving hyper-activation and consequential desensitisation/internalisation of CXCR2 by excessive EC junctional expression of CXCL1 (see section 7.1.2). In addition, neutrophil clearance is proposed to be mediated by CXCR4, a response linked to terminal relocation of neutrophils back to the BM (Martin et al., 2003; Furze and Rankin, 2008). Complementary to our finding of increased CXCR4 expression on rTEM neutrophils in the lung vasculature, Wang *et al*., detected increased CXCR4 on reverse migrated neutrophils in the lungs, in their model. In addition, through use of a CXCR4 antagonist, the number of PA neutrophils was increased in the lung but decreased in the BM (Wang et al., 2017). Overall, these findings suggest that CXCR4 could be important in homing of reversing cells from the lung back to the BM. Collectively, our data highlight key similarities between rTEM and rIM + rTEM neutrophils. Therefore, we propose that initially, after neutrophils reverse migrate, they are transported into the lungs during the acute phase of the reaction where they exhibit a typically pro-inflammatory/permeability phenotype. Then, during their increased retention time within the lung vasculature, the neutrophils may switch to a resolving phenotype, characterised by decreased pro-inflammatory markers, and increased CXCR4 expression, thus facilitating their terminal relocation to the BM at a later time-point (24 hr+).

7.1.4. Investigating the role of neutrophil-derived TNF and TNFRI/II in acute inflammation

Following a previous publication by our team, demonstrating that neutrophil-derived TNF is responsible for the initial vascular leakage induced by LTB_4 (Finsterbusch et al.,

2014), we sought to explore the role of neutrophil-derived TNF and TNFRs as mediators of neutrophil rTEM. To this end, we initiated an ambitious programme aimed at generating and validating a novel mouse line exhibiting a selective neutrophil TNF deficiency (neutrophil-selective TNF^{KO}; Neutro-TNF^{KO}). In addition, we sought to generate and investigate a chimeric haematopoietic-derived cell (HDC)-*TNFRI/II*^{KO} (TNFRI/II KO-BM->-WT) mouse model.

To generate the Neutro-TNF^{KO} line, we first crossed MRP8-Cre and TNF *loxP* floxed GM lines (Kim et al., 2018). MRP8 is an essential component of the anti-bacterial protein calprotectin that is mostly expressed by neutrophils, thus limiting the functional deletion of the TNF gene to this cell type. Genomic validation by PCR revealed that only Neutro-TNF^{KO} mice contained that *Cre* transgene (**Fig. 6.3A-B**). Additionally, flow cytometry of LPS-stimulated cells revealed that the majority of peripheral blood neutrophils were deficient in TNF (**Fig. 6.4A-C**). Moreover, we found deletion of TNF in ~20% of peripheral monocytes. This is in accordance with the literature whereby MRP8 has been shown to be expressed during early monocyte development (Elliott et al., 2011; Abram et al., 2014; Csepregi et al., 2018). Whilst a monocyte-TNF deficiency could be cause for concern in terms of determining the effects of neutrophil derived-TNF, our inflammatory models are acute reactions characterised by a disruption of endothelial integrity and leukocyte migration, mediated predominantly by neutrophils but not monocytes (McDonald et al., 2010; Lämmermann et al., 2013; Finsterbusch et al., 2014). Having said that, it would be essential to rule out the potential contribution of monocytes in any noted phenotypes (section 7.2.3.4). Unfortunately, whilst our results suggest the successful generation of the Neutro-TNF^{KO} line, due to time and resource constraints we did not extend these mice to analysis of inflammatory models.

The project also generated chimeric TNFRI/II KO-BM->-WT and control WT chimeric mice (*WT*-BM->-WT), in which BM from donor global *TNFRI/II*^{KO} or WT mice respectively, were injected i.v. into irradiated *LysM-EGFP*$^{ki/+}$ or WT recipient mice. Both chimeric animals, exhibited comparable reconstituted neutrophil blood counts at 6 weeks post-BM transplant (**Fig. 6.5C**). Interestingly, following IR-injury of the cremaster muscle, TNFRI/II KO-BM->-WT mice exhibited a complete loss of a vascular leakage response (**Fig. 6.6A**) and a significant (~40%) reduction in total neutrophil extravasation with respect to *WT*-BM->-WT control mice (**Fig. 6.6B-C**). Collectively, these experiments

suggest a critical role for neutrophil-TNFRI/II in the induction of vascular leakage and neutrophil migration. Finsterbusch *et al*., previously provided evidence that following LTB_4 stimulation, neutrophil-derived TNF signalling was fundamental in driving the vascular leakage response post leukocyte-EC adhesion (Finsterbusch et al., 2014). Together with our observations, it would appear that the assumed release of neutrophil-derived TNF alone during IR-injury, is not sufficient to induce vascular leakage. Therefore, it could be hypothesised that once released, TNF acts in an autocrine/paracrine manner *via* neutrophil-TNFRs to amplify the synthesis and release of neutrophil-derived pro-permeability factors such as ROS, LTB_4, VEGF, HBP as well as TNF, whereby the latter three are preformed and stored in neutrophil granules (Beil et al., 1995; Borregaard et al., 2007; Gong and Koh, 2010). This suggests the existence of a permeability threshold, whereby a minimum concentration of pro-permeability factors is required to induce a vascular leakage response. Indeed, autocrine and/or paracrine TNF-TNFR signaling has previously been reported for a number of immune cell types, including monocytes and macrophages (Lombardo et al., 2007; Caldwell et al., 2014), but most importantly also for neutrophils. In the latter case, neutrophil TNF production, as induced by TLR2 ligand stimulation, increased the synthesis of neutrophil-derived cytokines, chemokines and lipid mediators *via* TNFR1 activation (Deguine et al., 2017). This included the production of additional TNF, as well as CCL3, CCL4, CXCL1, CXCL2, LTB_4 and PGE_2. However, in this study amplification by TNF-TNFRI/II began at 90 min post zymosan-stimulation and peaked at 240 min, whereas we have shown that IR-injury-induced permeability occurs within a few min post reperfusion (see Chapter 3). Hence, it is possible that in our reaction, a lack of HDC-TNFRs prevents neutrophil degranulation, known to be induced by TNF (Richter et al., 1990). This would also be consistent with a lack of availability of preformed pro-permeability factors such as HBP (Borregaard et al., 2007) and VEGF (Gong and Koh, 2010; Zhou et al., 2017), which as suggested, may be required to surpass the 'permeability threshold'.

A deficiency in neutrophil degranulation may also explain our observed partial defect in the neutrophil extravasation response. Neutrophil TEM, in part, is mediated by surface molecules CD11b and LFA-1 that are known to be pre-formed in specific, gelatinase and secretory granules/vesicles, where they are released upon neutrophil activation (Borregaard et al., 2007). A defect in neutrophil extravasation is hence consistent with

a potential downregulation of CD11b and LFA-1, both of which are known to mediate TNF-induced leukocyte crawling and migration (Sumagin et al., 2010). Neutrophil migration would likely therefore be predominantly mediated by TNF-independent mechanisms, namely by PECAM-1, ICAM-2, JAM-A and ESAM (Nourshargh et al., 2006; Huang et al., 2006; Woodfin et al., 2009; Wegmann et al., 2006), however this hypothesis would require further investigations, initially looking at the surface expression of CD11b and LFA-1 (section 7.2.4).

Another potential explanation for our observed loss of vascular leakage and partial defect in neutrophil extravasation responses could be an initial absence of preformed TNF in neutrophil intracellular stores. Finsterbusch et al., previously showed that following neutrophil-EC interactions, preformed neutrophil-derived TNF is released and mediates LTB_4-induced permeability (Finsterbusch et al., 2014). Hence similar to their use of HDC-TNF^{KO} chimeras, the absence of preformed stores in our HDC-TNFRI/II^{KO} chimeras would result in the loss of TNF-induced vascular leakage. If correct, this would imply that HDC-TNFRI/II contribute to the development of intracellular TNF stores during granulopoiesis. However, evaluation of this postulate based on the current literature is difficult, as little is known about how TNF is stored by neutrophils (Beil et al., 1995). This hypothesis might be directly assessed by flow cytometry to measure intracellular TNF levels under basal and/or inflammatory conditions as described by Finsterbusch et al., (section 7.2.4.2) (Finsterbusch et al., 2014). Collectively, our findings in the context of the discussed literature and proposed hypotheses provide fruitful grounds for future investigations into the role of neutrophil-derived TNF and TNFRI/II.

7.2. Open questions and future perspectives

7.2.1. Deciphering the specific mechanisms of CXCL1-mediated neutrophil rTEM

This section will discuss potential future investigations aimed at shedding greater insight into the mechanisms through which augmented distribution of CXCL1 may lead to neutrophil rTEM, as summarised in **Fig. 7.2.**

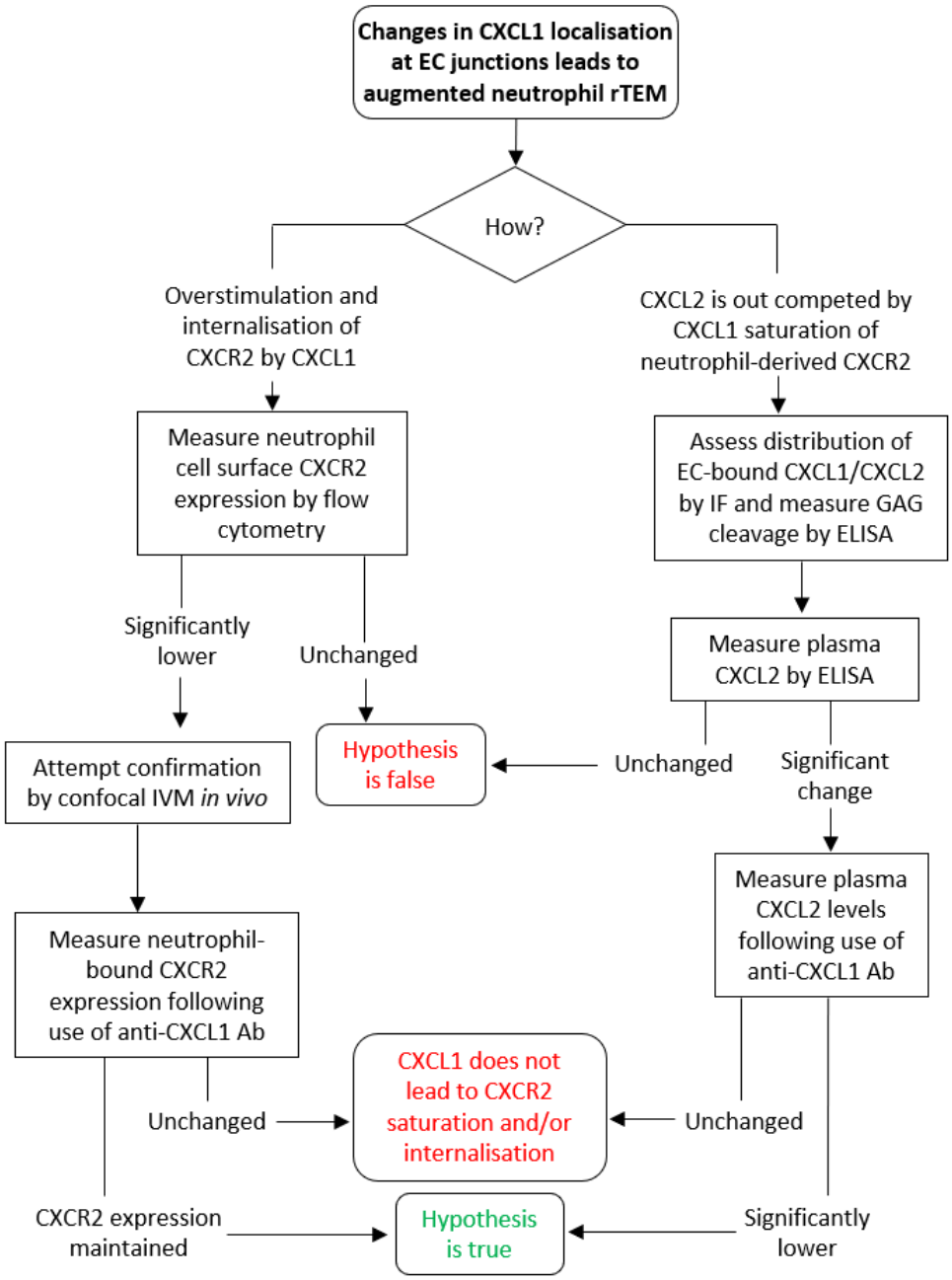

Figure 7.2. Future investigations to understand how disruption of CXCL1 mediates neutrophil rTEM. This flow diagram represents a series of proposed future investigations, extending the studies described in this thesis. See text for further details.

In this thesis, we have shown that vascular permeability induction facilitated the diffusion of tissue-generated CXCL1 through paracellular junctions into the vascular lumen and subsequently induced aberrant neutrophil TEM. However, the precise mechanisms as to how changes in CXCL1 localisation facilitate neutrophil rTEM remains unclear. To ascertain the direct regulation, expression and presentation of CXCL1, would require further investigation.

One possible explanation could be that increased diffusion of CXCL1 through EC junctions may result in excessive presentation of chemokine to its neutrophil-bound receptor, CXCR2, leading to its saturation and/or hyperactivation followed by receptor internalisation. Thus, potential internalisation of CXCR2 on rTEM neutrophils could be assessed by confocal IVM using commercially available fluorescently conjugated antibodies for CXCR2 (Haarmann et al., 2019). Additionally, flow cytometry could be employed to compare CXCR2 expression levels on strept-AF647^{+} vs. strept-AF647^{-} neutrophils isolated from the blood and LVWO. If a decrease in CXCR2 expression on rTEM neutrophils was identified, this may explain why these neutrophils are unable to progress into the extravascular space and instead move in a retrograde manner. Complementary to this, if excessive CXCL1 does indeed lead to CXCR2 internalisation, we may expect this augmented expression to be prevented following prophylactic treatment with an anti-CXCL1 Ab.

As binding of CXCL2 to its receptor is known to facilitate neutrophil TEM (Girbl et al., 2018), an alternative hypothesis could be that excess of CXCL1 in proximity to the migrating neutrophil may result in saturation of CXCR2, and consequently reduce and/or block receptor availability for CXCL2. If this is the case, we may detect enhanced levels of unbound CXCL2 in the plasma, a response that could be measured by ELISA. Additionally, we could compare the junctional presentation of CXCL1 and CXCL2 under inflammatory conditions that induce, or fail to induce, neutrophil rTEM by IF using fluorescently labelled anti-CXCL1 and anti-CXCL2.

Lastly, it would be useful to investigate other potential mechanisms that could account for elevated plasma CXCL1 levels following hyper-permeability induction. For example, we could assess the potential contribution of GAGs in retention of CXCL1 and hence assess its cleavage from EC membranes. GAGs are readily cleaved under certain

inflammatory conditions (Key et al., 1992; Crijns et al., 2020) and therefore their absence from the EC surface/junction may disrupt presentation of chemokines and thus directional cues for neutrophil migration. This question could be addressed by measuring cleaved GAGs using a commercially available ELISA kit to detect heparan sulfate (Rees et al., 2010) (i.e. GAGs known to retain CXCL1 and CXCL2) (Crijns et al., 2020), or *via* IF staining of CXCL1 on ECs, to determine if there are different levels and/or localisation of CXCL1 following models of vascular leakage. If evidence for GAG cleavage is obtained, the effect of GAG cleavage inhibitors (e.g. non-anticoagulant heparins, a heparanase inhibitor (Cassinelli et al., 2020)) on CXCL1 plasma levels and neutrophil rTEM could be investigated.

7.2.2. Understanding the pathophysiological relevance of rTEM neutrophils for the identification of novel therapeutic targets

This section will discuss potential future investigations regarding the characterisation of rTEM neutrophils and their pathophysiological impact, beyond the findings of this thesis as summarised in **Fig. 7.3** and described in more detail in sections 7.2.2.1 – 7.2.2.4.

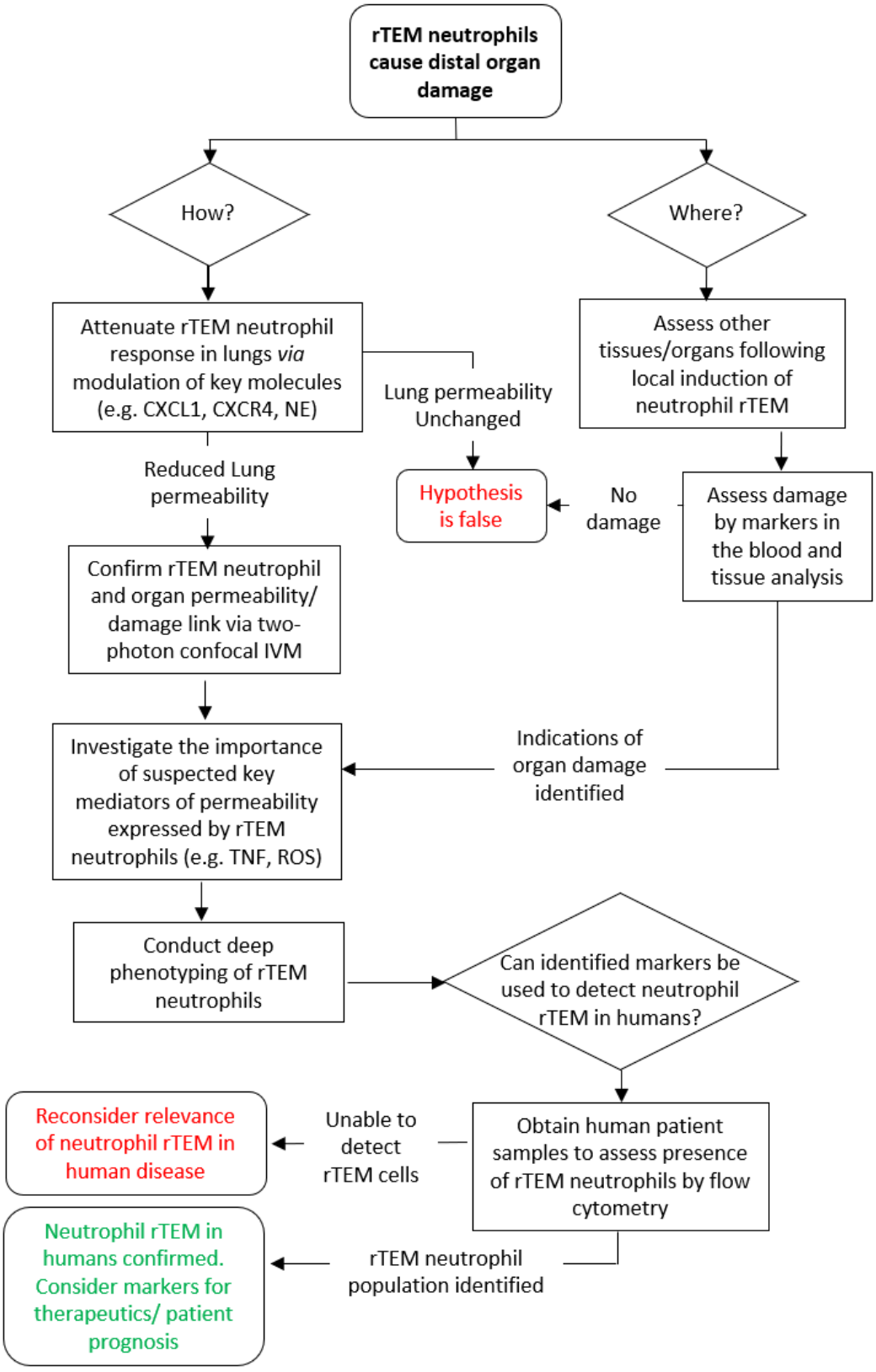

Figure 7.3. Future work to characterise rTEM neutrophils and their (patho)physiological impact. This flow diagram represents a series of proposed future investigations beyond completion of the work described in this thesis, as further described in sections 7.2.2.1 – 7.2.2.4.

7.2.2.1. How do rTEM neutrophils cause secondary organ vascular leakage/damage?

In Chapter 5, reverse transmigrating neutrophils were shown to be enriched in the lung vasculature where they displayed a pro-inflammatory phenotype characterised by higher cell surface expression of CD11b, ICAM-1, β1-integrin, CXCR4 and NE. As discussed in section 7.1.3, these molecules are known markers of neutrophil activation (ICAM-1), adhesion & TEM (CD11b & β1-integrin), lung margination (CXCR4) and vascular damage (NE) (Sumagin et al., 2010; Devi et al., 2013; Nourshargh and Alon, 2014). However, the precise mechanism(s) as to how reverse transmigrating neutrophils are retained in the lung vasculature, and more importantly, how they may induce vascular leakage requires further investigations.

To confirm definitively that rTEM neutrophils are responsible for pulmonary leakage/damage, we could seek to attenuate the impact of rTEM neutrophils. Firstly, as we found that use of an anti-CXCL1 Ab reduced the frequency of rTEM, we could use this approach to block the induction of rTEM followed by evaluation of the pulmonary vascular leakage response. Next, based on our initial phenotypic analysis of rTEM neutrophils, we hypothesise that CXCR4 may mediate margination of rTEM neutrophils in the lung vasculature. To address this, we could use pharmacological inhibitors of CXCR4 (Gaur et al., 2018). Complementary to this, we could measure the level of CXCL12, the ligand of CXCR4, from isolated lung tissue where CXCL12 has been shown to be upregulated under inflammatory conditions (Devi et al., 2013; Li et al., 2020). Lastly, we hypothesise that rTEM neutrophil-derived NE may be responsible for the observed pulmonary vascular leakage. This could be directly assessed *via* the use of commercially available NE inhibitors or NE^{KO} mice (Colom et al., 2015; Voisin et al., 2019), which if the hypothesis is correct would reduce the onset of damage to the endothelium. Targeting ICAM-1, CD11b or β2-integrins should be avoided as this may adversely affect neutrophil migration. Experimentally, a prophylactic i.v. injection of the aforementioned antagonists/inhibitors could be used in the inflammatory reactions of IL-1β + histamine or IR-injury in combination with our neutrophil rTEM tracking strategy (Chapter 5). Lung permeability could then be assessed in extracted tissues using an i.v. injection of fluorescent microspheres as detailed in Owen-Woods et al (Owen-Woods et al., 2020). This could then be correlated with the number of strept-$AF647^{+}$ neutrophils detected in

LVWOs at 2 hr, as assessed by flow cytometry. This approach could be extended to using two-photon confocal microscopy. Here, this would facilitate real-time imaging of the lung vasculature following local induction and tracking of rTEM neutrophils, thus allowing for visualisation of the arrival of rTEM neutrophils and the onset of vascular leakage. Such an approach would allow identification of the optimal time point to collect rTEM neutrophils from LVWOs to gain a more representative picture of the rTEM phenotype at the relevant time of vascular leakage induction.

In addition to the phenotyping performed in Chapter 5, we could look at other known neutrophil-derived pro-permeability factors, such as ROS, as suggested by Buckley et al., and Woodfin et al., (Buckley et al., 2006; Woodfin et al., 2011). To assess the intracellular neutrophil production of ROS, LVWO could be collected and incubated *ex vivo* with a ROS probe such as dihydrorhodamine (DHR). This probe is predominantly oxidised by superoxide radicals to produce the fluorescent product, 2-hydroxyethidium, hence, the greater ROS production the greater the fluorescent signal. This could then be analysed by flow cytometry to allow for a direct comparison between streptavidin^{-} and streptavidin^{+} neutrophils.

Another neutrophil-derived factor that could mediate vascular leakage is TNF, previously shown to be expressed in close proximity to ECs prior to transmigration (Finsterbusch et al., 2014). Thus, an interesting avenue of research would be to assess whether rTEM neutrophils express higher levels of TNF. For this purpose, Neutro-TNF^{KO} mice (validated in Chapter 6) could be used in inflammatory models that elicit rTEM to assess the contribution of TNF derived from rTEM neutrophils to remote organ damage. However, while antibodies are available to look at surface TNF expression, maintaining retention of TNF after extraction from the mouse remains difficult as TNF can be readily cleaved at the cell surface by the enzyme, TACE (Moss et al., 2008). Inhibition of TNF release could be achieved through the use of TACE-inhibitors (Wong et al., 2016), or commercially available iRhom2 KO mice. iRhom2, known to be expressed by neutrophils, is an essential shuttle protein that transports TACE (Adrain et al., 2012). If TNF derived from reverse migrating neutrophils is responsible for the vascular leakage in the lung, then it would be expected that absence of soluble/released TNF would suppress or reduce this lung vascular dysfunction. These experiments could be complemented by quantifying surface TNF expression on rTEM neutrophils.

7.2.2.2. Deeper exploration into the phenotype of rTEM neutrophils to identify novel therapeutic targets

With a better understanding of the expression profile of rTEM neutrophil in different tissues, future investigations can begin to suggest potential novel anti-inflammatory therapeutic strategies. For example, our current profiling revealed that rTEM neutrophils found in the lung express high levels of NE, a serine protease strongly linked to numerous acute lung diseases such as ALI (Dushianthan et al., 2011; Colom et al., 2015). As such, NE inhibitors have previously been used in the clinical setting to treat NE-induced lung injury (Polverino et al., 2017). Not only could our work help inform the wider impact of these inhibitors but they can also be used as a basis to better understand their mechanisms and hence their use. Use of flow cytometry provided insight into the phenotype of rTEM neutrophils but with this approach only a limited number of markers were assessed. Expanding the analysis of rTEM neutrophil phenotype could be achieved using time-of-flight mass cytometry (CyTOF), to enable deep phenotyping of reverse migrating neutrophils. CyTOF works on a similar principle to the flow cytometry employed in the thesis, however antigens are alternatively labelled with Abs conjugated to unique metal isotopes. Once labelled, cells are processed and analysed by mass spectrometry where the presence and abundance of the metal ion signal is used as a marker of antigen expression. Through this method, up to 40 different antigens can be detected simultaneously, enabling deeper understanding of the rTEM neutrophil phenotype. This technique has been used previously to assess the phenotype of leukocytes in human patients suffering from cancer and rheumatoid arthritis (Goldman et al., 2019; Leite Pereira et al., 2019). For example, Leite Pereira et al., demonstrated the power of this technique by examining 34 different makers on leukocytes, facilitating the identification of two potentially new subpopulation of neutrophils and T-cells. To further characterise rTEM neutrophils, we could assess potential changes at the level of transcription. This can be addressed following isolation of rTEM neutrophils by flow cytometry and subsequent analysis by single cell RNA-sequencing. Furthermore, as this can identify changes at the level of a single cell this may provide insight into the heterogeneity of this cell population (Haque et al., 2017).

7.2.2.3. Do rTEM neutrophils disseminate to other secondary organs and do they exhibit the same phenotype/pathogenic function?

In Chapter 5, neutrophils that have undergone rTEM were tracked into the peripheral circulation, lung vasculature followed by the BM at a later time-point. In the lung, they were identified to exhibit a pro-inflammatory phenotype as shown by enhanced surface expression levels of CD11b, ICAM-1, β1-integrins, CXCR4 and NE. However, it remains unknown whether reverse transmigrating neutrophils are retained and exhibit a similar pro-inflammatory phenotype in other key organs such as the liver, kidneys, heart and brain. This could be assessed by detecting the presence and phenotype of fluorescently labelled strept-AF647^{+} cells in these organs by flow cytometry as described in Chapter 5, or alternatively, tissue samples could be collected and processed for confocal microscopy. Furthermore, the potential pathophysiological consequences of rTEM neutrophils in these organs could be assessed following i.v. injection of fluorescent microspheres and subsequent analysis of the relevant tissues. Lastly, damage/dysfunction of specific tissues could be assessed by measurement of certain proteins in the blood. For example, tissue damage is often associated with elevated levels of non-specific markers, including c-reactive protein (Pepys and Hirschfield, 2003) and lactate dehydrogenase (Guzmán-de la Garza et al., 2013). In addition, levels of tissue specific markers, for example, troponin (heart) (Maynard et al., 2000), and aspartate aminotransferase and alanine aminotransferase (liver) (Guzmán-de la Garza et al., 2013), could be quantified.

7.2.2.4. Can phenotypic markers aid in the detection of rTEM neutrophils in humans and act as a prognosis marker?

Detection of reverse migrating neutrophils has proved difficult to translate towards humans. In part, this is due to the limited understanding of their phenotype and fate, rendering it challenging to know where to look for these cells and how to differentiate them from other neutrophils. Investigations discussed in Chapter 5 provided insight into the fate and phenotype of reverse transmigrating neutrophils and may thus form the basis for development of a bio-marker detection strategy. Phenotyping of rTEM neutrophils in humans has so far been limited to *in vitro* investigations. Here, Buckley et

al., identified rTEM neutrophils to be ICAM-1^{high} and interestingly they detected a population of ICAM-1^{high} neutrophils in the blood of patients suffering with chronic inflammatory disorders. This is complementary to the findings presented here and with those of Woodfin et al., where increased expression of ICAM-1 was detected on rTEM neutrophils in the blood and lung vasculature. However, the reported changes in ICAM-1 expression are subtle and may not represent the optimal marker for detection of rTEM neutrophils. This may be improved *via* deep phenotyping of this sub-population as discussed previously (section 7.2.2.2). Of note, since we detected increased levels of rTEM post IR-injury, a representative model of an insult incurred during pathologies such as trauma and organ transplantation, detection of rTEM in blood samples of such patients could potentially serve as a prognosis marker to predict the risk of developing secondary organ damage.

7.2.3. Deciphering the role of neutrophil-derived TNF in models of acute inflammation

The next two sections will discuss future work that could build upon the initial but potentially exciting findings of Chapter 6. These experiments will encompass characterising the role of neutrophil-derived TNF during the early acute phase of IR-injury, as summarised in **Fig. 7.4** and described in more detail in sections 7.2.3.1 – 7.2.3.4.

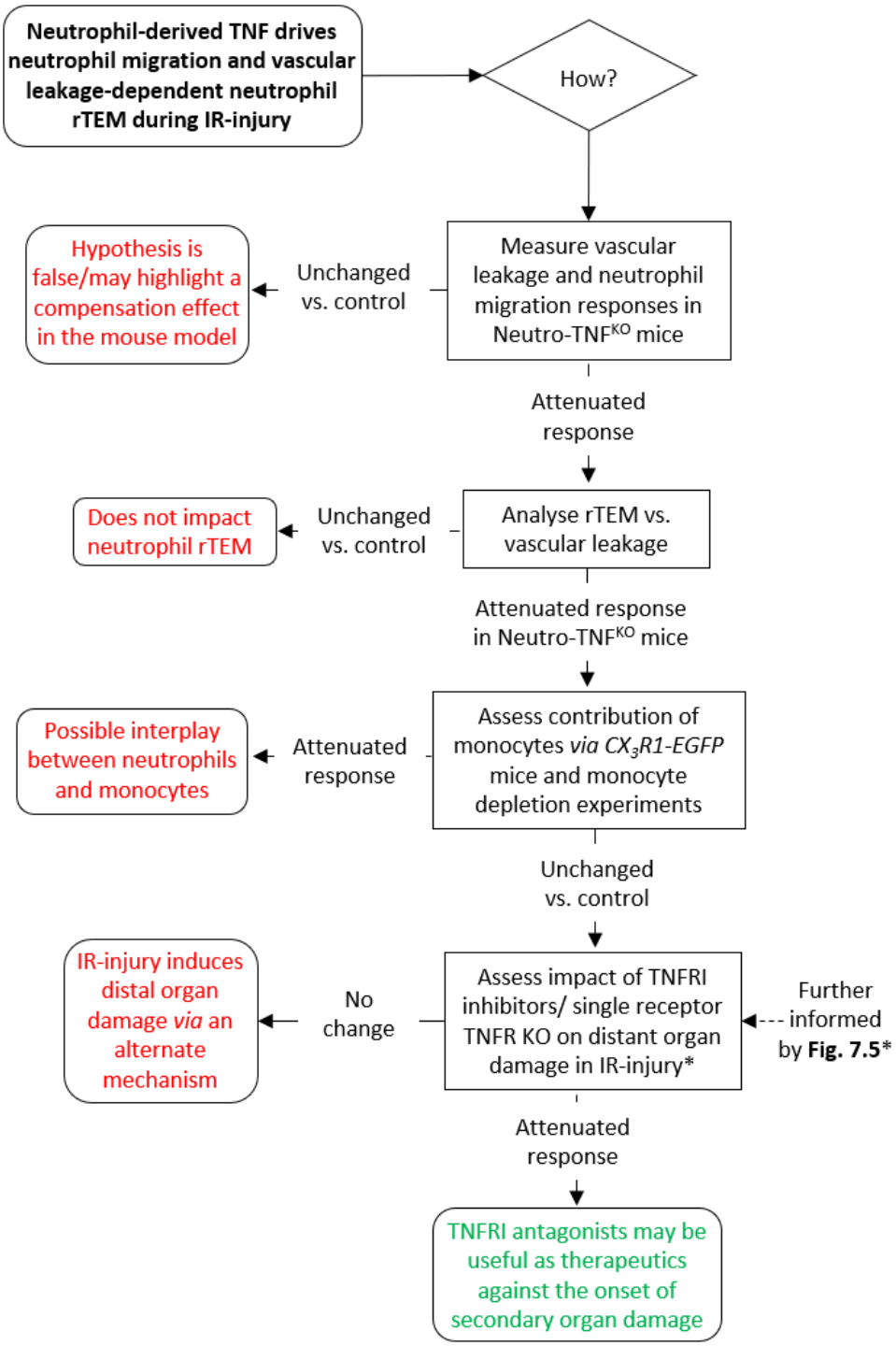

Figure 7.4. Future investigations into the role of neutrophil-derived TNF during the early acute phase of IR-injury. These experiments and concepts are further developed in sections 7.2.3.1 – 7.2.3.2. *Of note, highlighted experiments are also informed by TNFR studies summarised in **Fig. 7.5** and detailed in section 7.2.4.3.

7.2.3.1. Does neutrophil-derived TNF play a role in IR-mediated acute inflammatory responses?

Previous studies from our team (Finsterbusch et al., 2014) provided the first evidence that neutrophil-derived TNF is a key regulator of microvascular plasma leakage following induction of inflammation by neutrophil chemoattractants such as LTB_4, C5a and KC. However, whilst there is ample indirect evidence to illustrate the ability of neutrophil derived-TNF to induce microvascular leakage, direct verification is lacking. This led us to generate the selective neutrophil-TNF deficient mouse model, Neutro-TNF^{KO} (Chapter 6). This novel line could be used to provide direct evidence for the role of neutrophil-derived TNF in mediating vascular leakage, for example, following IR-injury. Experimentally, vascular leakage could be evaluated in multiple organs using the Evans blue assay in Neutro-TNF^{KO} mice. However, for real-time analysis of the leakage response, the TRITC-dextran strategy developed in Chapters 3 and 4 using confocal IVM of the cremaster muscle could be employed.

Furthermore, our group has previously shown that neutrophil rTEM during IR-injury is mediated by JAM-C cleavage at EC junctions (Woodfin et al., 2011). However, stabilisation of JAM-C only led to a partial inhibition of neutrophil rTEM. Since TNF is a key player in vascular permeability induction (Finsterbusch et al., 2014) and enhanced vascular leakage can lead to enhanced neutrophil rTEM in IR-injury (Owen-Woods et al., 2020), we hypothesise that neutrophil-derived TNF contributes to the induction of neutrophil rTEM during IR-injury. Application of confocal IVM, as stated above, would allow for simultaneous investigations into the impact on vascular permeability and neutrophil rTEM.

7.2.3.2. Does monocyte-TNF play a role in any identified phenomena?

MRP8 is expressed primarily by neutrophils but also by approximately 20% of monocytes, allowing for conditional deletion of floxed alleles in these two leukocyte populations (Abram et al., 2014). To directly associate any observed phenotype to the contribution of neutrophil-derived TNF it would be essential to understand the role of monocytes during early acute inflammation. Firstly, commercially available *CX_3R1-EGFP*

mice (Jung et al., 2000) could be used to specifically track monocytes *in vivo*, to assess their recruitment responses during the early phase of acute inflammation. Secondly, this could be followed by monocyte depletion experiments using an anti-CCR2 Ab (MC-21) (Mack et al., 2001; Hammond et al., 2014) to assess if the prospective phenotype of enhanced vascular leakage and neutrophil rTEM is monocyte-dependent. These experiments would also utilise the TRITC-dextran and confocal IVM strategy to evaluate neutrophil migratory dynamics and vascular leakage responses.

7.2.4. Understanding the role of HDC-TNFRI/II in vascular leakage and neutrophil extravasation during acute inflammation

This section will discuss additional future investigations stemming from Chapter 6 into the role of HDC-TNFRs. These investigations that are complementary to works detailed in section 7.2.3 would further our understanding of how TNF mediates the early acute phase of IR-injury, as summarised in **Fig. 7.5**, and detailed in sections 7.2.4.1 – 7.2.4.3.

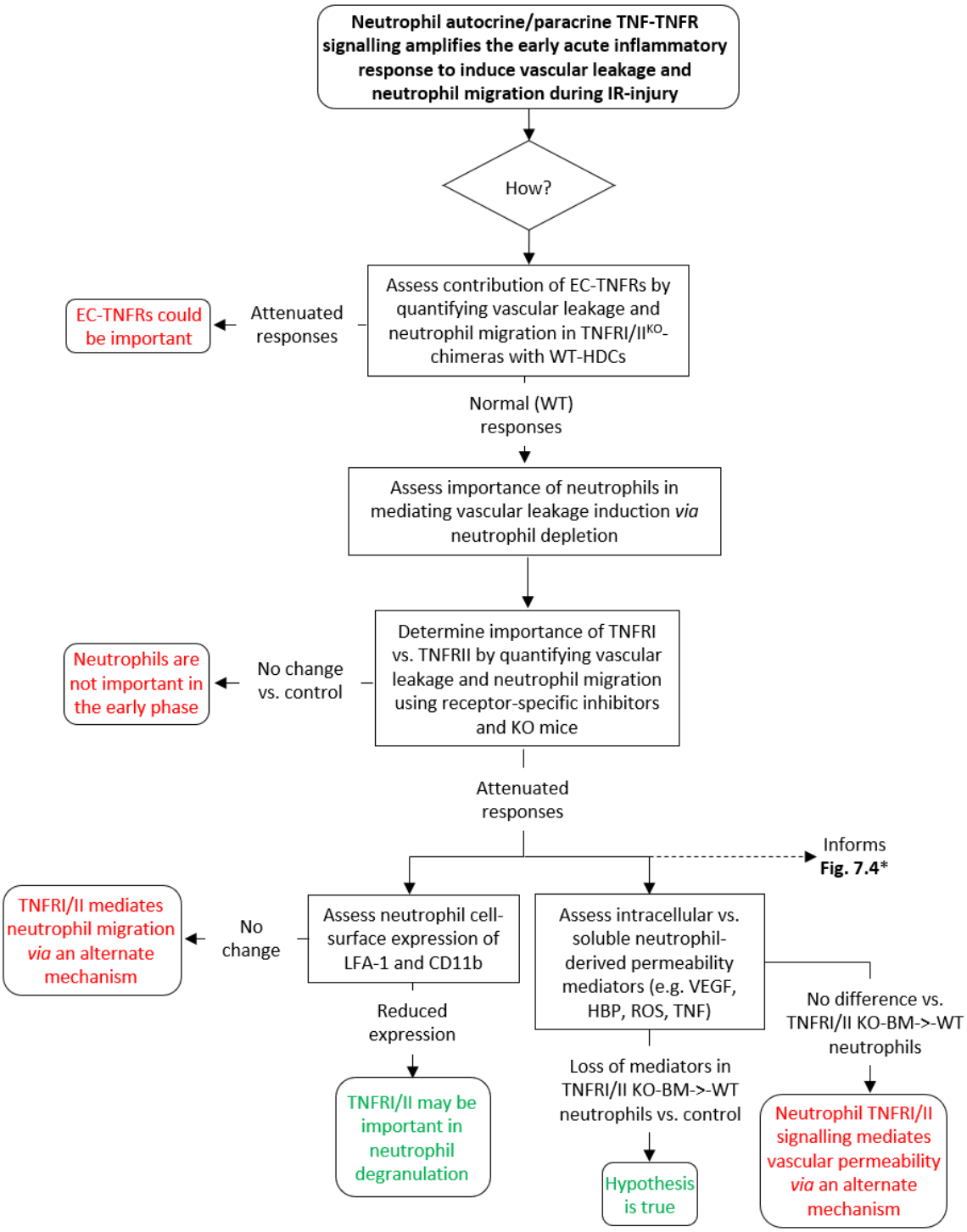

Figure 7.5. Future investigations into the role of HDC-TNFRs during the early acute phase of IR-injury. These experiments and concepts are further developed in sections 7.2.4.1 – 7.2.4.3. *Of note, highlighted experiments also inform the proposed investigations summarised in **Fig. 7.4** and detailed in section 7.2.4.3.

7.2.4.1. How does an absence of HDC-TNFRI/II result in a defect in leukocyte extravasation?

In Chapter 6, preliminary investigations identified a role for HDC-TNFRI/II in neutrophil extravasation and vascular leakage. However, to definitively determine the origin of this defect in neutrophil extravasation, further exploration would be required. As TNFRI is considered to be a predominately pro-inflammatory receptor, we hypothesise that loss of this receptor would lead to a similar defect in extravasation by reduced degranulation (Richter et al., 1990). To address, experiments could be conducted to explore the individual contribution of each TNFR on HDCs in driving neutrophil TEM. This could be assessed *via* the generation of chimeric animals, whereby WT mice are reconstituted with BM from *TNFRI*^{KO} or *TNFRII*^{KO} mice. To support these experiments, selective TNFRI (Zhang et al., 2020) or TNFRII (Torrey et al., 2017; Shaikh et al., 2018) inhibitors could be used.

Next, neutrophil migration is known to be dependent on chemotactic cues and presentation of neutrophil-surface molecules (Ley et al., 2007; Girbl et al., 2018). As one of our hypothesis involved a defect in degranulation (see Chapter 6, or section 7.1.4), flow cytometry could be used to assess neutrophil cell surface expression of β2-integrins following degranulation, which are involved in mediating neutrophil migration (Chapter 1, section 1.5 & 1.6) (Sumagin et al., 2010). For this purpose, blood samples could be collected at 30 min intervals during the 2 hr reperfusion period of an IR reaction. If the aforementioned hypothesis is correct, then it should be expected that some of these markers would be downregulated.

7.2.4.2. Is the vascular leakage response during IR-injury dependent on HDC-TNFRI/II?

If our hypothesis of TNF-TNFR autocrine/paracrine signal amplification is correct (section 7.1.4), then it would be expected that TNFRI/II KO-BM->-WT mice would secrete reduced levels of pre-formed pro-permeability mediators including TNF, VEGF and HBP, with reduced levels of *de novo* synthesised ROS and LTB_4. To examine this, it would be useful to determine the presence of intracellular vs. soluble levels of TNF by flow cytometry and ELISA, respectively (Finsterbusch et al., 2014), for both TNFRI/II KO-BM->-WT and *WT*-BM->-WT mice following stimulation by IR-injury. Similar experiments

could also be performed to look at neutrophil-derived HBP (Olofsson et al., 1999; Tapper et al., 2002) and VEGF (Gaudry et al., 1997; Krause et al., 2014). In addition, blood levels of mediators such as LTB_4 could be assessed by ELISA using samples collected throughout the 2 hr reperfusion period, while ROS could be detected using fluorescent probes by flow cytometry as described in section 7.2.2.1. Complimentary to this, if neutrophil-derived TNFRs are required for the release of pre-formed pro-permeability factors, then we may expect that vascular leakage induction following neutrophil depletion during IR-injury would be the same as that noted in TNFRI/II KO-BM->-WT chimeric mice. Hence, to assess this, neutrophil depletion experiments could be conducted during IR-injury using a high dose of anti-Ly6G Ab (e.g. 150 µg) to specifically target neutrophils (Pollenus et al., 2019).

Secondly, to directly address the importance of EC-derived TNFRs on the vascular leakage response chimeric mice expressing WT-HDCs and TNFRI/II^{KO} ECs would be expected to have comparable leakage response to those of WT mice if the vascular leakage response is purely mediated by HDC-TNFRs as indicated in Chapter 6.

7.2.4.3. Could selective blockade of TNFRI be therapeutically advantageous and prevent the development of secondary organ damage?

Currently, the predominant treatment for regulating pulmonary inflammatory disorders such as ALI in humans revolves around the use of blocking anti-TNF Ab (Raghavendran et al., 2008). A systemic inhibition of TNF and/or its respective receptors can however result in undesirable side effects due to its pivotal role in many biological functions (Horiuchi et al., 2010). Of note, TNFRI is generally considered to predominantly mediate pro-inflammatory effects, as opposed to the typically anti-inflammatory properties of TNFRII (Naudé et al., 2011; Cabal-Hierro and Lazo, 2012; Holbrook et al., 2019). As such, it has been hypothesised that blocking both receptors may result in loss of TNFRII-mediated attenuation of apoptotic activity and its role in promoting cell survival and proliferation (Proudfoot et al., 2018). This mandates the development of more selective therapy options. Recently, the therapeutic benefits of TNFR antagonists have been considered as a prophylactic treatment, whereby treatment with a selective TNFRI inhibitor has been used to combat pulmonary oedema as induced by inhaled LPS in non-

human primates (NHP) and in healthy humans (Proudfoot et al., 2018). Here, they observed reduced pulmonary vascular oedema in both species that received the pre-treatment. Furthermore, if neutrophil-derived TNF is identified as a key driver of IR-mediated secondary organ damage, as induced by disseminated rTEM neutrophils, then selective inhibition of TNFRI pathway could be therapeutically advantageous in preventing the onset of vascular oedema. Auxiliary investigations could be performed using TNFRI-/ TNFRII-specific inhibitors or *via* the use single receptor KO (*TNFRI*^{KO} & *TNFRII*^{KO}) mice, as described in section 7.2.4.1, to assess if TNFRI does indeed mediate these responses.

7.3. Concluding remarks

Acute inflammation is a fundamental innate process following infection and sterile injuries. Depending on the severity of inflammation, secondary pathologies can develop and adversely affect prognostic outcomes. This thesis has revisited two established features of inflammation, namely, vascular leakage and neutrophil migration. The findings provide comprehensive evidence for enhanced microvascular leakage in disrupting chemotactic directional cues that drive retrograde migration of neutrophils back into the circulation. Importantly, through the development of a novel methodology for exclusive labelling and tracking of rTEM neutrophils, the findings reveal that these neutrophils exhibit an activated phenotype in the blood that is further exacerbated in the lung vasculature where they accumulate and their presence is associated with sites of vascular damage (**Fig. 7.6**). This methodological advancement offers the first approach for labelling and tracking of rTEM neutrophils, facilitating direct insight into their phenotype and fate. Finally, the work identified crucial roles for HDC-TNFRs in both vascular permeability and neutrophil migration during IR-injury. Collectively, these results suggest that antagonism of CXCL1, CXCR2 or possibly NE could be therapeutically advantageous to prevent the onset of secondary organ damage, and provides a plausible basis for further investigations into the pathophysiological relevance of neutrophil rTEM.

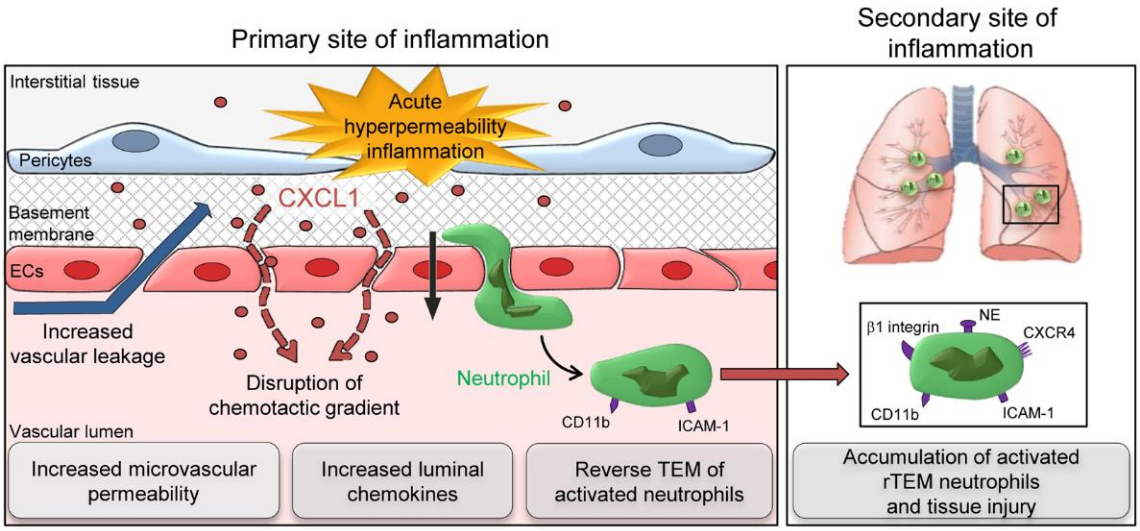

Figure 7.6. A working schematic presenting the proposed mechanism of how permeability regulates neutrophil TEM. Neutrophils that undergo rTEM in the cremaster muscle following models of hyper-permeability travel in the blood and exhibit increased retention in the lung vasculature. In the blood, these cells exhibit a pro-inflammatory phenotype which is further exacerbated in the lung vasculature, where they contribute to secondary organ damage. Figure reproduced from Owen-Woods et al., 2020.

8. References

Abram, C.L., and C.A. Lowell. 2013. The Ins and Outs of Leukocyte Integrin Signaling. *Annu. Rev. Immunol.* 185:974–981. doi:10.1038/mp.2011.182.doi.

Abram, C.L., G.L. Roberge, Y. Hu, and C.A. Lowell. 2014. Comparative analysis of the efficiency and specificity of myeloid-Cre deleting strains using ROSA-EYFP reporter mice. *J. Immunol. Methods*. 408:89–100. doi:10.1016/j.jim.2014.05.009.

Adrain, C., M. Zettl, Y. Christova, N. Taylor, and M. Freeman. 2012. Tumor necrosis factor signaling requires iRhom2 to promote trafficking and activation of TACE. *Science.* 335:225–228. doi:10.1126/science.1214400.

Adrover, J.M., C. del Fresno, G. Crainiciuc, M.I. Cuartero, M. Casanova-Acebes, L.A. Weiss, H. Huerga-Encabo, C. Silvestre-Roig, J. Rossaint, I. Cossío, A. V. Lechuga-Vieco, J. García-Prieto, M. Gómez-Parrizas, J.A. Quintana, I. Ballesteros, S. Martin-Salamanca, A. Aroca-Crevillen, S.Z. Chong, M. Evrard, K. Balabanian, J. López, K. Bidzhekov, F. Bachelerie, F. Abad-Santos, C. Muñoz-Calleja, A. Zarbock, O. Soehnlein, C. Weber, L.G. Ng, C. Lopez-Rodriguez, D. Sancho, M.A. Moro, B. Ibáñez, and A. Hidalgo. 2019. A Neutrophil Timer Coordinates Immune Defense and Vascular Protection. *Immunity*. 50:390-402.e10. doi:10.1016/j.immuni.2019.01.002.

Al-Sadi, R., S. Guo, K. Dokladny, M.A. Smith, D. Ye, A. Kaza, D.M. Watterson, and T.Y. Ma. 2012. Mechanism of Interleukin-1β induced-increase in mouse intestinal permeability in vivo. *J. Interf. Cytokine Res.* 32:474–484. doi:10.1089/jir.2012.0031.

Alon, R., S. Chen, K.D. Puri, E.B. Finger, and T.A. Springer. 1997. The kinetics of L-selectin tethers and the mechanics of selectin- mediated rolling. *J. Cell Biol.* 138:1169–1180. doi:10.1083/jcb.138.5.1169.

Alon, R., R. Hershkoviz, E.A. Bayer, M. Wilchek, and O. Lider. 1993. Streptavidin blocks immune reactions mediated by fibronectin-VLA-5 recognition through an Arg-Gly-Asp mimicking site. *Eur. J. Immunol.* 23:893–898. doi:10.1002/eji.1830230419.

Andonegui, G., H. Zhou, D. Bullard, M.M. Kelly, S.C. Mullaly, B. McDonald, E.M. Long, S.M. Robbins, and P. Kubes. 2009. Mice that exclusively express TLR4 on endothelial cells can efficiently clear a lethal systemic Gram-negative bacterial infection. *J. Clin. Invest.* 119:1921–1930. doi:10.1172/jci36411.

Arbonés, M.L., D.C. Ord, K. Ley, H. Ratech, C. Maynard-Curry, G. Otten, D.J. Capon, and T.F. Teddert. 1994. Lymphocyte homing and leukocyte rolling and migration are impaired in L-selectin-deficient mice. *Immunity*. 1:247–260. doi:10.1016/1074-7613(94)90076-0.

Arnaout, M.A., B. Mahalingam, and J.-P. Xiong. 2005. Integrin Structure, Allostery, and Bidirectional Signaling. *Annu. Rev. Cell Dev. Biol.* 21:381–410. doi:10.1146/annurev.cellbio.21.090704.151217.

Ashina, K., Y. Tsubosaka, T. Nakamura, K. Omori, K. Kobayashi, M. Hori, H. Ozaki, and T. Murata. 2015. Histamine induces vascular hyperpermeability by increasing blood flow and endothelial barrier disruption in vivo. *PLoS One*. 10:1–16.

doi:10.1371/journal.pone.0132367.

Ashrafpour, H., N. Huang, P.C. Neligan, C.R. Forrest, P.D. Addison, M.A. Moses, R.H. Levine, and C.Y. Pang. 2004. Vasodilator effect and mechanism of action of vascular endothelial growth factor in skin vasculature. *Am. J. Physiol. - Hear. Circ. Physiol.* 286:946–954. doi:10.1152/ajpheart.00901.2003.

Aurrand-Lions, M., C. Lamagna, J.P. Dangerfield, S. Wang, P. Herrera, S. Nourshargh, and B.A. Imhof. 2005. Junctional Adhesion Molecule-C Regulates the Early Influx of Leukocytes into Tissues during Inflammation. *J. Immunol.* 174:6406–6415. doi:10.4049/jimmunol.174.10.6406.

Azzi, S., J.K. Hebda, and J. Gavard. 2013. Vascular Permeability and Drug Delivery in Cancers. *Front. Oncol.* 3:1–14. doi:10.3389/fonc.2013.00211.

Ballet, R., Y. Emre, S. Jemelin, M. Charmoy, F. Tacchini-Cottier, and B.A. Imhof. 2014. Blocking Junctional Adhesion Molecule C Enhances Dendritic Cell Migration and Boosts the Immune Responses against Leishmania major. *PLoS Pathog.* 10. doi:10.1371/journal.ppat.1004550.

Baluk, P., P. Bolton, A. Hirata, G. Thurston, and D.M. McDonald. 1998. Endothelial gaps and adherent leukocytes in allergen-induced early- and late-phase plasma leakage in rat airways. *Am. J. Pathol.* 152:1463–1476.

Barash, J., D. Dushnitzki, Y. Barak, S. Miron, and T. Hahn. 2003. Tumor necrosis factor (TNF)α and its soluble receptor (sTNFR) p75 during acute human parvovirus B19 infection in children. *Immunol. Lett.* 88:109–112. doi:10.1016/S0165-2478(03)00075-0.

Barreiro, O., M. Yáñez-Mó, J.M. Serrador, M.C. Montoya, M. Vicente-Manzanares, R. Tejedor, H. Furthmayr, and F. Sánchez-Madrid. 2002. Dynamic interaction of VCAM-1 and ICAM-1 with moesin and ezrin in a novel endothelial docking structure for adherent leukocytes. *J. Cell Biol.* 157:1233–1245. doi:10.1083/jcb.200112126.

Bartels, K., J. Karhausen, E.T. Clambey, A. Grenz, and H.K. Eltzschig. 2013. Perioperative Organ Injury. *Anesthesiology*. 119:1474–1489. doi:10.1097/ALN.0000000000000022.

Bates, D.O. 2010. Vascular endothelial growth factors and vascular permeability. *Cardiovasc. Res.* 87:262–271. doi:10.1093/cvr/cvq105.

Bates, D.O., and S.J. Harper. 2002. Regulation of vascular permeability by vascular endothelial growth factors. *Vascul. Pharmacol.* 39:225–237. doi:10.1016/S1537-1891(03)00011-9.

Baud, V., M. Karin, and M. Karin. 2001. Signal transduction by TNF and its relatives. *Trends Cell Biol.* 11:372–377.

Beauvillain, C., P. Cunin, A. Doni, M. Scotet, S. Jaillon, M.L. Loiry, G. Magistrelli, K. Masternak, A. Chevailler, Y. Delneste, and P. Jeannin. 2011. CCR7 is involved in the migration of neutrophils to lymph nodes. *Blood*. 117:1196–1204. doi:10.1182/blood-2009-11-254490.

Becker, D.J., and J.B. Lowe. 1999. Leukocyte adhesion deficiency type II. *Biochim. Biophys. Acta - Mol. Basis Dis.* 1455:193–204. doi:10.1016/S0925-4439(99)00071-X.

Becker, S., J. Quay, H.S. Koren, and J.S. Haskill. 1994. Constitutive and stimulated MCP-1, GRO alpha, beta, and gamma expression in human airway epithelium and bronchoalveolar macrophages. *Am. J. Physiol. Cell. Mol. Physiol.* 266:L278–L286. doi:10.1152/ajplung.1994.266.3.L278.

Beil, W.J., P.F. Weller, M.A. Peppercorn, S.J. Galli, and A.M. Dvorak. 1995. Ultrastructural immunogold localization of subcellular sites of TNF-α in colonic Crohn's disease. *J. Leukoc. Biol.* 58:284–298. doi:10.1002/jlb.58.3.284.

Benly, P. 2015. Role of histamine in acute inflammation. *J. Pharm. Sci. Res.* 7:373–376.

Bevilacqua, M.P., and R.M. Nelson. 1993. Selectins. *J. Clin. Invest.* 91:379–387. doi:10.1172/JCI116210.

Bian, T., H. Li, Q. Zhou, C. Ni, Y. Zhang, and F. Yan. 2017. Human β -Defensin 3 Reduces TNF- α -Induced Inflammation and Monocyte Adhesion in Human Umbilical Vein Endothelial Cells. *Mediators Inflamm.* 1–11. doi:10.1155/2017/8529542.

Biondo, C., G. Mancuso, A. Midiri, G. Signorino, M. Domina, V. Lanza Cariccio, N. Mohammadi, M. Venza, I. Venza, G. Teti, and C. Beninati. 2014. The interleukin-1β/CXCL1/2/neutrophil axis mediates host protection against group B streptococcal infection. *Infect. Immun.* 82:4508–4517. doi:10.1128/IAI.02104-14.

Bixel, M.G., B. Petri, A.G. Khandoga, A. Khandoga, K. Wolburg-Buchholz, H. Wolburg, S. März, F. Krombach, and D. Vestweber. 2007. A CD99-related antigen on endothelial cells mediates neutrophil but not lymphocyte extravasation in vivo. *Blood*. 109:5327–5336. doi:10.1182/blood-2006-08-043109.

Bjork, J., P. Hedqvist, and K.-E. Arfors. 1982. Increase in vascular permeability induced by leukotriene b4 and the role of polymorphonuclear leukocytes. *Inflammation*. 6:189–200. doi:10.1007/BF00916243.

Blasi, E., L. Pitzurra, A. Bartoli, M. Puliti, and F. Bistoni. 1994. Tumor necrosis factor as an autocrine and paracrine signal controlling the macrophage secretory response to Candida albicans. *Infect. Immun.* 62:1199–1206. doi:10.1128/IAI.62.4.1199-1206.1994.

Bonecchi, R., and G.J. Graham. 2016. Atypical chemokine receptors and their roles in the resolution of the inflammatory response. *Front. Immunol.* 7:1–7. doi:10.3389/fimmu.2016.00224.

Bonvin, P., F. Gueneau, V. Buatois, M. Charreton-Galby, S. Lasch, M. Messmer, U. Christen, A.D. Luster, Z. Johnson, W. Ferlin, M. Kosco-Vilbois, A. Proudfoot, and N. Fischer. 2017. Antibody neutralization of CXCL10 in vivo is dependent on binding to free and not endothelial-bound chemokine: Implications for the design of a new generation of anti-chemokine therapeutic antibodies. *J. Biol. Chem.* 292:4185–4197. doi:10.1074/jbc.M116.745877.

Borregaard, N., L. Kjeldsen, K. Lollike, and H. Sengelov. 1996. Granules and secretory vesicles of the human neutrophil. *Int. J. Pediatr. Hematol.* 3:307–319.

Borregaard, N., O.E. Sørensen, and K. Theilgaard-Mönch. 2007. Neutrophil granules: a library of innate immunity proteins. *Trends Immunol.* 28:340–345. doi:10.1016/j.it.2007.06.002.

Bouwmeester, T., A. Bauch, H. Ruffner, P.O. Angrand, G. Bergamini, K. Croughton, C. Cruciat, D. Eberhard, J. Gagneur, S. Ghidelli, C. Hopf, B. Huhse, R. Mangano, A.M.

Michon, M. Schirle, J. Schlegl, M. Schwab, M.A. Stein, A. Bauer, G. Casari, G. Drewes, A.C. Gavin, D.B. Jackson, G. Joberty, G. Neubauer, J. Rick, B. Kuster, and G. Superti-Furga. 2004. A physical and functional map of the human TNF-α/NF-κB signal transduction pathway. *Nat. Cell Biol.* 6:97–105. doi:10.1038/ncb1086.

Bowers, E., A. Slaughter, P.S. Frenette, R. Kuick, O.M. Pello, and D. Lucas. 2018. Granulocyte-derived TNFα promotes vascular and hematopoietic regeneration in the bone marrow. *Nat. Med.* 24:95–102. doi:10.1038/nm.4448.

Bradfield, P.F., S. Nourshargh, M. Aurrand-Lions, and B.A. Imhof. 2007a. JAM Family and Related Proteins in Leukocyte Migration (Vestweber Series). *Arterioscler. Thromb. Vasc. Biol.* 27:2104–2112. doi:10.1161/ATVBAHA.107.147694.

Bradfield, P.F., C. Scheiermann, S. Nourshargh, C. Ody, F.W. Luscinskas, G.E. Rainger, G.B. Nash, M. Miljkovic-Licina, M. Aurrand-Lions, and B.A. Imhof. 2007b. JAM-C regulates unidirectional monocyte transendothelial migration in inflammation. *Blood*. 110:2545–2555. doi:10.1182/blood-2007-03-078733.

Bradley, J. 2008. TNF-mediated inflammatory disease. *J. Pathol.* 214:149–160. doi:10.1002/path.2287.

Braun, L.J., M. Zinnhardt, M. Vockel, H.C. Drexler, K. Peters, and D. Vestweber. 2019. VE-PTP inhibition stabilizes endothelial junctions by activating FGD5. *EMBO Rep.* 20:1–18. doi:10.15252/embr.201847046.

Broermann, A., M. Winderlich, H. Block, M. Frye, J. Rossaint, A. Zarbock, G. Cagna, R. Linnepe, D. Schulte, A.F. Nottebaum, and D. Vestweber. 2011. Dissociation of VE-PTP from ve-cadherin is required for leukocyte extravasation and for VEGF-induced vascular permeability in vivo. *J. Exp. Med.* 208:2393–2401. doi:10.1084/jem.20110525.

Buckley, C.D., E.A. Ross, H.M. McGettrick, C.E. Osborne, O. Haworth, C. Schmutz, P.C.W. Stone, M. Salmon, N.M. Matharu, R.K. Vohra, G.B. Nash, and G.E. Rainger. 2006. Identification of a phenotypically and functionally distinct population of long-lived neutrophils in a model of reverse endothelial migration. *J. Leukoc. Biol.* 79:303–311. doi:10.1189/jlb.0905496.

Bullard, D.C., E.J. Kunkel, H. Kubo, M.J. Hicks, I. Lorenzo, N.A. Doyle, C.M. Doerschuk, K. Ley, and A.L. Beaudet. 1996. Infectious susceptibility and severe deficiency of leukocyte rolling and recruitment in E-selectin and P-selectin double mutant mice. *J. Exp. Med.* 183:2329–2336. doi:10.1084/jem.183.5.2329.

Van Buul, J.D., E. Kanters, and P.L. Hordijk. 2007. Endothelial signaling by Ig-like cell adhesion molecules. *Arterioscler. Thromb. Vasc. Biol.* 27:1870–1876. doi:10.1161/ATVBAHA.107.145821.

Cabal-Hierro, L., and P.S. Lazo. 2012. Signal transduction by tumor necrosis factor receptors. *Cell. Signal.* 24:1297–1305. doi:10.1016/j.cellsig.2012.02.006.

Caldwell, A.B., H.A. Birnbaum, Z. Cheng, A. Hoffmann, and J.D. Vargas. 2014. Network dynamics determine the autocrine and paracrine signaling functions of TNF. *Genes Dev.* 28:2120–2133. doi:10.1101/gad.244749.114.

Carden, D., F. Xiao, C. Moak, B.H. Willis, S. Robinson-Jackson, and S. Alexander. 1998. Neutrophil elastase promotes lung microvascular injury and proteolysis of endothelial cadherins. *Am. J. Physiol. Circ. Physiol.* 275:H385–H392.

doi:10.1152/ajpheart.1998.275.2.H385.

Carlos, D., F. Spiller, F.O. Souto, S.C. Trevelin, V.F. Borges, A. de Freitas, J.C. Alves-Filho, J.S. Silva, B. Ryffel, and F.Q. Cunha. 2013. Histamine H 2 Receptor Signaling in the Pathogenesis of Sepsis: Studies in a Murine Diabetes Model. *J. Immunol.* 191:1373–1382. doi:10.4049/jimmunol.1202907.

Carlsson, A.C., T.E. Larsson, J. Helmersson-Karlqvist, A. Larsson, L. Lind, and J. Ärnlöv. 2014. Soluble TNF receptors and kidney dysfunction in the elderly. *J. Am. Soc. Nephrol.* 25:1313–1320. doi:10.1681/ASN.2013080860.

Carman, C. V., P.T. Sage, T.E. Sciuto, M.A. de la Fuente, R.S. Geha, H.D. Ochs, H.F. Dvorak, A.M. Dvorak, and T.A. Springer. 2007. Transcellular Diapedesis Is Initiated by Invasive Podosomes. *Immunity*. 26:784–797. doi:10.1016/j.immuni.2007.04.015.

Carman, C. V., and T.A. Springer. 2004. A transmigratory cup in leukocyte diapedesis both through individual vascular endothelial cells and between them. *J. Cell Biol.* 167:377–388. doi:10.1083/jcb.200404129.

Carpentier, I., B. Coornaert, and R. Beyaert. 2004. Function and Regulation of Tumor Necrosis Factor Receptor Type 2. *Curr. Med. Chem.* 11:2205–2212. doi:10.2174/0929867043364694.

Carswell, E.A., L.J. Old, R.L. Kassel, S. Green, N. Fiore, and B. Williamson. 1975. An endotoxin induced serum factor that causes necrosis of tumors. *Proc. Natl. Acad. Sci. U. S. A.* 72:3666–3670. doi:10.1073/pnas.72.9.3666.

Caruso, R.A., G. Speciale, A. Inferrera, L. Rigoli, and C. Inferrera. 2001. Ultrastructural observations on the microvasculature in advanced gastric carcinomas. *Histol. Histopathol.* 16:785–792. doi:10.14670/HH-16.785.

Cassatella, M.A., L. Meda, S. Bonora, M. Ceska, and G. Constantin. 1993. Interleukin 10 (IL-10) inhibits the release of proinflammatory cytokines from human polymorphonuclear leukocytes. Evidence for an autocrine role of tumor necrosis factor and IL-1 beta in mediating the production of IL-8 triggered by lipopolysaccharide. *J. Exp. Med.* 178:2207–2211. doi:10.1084/jem.178.6.2207.

Cassinelli, G., G. Torri, and A. Naggi. 2020. Non-Anticoagulant Heparins as Heparanase Inhibitors. *In* Advances in experimental medicine and biology. 493–522.

Champagne, B., P. Tremblay, A. Cantin, and Y. St Pierre. 1998. Proteolytic cleavage of ICAM-1 by human neutrophil elastase. *J. Immunol.* 161:6398–405.

Chan, B.P., W.M. Reichert, and G.A. Truskey. 2004. Effect of streptavidin-biotin on endothelial vasoregulation and leukocyte adhesion. *Biomaterials*. 25:3951–3961. doi:10.1016/j.biomaterials.2003.10.077.

Chang, S.H., D. Feng, J.A. Nagy, T.E. Sciuto, A.M. Dvorak, and H.F. Dvorak. 2009. Vascular permeability and pathological angiogenesis in caveolin-1-null mice. *Am. J. Pathol.* 175:1768–1776. doi:10.2353/ajpath.2009.090171.

Chavakis, T., T. Keiper, R. Matz-Westphal, K. Hersemeyer, U.J. Sachs, P.P. Nawroth, K.T. Preissner, and S. Santoso. 2004. The junctional adhesion molecule-C promotes neutrophil transendothelial migration in vitro and in vivo. *J. Biol. Chem.* 279:55602–55608. doi:10.1074/jbc.M404676200.

Chen, G., and D. V Goeddel. 2002. TNF-R1 Signaling: A Beautiful Pathway. *Science.* 296:1634–1636.

Chen, L., H. Deng, H. Cui, J. Fang, Z. Zuo, J. Deng, Y. Li, X. Wang, and L. Zhao. 2018. Inflammatory responses and inflammation-associated diseases in organs. *Oncotarget*. 9:7204–7218. doi:10.18632/oncotarget.23208.

Chistiakov, D.A., A.N. Orekhov, and Y. V. Bobryshev. 2015. Endothelial barrier and its abnormalities in cardiovascular disease. *Front. Physiol.* 6:1–11. doi:10.3389/fphys.2015.00365.

Chomarat, P., C. Dantin, L. Bennett, J. Banchereau, and A.K. Palucka. 2003. TNF Skews Monocyte Differentiation from Macrophages to Dendritic Cells. *J. Immunol.* 171:2262–2269. doi:10.4049/jimmunol.171.5.2262.

Chua, F., and G.J. Laurent. 2006. Neutrophil elastase: Mediator of extracellular matrix destruction and accumulation. *Proc. Am. Thorac. Soc.* 3:424–427. doi:10.1513/pats.200603-078AW.

Cicha, I., and K. Urschel. 2015. TNF-α in the cardiovascular system: from physiology to therapy. *Int. J. Interf. Cytokine Mediat. Res.* 7:9. doi:10.2147/IJICMR.S64894.

Claesson-Welsh, L. 2015. Vascular permeability - The essentials. *Ups. J. Med. Sci.* 120:135–143. doi:10.3109/03009734.2015.1064501.

Clausen, B.E., C. Burkhardt, W. Reith, R. Renkawitz, and I. Förster. 1999. Conditional gene targeting in macrophages and granulocytes using LysMcre mice. *Transgenic Res.* 8:265–277. doi:10.1023/A:1008942828960.

Colom, B., J. V. Bodkin, M. Beyrau, A. Woodfin, C. Ody, C. Rourke, T. Chavakis, K. Brohi, B.A. Imhof, and S. Nourshargh. 2015. Leukotriene B4-Neutrophil Elastase Axis Drives Neutrophil Reverse Transendothelial Cell Migration In Vivo. *Immunity*. 42:1075–1086. doi:10.1016/j.immuni.2015.05.010.

Condliffe, A.M., E. Kitchen, and E.R. Chilvers. 1998. Neutrophil priming: Pathophysiological consequences and underlying mechanisms. *Clin. Sci.* 94:461–471. doi:10.1042/cs0940461.

Cowland, J.B., and N. Borregaard. 2016. Granulopoiesis and granules of human neutrophils. *Immunol. Rev.* 273:11–28. doi:10.1111/imr.12440.

Crijns, H., V. Vanheule, and P. Proost. 2020. Targeting Chemokine—Glycosaminoglycan Interactions to Inhibit Inflammation. *Front. Immunol.* 11:1–30. doi:10.3389/fimmu.2020.00483.

Csepregi, J.Z., A. Orosz, E. Zajta, O. Kása, T. Németh, E. Simon, S. Fodor, K. Csonka, B.L. Barátki, D. Kövesdi, Y.-W. He, A. Gácser, and A. Mócsai. 2018. Myeloid-Specific Deletion of Mcl-1 Yields Severely Neutropenic Mice That Survive and Breed in Homozygous Form. *J. Immunol.* 201:3793–3803. doi:10.4049/jimmunol.1701803.

Cui, X., L. Chang, Y. Li, Q. Lv, F. Wang, Y. Lin, W. Li, J.D. Meade, J.C. Walden, and P. Liang. 2018. Trivalent soluble TNF Receptor, a potent TNF-α antagonist for the treatment collagen-induced arthritis. *Sci. Rep.* 8:1–11. doi:10.1038/s41598-018-25652-w.

Cunin, P., P.Y. Lee, E. Kim, A.B. Schmider, N. Cloutier, A. Pare, M. Gunzer, R.J.

Soberman, S. Lacroix, E. Boilard, C.T. Lefort, and P.A. Nigrovic. 2019. Differential attenuation of b2 integrin–dependent and –independent neutrophil migration by Ly6G ligation. *Blood Adv.* 3:256–267. doi:10.1182/bloodadvances.2018026732.

Cunningham, S.A., J.M. Rodriguez, M. Pia Arrate, T.M. Tran, and T.A. Brock. 2002. JAM2 interacts with α4β1. Facilitation by JAM3. *J. Biol. Chem.* 277:27589–27592. doi:10.1074/jbc.C200331200.

Dangerfield, J., K.Y. Larbi, M.T. Huang, A. Dewar, and S. Nourshargh. 2002. PECAM-1 (CD31) homophilic interaction up-regulates α6β1 on transmigrated neutrophils in vivo and plays a functional role in the ability of α6 integrins to mediate leukocyte migration through the perivascular basement membrane. *J. Exp. Med.* 196:1201–1211. doi:10.1084/jem.20020324.

Darbonne, W.C., G.C. Rice, M.A. Mohler, T. Apple, C.A. Hébert, A.J. Valente, and J.B. Baker. 1991. Red blood cells are a sink for interleukin 8, a leukocyte chemotaxin. *J. Clin. Invest.* 88:1362–1369. doi:10.1172/JCI115442.

David, B.A., and P. Kubes. 2019. Exploring the complex role of chemokines and chemoattractants in vivo on leukocyte dynamics. *Immunol. Rev.* 289:9–30. doi:10.1111/imr.12757.

Davis, G.E., and D.R. Senger. 2005. Endothelial extracellular matrix: Biosynthesis, remodeling, and functions during vascular morphogenesis and neovessel stabilization. *Circ. Res.* 97:1093–1107. doi:10.1161/01.RES.0000191547.64391.e3.

Deaglio, S., M. Morra, R. Mallone, C.M. Ausiello, E. Prager, G. Garbarino, U. Dianzani, H. Stockinger, and F. Malavasi. 1998. Human CD38 (ADP-ribosyl cyclase) is a counter-receptor of CD31, an Ig superfamily member. *J. Immunol.* 160:395–402.

Deguine, J., J. Wei, R. Barbalat, K. Gronert, and G.M. Barton. 2017. Local TNFR1 Signaling Licenses Murine Neutrophils for Increased TLR-Dependent Cytokine and Eicosanoid Production. *J. Immunol.* 198:2865–2875. doi:10.4049/jimmunol.1601465.

Dejana, E. 2004. Endothelial cell-cell junctions: Happy together. *Nat. Rev. Mol. Cell Biol.* 5:261–270. doi:10.1038/nrm1357.

Dejana, E., and F. Orsenigo. 2013. Endothelial adherens junctions at a glance. *J. Cell Sci.* 126:2545–2549. doi:10.1242/jcs.124529.

Dejana, E., F. Orsenigo, and M.G. Lampugnani. 2008. The role of adherens junctions and VE-cadherin in the control of vascular permeability. *J. Cell Sci.* 121:2115–2122. doi:10.1242/jcs.017897.

DeLisser, H.M., Horng Chin Yan, P.J. Newman, W.A. Muller, C.A. Buck, and S.M. Albelda. 1993. Platelet/endothelial cell adhesion molecule-1 (CD31)-mediated cellular aggregation involves cell surface glycosaminoglycans. *J. Biol. Chem.* 268:16037–16046.

Deng, Q., and A. Huttenlocher. 2012. Leukocyte migration from a fish eye's view. *J. Cell Sci.* 125:3949–3956. doi:10.1242/jcs.093633.

Devi, S., Y. Wang, W.K. Chew, R. Lima, N. A-González, C.N.Z. Mattar, S.Z. Chong, A. Schlitzer, N. Bakocevic, S. Chew, J.L. Keeble, C.C. Goh, J.L.Y. Li, M. Evrard, B. Malleret, A. Larbi, L. Renia, M. Haniffa, S.M. Tan, J.K.Y. Chan, K. Balabanian, T. Nagasawa, F. Bachelerie, A. Hidalgo, F. Ginhoux, P. Kubes, and L.G. Ng. 2013.

Neutrophil mobilization via plerixaformediated CXCR4 inhibition arises from lung demargination and blockade of neutrophil homing to the bone marrow. *J. Exp. Med.* 210:2321–2336. doi:10.1084/jem.20130056.

Di, A., D. Mehta, and A.B. Malik. 2016. ROS-activated calcium signaling mechanisms regulating endothelial barrier function. *Cell Calcium*. 60:163–171. doi:10.1016/j.ceca.2016.02.002.

Dinarello, C.A. 2018. Overview of the IL-1 family in innate inflammation and acquired immunity. *Immunol. Rev.* 281:8–27. doi:10.1111/imr.12621.

DiStasi, M.R., and K. Ley. 2009. Opening the flood-gates: how neutrophil-endothelial interactions regulate permeability. *Trends Immunol.* 30:547–556. doi:10.1016/j.it.2009.07.012.

Djeu, J.Y., D. Serbousek, and D.K. Blanchard. 1990. Release of Tumor Necrosis Factor by Human Polymorphonuclear Leukocytes. *Blood*. 76:1405–1409. doi:10.1017/CBO9780511546198.032.

Dopp, J.M., T.A. Sarafian, F.M. Spinella, M.A. Kahn, H. Shau, and J. De Vellis. 2002. Expression of the p75 TNF receptor is linked to TNF-induced NFκB translocation and oxyradical neutralization in glial cells. *Neurochem. Res.* 27:1535–1542. doi:10.1023/A:1021608724117.

Duah, E., R.K. Adapala, N. Al-Azzam, V. Kondeti, F. Gombedza, C.K. Thodeti, and S. Paruchuri. 2013. Cysteinyl leukotrienes regulate endothelial cell inflammatory and proliferative signals through CysLT 2 and CysLT 1 receptors. *Sci. Rep.* 3:1–6. doi:10.1038/srep03274.

Dufour, E.M., A. Deroche, Y. Bae, and W.A. Muller. 2008. CD99 is essential for leukocyte diapedesis in vivo. *Cell Commun. Adhes.* 15:351–363. doi:10.1080/15419060802442191.

Duong, C.N., and D. Vestweber. 2020. Mechanisms Ensuring Endothelial Junction Integrity Beyond VE-Cadherin. *Front. Physiol.* 11:1–9. doi:10.3389/fphys.2020.00519.

Dushianthan, A., M.P.W. Grocott, A.D. Postle, and R. Cusack. 2011. Acute respiratory distress syndrome and acute lung injury. *Postgrad. Med. J.* 87:612–622. doi:10.1136/pgmj.2011.118398.

Dvorak, A.M., and D. Feng. 2001. The vesiculo-vacuolar organelle (VVO): A new endothelial cell permeability organelle. *J. Histochem. Cytochem.* 49:419–431. doi:10.1177/002215540104900401.

Ebeigbe Anthony, B., and O. Talabi Olufunke. 2014. Vascular effects of histamine. *Niger. J. Physiol. Sci.* 29:007–010.

Egawa, G., S. Nakamizo, Y. Natsuaki, H. Doi, Y. Miyachi, and K. Kabashima. 2013. Intravital analysis of vascular permeability in mice using two-photon microscopy. *Sci. Rep.* 3:1–6. doi:10.1038/srep01932.

Elks, P.M., F.J. Van Eeden, G. Dixon, X. Wang, C.C. Reyes-Aldasoro, P.W. Ingham, M.K.B. Whyte, S.R. Walmsley, and S.A. Renshaw. 2011. Activation of hypoxia-inducible factor-1α (hif-1α) delays inflammation resolution by reducing neutrophil apoptosis and reverse migration in a zebrafish inflammation model. *Blood*. 118:712–722. doi:10.1182/blood-2010-12-324186.

Ellett, F., P.M. Elks, A.L. Robertson, N. V. Ogryzko, and S.A. Renshaw. 2015. Defining the phenotype of neutrophils following reverse migration in zebrafish. *J. Leukoc. Biol.* 98:975–981. doi:10.1189/jlb.3ma0315-105r.

Elliott, E.R., J.A. Van Ziffle, P. Scapini, B.M. Sullivan, R.M. Locksley, and C.A. Lowell. 2011. Deletion of Syk in Neutrophils Prevents Immune Complex Arthritis. *J. Immunol.* 187:4319–4330. doi:10.4049/jimmunol.1100341.

Engelhardt, B., and H. Wolburg. 2004. Mini review: Transendothelial migration of leukocytes: Through the front door or around the side of the house? *Eur. J. Immunol.* 34:2955–2963. doi:10.1002/eji.200425327.

Fahey, E., and S.L. Doyle. 2019. IL-1 family cytokine regulation of vascular permeability and angiogenesis. *Front. Immunol.* 10:1–15. doi:10.3389/fimmu.2019.01426.

Fan, E., D. Brodie, and A.S. Slutsky. 2018. Acute respiratory distress syndrome advances in diagnosis and treatment. *JAMA - J. Am. Med. Assoc.* 319:698–710. doi:10.1001/jama.2017.21907.

Faubel, S., and C.L. Edelstein. 2016. Mechanisms and mediators of lung injury after acute kidney injury. *Nat. Rev. Nephrol.* 12:48–60. doi:10.1038/nrneph.2015.158.

Faust, N., F. Varas, L.M. Kelly, S. Heck, and T. Graf. 2000. Insertion of enhanced green fluorescent protein into the lysozyme gene creates mice with green fluorescent granulocytes and macrophages. *Blood*. 96:719–726. doi:10.1182/blood.v96.2.719.014k29_719_726.

Feng, D., J.A. Nagy, K. Pyne, H.F. Dvorak, and A.M. Dvorak. 1998. Neutrophils emigrate from venules by a transendothelial cell pathway in response to FMLP. *J. Exp. Med.* 187:903–915. doi:10.1084/jem.187.6.903.

Ferrara, N. 2004. Vascular endothelial growth factor: Basic science and clinical progress. *Endocr. Rev.* 25:581–611. doi:10.1210/er.2003-0027.

Fielding, C.A., R.M. McLoughlin, L. McLeod, C.S. Colmont, M. Najdovska, D. Grail, M. Ernst, S.A. Jones, N. Topley, and B.J. Jenkins. 2008. IL-6 Regulates Neutrophil Trafficking during Acute Inflammation via STAT3. *J. Immunol.* 181:2189–2195. doi:10.4049/jimmunol.181.3.2189.

Filippi, M.-D. 2016. Mechanism of Diapedesis: Importance of the Transcellular Route. *Adv. Immunol.* 129:25–53. doi:10.1016/bs.ai.2015.09.001.

De Filippo, K., A. Dudeck, M. Hasenberg, E. Nye, N. Van Rooijen, K. Hartmann, M. Gunzer, A. Roers, and N. Hogg. 2013. Mast cell and macrophage chemokines CXCL1/CXCL2 control the early stage of neutrophil recruitment during tissue inflammation. *Blood*. 121:4930–4937. doi:10.1182/blood-2013-02-486217.

De Filippo, K., R.B. Henderson, M. Laschinger, and N. Hogg. 2008. Neutrophil Chemokines KC and Macrophage-Inflammatory Protein-2 Are Newly Synthesized by Tissue Macrophages Using Distinct TLR Signaling Pathways. *J. Immunol.* 180:4308–4315. doi:10.4049/jimmunol.180.6.4308.

Finsterbusch, M., M.B. Voisin, M. Beyrau, T.J. Williams, and S. Nourshargh. 2014. Neutrophils recruited by chemoattractants in vivo induce microvascular plasma protein leakage through secretion of TNF. *J. Exp. Med.* 211:1307–1314. doi:10.1084/jem.20132413.

Flemming, S., N. Burkard, M. Renschler, F. Vielmuth, M. Meir, M.A. Schick, C. Wunder, C.T. Germer, V. Spindler, J. Waschke, and N. Schlegel. 2015. Soluble VE-cadherin is involved in endothelial barrier breakdown in systemic inflammation and sepsis. *Cardiovasc. Res.* 107:32–44. doi:10.1093/cvr/cvv144.

Flynn, J.A.L., M.M. Goldstein, J. Chan, K.J. Triebold, K. Pfeffer, C.J. Lowenstein, R. Schrelber, T.W. Mak, and B.R. Bloom. 1995. Tumor necrosis factor-α is required in the protective immune response against mycobacterium tuberculosis in mice. *Immunity*. 2:561–572. doi:10.1016/1074-7613(95)90001-2.

Folco, G., and R.C. Murphy. 2006. Eicosanoid transcellular biosynthesis: From cell-cell interactions to in vivo tissue responses. *Pharmacol. Rev.* 58:375–388. doi:10.1124/pr.58.3.8.

Foxman, E.F., J.J. Campbell, and E.C. Butcher. 1997. Multistep navigation and the combinatorial control of leukocyte chemotaxis. *J. Cell Biol.* 139:1349–1360. doi:10.1083/jcb.139.5.1349.

Frenette, P.S., H. Rayburn, R.O. Hynes, and D.D. Wagner. 1996. Double Knockout value of Endothelial Selectins. *Immunol. Today*. 17:203.

Frye, M., M. Dierkes, V. Küppers, M. Vockel, J. Tomm, D. Zeuschner, J. Rossaint, A. Zarbock, G.Y. Koh, K. Peters, A.F. Nottebaum, and D. Vestweber. 2015. Interfering with VE-PTP stabilizes endothelial junctions in vivo via Tie-2 in the absence of VE-cadherin. *J. Exp. Med.* 212:2267–2287. doi:10.1084/jem.20150718.

Fukuhra, S., A. Sakurai, A. Yamagishi, K. Sako, and N. Moehizuki. 2006. Vascular endothelial cadherin-mediated cell-cell adhesion regulated by a small GTPase, Rap1. *J. Biochem. Mol. Biol.* 39:132–139. doi:10.5483/bmbrep.2006.39.2.132.

Furze, R.C., and S.M. Rankin. 2008. Neutrophil mobilization and clearance in the bone marrow. *Immunology*. 125:281–288. doi:10.1111/j.1365-2567.2008.02950.x.

Futosi, K., S. Fodor, and A. Mócsai. 2013. Neutrophil cell surface receptors and their intracellular signal transduction pathways. *Int. Immunopharmacol.* 17:638–650. doi:10.1016/j.intimp.2013.06.034.

Gane, J.M., R.A. Stockley, and E. Sapey. 2016. TNF- α Autocrine Feedback Loops in Human Monocytes: The Pro- and Anti-Inflammatory Roles of the TNF- α Receptors Support the Concept of Selective TNFR1 Blockade in Vivo. *J. Immunol. Res.* 2016. doi:10.1155/2016/1079851.

Gao, C., Y. Liu, Q. Yu, Q. Yang, B. Li, L. Sun, W. Yan, X. Cai, E. Gao, L. Xiong, H. Wang, and L. Tao. 2015. TNF-α antagonism ameliorates myocardial ischemia-reperfusion injury in mice by upregulating adiponectin. *Am. J. Physiol. - Hear. Circ. Physiol.* 308:H1583–H1591. doi:10.1152/ajpheart.00346.2014.

Gaudry, M., O. Brégerie, V. Andrieu, J. El Benna, M.A. Pocidalo, and J. Hakim. 1997. Intracellular pool of vascular endothelial growth factor in human neutrophils. *Blood*. 90:4153–4161. doi:10.1182/blood.v90.10.4153.

Gaur, P., V. Verma, S. Gupta, E. Sorani, A. Vainstein Haras, G. Oberkovitz, A. Peled, and S. Khleif. 2018. CXCR4 antagonist (BL-8040) to enhance antitumor effects by increasing tumor infiltration of antigen-specific effector T-cells. *J. Clin. Oncol.* 36:73–73. doi:10.1200/JCO.2018.36.5_suppl.73.

Gautam, N., A. Maria Olofsson, H. Herwald, L.F. Iversen, E. Lundgren-Åkerlund, P.

Hedqvist, K.E. Arfors, H. Flodgaard, and L. Lindbom. 2001. Heparin-binding protein (HBP/CAP37): A missing link in neutrophil-evoked alteration of vascular permeability. *Nat. Med.* 7:1123–1127. doi:10.1038/nm1001-1123.

Gavard, J. 2014. Endothelial permeability and VE-cadherin. A wacky comradeship. *Cell Adhes. Migr.* 8:158–164.

Di Gennaro, A., E. Kenne, M. Wan, O. Soehnlein, L. Lindbom, and J.Z. Haeggström. 2009. Leukotriene B 4 - induced changes in vascular permeability are mediated by neutrophil release of heparin-binding protein (HBP/CAP37/azurocidin). *FASEB J.* 23:1750–1757. doi:10.1096/fj.08-121277.

Giagulli, C., L. Ottoboni, E. Caveggion, B. Rossi, C. Lowell, G. Constantin, C. Laudanna, and G. Berton. 2006. The Src Family Kinases Hck and Fgr Are Dispensable for Inside-Out, Chemoattractant-Induced Signaling Regulating β2 Integrin Affinity and Valency in Neutrophils, but Are Required for β2 Integrin-Mediated Outside-In Signaling Involved in Sustained Adhesion. *J. Immunol.* 177:604–611. doi:10.4049/jimmunol.177.1.604.

Girbl, T., T. Lenn, L. Perez, L. Rolas, A. Barkaway, A. Thiriot, C. del Fresno, E. Lynam, E. Hub, M. Thelen, G. Graham, R. Alon, D. Sancho, U.H. von Andrian, M.B. Voisin, A. Rot, and S. Nourshargh. 2018. Distinct Compartmentalization of the Chemokines CXCL1 and CXCL2 and the Atypical Receptor ACKR1 Determine Discrete Stages of Neutrophil Diapedesis. *Immunity*. 49:1062–1076. doi:10.1016/j.immuni.2018.09.018.

Goebeler, M., T. Yoshimura, A. Toksoy, U. Ritter, E.B. Bröcker, and R. Gillitzer. 1997. The chemokine repertoire of human dermal microvascular endothelial cells and its regulation by inflammatory cytokines. *J. Invest. Dermatol.* 108:445–451. doi:10.1111/1523-1747.ep12289711.

Goldman, S.L., R.N. Nagel, K. Preiss, and H.J. Warnecke. 2019. CyTOF reveals phenotypically-distinct human blood neutrophil populations differentially correlated with melanoma stage. *In* Climate Change 2013 - The Physical Science Basis. Intergovernmental Panel on Climate Change, editor. Cambridge University Press, Cambridge. 1–30.

Gong, Y., and D.R. Koh. 2010. Neutrophils promote inflammatory angiogenesis via release of preformed VEGF in an in vivo corneal model. *Cell Tissue Res.* 339:437–448. doi:10.1007/s00441-009-0908-5.

Gotsch, U., E. Borges, R. Bosse, E. Böggemeyer, M. Simon, H. Mossmann, and D. Vestweber. 1997. VE-cadherin antibody accelerates neutrophil recruitment in vivo. *J. Cell Sci.* 110:583–588.

Grace, P.A. 1994. Ischaemia-reperfusion injury. *Br. J. Surg.* 81:637–647.

Green, N.M. 1975. Avidin. *In* Advances in Protein Chemistry Volume 29. 85–133.

Griffin, G.K., G. Newton, M.L. Tarrio, D. Bu, E. Maganto-Garcia, V. Azcutia, P. Alcaide, N. Grabie, F.W. Luscinskas, K.J. Croce, and A.H. Lichtman. 2012. IL-17 and TNF-α Sustain Neutrophil Recruitment during Inflammation through Synergistic Effects on Endothelial Activation. *J. Immunol.* 188:6287–6299. doi:10.4049/jimmunol.1200385.

Grivennikov, S.I., A. V. Tumanov, D.J. Liepinsh, A.A. Kruglov, B.I. Marakusha, A.N.

Shakhov, T. Murakami, L.N. Drutskaya, I. Förster, B.E. Clausen, L. Tessarollo, B. Ryffel, D. V. Kuprash, and S.A. Nedospasov. 2005. Distinct and nonredundant in vivo functions of TNF produced by T cells and macrophages/neutrophils: Protective and deleterious effects. *Immunity*. 22:93–104. doi:10.1016/j.immuni.2004.11.016.

Grommes, J., and O. Soehnlein. 2011. Contribution of neutrophils to acute lung injury. *Mol. Med.* 17:293–307. doi:10.2119/molmed.2010.00138.

Guo, M., J.W. Breslin, M.H. Wu, C.J. Gottardi, and S.Y. Yuan. 2008. VE-cadherin and β-catenin binding dynamics during histamine-induced endothelial hyperpermeability. *Am. J. Physiol. Physiol.* 294:C977–C984. doi:10.1152/ajpcell.90607.2007.

Guzmán-de la Garza, F.J., J.M. Ibarra-Hernáez, P. Cordero-Pérez, P. Villegas-Quintero, C.I. Villarreal-Ovalle, L. Torres-González, N.E. Oliva-Sosa, G. Alarcón-Galvÿn, N.E. Fernández-Garza, L.E. Muñoz-Espinosa, C.R. Cámara-Lemarroy, and J.G. Carrillo-Arriaga. 2013. Temporal relationship of serum markers and tissue damage during acute intestinal ischemia/reperfusion. *Clinics*. 68:1034–1038. doi:10.6061/clinics/2013(07)23.

Haarmann, A., M.K. Schuhmann, C. Silwedel, C.M. Monoranu, G. Stoll, and M. Buttmann. 2019. Human brain endothelial CXCR2 is inflammation-inducible and mediates CXCL5-and CXCL8-triggered paraendothelial barrier breakdown. *Int. J. Mol. Sci.* 20:1–14. doi:10.3390/ijms20030602.

Halai, K., J. Whiteford, B. Ma, S. Nourshargh, and A. Woodfin. 2014. ICAM-2 facilitates luminal interactions between neutrophils and endothelial cells in vivo. *J. Cell Sci.* 127:620–629. doi:10.1242/jcs.137463.

Hallett, M.B., and D. Lloyds. 1995. Neutrophil priming: the cellular signals that say “amber” but not “green.” *Immunol. Today*. 16:264–268. doi:10.1016/0167-5699(95)80178-2.

Hallmann, R., N. Horn, M. Selg, O. Wendler, F. Pausch, and L.M. Sorokin. 2005. Expression and function of laminins in the embryonic and mature vasculature. *Physiol. Rev.* 85:979–1000. doi:10.1152/physrev.00014.2004.

Hammond, M.D., R.A. Taylor, M.T. Mullen, Y. Ai, H.L. Aguila, M. Mack, S.E. Kasner, L.D. McCullough, and L.H. Sansing. 2014. CCR2+Ly6Chi inflammatory monocyte recruitment exacerbates acute disability following intracerebral hemorrhage. *J. Neurosci.* 34:3901–3909. doi:10.1523/JNEUROSCI.4070-13.2014.

Hampton, H.R., J. Bailey, M. Tomura, R. Brink, and T. Chtanova. 2015. Microbe-dependent lymphatic migration of neutrophils modulates lymphocyte proliferation in lymph nodes. *Nat. Commun.* 6:7139. doi:10.1038/ncomms8139.

Hampton, H.R., and T. Chtanova. 2016. The lymph node neutrophil. *Semin. Immunol.* 28:129–136. doi:10.1016/j.smim.2016.03.008.

Haque, A., J. Engel, S.A. Teichmann, and T. Lönnberg. 2017. A practical guide to single-cell RNA-sequencing for biomedical research and clinical applications. *Genome Med.* 9:1–12. doi:10.1186/s13073-017-0467-4.

Hara, T., T. Ishida, H.M. Cangara, and K. ichi Hirata. 2009. Endothelial cell-selective adhesion molecule regulates albuminuria in diabetic nephropathy. *Microvasc.*

Res. 77:348–355. doi:10.1016/j.mvr.2009.01.002.

He, P. 2010. Leucocyte/endothelium interactions and microvessel permeability: Coupled or uncoupled? *Cardiovasc. Res.* 87:281–290. doi:10.1093/cvr/cvq140.

Heemskerk, N., L. Schimmel, C. Oort, J. van Rijssel, T. Yin, B. Ma, J. van Unen, B. Pitter, S. Huveneers, J. Goedhart, Y. Wu, E. Montanez, A. Woodfin, and J.D. van Buul. 2016. F-actin-rich contractile endothelial pores prevent vascular leakage during leukocyte diapedesis through local RhoA signalling. *Nat. Commun.* 7:10493–10500. doi:10.1038/ncomms10493.

Heit, J.A., W. Michael O'Fallon, T.M. Petterson, C.M. Lohse, M.D. Silverstein, D.N. Mohr, and L. Joseph Melton. 2002. Relative impact of risk factors for deep vein thrombosis and pulmonary embolism: A population-based study. *Arch. Intern. Med.* 162:1245–1248. doi:10.1001/archinte.162.11.1245.

Hellebrekers, P., N. Vrisekoop, and L. Koenderman. 2018. Neutrophil phenotypes in health and disease. *Eur. J. Clin. Invest.* 48. doi:10.1111/eci.12943.

Herron, C.R., A.M. Lowery, P.R. Hollister, A.B. Reynolds, and P.A. Vincent. 2011. p120 regulates endothelial permeability independently of its NH2 terminus and Rho binding. *Am. J. Physiol. - Hear. Circ. Physiol.* 300:36–48. doi:10.1152/ajpheart.00812.2010.

Hidalgo, A., A.J. Peired, M. Wild, D. Vestweber, and P.S. Frenette. 2007. Complete identification of E-selectin ligand activity on neutrophils reveals a dynamic interplay and distinct functions of PSGL-1, ESL-1 and CD44. *Immunity*. 26:477–489. doi:10.1016/j.pain.2013.06.005.Re-Thinking.

Holbrook, J., S. Lara-Reyna, H. Jarosz-Griffiths, and M.F. McDermott. 2019. Tumour necrosis factor signalling in health and disease. *F1000Research*. 8:111. doi:10.12688/f1000research.17023.1.

Horiuchi, T., H. Mitoma, S.I. Harashima, H. Tsukamoto, and T. Shimoda. 2010. Transmembrane TNF-α: Structure, function and interaction with anti-TNF agents. *Rheumatology*. 49:1215–1228. doi:10.1093/rheumatology/keq031.

Huang, M.T., K.Y. Larbi, C. Scheiermann, A. Woodfin, N. Gerwin, D.O. Haskard, and S. Nourshargh. 2006. ICAM-2 mediates neutrophil transmigration in vivo: Evidence for stimulus specificity and a role in PECAM-1-independent transmigration. *Blood*. 107:4721–4727. doi:10.1182/blood-2005-11-4683.

Huo, Y., A. Schober, S.B. Forlow, D.F. Smith, M.C. Hyman, S. Jung, D.R. Littman, C. Weber, and K. Ley. 2003. Circulating activated platelets exacerbate atherosclerosis in mice deficient in apolipoprotein E. *Nat. Med.* 9:61–67. doi:10.1038/nm810.

Hurley, J. 1963. An Electron Microscopic Study of Leukocyte Emigration and Vascular Permeability in Rat Skin. *Aust. J. Exp. Biol. Med. Sci.* 41:171–186. doi:10.1038/icb.1963.17.

Jablonska, J., S. Leschner, K. Westphal, S. Lienenklaus, and S. Weiss. 2010. Neutrophils responsive to endogenous IFN-γ regulate tumor angiogenesis and growth in a mouse tumor model. *J. Clin. Invest.* 120:4163–4163. doi:10.1172/JCI37223C1.

Jaffe, E.A., C.R. Minick, B. Adelman, C.G. Becker, and R. Nachman. 1976. Synthesis of basement membrane collagen by cultured human endothelial cells. *J. Exp. Med.*

144:209–225. doi:10.1084/jem.144.1.209.

Janetopoulos, C., and R.A. Firtel. 2008. Directional sensing during chemotaxis. *FEBS Lett.* 582:2075–2085. doi:10.1016/j.febslet.2008.04.035.

Jin, T. 2013. Gradient sensing during chemotaxis. *Curr. Opin. Cell Biol.* 25:532–537. doi:10.1016/j.ceb.2013.06.007.

Johnson, E.R., and M.A. Matthay. 2010. Acute Lung Injury: Epidemiology, Pathogenesis, and Treatment. *J. Aerosol Med. Pulm. Drug Deliv.* 23:243–252. doi:10.1089/jamp.2009.0775.

Jones, D.A., O. Abbassi, L. V. McIntire, R.P. McEver, and C.W. Smith. 1993. P-selectin mediates neutrophil rolling on histamine-stimulated endothelial cells. *Biophys. J.* 65:1560–1569. doi:10.1016/S0006-3495(93)81195-0.

Josephs, S.F., T.E. Ichim, S.M. Prince, S. Kesari, F.M. Marincola, A.R. Escobedo, and A. Jafri. 2018. Unleashing endogenous TNF-alpha as a cancer immunotherapeutic. *J. Transl. Med.* 16:1–8. doi:10.1186/s12967-018-1611-7.

Julier, Z., A.J. Park, P.S. Briquez, and M.M. Martino. 2017. Promoting tissue regeneration by modulating the immune system. *Acta Biomater.* 53:13–28. doi:10.1016/j.actbio.2017.01.056.

Jung, S., J. Aliberti, P. Graemmel, M.J. Sunshine, G.W. Kreutzberg, A. Sher, and D.R. Littman. 2000. Analysis of Fractalkine Receptor CX3CR1 Function by Targeted Deletion and Green Fluorescent Protein Reporter Gene Insertion. *Mol. Cell. Biol.* 20:4106–4114. doi:10.1128/mcb.20.11.4106-4114.2000.

Kalia, N., N.J. Brown, R.F.M. Wood, and A.G. Pockley. 2005. Ketotifen abrogates local and systemic consequences of rat intestinal ischemia-reperfusion injury. *J. Gastroenterol. Hepatol.* 20:1032–1038. doi:10.1111/j.1440-1746.2005.03767.x.

Kalogeris, T., C.P. Baines, M. Krenz, and R.J. Korthuis. 2012. Cell Biology of Ischemia/Reperfusion Injury. 298. 229–317 pp.

Kansas, G.S. 1996. Selectins and Their Ligands: Current Concepts and Controversies. *Blood*. 88:3259–3287.

Kany, S., J.T. Vollrath, and B. Relja. 2019. Cytokines in inflammatory disease. *Int. J. Mol. Sci.* 20:1–31. doi:10.3390/ijms20236008.

Kenne, E., J. Rasmuson, T. Renné, M.L. Vieira, W. Müller-Esterl, H. Herwald, and L. Lindbom. 2019. Neutrophils engage the kallikrein-kinin system to open up the endothelial barrier in acute inflammation. *FASEB J.* 33:2599–2609. doi:10.1096/fj.201801329R.

Key, N.S., J.L. Platt, and G.M. Vercellotti. 1992. Vascular endothelial cell proteoglycans are susceptible to cleavage by neutrophils. *Arterioscler. Thromb. Vasc. Biol.* 12:836–842. doi:10.1161/01.ATV.12.7.836.

Kienle, K., and T. Lämmermann. 2016. Neutrophil swarming: an essential process of the neutrophil tissue response. *Immunol. Rev.* 273:76–93. doi:10.1111/imr.12458.

Kim, H., M. Kim, S.-K. Im, and S. Fang. 2018. Mouse Cre-LoxP system: general principles to determine tissue-specific roles of target genes. *Lab. Anim. Res.* 34:147. doi:10.5625/lar.2018.34.4.147.

Kim, M.M., L. Schlussel, L. Zhao, and H.A. Himburg. 2019. Dickkopf-1 Treatment Stimulates Hematopoietic Regenerative Function in Infused Endothelial Progenitor Cells. *Radiat. Res.* 192:53. doi:10.1667/rr15361.1.

Kinashi, T., and K. Katagiri. 2005. Regulation of immune cell adhesion and migration by regulator of adhesion and cell polarization enriched in lymphoid tissues. *Immunology*. 116:164–171. doi:10.1111/j.1365-2567.2005.02214.x.

Koga, K., Y. Osuga, O. Tsutsumi, R. Okagaki, M. Momoeda, T. Yano, T. Fujiwara, Y. Takai, K. Kugu, Y. Morita, and Y. Taketani. 2000. Increased concentrations of soluble tumour necrosis factor receptor (sTNFR) I and II in peritoneal fluid from women with endometriosis. *Mol. Hum. Reprod.* 6:929–933. doi:10.1093/molehr/6.10.929.

Kolaczkowska, E., and P. Kubes. 2013. Neutrophil recruitment and function in health and inflammation. *Nat. Rev. Immunol.* 13:159–175. doi:10.1038/nri3399.

Koltsova, E.K., and K. Ley. 2010. The Mysterious Ways of the Chemokine CXCL5. *Immunity*. 33:7–9. doi:10.1016/j.immuni.2010.07.012.

Kotovuori, P., E. Tontti, R. Pigott, M. Shepherd, M. Kiso, A. Hasegawa, R. Renkonen, P. Nortamo, D.C. Altieri, and C.G. Gahmberg. 1993. The vascular E-selectin binds to the leukocyte integrins CD11/CD18. *Glycobiology*. 3:131–136. doi:10.1093/glycob/3.2.131.

Krause, T.A., A.F. Alex, D.R. Engel, C. Kurts, and N. Eter. 2014. VEGF-production by CCR2-dependent macrophages contributes to laser-induced choroidal neovascularization. *PLoS One*. 9. doi:10.1371/journal.pone.0094313.

Kumar, P., Q. Shen, C.D. Pivetti, E.S. Lee, M.H. Wu, and S.Y. Yuan. 2009. Molecular mechanisms of endothelial hyperpermeability: Implications in inflammation. *Expert Rev. Mol. Med.* 11:1–20. doi:10.1017/S1462399409001112.

Kuzuya, A., K. Numajiri, M. Kimura, and M. Komiyama. 2008. Single-molecule accommodation of streptavidin in nanometer-scale wells formed in DNA nanostructures. *Nucleic Acids Symp. Ser. (Oxf).* 681–682. doi:10.1093/nass/nrn344.

Lacy, P. 2006. Mechanisms of degranulation in neutrophils. *Allergy, Asthma Clin. Immunol.* 2:98–108. doi:10.2310/7480.2006.00012.

Lämmermann, T., P. V. Afonso, B.R. Angermann, J.M. Wang, W. Kastenmüller, C.A. Parent, and R.N. Germain. 2013. Neutrophil swarms require LTB4 and integrins at sites of cell death in vivo. *Nature*. 498:371–375. doi:10.1038/nature12175.

Lampugnani, M.G. 2012. Endothelial cell-to-cell junctions: Adhesion and signaling in physiology and pathology. *Cold Spring Harb. Perspect. Med.* 2:1–14. doi:10.1101/cshperspect.a006528.

Lee, J.S., C.W. Frevert, M.M. Wurfel, S.C. Peiper, V.A. Wong, K.K. Ballman, J.T. Ruzinski, J.S. Rhim, T.R. Martin, and R.B. Goodman. 2003. Duffy Antigen Facilitates Movement of Chemokine Across the Endothelium In Vitro and Promotes Neutrophil Transmigration In Vitro and In Vivo. *J. Immunol.* 170:5244–5251. doi:10.4049/jimmunol.170.10.5244.

Lee, P.Y., J.-X. Wang, E. Parisini, C.C. Dascher, and P.A. Nigrovic. 2013. Ly6 family proteins in neutrophil biology. *J. Leukoc. Biol.* 94:585–594.

doi:10.1189/jlb.0113014.

Leite Pereira, A., S. Bitoun, A. Paoletti, G. Nocturne, E. Marcos Lopez, A. Cosma, R. Le Grand, X. Mariette, and N. Tchitchek. 2019. Characterization of Phenotypes and Functional Activities of Leukocytes From Rheumatoid Arthritis Patients by Mass Cytometry. *Front. Immunol.* 10. doi:10.3389/fimmu.2019.02384.

Ley, K. 1994. Histamine can induce leukocyte rolling in rat mesenteric venules. *Am. J. Physiol. Circ. Physiol.* 267:H1017–H1023. doi:10.1152/ajpheart.1994.267.3.H1017.

Ley, K., C. Laudanna, M.I. Cybulsky, and S. Nourshargh. 2007. Getting to the site of inflammation: The leukocyte adhesion cascade updated. *Nat. Rev. Immunol.* 7:678–689. doi:10.1038/nri2156.

Li, F., X. Xu, J. Geng, X. Wan, and H. Dai. 2020. The autocrine CXCR4/CXCL12 axis contributes to lung fibrosis through modulation of lung fibroblast activity. *Exp. Ther. Med.* 1844–1854. doi:10.3892/etm.2020.8433.

Lim, K., T. hyoun Kim, A. Trzeciak, A.M. Amitrano, E.C. Reilly, H. Prizant, D.J. Fowell, D.J. Topham, and M. Kim. 2020. In situ neutrophil efferocytosis shapes T cell immunity to influenza infection. *Nat. Immunol.* 21:1046–1057. doi:10.1038/s41590-020-0746-x.

Lindner, J.R., M.L. Kahn, S.R. Coughlin, G.R. Sambrano, E. Schauble, D. Bernstein, D. Foy, A. Hafezi-Moghadam, and K. Ley. 2000. Delayed Onset of Inflammation in Protease-Activated Receptor-2-Deficient Mice. *J. Immunol.* 165:6504–6510. doi:10.4049/jimmunol.165.11.6504.

Lipowsky, H.H., and B.W. Zweifach. 1978. Application of the “two-slit” photometric technique to the measurement of microvascular volumetric flow rates. *Microvasc. Res.* 15:93–101. doi:10.1016/0026-2862(78)90009-2.

Lombardo, E., A. Alvarez-Barrientos, B. Maroto, L. Boscá, and U.G. Knaus. 2007. TLR4-Mediated Survival of Macrophages Is MyD88 Dependent and Requires TNF-α Autocrine Signalling. *J. Immunol.* 178:3731–3739. doi:10.4049/jimmunol.178.6.3731.

Di Lorenzo, A., C. Fernández-Hernando, G. Cirino, and W.C. Sessa. 2009. Akt1 is critical for acute inflammation and histamine-mediated vascular leakage. *Proc. Natl. Acad. Sci. U. S. A.* 106:14552–14557. doi:10.1073/pnas.0904073106.

Lou, O., P. Alcaide, F.W. Luscinskas, and W.A. Muller. 2007. CD99 Is a Key Mediator of the Transendothelial Migration of Neutrophils. *J. Immunol.* 178:1136–1143. doi:10.4049/jimmunol.178.2.1136.

Mack, M., J. Cihak, C. Simonis, B. Luckow, A.E.I. Proudfoot, J. Plachý, H. Brühl, M. Frink, H.-J. Anders, V. Vielhauer, J. Pfirstinger, M. Stangassinger, and D. Schlöndorff. 2001. Expression and Characterization of the Chemokine Receptors CCR2 and CCR5 in Mice. *J. Immunol.* 166:4697–4704. doi:10.4049/jimmunol.166.7.4697.

Madge, L.A., and J.S. Pober. 2001. TNF signaling in vascular endothelial cells. *Exp. Mol. Pathol.* 70:317–325. doi:10.1006/exmp.2001.2368.

Majno, G., and I. Joris. 2004. Cells, Tissues, and Disease. 2nd ed. Oxford University Press, New York.

Majno, G., S.M. Shea, and M. Leventhal. 1969. Endothelial contraction induced by

histamine-type mediators. *J. Cell Biol.* 42:647–672. doi:10.1083/jcb.42.3.647.

Majumdar, R., M. Sixt, and C.A. Parent. 2014. New paradigms in the establishment and maintenance of gradients during directed cell migration. *Curr. Opin. Cell Biol.* 30:33–40. doi:10.1016/j.ceb.2014.05.010.

Majumdar, R., A. Tavakoli Tameh, and C.A. Parent. 2016. Exosomes Mediate LTB4 Release during Neutrophil Chemotaxis. *PLoS Biol.* 14:1–28. doi:10.1371/journal.pbio.1002336.

Mamdouh, Z., X. Chen, L.M. Plerini, F.R. Maxfield, and W.A. Muller. 2003. Targeted recycling of PECAM from endothelial surface-connected compartments during diapedesis. *Nature*. 421:748–753. doi:10.1038/nature01300.

Mamdouh, Z., A. Mikhailov, and W.A. Muller. 2009. Transcellular migration of leukocytes is mediated by the endothelial lateral border recycling compartment. *J. Exp. Med.* 206:2795–2808. doi:10.1084/jem.20082745.

Martìn-Padura, I., S. Lostaglio, M. Schneemann, L. Williams, M. Romano, P. Fruscella, C. Panzeri, A. Stoppacciaro, L. Ruco, A. Villa, D. Simmons, and E. Dejana. 1998. Junctional adhesion molecule, a novel member of the immunoglobulin superfamily that distributes at intercellular junctions and modulates monocyte transmigration. *J. Cell Biol.* 142:117–127. doi:10.1083/jcb.142.1.117.

Martin, C., P.C.E. Burdon, G. Bridger, J.C. Gutierrez-Ramos, T.J. Williams, and S.M. Rankin. 2003. Chemokines acting via CXCR2 and CXCR4 control the release of neutrophils from the bone marrow and their return following senescence. *Immunity*. 19:583–593. doi:10.1016/S1074-7613(03)00263-2.

Martins, P.D.C., J.J. García-Vallejo, J. V. Van Thienen, M. Fernandez-Borja, J.M. Van Gils, C. Beckers, A.J. Horrevoets, P.L. Hordijk, and J.J. Zwaginga. 2007. P-selectin glycoprotein ligand-1 is expressed on endothelial cells and mediates monocyte adhesion to activated endothelium. *Arterioscler. Thromb. Vasc. Biol.* 27:1023–1029. doi:10.1161/ATVBAHA.107.140442.

Massena, S. 2015. A close-up on neutrophils. Uppsala Universitet. 1–49 pp.

Massena, S., G. Christoffersson, E. Hjertström, E. Zcharia, I. Vlodavsky, N. Ausmees, C. Rolny, J.P. Li, and M. Phillipson. 2010. A chemotactic gradient sequestered on endothelial heparan sulfate induces directional intraluminal crawling of neutrophils. *Blood*. 116:1924–1931. doi:10.1182/blood-2010-01-266072.

Massena, S., G. Christoffersson, E. Vågesjö, C. Seignez, K. Gustafsson, F. Binet, C.H. Hidalgo, A. Giraud, J. Lomei, S. Weström, M. Shibuya, L. Claesson-Welsh, P. Gerwins, M. Welsh, J. Kreuger, and M. Phillipson. 2015. Identification and characterization of VEGF-A-responsive neutrophils expressing CD49d, VEGFR1, and CXCR4 in mice and humans. *Blood*. 126:2016–2026. doi:10.1182/blood-2015-03-631572.

Mathias, J.R., B.J. Perrin, T.-X. Liu, J. Kanki, A.T. Look, and A. Huttenlocher. 2006. Resolution of inflammation by retrograde chemotaxis of neutrophils in transgenic zebrafish. *J. Leukoc. Biol.* 80:1281–1288. doi:10.1189/jlb.0506346.

Matter, K., and M.S. Balda. 2003. Signalling to and from tight junctions. *Nat. Rev. Mol. Cell Biol.* 4:225–236. doi:10.1038/nrm1055.

Mayadas, T.N., R.C. Johnson, H. Rayburn, R.O. Hynes, and D.D. Wagner. 1993.

Leukocyte rolling and extravasation are severely compromised in P selectin-deficient mice. *Cell*. 74:541–554. doi:10.1016/0092-8674(93)80055-J.

Maynard, S.J., I.B.A. Menown, and A.A.J. Adgey. 2000. Troponin T or troponin I as cardiac markers in ischaemic heart disease. *Heart*. 83:371–373. doi:10.1136/heart.83.4.371.

McCormick, B., H.E. Craig, J.Y. Chu, L.M. Carlin, M. Canel, F. Wollweber, M. Toivakka, M. Michael, A.L. Astier, L. Norton, J. Lilja, J.M. Felton, T. Sasaki, J. Ivaska, I. Hers, I. Dransfield, A.G. Rossi, and S. Vermeren. 2019. A Negative Feedback Loop Regulates Integrin Inactivation and Promotes Neutrophil Recruitment to Inflammatory Sites. *J. Immunol.* 203:1579–1588. doi:10.4049/jimmunol.1900443.

McDonald, B., K. Pittman, G.B. Menezes, S.A. Hirota, I. Slaba, C.C.M. Waterhouse, P.L. Beck, D.A. Muruve, and P. Kubes. 2010. Intravascular Danger Signals Guide Neutrophils to Sites of Sterile Inflammation. *Science.* 330:362–366. doi:10.1126/science.1195491.

McEver, R.P. 2015. Selectins: Initiators of leucocyte adhesion and signalling at the vascular wall. *Cardiovasc. Res.* 107:331–339. doi:10.1093/cvr/cvv154.

Michlewska, S., I. Dransfield, I.L. Megson, and A.G. Rossi. 2009. Macrophage phagocytosis of apoptotic neutrophils is critically regulated by the opposing actions of pro-inflammatory and anti-inflammatory agents: key role for TNF-α. *FASEB J.* 23:844–854. doi:10.1096/fj.08-121228.

Middleton, J., S. Neil, J. Wintle, I. Clark-Lewis, H. Moore, L. Charles, M. Auer, H. Elin, and R. Antal. 1997. Transcytosis and surface presentation of IL-8 by venular endothelial cells. *Cell*. 91:385–395. doi:10.1016/S0092-8674(00)80422-5.

Millán, J., L. Hewlett, M. Glyn, D. Toomre, P. Clark, and A.J. Ridley. 2006. Lymphocyte transcellular migration occurs through recruitment of endothelial ICAM-1 to caveola- and F-actin-rich domains. *Nat. Cell Biol.* 8:113–123. doi:10.1038/ncb1356.

Monneau, Y., F. Arenzana-Seisdedos, and H. Lortat-Jacob. 2016. The sweet spot: how GAGs help chemokines guide migrating cells. *J. Leukoc. Biol.* 99:935–953. doi:10.1189/jlb.3mr0915-440r.

Moss, M.L., L. Sklair-Tavron, and R. Nudelman. 2008. Drug Insight: Tumor necrosis factor-converting enzyme as a pharmaceutical target for rheumatoid arthritis. *Nat. Clin. Pract. Rheumatol.* 4:300–309. doi:10.1038/ncprheum0797.

Mukhopadhyay, S., J.R. Hoidal, and T.K. Mukherjee. 2006. Role of TNFα in pulmonary pathophysiology. *Respir. Res.* 7:1–9. doi:10.1186/1465-9921-7-125.

Muller, W.A. 1995. The role of PECAM-1 (CD31) in leukocyte emigration: studies in vitro and in vivo. *J. Leukoc. Biol.* 57:523–528. doi:10.1002/jlb.57.4.523.

Muller, W.A. 2003. Leukocyte-endothelial-cell interactions in leukocyte transmigration and the inflammatory response. *Trends Immunol.* 24:326–333. doi:10.1016/S1471-4906(03)00117-0.

Muller, W.A. 2011. Mechanisms of Leukocyte Transendothelial Migration. *Annu. Rev. Pathol. Mech. Dis.* 6:323–344. doi:10.1146/annurev-pathol-011110-130224.

Muller, W.A. 2013. Getting Leukocytes to the Site of Inflammation. *Vet. Pathol.* 50:7–

22. doi:10.1177/0300985812469883.

Muller, W.A. 2016. Transendothelial migration: unifying principles from the endothelial perspective. *Immunol. Rev.* 273:61–75. doi:10.1111/imr.12443.

Nagy, J.A., L. Benjamin, H. Zeng, A.M. Dvorak, and H.F. Dvorak. 2008. Vascular permeability, vascular hyperpermeability and angiogenesis. *Angiogenesis*. 11:109–119. doi:10.1007/s10456-008-9099-z.

Naikawadi, R.P., N. Cheng, S.M. Vogel, F. Qian, D. Wu, A.B. Malik, and R.D. Ye. 2012. A critical role for phosphatidylinositol (3,4,5)-trisphosphate-dependent rac exchanger 1 in endothelial junction disruption and vascular hyperpermeability. *Circ. Res.* 111:1517–1527. doi:10.1161/CIRCRESAHA.112.273078.

Nasdala, I., K. Wolburg-Buchholz, H. Wolburg, A. Kuhn, K. Ebnet, G. Brachtendorf, U. Samulowitz, B. Kuster, B. Engelhardt, D. Vestweber, and S. Butz. 2002. A transmembrane tight junction protein selectively expressed on endothelial cells and platelets. *J. Biol. Chem.* 277:16294–16303. doi:10.1074/jbc.M111999200.

Naudé, P.J.W., J.A. Den Boer, P.G.M. Luiten, and U.L.M. Eisel. 2011. Tumor necrosis factor receptor cross-talk. *FEBS J.* 278:888–898. doi:10.1111/j.1742-4658.2011.08017.x.

Németh, T., K. Futosi, C. Sitaru, J. Ruland, and A. Mócsai. 2016. Neutrophil-specific deletion of the CARD9 gene expression regulator suppresses autoantibody-induced inflammation in vivo. *Nat. Commun.* 7:1–13. doi:10.1038/ncomms11004.

Németh, T., M. Sperandio, and A. Mócsai. 2020. Neutrophils as emerging therapeutic targets. *Nat. Rev. Drug Discov.* 19:253–275. doi:10.1038/s41573-019-0054-z.

Newton, K., and V.M. Dixit. 2012. Signaling in Innate Immunity and Inflammation. *Cold Spring Harb. Perspect. Biol.* 4:1–19. doi:10.1101/cshperspect.a006049.

Ng, L.G., R. Ostuni, and A. Hidalgo. 2019. Heterogeneity of neutrophils. *Nat. Rev. Immunol.* 19:255–265. doi:10.1038/s41577-019-0141-8.

Nieminen, M., T. Henttinen, M. Merinen, F. Marttila-Ichihara, J.E. Eriksson, and S. Jalkanen. 2006. Vimentin function in lymphocyte adhesion and transcellular migration. *Nat. Cell Biol.* 8:156–162. doi:10.1038/ncb1355.

Nottebaum, A.F., G. Cagna, M. Winderlich, A.C. Gamp, R. Linnepe, C. Polaschegg, K. Filippova, R. Lyck, B. Engelhardt, O. Kamenyeva, M.G. Bixel, S. Butz, and D. Vestweber. 2008. VE-PTP maintains the endothelial barrier via plakoglobin and becomes dissociated from VE-cadherin by leukocytes and by VEGF. *J. Exp. Med.* 205:2929–2945. doi:10.1084/jem.20080406.

Nourshargh, S., and R. Alon. 2014. Leukocyte Migration into Inflamed Tissues. *Immunity*. 41:694–707. doi:10.1016/j.immuni.2014.10.008.

Nourshargh, S., P.L. Hordijk, and M. Sixt. 2010. Breaching multiple barriers: Leukocyte motility through venular walls and the interstitium. *Nat. Rev. Mol. Cell Biol.* 11:366–378. doi:10.1038/nrm2889.

Nourshargh, S., F. Krombach, and E. Dejana. 2006. The role of JAM-A and PECAM-1 in modulating leukocyte infiltration in inflamed and ischemic tissues. *J. Leukoc. Biol.* 80:714–718. doi:10.1189/jlb.1105645.

Nourshargh, S., S.A. Renshaw, and B.A. Imhof. 2016. Reverse Migration of Neutrophils:

Where, When, How, and Why? *Trends Immunol.* 37:273–286. doi:10.1016/j.it.2016.03.006.

Novitzky-Basso, I., and A. Rot. 2012. Duffy antigen receptor for chemokines and its involvement in patterning and control of inflammatory chemokines. *Front. Immunol.* 3:1–6. doi:10.3389/fimmu.2012.00266.

Nwariaku, F.E., P. Rothenbach, Z. Liu, X. Zhu, R.H. Turnage, and L.S. Terada. 2003. Rho inhibition decreases TNF-induced endothelial MAPK activation and monolayer permeability. *J. Appl. Physiol.* 95:1889–1895. doi:10.1152/japplphysiol.00225.2003.

Okamoto, T., and K. Suzuki. 2017. The Role of Gap Junction-Mediated Endothelial Cell–Cell Interaction in the Crosstalk between Inflammation and Blood Coagulation. *Int. J. Mol. Sci.* 18:2254. doi:10.3390/ijms18112254.

Olofsson, A.M., M. Vestberg, H. Herwald, J. Rygaard, G. David, K.E. Arfors, V. Linde, H. Flodgaard, J. Dedio, W. Müller-Esterl, and E. Lundgren-Åkerlund. 1999. Heparin-binding protein targeted to mitochondrial compartments protects endothelial cells from apoptosis. *J. Clin. Invest.* 104:885–894. doi:10.1172/JCI6671.

Olson, T.S., and K. Ley. 2002. Chemokines and chemokine receptors in leukocyte trafficking. *Am. J. Physiol. Integr. Comp. Physiol.* 283:R7–R28. doi:10.1152/ajpregu.00738.2001.

Orlova, V. V., M. Economopoulou, F. Lupu, S. Santoso, and T. Chavakis. 2006. Junctional adhesion molecule-C regulates vascular endothelial permeability by modulating VE-cadherin-mediated cell-cell contacts. *J. Exp. Med.* 203:2703–2714. doi:10.1084/jem.20051730.

Orsenigo, F., C. Giampietro, A. Ferrari, M. Corada, A. Galaup, S. Sigismund, G. Ristagno, L. Maddaluno, G. Young Koh, D. Franco, V. Kurtcuoglu, D. Poulikakos, P. Baluk, D. McDonald, M. Grazia Lampugnani, and E. Dejana. 2012. Phosphorylation of VE-cadherin is modulated by haemodynamic forces and contributes to the regulation of vascular permeability in vivo. *Nat. Commun.* 3:1208. doi:10.1038/ncomms2199.

Ortiz, D., J.C. Briceño, and P. Cabrales. 2014. Microhemodynamic parameters quantification from intravital microscopy videos. *Physiol. Meas.* 35:351–367. doi:10.1088/0967-3334/35/3/351.

Ostermann, G., K.S.C. Weber, A. Zernecke, A. Schröder, and C. Weber. 2002. JAM-I is a ligand of the β2 integrin LFA-I involved in transendothelial migration of leukocytes. *Nat. Immunol.* 3:151–158. doi:10.1038/ni755.

Owen-Woods, C., R. Joulia, A. Barkaway, L. Rolas, B. Ma, A.F. Nottebaum, K.P. Arkill, M. Stein, T. Girbl, M. Golding, D.O. Bates, D. Vestweber, M.-B. Voisin, and S. Nourshargh. 2020. Local microvascular leakage promotes trafficking of activated neutrophils to remote organs. *J. Clin. Invest.* 130:2301–2318. doi:10.1172/JCI133661.

Papayannopoulos, V. 2018. Neutrophil extracellular traps in immunity and disease. *Nat. Rev. Immunol.* 18:134–147. doi:10.1038/nri.2017.105.

Park-Windhol, C., and P.A. D'Amore. 2016. Disorders of Vascular Permeability. *Annu. Rev. Pathol. Mech. Dis.* 11:251–281. doi:10.1146/annurev-pathol-012615-044506.

Park, S.A., S. Jeong, Y.H. Choe, and Y.M. Hyun. 2018. Sensing of Vascular Permeability in Inflamed Vessel of Live Animal. *J. Anal. Methods Chem.* 2018:2–7. doi:10.1155/2018/5797152.

Pasparakis, M., L. Alexopoulou, V. Episkopou, and G. Kollias. 1996. Immune and inflammatory responses in TNFα-deficient mice: A critical requirement for TNFα in the formation of primary B cell follicles, follicular dendritic cell networks and germinal centers, and in the maturation of the humoral immune response. *J. Exp. Med.* 184:1397–1411. doi:10.1084/jem.184.4.1397.

Passegué, E., E.F. Wagner, and I.L. Weissman. 2004. JunB deficiency leads to a myeloproliferative disorder arising from hematopoietic stem cells. *Cell*. 119:431–443. doi:10.1016/j.cell.2004.10.010.

Pękalski, J., P.J. Zuk, M. Kochańczyk, M. Junkin, R. Kellogg, S. Tay, and T. Lipniacki. 2013. Spontaneous NF-κB Activation by Autocrine TNFα Signaling: A Computational Analysis. *PLoS One*. 8:e78887. doi:10.1371/journal.pone.0078887.

Pepys, M.B., and G.M. Hirschfield. 2003. C-reactive protein: a critical update. *J. Clin. Invest.* 111:1805–1812. doi:10.1172/JCI200318921.

Peschon, J.J., D.S. Torrance, K.L. Stocking, M.B. Glaccum, C. Otten, C.R. Willis, K. Charrier, P.J. Morrissey, C.B. Ware, and K.M. Mohler. 1998. TNF Receptor-Deficient Mice Reveal Divergent Roles for p55 and p75 in Several Models of Inflammation. *J. Immunol.* 160:943–952.

Pfeffer, K., T. Matsuyama, T.M. Kündig, A. Wakeham, K. Kishihara, A. Shahinian, K. Wiegmann, P.S. Ohashi, M. Krönke, and T.W. Mak. 1993. Mice deficient for the 55 kd tumor necrosis factor receptor are resistant to endotoxic shock, yet succumb to L. monocytogenes infection. *Cell*. 73:457–467. doi:10.1016/0092-8674(93)90134-C.

Phillipson, M., B. Heit, P. Colarusso, L. Liu, C.M. Ballantyne, and P. Kubes. 2006. Intraluminal crawling of neutrophils to emigration sites: A molecularly distinct process from adhesion in the recruitment cascade. *J. Exp. Med.* 203:2569–2575. doi:10.1084/jem.20060925.

Phillipson, M., J. Kaur, P. Colarusso, C.M. Ballantyne, and P. Kubes. 2008. Endothelial Domes Encapsulate Adherent Neutrophils and Minimize Increases in Vascular Permeability in Paracellular and Transcellular Emigration. *PLoS One*. 3:e1649. doi:10.1371/journal.pone.0001649.

Pillay, J., V.M. Kamp, E. van Hoffen, T. Visser, T. Tak, J. Lammers, L.H. Ulfman, L.P. Leenen, P. Pickkers, and L. Koenderman. 2012. A subset of neutrophils in human systemic inflammation inhibits T cell responses through Mac-1. *J. Clin. Invest.* 122:327–336. doi:10.1172/JCI57990.

Pillay, J., B.P. Ramakers, V.M. Kamp, A.L.T. Loi, S.W. Lam, F. Hietbrink, L.P. Leenen, A.T. Tool, P. Pickkers, and L. Koenderman. 2010. Functional heterogeneity and differential priming of circulating neutrophils in human experimental endotoxemia. *J. Leukoc. Biol.* 88:211–220. doi:10.1189/jlb.1209793.

Pink, D.B.S., W. Schulte, M.H. Parseghian, A. Zijlstra, and J.D. Lewis. 2012. Real-time visualization and quantitation of vascular permeability in vivo: Implications for drug delivery. *PLoS One*. 7:1–10. doi:10.1371/journal.pone.0033760.

Pitchford, S., D. Pan, and H.C.E. Welch. 2017. Platelets in neutrophil recruitment to sites of inflammation. *Curr. Opin. Hematol.* 24:23–31. doi:10.1097/MOH.0000000000000297.

Pitsillides, C.M., J.M. Runnels, J.A. Spencer, L. Zhi, M.X. Wu, and C.P. Lin. 2011. Cell labeling approaches for fluorescence-based in vivo flow cytometry. *Cytom. Part A*. 79 A:758–765. doi:10.1002/cyto.a.21125.

Pollenus, E., B. Malengier-Devlies, L. Vandermosten, T.T. Pham, T. Mitera, H. Possemiers, L. Boon, G. Opdenakker, P. Matthys, and P.E. Van den Steen. 2019. Limitations of neutrophil depletion by anti-Ly6G antibodies in two heterogenic immunological models. *Immunol. Lett.* 212:30–36. doi:10.1016/j.imlet.2019.06.006.

Polverino, E., E. Rosales-Mayor, G.E. Dale, K. Dembowsky, and A. Torres. 2017. The Role of Neutrophil Elastase Inhibitors in Lung Diseases. *Chest*. 152:249–262. doi:10.1016/j.chest.2017.03.056.

Potter, M.D., S. Barbero, and D.A. Cheresh. 2005. Tyrosine phosphorylation of VE-cadherin prevents binding of p120- and β-catenin and maintains the cellular mesenchymal state. *J. Biol. Chem.* 280:31906–31912. doi:10.1074/jbc.M505568200.

Powell, D., S. Tauzin, L.E. Hind, Q. Deng, D.J. Beebe, and A. Huttenlocher. 2017. Chemokine Signaling and the Regulation of Bidirectional Leukocyte Migration in Interstitial Tissues. *Cell Rep.* 19:1572–1585. doi:10.1016/j.celrep.2017.04.078.

Prince, L.R., L. Allen, E.C. Jones, P.G. Hellewell, S.K. Dower, M.K.B. Whyte, and I. Sabroe. 2004. The role of interleukin-1β in direct and toll-like receptor 4-mediated neutrophil activation and survival. *Am. J. Pathol.* 165:1819–1826. doi:10.1016/S0002-9440(10)63437-2.

Proebstl, D., M.B. Voisin, A. Woodfin, J. Whiteford, F. D'Acquisto, G.E. Jones, D. Rowe, and S. Nourshargh. 2012. Pericytes support neutrophil subendothelial cell crawling and breaching of venular walls in vivo. *J. Exp. Med.* 209:1219–1234. doi:10.1084/jem.20111622.

Proudfoot, A., A. Bayliffe, C.M. O'Kane, T. Wright, A. Serone, P.J. Bareille, V. Brown, U.I. Hamid, Y. Chen, R. Wilson, J. Cordy, P. Morley, R. De Wildt, S. Elborn, M. Hind, E.R. Chilvers, M. Griffiths, C. Summers, and D.F. McAuley. 2018. Novel anti-tumour necrosis factor receptor-1 (TNFR1) domain antibody prevents pulmonary inflammation in experimental acute lung injury. *Thorax*. 73:723–730. doi:10.1136/thoraxjnl-2017-210305.

Proudfoot, A., Z. Johnson, P. Bonvin, and T. Handel. 2017. Glycosaminoglycan Interactions with Chemokines Add Complexity to a Complex System. *Pharmaceuticals*. 10:70. doi:10.3390/ph10030070.

Proudfoot, A.E.I. 2015. Chemokines and glycosaminoglycans. *Front. Immunol.* 6:1–3. doi:10.3389/fimmu.2015.00246.

Proudfoot, A.E.I., T.M. Handel, Z. Johnson, E.K. Lau, P. LiWang, I. Clark-Lewis, F. Borlat, T.N.C. Wells, and M.H. Kosco-Vilbois. 2003. Glycosaminoglycan binding and oligomerization are essential for the in vivo activity of certain chemokines. *Proc. Natl. Acad. Sci. U. S. A.* 100:1885–1890. doi:10.1073/pnas.0334864100.

Pruenster, M., L. Mudde, P. Bombosi, S. Dimitrova, M. Zsak, J. Middleton, A. Richmond, G.J. Graham, S. Segerer, R.J.B. Nibbs, and A. Rot. 2009. The Duffy antigen receptor for chemokines transports chemokines and supports their promigratory activity. *Nat. Immunol.* 10:101–108. doi:10.1038/ni.1675.

Puga, I., M. Cols, C.M. Barra, B. He, L. Cassis, M. Gentile, L. Comerma, A. Chorny, M. Shan, W. Xu, G. Magri, D.M. Knowles, W. Tam, A. Chiu, J.B. Bussel, S. Serrano, J.A. Lorente, B. Bellosillo, J. Lloreta, N. Juanpere, F. Alameda, T. Baró, C.D. De Heredia, N. Torán, A. Català, M. Torrebadell, C. Fortuny, V. Cusí, C. Carreras, G.A. Diaz, J.M. Blander, C.M. Farber, G. Silvestri, C. Cunningham-Rundles, M. Calvillo, C. Dufour, L.D. Notarangelo, V. Lougaris, A. Plebani, J.L. Casanova, S.C. Ganal, A. Diefenbach, J.I. Aróstegui, M. Juan, J. Yagüe, N. Mahlaoui, J. Donadieu, K. Chen, and A. Cerutti. 2012. B cell-helper neutrophils stimulate the diversification and production of immunoglobulin in the marginal zone of the spleen. *Nat. Immunol.* 13:170–180. doi:10.1038/ni.2194.

Qiang, S., M.H. Wu, and S. Yuan. 2009. Endothelial contractile cytoskeleton and microvascular permeability. *Cell Health Cytoskelet.* Volume 1:43–50. doi:10.2147/CHC.S5118.

Raghavendran, K., G. Pryhuber, P. Chess, B. Davidson, P. Knight, and R. Notter. 2008. Pharmacotherapy of Acute Lung Injury and Acute Respiratory Distress Syndrome. *Curr. Med. Chem.* 15:1911–1924. doi:10.2174/092986708785132942.

Raghu, G., K.K. Brown, U. Costabel, V. Cottin, R.M. Du Bois, J.A. Lasky, M. Thomeer, J.P. Utz, R.K. Khandker, L. McDermott, and S. Fatenejad. 2008. Treatment of idiopathic pulmonary fibrosis with etanercept: An exploratory, placebo-controlled trial. *Am. J. Respir. Crit. Care Med.* 178:948–955. doi:10.1164/rccm.200709-1446OC.

Ramachandran, V., M. Williams, T. Yago, D.W. Schmidtke, and R.P. McEver. 2004. Dynamic alterations of membrane tethers stabilize leukocyte rolling on P-selectin. *Proc. Natl. Acad. Sci. U. S. A.* 101:13519–13524. doi:10.1073/pnas.0403608101.

Randolph, G.J., and M.B. Furie. 1996. Mononuclear phagocytes egress from an in vitro model of the vascular wall by migrating across endothelium in the basal to apical direction: role of intercellular adhesion molecule 1 and the CD11/CD18 integrins. *J. Exp. Med.* 183:451–462. doi:10.1084/jem.183.2.451.

Randolph, G.J., S. Ivanov, B.H. Zinselmeyer, and J.P. Scallan. 2017. The Lymphatic System: Integral Roles in Immunity. *Annu. Rev. Immunol.* 35:31–52. doi:10.1146/annurev-immunol-041015-055354.

Rees, M.D., J.M. Whitelock, E. Malle, C.Y. Chuang, R. V. Iozzo, A. Nilasaroya, and M.J. Davies. 2010. Myeloperoxidase-derived oxidants selectively disrupt the protein core of the heparan sulfate proteoglycan perlecan. *Matrix Biol.* 29:63–73. doi:10.1016/j.matbio.2009.09.005.

Reeves, K.J., Z.L.S. Brookes, M.W.R. Reed, and N.J. Brown. 2012. Evaluation of fluorescent plasma markers for in vivo microscopy of the microcirculation. *J. Vasc. Res.* 49:132–143. doi:10.1159/000331281.

Reichel, C.A., M. Rehberg, M. Lerchenberger, N. Berberich, P. Bihari, A.G. Khandoga, S. Zahler, and F. Krombach. 2009. Ccl2 and Ccl3 Mediate Neutrophil Recruitment via Induction of Protein Synthesis and Generation of Lipid Mediators. *Arterioscler.*

Thromb. Vasc. Biol. 29:1787–1793. doi:10.1161/ATVBAHA.109.193268.

Reitsma, S., D.W. Slaaf, H. Vink, M.A.M.J. Van Zandvoort, and M.G.A. Oude Egbrink. 2007. The endothelial glycocalyx: Composition, functions, and visualization. *Pflugers Arch. Eur. J. Physiol.* 454:345–359. doi:10.1007/s00424-007-0212-8.

Ribaux, P., J.A. Ehses, N. Lin-Marq, F. Carrozzino, M. Böni-Schnetzler, E. Hammar, J.C. Irminger, M.Y. Donath, and P.A. Halban. 2007. Induction of CXCL1 by extracellular matrix and autocrine enhancement by interleukin-1 in rat pancreatic β-cells. *Endocrinology*. 148:5582–5590. doi:10.1210/en.2007-0325.

Richter, J., J. Ng-Sikorski, I. Olsson, and T. Andersson. 1990. Tumor necrosis factor-induced degranulation in adherent human neutrophils is dependent on CD11b/CD18-integrin-triggered oscillations of cytosolic free Ca2+. *Proc. Natl. Acad. Sci.* 87:9472–9476. doi:10.1073/pnas.87.23.9472.

Roberts, W.G., and G.E. Palade. 1995. Increased microvascular permeability and endothelial fenestration induced by vascular endothelial growth factor. *J. Cell Sci.* 108:2369–2379.

Robertson, A.L., G.R. Holmes, A.N. Bojarczuk, J. Burgon, C.A. Loynes, M. Chimen, A.K. Sawtell, B. Hamza, J. Willson, S.R. Walmsley, S.R. Anderson, M.C. Coles, S.N. Farrow, R. Solari, S. Jones, L.R. Prince, D. Irimia, G. Ed Rainger, V. Kadirkamanathan, M.K.B. Whyte, and S.A. Renshaw. 2014. A zebrafish compound screen reveals modulation of neutrophil reverse migration as an anti-inflammatory mechanism. *Sci. Transl. Med.* 6:1–10. doi:10.1126/scitranslmed.3007672.

Rodrigues, S.F., and D.N. Granger. 2010. Role of blood cells in ischaemia-reperfusion induced endothelial barrier failure. *Cardiovasc. Res.* 87:291–299. doi:10.1093/cvr/cvq090.

Rosales, C. 2018. Neutrophil: A cell with many roles in inflammation or several cell types? *Front. Physiol.* 9:1–17. doi:10.3389/fphys.2018.00113.

Rosen, S.D. 2004. Ligands for L-Selectin: Homing, Inflammation, and Beyond. *Annu. Rev. Immunol.* 22:129–156. doi:10.1146/annurev.immunol.21.090501.080131.

Rosenberger, P., J.M. Schwab, V. Mirakaj, E. Masekowsky, A. Mager, J.C. Morote-Garcia, K. Unertl, and H.K. Eltzschig. 2009. Hypoxia-inducible factor-dependent induction of netrin-1 dampens inflammation caused by hypoxia. *Nat. Immunol.* 10:195–202. doi:10.1038/ni.1683.

Rot, A. 1991. Some Aspects of NAP-1 Pathophysiology: Lung Damage Caused by a Blood-Borne Cytokine. *In* Chemotactic Cytokine. Advances in Experimental Medicine and Biology. J. Westwick, I.J.D. Lindley, and S.L. Kunkel, editors. Springer, Boston, MA. 127–135.

Rot, A. 2010. Chemokine patterning by glycosaminoglycans and interceptors. *Front. Biosci.* 15:645. doi:10.2741/3638.

Rot, A., and U.H. von Andrian. 2004. CHEMOKINES IN INNATE AND ADAPTIVE HOST DEFENSE: Basic Chemokinese Grammar for Immune Cells. *Annu. Rev. Immunol.* 22:891–928. doi:10.1146/annurev.immunol.22.012703.104543.

Rothe, J., W. Lesslauer, H. Lötscher, Y. Lang, P. Koebel, F. Köntgen, A. Althage, R. Zinkernagel, M. Steinmetz, and H. Bluethmann. 1993. Mice lacking the tumour

necrosis factor receptor 1 are resistant to IMF-mediated toxicity but highly susceptible to infection by Listeria monocytogenes. *Nature*. 364:798–802. doi:10.1038/364798a0.

Roussel, E., and M.-C. Gingras. 1997. Transendothelial migration induces rapid expression on neutrophils of granule-release VLA6 used for tissue infiltration. *J. Leukoc. Biol.* 62:356–362. doi:10.1002/jlb.62.3.356.

Rullo, J., H. Becker, S.J. Hyduk, J.C. Wong, G. Digby, P.D. Arora, A.P. Cano, J. Hartwig, C.A. McCulloch, and M.I. Cybulsky. 2012. Actin polymerization stabilizes α4β1 integrin anchors that mediate monocyte adhesion. *J. Cell Biol.* 197:115–129. doi:10.1083/jcb.201107140.

Sachs, U.J.H., C.L. Andrei-Selmer, A. Maniar, T. Weiss, C. Paddock, V. V. Orlova, Y.C. Eun, P.J. Newman, K.T. Preissner, T. Chavakis, and S. Santoso. 2007. The neutrophil-specific antigen CD177 is a counter-receptor for platelet endothelial cell adhesion molecule-1 (CD31). *J. Biol. Chem.* 282:23603–23612. doi:10.1074/jbc.M701120200.

Sagiv, J.Y., J. Michaeli, S. Assi, I. Mishalian, H. Kisos, L. Levy, P. Damti, D. Lumbroso, L. Polyansky, R. V. Sionov, A. Ariel, A.H. Hovav, E. Henke, Z.G. Fridlender, and Z. Granot. 2015. Phenotypic diversity and plasticity in circulating neutrophil subpopulations in cancer. *Cell Rep.* 10:562–573. doi:10.1016/j.celrep.2014.12.039.

Sawant, K. V., K.M. Poluri, A.K. Dutta, K.M. Sepuru, A. Troshkina, R.P. Garofalo, and K. Rajarathnam. 2016. Chemokine CXCL1 mediated neutrophil recruitment: Role of glycosaminoglycan interactions. *Sci. Rep.* 6:4–11. doi:10.1038/srep33123.

Scapini, P., M. Morini, C. Tecchio, S. Minghelli, E. Di Carlo, E. Tanghetti, A. Albini, C. Lowell, G. Berton, D.M. Noonan, and M.A. Cassatella. 2004. CXCL1/Macrophage Inflammatory Protein-2-Induced Angiogenesis In Vivo Is Mediated by Neutrophil-Derived Vascular Endothelial Growth Factor-A. *J. Immunol.* 172:5034–5040. doi:10.4049/jimmunol.172.8.5034.

Schenkel, A.R., T.W. Chew, E. Chlipala, M.W.N. Harbord, and W.A. Muller. 2006. Different susceptibilities of PECAM-deficient mouse strains to spontaneous idiopathic pneumonitis. *Exp. Mol. Pathol.* 81:23–30. doi:10.1016/j.yexmp.2005.11.007.

Schenkel, A.R., T.W. Chew, and W.A. Muller. 2004. Platelet Endothelial Cell Adhesion Molecule Deficiency or Blockade Significantly Reduces Leukocyte Emigration in a Majority of Mouse Strains. *J. Immunol.* 173:6403–6408. doi:10.4049/jimmunol.173.10.6403.

Schenkel, A.R., E.M. Dufour, T.W. Chew, E. Sorg, and W.A. Muller. 2007. The murine CD99-related molecule CD99-like 2 (CD99L2) is an adhesion molecule involved in the inflammatory response. *Cell Commun. Adhes.* 14:227–237. doi:10.1080/15419060701755966.

Schenkel, A.R., Z. Mamdouh, X. Chen, R.M. Liebman, and W.A. Muller. 2002. CD99 plays a major role in the migration of monocytes through endothelial junctions. *Nat. Immunol.* 3:143–150. doi:10.1038/ni749.

Schmitt, M.M.N., R.T.A. Megens, A. Zernecke, K. Bidzhekov, N.M. Van Den Akker, T.

Rademakers, M.A. Van Zandvoort, T.M. Hackeng, R.R. Koenen, and C. Weber. 2014. Endothelial junctional adhesion molecule-a guides monocytes into flow-dependent predilection sites of atherosclerosis. *Circulation*. 129:66–76. doi:10.1161/CIRCULATIONAHA.113.004149.

Schubert, W., P.G. Frank, B. Razani, D.S. Park, C.W. Chow, and M.P. Lisanti. 2001. Caveolae-deficient Endothelial Cells Show Defects in the Uptake and Transport of Albumin in Vivo. *J. Biol. Chem.* 276:48619–48622. doi:10.1074/jbc.C100613200.

Schulte, D., V. Küppers, N. Dartsch, A. Broermann, H. Li, A. Zarbock, O. Kamenyeva, F. Kiefer, A. Khandoga, S. Massberg, and D. Vestweber. 2011. Stabilizing the VE-cadherin-catenin complex blocks leukocyte extravasation and vascular permeability. *EMBO J.* 30:4157–4170. doi:10.1038/emboj.2011.304.

Seelige, R., C. Natsch, S. März, D. Jing, M. Frye, S. Butz, and D. Vestweber. 2013. Cutting Edge: Endothelial-Specific Gene Ablation of CD99L2 Impairs Leukocyte Extravasation In Vivo. *J. Immunol.* 190:892–896. doi:10.4049/jimmunol.1202721.

Segal, A.W., and O.T.G. Jones. 1978. Novel cytochrome b system in phagocytic vacuoles of human granulocytes. *Nature*. 276:515–517. doi:10.1038/276515a0.

Serhan, C.N., N. Chiang, and T.E. Van Dyke. 2008. Resolving inflammation: dual anti-inflammatory and pro-resolution lipid mediators. *Nat. Rev. Immunol.* 8:349–361. doi:10.1038/nri2294.

Shaikh, F., J. He, P. Bhadra, X. Chen, and S.W.I. Siu. 2018. TNF receptor type II as an emerging drug target for the treatment of cancer, autoimmune diseases, and graft-versus-host disease: Current perspectives and in silico search for small molecule binders. *Front. Immunol.* 9:1–6. doi:10.3389/fimmu.2018.01382.

Shamri, R., V. Grabovsky, J.M. Gauguet, S. Feigelson, E. Manevich, W. Kolanus, M.K. Robinson, D.E. Staunton, U.H. Von Andrian, and R. Alon. 2005. Lymphocyte arrest requires instantaneous induction of an extended LFA-1 conformation mediated by endothelium-bound chemokines. *Nat. Immunol.* 6:497–506. doi:10.1038/ni1194.

Shattil, S.J. 2005. Integrins and Src: Dynamic duo of adhesion signaling. *Trends Cell Biol.* 15:399–403. doi:10.1016/j.tcb.2005.06.005.

Shattil, S.J., C. Kim, and M.H. Ginsberg. 2010. The final steps of integrin activation: the end game. *Nat. Rev. Mol. Cell Biol.* 11:288–300. doi:10.1038/nrm2871.

Shaw, S.K., P.S. Bamba, B.N. Perkins, and F.W. Luscinskas. 2001. Real-Time Imaging of Vascular Endothelial-Cadherin During Leukocyte Transmigration Across Endothelium. *J. Immunol.* 167:2323–2330. doi:10.4049/jimmunol.167.4.2323.

Shaw, S.K., S. Ma, M.B. Kim, R.M. Rao, C.U. Hartman, R.M. Froio, L. Yang, T. Jones, Y. Liu, A. Nusrat, C.A. Parkos, and F.W. Luscinskas. 2004. Coordinated redistribution of leukocyte LFA-1 and endothelial cell ICAM-1 accompany neutrophil transmigration. *J. Exp. Med.* 200:1571–1580. doi:10.1084/jem.20040965.

Sidibé, A., and B.A. Imhof. 2014. VE-cadherin phosphorylation decides: Vascular permeability or diapedesis. *Nat. Immunol.* 15:215–217. doi:10.1038/ni.2825.

Sigal, A., D.A. Bleijs, V. Grabovsky, S.J. van Vliet, O. Dwir, C.G. Figdor, Y. van Kooyk, and R. Alon. 2000. The LFA-1 Integrin Supports Rolling Adhesions on ICAM-1 Under Physiological Shear Flow in a Permissive Cellular Environment. *J. Immunol.* 165:442–452. doi:10.4049/jimmunol.165.1.442.

Silvestre-Roig, C., A. Hidalgo, and O. Soehnlein. 2016. Neutrophil heterogeneity: Implications for homeostasis and pathogenesis. *Blood*. 127:2173–2181. doi:10.1182/blood-2016-01-688887.

Simon, S.I., Y. Hu, D. Vestweber, and C.W. Smith. 2000. Neutrophil Tethering on E-Selectin Activates β 2 Integrin Binding to ICAM-1 Through a Mitogen-Activated Protein Kinase Signal Transduction Pathway . *J. Immunol.* 164:4348–4358. doi:10.4049/jimmunol.164.8.4348.

Skaria, T., E. Bachli, and G. Schoedon. 2017. Wnt5A/Ryk signaling critically affects barrier function in human vascular endothelial cells. *Cell Adhes. Migr.* 11:24–38. doi:10.1080/19336918.2016.1178449.

Smith, J.A. 1994. Neutrophils, host defense, and inflammation: a double-edged sword. *J. Leukoc. Biol.* 56:672–686. doi:10.1002/jlb.56.6.672.

Soehnlein, O., S. Oehmcke, X. Ma, A.G. Rothfuchs, R. Frithiof, N. Van Rooijen, M. Mörgelin, H. Herwald, and L. Lindbom. 2008. Neutrophil degranulation mediates severe lung damage triggered by streptococcal M1 protein. *Eur. Respir. J.* 32:405–412. doi:10.1183/09031936.00173207.

Sokulsky, L.A., K. Garcia-Netto, T.H. Nguyen, J.L.N. Girkin, A. Collison, J. Mattes, G. Kaiko, C. Liu, N.W. Bartlett, M. Yang, and P.S. Foster. 2020. A Critical Role for the CXCL3/CXCL5/CXCR2 Neutrophilic Chemotactic Axis in the Regulation of Type 2 Responses in a Model of Rhinoviral-Induced Asthma Exacerbation. *J. Immunol.* 205:2468–2478. doi:10.4049/jimmunol.1901350.

Sperandio, M., C.A. Gleissner, and K. Ley. 2009. Glycosylation in immune cell trafficking. *Immunol. Rev.* 230:97–113. doi:10.1111/j.1600-065X.2009.00795.x.

Stackowicz, J., F. Jönsson, and L.L. Reber. 2020. Mouse Models and Tools for the in vivo Study of Neutrophils. *Front. Immunol.* 10:1–19. doi:10.3389/fimmu.2019.03130.

Stark, M.A., Y. Huo, T.L. Burcin, M.A. Morris, T.S. Olson, and K. Ley. 2005. Phagocytosis of apoptotic neutrophils regulates granulopoiesis via IL-23 and IL-17. *Immunity*. 22:285–294. doi:10.1016/j.immuni.2005.01.011.

Stoler-Barak, L., C. Moussion, E. Shezen, M. Hatzav, M. Sixt, and R. Alon. 2014. Blood vessels pattern heparan sulfate gradients between their apical and basolateral aspects. *PLoS One*. 9. doi:10.1371/journal.pone.0085699.

Stratman, A.N., and G.E. Davis. 2012. Endothelial Cell-Pericyte Interactions Stimulate Basement Membrane Matrix Assembly: Influence on Vascular Tube Remodeling, Maturation, and Stabilization. *Microsc. Microanal.* 18:68–80. doi:10.1017/S1431927611012402.

Su, Y., and A. Richmond. 2015. Chemokine Regulation of Neutrophil Infiltration of Skin Wounds. *Adv. Wound Care*. 4:631–640. doi:10.1089/wound.2014.0559.

Sugimoto, M.A., L.P. Sousa, V. Pinho, M. Perretti, and M.M. Teixeira. 2016. Resolution of Inflammation: What Controls Its Onset? *Front. Immunol.* 7. doi:10.3389/fimmu.2016.00160.

Sukriti, S., M. Tauseef, P. Yazbeck, and D. Mehta. 2014. Mechanisms regulating endothelial permeability. *Pulm. Circ.* 4:535–551. doi:10.1086/677356.

Sumagin, R., H. Prizant, E. Lomakina, R.E. Waugh, and I.H. Sarelius. 2010. LFA-1 and

Mac-1 Define Characteristically Different Intralumenal Crawling and Emigration Patterns for Monocytes and Neutrophils In Situ. *J. Immunol.* 185:7057–7066. doi:10.4049/jimmunol.1001638.

Sumagin, R., and I.H. Sarelius. 2010. Intercellular Adhesion Molecule-1 Enrichment near Tricellular Endothelial Junctions Is Preferentially Associated with Leukocyte Transmigration and Signals for Reorganization of These Junctions To Accommodate Leukocyte Passage. *J. Immunol.* 184:5242–5252. doi:10.4049/jimmunol.0903319.

Summers, C., S.M. Rankin, A.M. Condliffe, N. Singh, A.M. Peters, and E.R. Chilvers. 2010. Neutrophil kinetics in health and disease. *Trends Immunol.* 31:318–324. doi:10.1016/j.it.2010.05.006.

Sun, Z., X. Li, S. Massena, S. Kutschera, N. Padhan, L. Gualandi, V. Sundvold-Gjerstad, K. Gustafsson, W.W. Choy, G. Zang, M. Quach, L. Jansson, M. Phillipson, M.R. Abid, A. Spurkland, and L. Claesson-Welsh. 2012. VEGFR2 induces c-Src signaling and vascular permeability in vivo via the adaptor protein TSAD. *J. Exp. Med.* 209:1363–1377. doi:10.1084/jem.20111343.

Sundd, P., E. Gutierrez, E.K. Koltsova, Y. Kuwano, S. Fukuda, M.K. Pospieszalska, A. Groisman, and K. Ley. 2012. Slings enable neutrophil rolling at high shear. *Nature*. 488:399–403. doi:10.1038/nature11248.

Sundd, P., M.K. Pospieszalska, and K. Ley. 2013. Neutrophil rolling at high shear: Flattening, catch bond behavior, tethers and slings. *Mol. Immunol.* 55:59–69. doi:10.1016/j.molimm.2012.10.025.

Szocs, K. 2004. Endothelial dysfunction and reactive oxygen species production in ischemia/reperfusion and intrate tolerance. *Gen. Physiol. Biophys.* 23:265–295.

Tapper, H., A. Karlsson, M. Mörgelin, H. Flodgaard, and H. Herwald. 2002. Secretion of heparin-binding protein from human neutrophils is determined by its localization in azurophilic granules and secretory vesicles. *Blood*. 99:1785–1793. doi:10.1182/blood.V99.5.1785.

Taylor, S., O. Dirir, R.T. Zamanian, M. Rabinovitch, and A.A.R. Thompson. 2018. The role of neutrophils and neutrophil elastase in pulmonary arterial hypertension. *Front. Med.* 5:1–1. doi:10.3389/fmed.2018.00217.

Tecchio, C., A. Micheletti, and M.A. Cassatella. 2014. Neutrophil-Derived Cytokines: Facts Beyond Expression. *Front. Immunol.* 5:1–7. doi:10.3389/fimmu.2014.00508.

Tedder, T.F., D.A. Steeber, and P. Pizcueta. 1995. L-selectin-deficient mice have impaired leukocyte recruitment into inflammatory sites. *J. Exp. Med.* 181:2259–2264. doi:10.1084/jem.181.6.2259.

Tharp, W.G., R. Yadav, D. Irimia, A. Upadhyaya, A. Samadani, O. Hurtado, S.-Y. Liu, S. Munisamy, D.M. Brainard, M.J. Mahon, S. Nourshargh, A. van Oudenaarden, M.G. Toner, and M.C. Poznansky. 2006. Neutrophil chemorepulsion in defined interleukin-8 gradients in vitro and in vivo. *J. Leukoc. Biol.* 79:539–554. doi:10.1189/jlb.0905516.

Thiriot, A., C. Perdomo, G. Cheng, I. Novitzky-Basso, S. McArdle, J.K. Kishimoto, O. Barreiro, I. Mazo, R. Triboulet, K. Ley, A. Rot, and U.H. von Andrian. 2017. Differential DARC/ACKR1 expression distinguishes venular from non-venular

endothelial cells in murine tissues. *BMC Biol.* 15:1–19. doi:10.1186/s12915-017-0381-7.

Thomas, C.J., and K. Schroder. 2013. Pattern recognition receptor function in neutrophils. *Trends Immunol.* 34:317–328. doi:10.1016/j.it.2013.02.008.

Thompson, R.D., K.E. Noble, K.Y. Larbi, A. Dewar, G.S. Duncan, T.W. Mak, and S. Nourshargh. 2001. Platelet-endothelial cell adhesion molecule-1 (PECAM-1)–deficient mice demonstrate a transient and cytokine-specific role for PECAM-1 in leukocyte migration through the perivascular basement membrane. *Blood*. 97:1854–1860. doi:10.1182/blood.V97.6.1854.

Thompson, S., B. Martínez-Burgo, K.M. Sepuru, K. Rajarathnam, J.A. Kirby, N.S. Sheerin, and S. Ali. 2017. Regulation of chemokine function: The roles of GAG-binding and post-translational nitration. *Int. J. Mol. Sci.* 18:1–17. doi:10.3390/ijms18081692.

Torrey, H., J. Butterworth, T. Mera, Y. Okubo, L. Wang, D. Baum, A. Defusco, S. Plager, S. Warden, D. Huang, E. Vanamee, R. Foster, and D.L. Faustman. 2017. Targeting TNFR2 with antagonistic antibodies inhibits proliferation of ovarian cancer cells and tumor-associated T regs. *Sci. Signal.* 10:eaaf8608. doi:10.1126/scisignal.aaf8608.

Tuinstra, R., F. Peterson, S. Kutlesa, E.S. Elgin, M. Kron, and B. Volkman. 2008. Interconversion between two unrelated protein folds in the lymphotactin native state. *Chemtracts*. 21:94–95.

Uchimido, R., E.P. Schmidt, and N.I. Shapiro. 2019. The glycocalyx: a novel diagnostic and therapeutic target in sepsis. *Crit. Care*. 23:16. doi:10.1186/s13054-018-2292-6.

Urban, C.F., D. Ermert, M. Schmid, U. Abu-Abed, C. Goosmann, W. Nacken, V. Brinkmann, P.R. Jungblut, and A. Zychlinsky. 2009. Neutrophil extracellular traps contain calprotectin, a cytosolic protein complex involved in host defense against Candida albicans. *PLoS Pathog.* 5. doi:10.1371/journal.ppat.1000639.

Veldkamp, C.T., C. Seibert, F.C. Peterson, N.B. De La Cruz, J.C. Haugner, H. Basnet, T.P. Sakmar, and B.F. Volkman. 2008. Structural basis of CXCR4 sulfotyrosine recognition by the chemokine SDF-1/CXCL12. *Sci. Signal.* 1:1–11. doi:10.1126/scisignal.1160755.

Vestweber, D. 2007. Adhesion and signaling molecules controlling the transmigration of leukocytes through endothelium. *Immunol. Rev.* 218:178–196. doi:10.1111/j.1600-065X.2007.00533.x.

Vestweber, D. 2012. Relevance of endothelial junctions in leukocyte extravasation and vascular permeability. *Ann. N. Y. Acad. Sci.* 1257:184–192. doi:10.1111/j.1749-6632.2012.06558.x.

Vestweber, D. 2015. How leukocytes cross the vascular endothelium. *Nat. Rev. Immunol.* 15:692–704. doi:10.1038/nri3908.

Vestweber, D., and J.E. Blanks. 1999. Mechanisms that regulate the function of the selectins and their ligands. *Physiol. Rev.* 79:181–213. doi:10.1152/physrev.1999.79.1.181.

Vestweber, D., F. Wessel, and A.F. Nottebaum. 2014. Similarities and differences in the regulation of leukocyte extravasation and vascular permeability. *Semin.*

Immunopathol. 36:177–192. doi:10.1007/s00281-014-0419-7.

Vogl, T., K. Tenbrock, S. Ludwig, N. Leukert, C. Ehrhardt, M.A.D. Van Zoelen, W. Nacken, D. Foell, T. Van Der Poll, C. Sorg, and J. Roth. 2007. Mrp8 and Mrp14 are endogenous activators of Toll-like receptor 4, promoting lethal, endotoxin-induced shock. *Nat. Med.* 13:1042–1049. doi:10.1038/nm1638.

Voisin, M.B., G. Leoni, A. Woodfin, L. Loumagne, N.S.A. Patel, R. Di Paola, S. Cuzzocrea, C. Thiemermann, M. Perretti, and S. Nourshargh. 2019. Neutrophil elastase plays a non-redundant role in remodeling the venular basement membrane and neutrophil diapedesis post-ischemia/reperfusion injury. *J. Pathol.* 248:88–102. doi:10.1002/path.5234.

Voisin, M.B., and S. Nourshargh. 2013. Neutrophil transmigration: Emergence of an adhesive cascade within venular walls. *J. Innate Immun.* 5:336–347. doi:10.1159/000346659.

Voisin, M.B., D. Pröbstl, and S. Nourshargh. 2010. Venular basement membranes ubiquitously express matrix protein low-expression regions: Characterization in multiple tissues and remodeling during inflammation. *Am. J. Pathol.* 176:482–495. doi:10.2353/ajpath.2010.090510.

Voisin, M.B., A. Woodfin, and S. Nourshargh. 2009. Monocytes and neutrophils exhibit both distinct and common mechanisms in penetrating the vascular basement membrane in vivo. *Arterioscler. Thromb. Vasc. Biol.* 29:1193–1199. doi:10.1161/ATVBAHA.109.187450.

Wang, J., M. Hossain, A. Thanabalasuriar, M. Gunzer, C. Meininger, and P. Kubes. 2017. Visualizing the function and fate of neutrophils in sterile injury and repair. *Science.* 358:111–116. doi:10.1126/science.aam9690.

Wang, J.X., A.M. Bair, S.L. King, R. Shnayder, Y.F. Huang, C.C. Shieh, R.J. Soberman, R.C. Fuhlbrigge, and P.A. Nigrovic. 2012. Ly6G ligation blocks recruitment of neutrophils via a β2-integrin- dependent mechanism. *Blood*. 120:1489–1498. doi:10.1182/blood-2012-01-404046.

Wang, S., M.B. Voisin, K.Y. Larbi, J. Dangerfield, C. Scheiermann, M. Tran, P.H. Maxwell, L. Sorokin, and S. Nourshargh. 2006. Venular basement membranes contain specific matrix protein low expression regions that act as exit points for emigrating neutrophils. *J. Exp. Med.* 203:1519–1532. doi:10.1084/jem.20051210.

Weber, C., L. Fraemohs, and E. Dejana. 2007. The role of junctional adhesion molecules in vascular inflammation. *Nat. Rev. Immunol.* 7:467–477. doi:10.1038/nri2096.

Weber, P.C., D.H. Ohlendorf, J.J. Wendoloski, and F.R. Salemme. 1989. Structural origins of high-affinity biotin binding to streptavidin. *Science.* 243:85–88. doi:10.1126/science.2911722.

Wedmore, C. V., and T.J. Williams. 1981. Control of vascular permeability by polymorphonuclear leukocytes in inflammation. *Nature*. 289:646–650.

Wegmann, F., B. Petri, A.A.G. Khandoga, C. Moser, A.A.G. Khandoga, S. Volkery, H. Li, I. Nasdala, O. Brandau, R. Fässler, S. Butz, F. Krombach, and D. Vestweber. 2006. ESAM supports neutrophil extravasation, activation of Rho, and VEGF-induced vascular permeability. *J. Exp. Med.* 203:1671–1677. doi:10.1084/jem.20060565.

Wessel, F., M. Winderlich, M. Holm, M. Frye, R. Rivera-Galdos, M. Vockel, R. Linnepe,

U. Ipe, A. Stadtmann, A. Zarbock, A.F. Nottebaum, and D. Vestweber. 2014. Leukocyte extravasation and vascular permeability are each controlled in vivo by different tyrosine residues of VE-cadherin. *Nat. Immunol.* 15:223–230. doi:10.1038/ni.2824.

Wiekowski, M.T., S.-C. Chen, P. Zalamea, B.P. Wilburn, D.J. Kinsley, W.W. Sharif, K.K. Jensen, J.A. Hedrick, D. Manfra, and S.A. Lira. 2001. Disruption of Neutrophil Migration in a Conditional Transgenic Model: Evidence for CXCR2 Desensitization In Vivo. *J. Immunol.* 167:7102–7110. doi:10.4049/jimmunol.167.12.7102.

Winderlich, M., L. Keller, G. Cagna, A. Broermann, O. Kamenyeva, F. Kiefer, U. Deutsch, A.F. Nottebaum, and D. Vestweber. 2009. VE-PTP controls blood vessel development by balancing Tie-2 activity. *J. Cell Biol.* 185:657–671. doi:10.1083/jcb.200811159.

Winter, M.C., S.S. Shasby, D.R. Ries, and D.M. Shasby. 2004. Histamine selectively interrupts VE-cadherin adhesion independently of capacitive calcium entry. *Am. J. Physiol. - Lung Cell. Mol. Physiol.* 287:816–823. doi:10.1152/ajplung.00056.2004.

Wojciak-Stothard, B., and A.J. Ridley. 2002. Rho GTPases and the regulation of endothelial permeability. *Vascul. Pharmacol.* 39:187–199. doi:10.1016/S1537-1891(03)00008-9.

Wolf, Y., A. Shemer, M. Polonsky, M. Gross, A. Mildner, S. Yona, E. David, K.W. Kim, T. Goldmann, I. Amit, M. Heikenwalder, S. Nedospasov, M. Prinz, N. Friedman, and S. Jung. 2017. Autonomous TNF is critical for in vivo monocyte survival in steady state and inflammation. *J. Exp. Med.* 214:905–917. doi:10.1084/jem.20160499.

Wong, D., K. Dorovini-Zis, and S.R. Vincent. 2004. Cytokines, nitric oxide, and cGMP modulate the permeability of an in vitro model of the human blood-brain barrier. *Exp. Neurol.* 190:446–455. doi:10.1016/j.expneurol.2004.08.008.

Wong, E., T. Cohen, E. Romi, M. Levin, Y. Peleg, U. Arad, A. Yaron, M.E. Milla, and I. Sagi. 2016. Harnessing the natural inhibitory domain to control TNFα Converting Enzyme (TACE) activity in vivo. *Sci. Rep.* 6:1–12. doi:10.1038/srep35598.

Woodfin, A., M. Beyrau, M.B. Voisin, B. Ma, J.R. Whiteford, P.L. Hordijk, N. Hogg, and S. Nourshargh. 2016. ICAM-1-expressing neutrophils exhibit enhanced effector functions in murine models of endotoxemia. *Blood*. 127:898–907. doi:10.1182/blood-2015-08-664995.

Woodfin, A., C.A. Reichel, A. Khandoga, M. Corada, M.B. Voisin, C. Scheiermann, D.O. Haskard, E. Dejana, F. Krombach, and S. Nourshargh. 2007a. JAM-A mediates neutrophil transmigration in a stimulus-specific manner in vivo: Evidence for sequential roles for JAM-A and PECAM-1 in neutrophil transmigration. *Blood*. 110:1848–1856. doi:10.1182/blood-2006-09-047431.

Woodfin, A., M.B. Voisin, M. Beyrau, B. Colom, D. Caille, F.M. Diapouli, G.B. Nash, T. Chavakis, S.M. Albelda, G.E. Rainger, P. Meda, B.A. Imhof, and S. Nourshargh. 2011. The junctional adhesion molecule JAM-C regulates polarized transendothelial migration of neutrophils in vivo. *Nat. Immunol.* 12:761–769. doi:10.1038/ni.2062.

Woodfin, A., M.B. Voisin, B.A. Imhof, E. Dejana, B. Engelhardt, and S. Nourshargh. 2009. Endothelial cell activation leads to neutrophil transmigration as supported

by the sequential roles of ICAM-2, JAM-A, and PECAM-1. *Blood*. 113:6246–6257. doi:10.1182/blood-2008-11-188375.

Woodfin, A., M.B. Voisin, and S. Nourshargh. 2007b. PECAM-1: A multi-functional molecule in inflammation and vascular biology. *Arterioscler. Thromb. Vasc. Biol.* 27:2514–2523. doi:10.1161/ATVBAHA.107.151456.

Wright, H.L., R.J. Moots, R.C. Bucknall, and S.W. Edwards. 2010. Neutrophil function in inflammation and inflammatory diseases. *Rheumatology*. 49:1618–1631. doi:10.1093/rheumatology/keq045.

Wu, D., Y. Zeng, Y. Fan, J. Wu, T. Mulatibieke, J. Ni, G. Yu, R. Wan, X. Wang, and G. Hu. 2016. Reverse-migrated neutrophils regulated by JAM-C are involved in acute pancreatitis-associated lung injury. *Sci. Rep.* 6:1–15. doi:10.1038/srep20545.

Wu, H., and S.G. Hymowitz. 2010. Chapter 40: Structure and function of tumor necrosis factor (TNF) at the cell surface. 1. Second Edi. Elsevier Inc. 265–275 pp.

Wu, M.Y., G.T. Yiang, W.T. Liao, A.P.Y. Tsai, Y.L. Cheng, P.W. Cheng, C.Y. Li, and C.J. Li. 2018. Current Mechanistic Concepts in Ischemia and Reperfusion Injury. *Cell. Physiol. Biochem.* 46:1650–1667. doi:10.1159/000489241.

Xu, J., F. Wang, A. Van Keymeulen, M. Rentel, and H.R. Bourne. 2005. Neutrophil microtubules suppress polarity and enhance directional migration. *Proc. Natl. Acad. Sci. U. S. A.* 102:6884–6889. doi:10.1073/pnas.0502106102.

Xu, N., X. Lei, and L. Liu. 2011. Tracking neutrophil intraluminal crawling, transendothelial migration and chemotaxis in tissue by intravital video microscopy. *J. Vis. Exp.* 2–5. doi:10.3791/3296.

Yamaki, K., H. Thorlacius, X. Xie, L. Lindbom, P. Hedqvist, and J. Raud. 1998. Characteristics of histamine-induced leukocyte rolling in the undisturbed microcirculation of the rat mesentery. *Br. J. Pharmacol.* 123:390–399. doi:10.1038/sj.bjp.0701614.

Yang, L. 2005. ICAM-1 regulates neutrophil adhesion and transcellular migration of TNF- -activated vascular endothelium under flow. *Blood*. 106:584–592. doi:10.1182/blood-2004-12-4942.

Yarilina, A., K.H. Park-Min, T. Antoniv, X. Hu, and L.B. Ivashkiv. 2008. TNF activates an IRF1-dependent autocrine loop leading to sustained expression of chemokines and STAT1-dependent type I interferon-response genes. *Nat. Immunol.* 9:378–387. doi:10.1038/ni1576.

Ye, F., S. Yin, M. Li, Y. Li, and J. Zhong. 2020. In-vivo full-field measurement of microcirculatory blood flow velocity based on intelligent object identification. *J. Biomed. Opt.* 25:1. doi:10.1117/1.jbo.25.1.016003.

Yipp, B.G., and P. Kubes. 2013. Antibodies against neutrophil LY6G do not inhibit leukocyte recruitment in mice in vivo. *Blood*. 121:241–242. doi:10.1182/blood-2012-09-454348.

Yoo, S.K., and A. Huttenlocher. 2011. Spatiotemporal photolabeling of neutrophil trafficking during inflammation in live zebrafish. *J. Leukoc. Biol.* 89:661–667. doi:10.1189/jlb.1010567.

Yu, C., S. Zhang, Y. Wang, S. Zhang, L. Luo, and H. Thorlacius. 2016. Platelet-Derived

CCL5 Regulates CXC Chemokine Formation and Neutrophil Recruitment in Acute Experimental Colitis. *J. Cell. Physiol.* 231:370–376. doi:10.1002/jcp.25081.

Zarbock, A., K. Ley, R.P. McEver, and A. Hidalgo. 2011. Leukocyte ligands for endothelial selectins: Specialized glycoconjugates that mediate rolling and signaling under flow. *Blood*. 118:6743–6751. doi:10.1182/blood-2011-07-343566.

Zhang, N., Z. Wang, and Y. Zhao. 2020. Selective inhibition of Tumor necrosis factor receptor-1 (TNFR1) for the treatment of autoimmune diseases. *Cytokine Growth Factor Rev.* 1:1–6. doi:10.1016/j.cytogfr.2020.03.002.

Zhou, P., S. Lu, Y. Luo, S. Wang, K. Yang, Y. Zhai, G. Sun, and X. Sun. 2017. Attenuation of TNF-α-induced inflammatory injury in endothelial cells by ginsenoside Rb1 via inhibiting NF-κB, JNK and p38 signaling pathways. *Front. Pharmacol.* 8:1–13. doi:10.3389/fphar.2017.00464.

Zhou, Z., P. Gengaro, W. Wang, X.Q. Wang, C. Li, S. Faubel, C. Rivard, and R.W. Schrier. 2008. Role of NF-κB and PI 3-kinase/Akt in TNF-α-induced cytotoxicity in microvascular endothelial cells. *Am. J. Physiol. - Ren. Physiol.* 295:932–941. doi:10.1152/ajprenal.00066.2008.

Zindel, J., and P. Kubes. 2020. DAMPs, PAMPs, and LAMPs in Immunity and Sterile Inflammation. *Annu. Rev. Pathol. Mech. Dis.* 15:493–518. doi:10.1146/annurev-pathmechdis-012419-032847.

9. Appendices

All videos and the publication arising from investigations conducted in this thesis are available in OneDrive shared file, accessible using the link sent *via* email.

9.1. Appendix 1

The videos and their respective descriptive legends below demonstrate examples of neutrophil migration (normal and reverse TEM), vascular leakage responses and labelling of rTEM neutrophils. *LysM-EGFP*$^{ki/+}$ mice were used for visualisation of neutrophils (Video 1-4 - green and video 5 - blue). ECs are labelled using a fluorescently labelled, non-blocking anti-CD31 Ab (Video 1-4 - red and video 5 – green). All images were acquired using a confocal microscope at a speed of 1 frame/min. All reactions are clearly highlighted in each video and in the complementary descriptions. Lastly, for the examples of normal and reverse TEM events an isosurface was generated using IMARIS Bitplane software to remove the other surrounding neutrophils for the purpose of clarity.

Video 1: A representative example of the neutrophil TEM & vascular leakage response during IR-injury induced cremasteric inflammation

This video shows an inflamed post-capillary venule as induced by IR-injury. Here, during the 1 hr reperfusion period, neutrophils (green) can be seen to undergo TEM and concomitantly, TRITC-Dextran (blue) can be seen to rapidly leak into the interstitial tissue, whereby the latter is seen to decrease after 30 min.

Video 2: An example of normal neutrophil TEM (nTEM) during IR-injury induced cremasteric inflammation

This video represents a typical/normal neutrophil TEM in a post-capillary venule during the reperfusion phase as induced during a model of IR-injury. Here, the video focuses on one neutrophil (green) of interest and the cell can be seen to protrude through an EC

junctional pore (red), which is clearly observed upon the brief removal of the neutrophil fluorescence channel (green). The neutrophil takes approximately 7 min to fully migrate into the sub-EC space, which is clearly observable following rotation of the blood vessel.

Video 3: An example of neutrophil reverse TEM (rTEM) during IR-injury induced cremasteric inflammation

This video shows a typical example of a neutrophil undergoing rTEM in a post-capillary venule during the reperfusion phase of cremasteric IR-injury. Here, the neutrophil (green) can be seen to initiate breaching through the EC wall (red) into the sub-EC space as is clearly observed following the temporary removal of the neutrophil fluorescence channel and rotation of the blood vessel. The cell is then seen to move in a retrograde manner, returning into the vascular lumen and detaching from the venular wall.

Video 4: Neutrophil TEM, vascular leakage and neutrophil rTEM as induced by IL-1β + histamine cremasteric inflammation

This video demonstrates the neutrophil TEM (green) response in a fluorescently labelled post-capillary venule (red) as induced following local IL-1β stimulation. Following the application of topical histamine over the surface of the cremaster tissue, TRITC-dextran can be seen to rapidly leak into the interstitial tissue, a response which declines after 30 min and is minimal after 1 hr. The second part of the video shows a representative example of a neutrophil undergoing rTEM following the application of histamine and as is described for video 3.

Video 5: Labelling of rTEM neutrophils in the cremaster muscle with anti-Ly6G-biotin Ab and strept-AF647

This video demonstrates our novel labelling strategy of rTEM neutrophils. Here, an anti-Ly6G-biotin labelled neutrophil (blue) initiates breaching through an EC junction (green) and becomes rapidly labelled with strept-AF647 (red) after its topical application. The neutrophil then initiates retrograde motility and returns to the vascular lumen and

detaches from the vascular wall. This approach allowed for distinction from other (non-reverse) neutrophils, thus facilitating their tracking.

9.2. Appendix 2

This section provides full access to our recent publication in JCI (2020) *via* the OneDrive, which included the experimental investigations presented in Chapters 3-5 in this thesis.

9.3. Appendix 3

This section specifies key experiment details in a timeline for confocal IVM experiments conducted in this thesis.

9.3.1. IL-1β or LTB_4 stimulation – (*LysM-EGFP*$^{ki/+}$, Chapter 3):

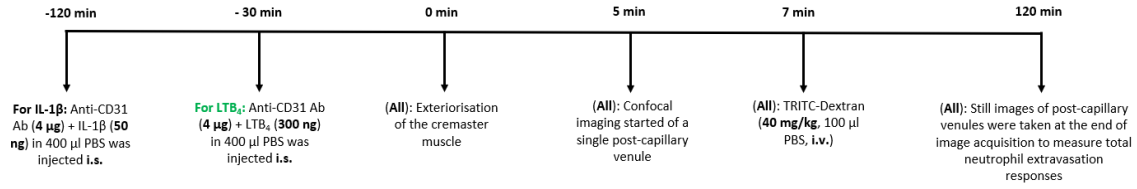

NB: Control treated mice were alternatively treated with an anti-CD31 Ab (4 µg) in 400 µl PBS, **i.s.**

9.3.2. IR-injury - (*LysM-EGFP*$^{ki/+}$, Chapter 3) or (TNFRI/II KO-BM->-WT & WT-BM->-WT, Chapter 6):

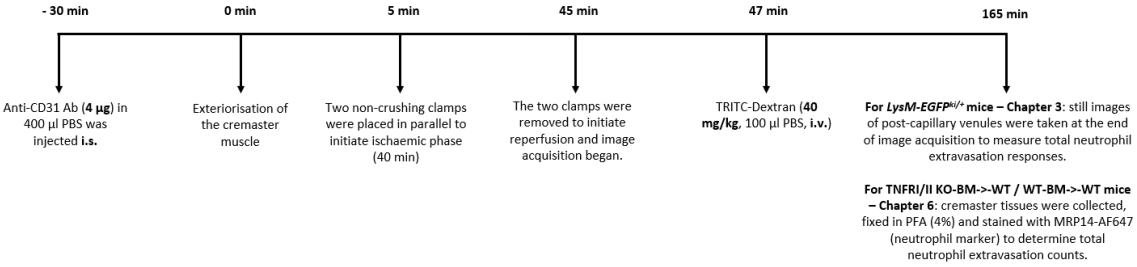

NB: For sham operated control mice there was no placement of the clamps.

9.3.3. IL-1β +/- histamine or VEGF - (*LysM-EGFP*$^{ki/+}$, Chapter 4) or *VEC-Y685F & VEC-WT*, Chapter 4 - IL-1β +/- Histamine only):

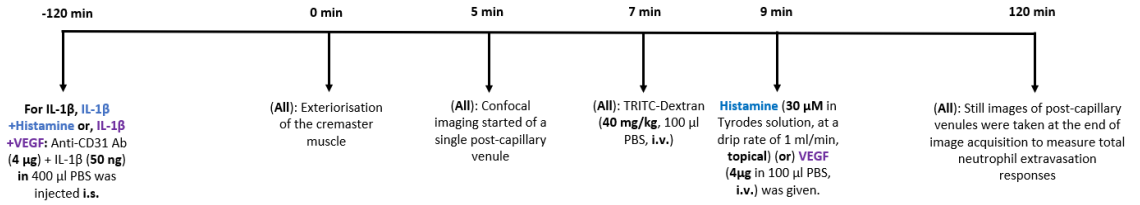

NB: Control PBS treated mice were alternatively treated with anti-CD31 Ab (4 µg) in 400 µl PBS, i.s. and were topically applied with Tyrodes solution alone.

9.3.4. IL-1β + histamine +/- Anti-VE-PTP - (WT, Chapter 4):

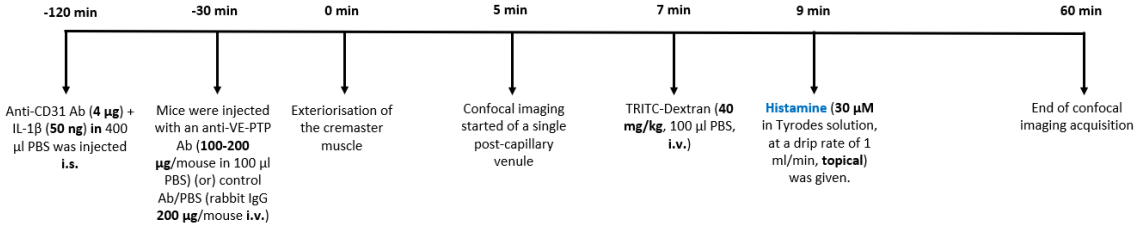

NB: For plasma and tissue CXCL1 analysis: Alternatively, WT mice were subjected to a local injection of IL-1β (200 µl of a 50 ng solution, i.s.) or PBS, 2 hr prior to a local injection of histamine (200 µl of a 30 µM solution, i.s.) or PBS control (200 µl) or 30 min prior to induction of cremaster ischaemia. Plasma and cremaster tissue samples were then collected after the peak of the vascular leakage response for each reaction i.e. following 30 min post reperfusion or 30 min post topical histamine treatment. Additionally, in some mice an anti-VE-PTP/isotype control Ab were injected as depicted and plasma was collected 60 min post local histamine treatment.

9.3.5. IL1β + histamine +/- anti-CXCL1 - (*LysM-EGFP*$^{ki/+}$, Chapter 4):

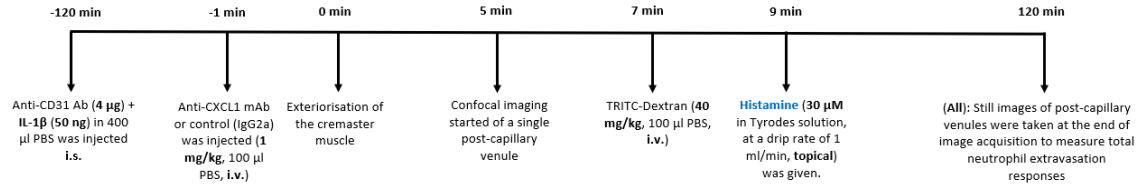

9.3.6. IR-injury +/- anti-CXCL1 - (*LysM-EGFP*$^{ki/+}$, Chapter 4):

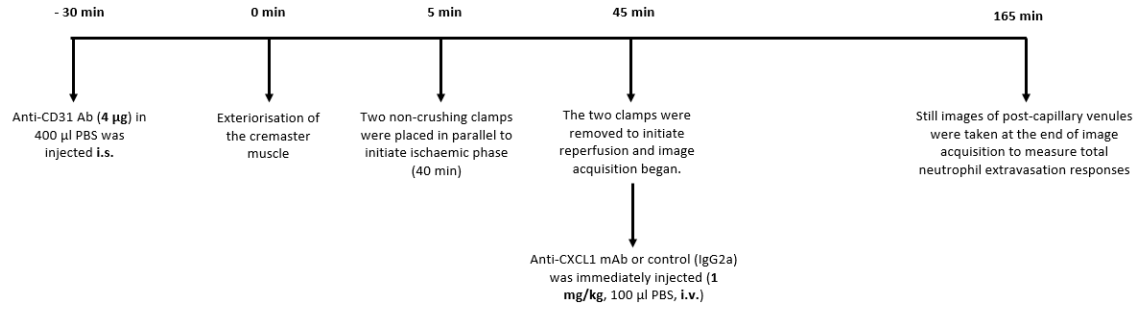

9.3.7. IL-1β + histamine + anti-Ly6G-biotin & strept-AF647 - (*LysM-EGFP*$^{ki/+}$, Chapter 5):

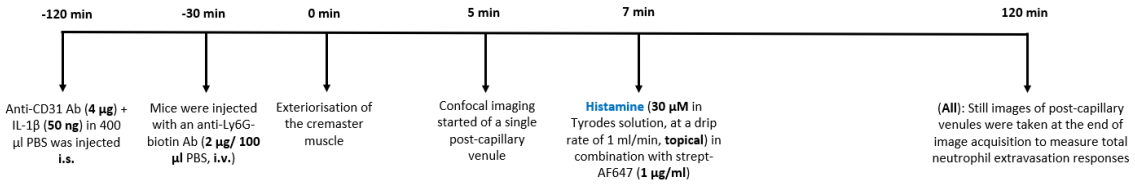

NB: Control IL-1β alone treated mice were alternatively just topically applied with Tyrodes solution alone. Alternatively, in some experiments control mice received no injection of anti-Ly6G Ab and topical application strept-AF647.